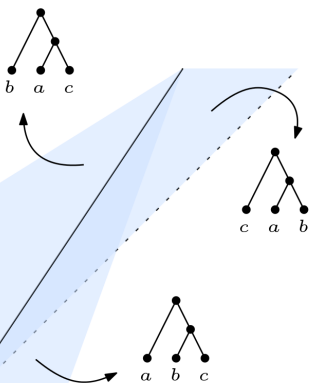

TORIC NEWTON–OKOUNKOV FUNCTIONS, THE KINGMAN COALESCENT, AND FULLY MIXED CELLS

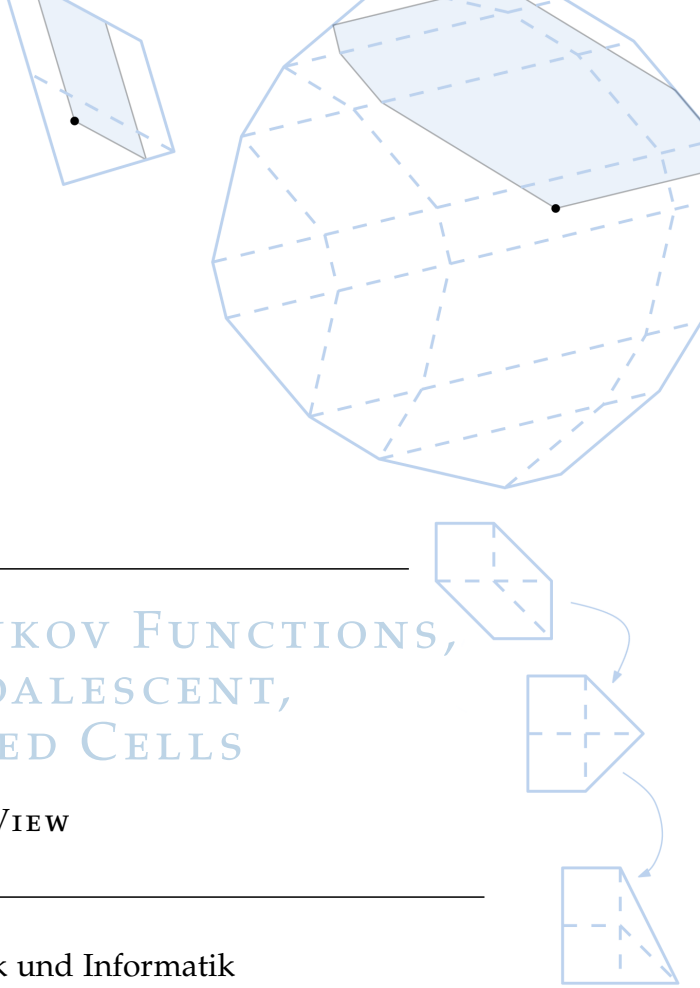
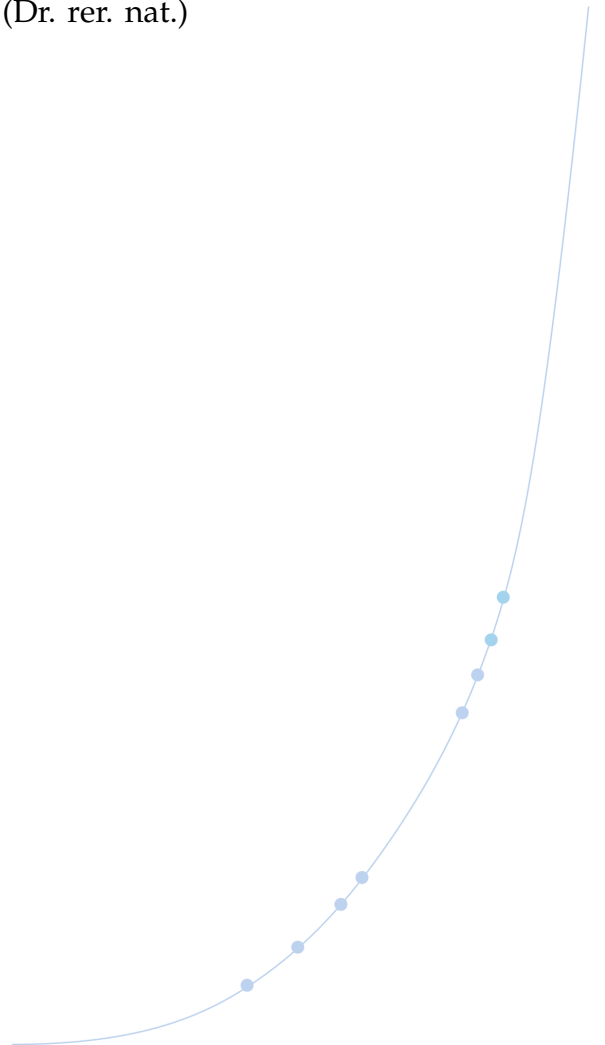
A POLYHEDRAL VIEW

beim Fachbereich Mathematik und Informatik
der Freien Universität Berlin
eingereichte DISSERTATION
zur Erlangung des Grades eines
Doktors der Naturwissenschaften (Dr. rer. nat.)

vorgelegt von
LENA WALTER



Berlin 2020



Lena Walter:

TORIC NEWTON–OKOUNKOV FUNCTIONS, THE KINGMAN COALESCENT,
AND FULLY MIXED CELLS

Tag der Disputation: 04. Mai 2021

BETREUER:

Prof. Dr. Christian Haase

GUTACHTER:

Prof. Dr. Christian Haase

Prof. Dr. Alex Küronya

ACKNOWLEDGMENTS



People claim that 2020 is the year of things that do not happen, get canceled, or postponed. One of the many things that Christian has taught me, is that most conjectures are false and that you should rather go out and look for counterexamples instead of proof. In this sense, I want to give a counterexample to the hypothesis above by making this thesis happen.¹

Of course, doing a PhD wasn't all just about quarantining myself with the very same \LaTeX file for months, but about the great math that I have learned and about the great people who have accompanied me on my way (and also a little about the great food, maybe).

First and foremost, I want thank my advisor Christian Haase. I am extremely grateful for your incomparable excitement for all kinds of mathematical problems and that you truly care sharing it with, and passing it on to all of your students. Thank you for being there and taking the time to discuss math, teaching, and life with me although there were always 547896724 emails and a full calendar waiting. You have made my time in Berlin very special and will make it hard to leave.

I would like to extend my sincere thanks to Alex Küronya for introducing me to the beautiful world of Newton–Okounkov bodies, for the valuable collaboration, and for the opportunity to experience a lot of interesting math and great desserts at BIRS. I also had the great pleasure of working with Giulia Codenotti and Francisco Santos, thanks for all the interesting discussions.

I cannot begin to express my gratitude to all members of 'Team Haase'! I have had an amazing time, thanks to Jan Hofmann and Florian Kohl, who used to be my colleagues and office mates and who became my friends. It would have been way harder and a lot less fun without you, guys. Special thanks to Carlos Améndola for all the board games in between and after work and to Karin Schaller for all the waffle lunches.

Even though I have technically not been part of the Villa, I really enjoyed all the time I have spent there, talking (math) and eating cake. Thanks to all the inhabitants of the Villa, in particular to Matthias Beck for making everyone feel like they belong. Special thanks to Giulia Codenotti for your friendship, our talks and for getting upset together, when necessary. A heartfelt thank-you goes out to the members of my amazing

¹Rumor has it that people only tend to read this particular page of one's thesis — but there is also a lot of great math about to come. I promise.

'infection/toric reading group' Marie-Charlotte Brandenburg and Amy Wiebe. What can I say, it has been a great opportunity and always a pleasure. Thanks for making it through quarantine with me, online and offline — this is how we do toric reading group!

Math brings people together, not only in Berlin. I have had the pleasure to visit great places and meet great people from all around the world. I am particularly happy that I kept meeting Christopher Borger, thanks for all our talks.

I am truly grateful to Christopher Borger, Marie-Charlotte Brandenburg, Jan Hofmann, Florian Kohl, Karin Schaller, Annika Walter, Benedikt Weygandt, Amy Wiebe, and Jan-Hendrik de Wiljes, for reading parts of this thesis, searching for typos or even trying to make it through the math.

Finally, I want to express my gratitude to my family and friends for their unconditional support from outside the math bubble. And thanks to Benedikt Weygandt for also being a part of it. We discussed my first Analysis 1 exercise sheet together and now we have finished our theses. There is no one I would rather have done this with, thanks for everything.

CONTENTS

| | |
|--|-----|
| ACKNOWLEDGMENTS | iii |
| NOTATION | vii |
| 1 INTRODUCTION | 1 |
| 1.1 Polyhedral Geometry: Background and Notation | 3 |
| 1.1.1 Polyhedra and Polytopes | 3 |
| 1.1.2 Cones and Fans | 5 |
| 2 TORIC NEWTON–OKOUNKOV FUNCTIONS | 7 |
| 2.1 Introduction | 7 |
| 2.2 Background and Notation | 11 |
| 2.2.1 Positivity | 11 |
| 2.2.2 Toric Varieties | 14 |
| 2.2.3 Newton–Okounkov Bodies | 16 |
| 2.2.4 Functions on Newton–Okounkov Bodies | 21 |
| 2.3 Zariski Decomposition | 24 |
| 2.3.1 The ‘Tilting-Isomorphism’ for Newton-Okounkov Bodies | 31 |
| 2.4 Newton–Okounkov Functions on Toric Varieties | 38 |
| 2.4.1 The Completely Toric Case | 38 |
| 2.4.2 Interpretation of a Subgraph as a Newton–Okounkov Body | 41 |
| 2.4.3 Geometric Valuation Coming from a General Point | 48 |
| 2.5 Rationality of Certain Seshadri Constants | 65 |
| 2.6 Outlook | 77 |
| 3 COALESCENTS AS DENSITIES ON A SPACE OF TREES | 79 |
| 3.1 Introduction | 79 |
| 3.2 The Fisher–Wright Model and the Kingman n -Coalescent | 80 |
| 3.2.1 The Fisher–Wright Model | 81 |
| 3.2.2 Tree Topology | 82 |
| 3.2.3 Waiting Times | 84 |
| 3.2.4 The Kingman n -Coalescent | 86 |
| 3.3 Spaces of Trees | 86 |
| 3.3.1 The Geometry of the Space of Trees MUM_n | 89 |
| 3.3.2 The Connection to Tropical Geometry | 94 |
| 3.4 The Kingman n -Coalescent as a Density on a Space of Trees | 96 |
| 3.5 The Kingman Coalescent | 97 |
| 3.5.1 The Kingman n -Coalescent as a Markov-Chain Process | 97 |
| 3.5.2 A Forgetful Map on the Space of Trees | 98 |
| 3.6 The Multispecies Coalescent | 102 |
| 3.6.1 A Polyhedral Description of Compatibility | 104 |
| 3.6.2 The Distribution of Gene Tree Topologies | 107 |

CONTENTS

| | | |
|-------|--|-----|
| 4 | ON FINDING A FULLY MIXED CELL | 115 |
| 4.1 | Introduction | 115 |
| 4.2 | Background and Notation | 116 |
| 4.2.1 | Regular Subdivisions and Triangulations | 117 |
| 4.2.2 | Minkowski Sums and Mixed Cells | 118 |
| 4.2.3 | The Cayley Trick | 119 |
| 4.2.4 | The Secondary Polytope and the Secondary Fan | 122 |
| 4.3 | A Lower Bound | 125 |
| 4.3.1 | A Matroid Intersection Algorithm | 126 |
| 4.3.2 | A Lower Bound on the Number of Flips | 126 |
| A | APPENDIX | 131 |
| | BIBLIOGRAPHY | 137 |
| | LIST OF FIGURES | 147 |
| | LIST OF TABLES | 149 |

NOTATION

POLYHEDRAL GEOMETRY

| | |
|--------------------------|---|
| H | hyperplane defined by $\alpha(x) = 0$ for some $\alpha \in (\mathbb{R}^n)^*$ |
| H^+ | half space defined by $\alpha(x) \geq 0$ for some $\alpha \in (\mathbb{R}^n)^*$ |
| $\text{cone}(A)$ | convex cone generated by A |
| σ | rational convex polyhedral cone in $N_{\mathbb{R}}$ |
| σ^\vee | dual cone of σ |
| ρ | 1-dimensional strongly convex cone (a ray) in $N_{\mathbb{R}}$ |
| u_ρ | minimal ray generator of $\rho \cap N$, ρ a rational ray in $N_{\mathbb{R}}$ |
| N_σ | sublattice $\mathbb{Z}(\sigma \cap N)$ |
| $N(\sigma)$ | quotient lattice N/N_σ |
| Σ | fan in $N_{\mathbb{R}}$ |
| $\Sigma(i)$ | i -dimensional cones in Σ |
| $\text{star}(\sigma)$ | star of σ , a fan in $N(\sigma)$ |
| $\Sigma^*(\sigma)$ | star subdivision of Σ for $\sigma \in \Sigma$ |
| $ \Sigma $ | support of a fan Σ |
| $\text{conv}(A)$ | convex hull of A |
| P | polytope or polyhedron |
| $\dim(P)$ | dimension of a polyhedron P |
| $\text{deg}(P)$ | normalized volume of a polytope P |
| $F \preceq P$ | F is a face of P |
| $\text{vert}(P)$ | set of vertices of a polytope or polyhedron |
| $\text{vert}(P, v)$ | relevant vertex set of a polytope w.r.t a direction v |
| P^\vee | polar dual of a polytope P |
| \mathcal{N}_P | normal fan of a polytope or polyhedron P |
| $\text{NP}(f)$ | Newton polytope of a Laurent polynomial f |
| $\text{length}_M(L)$ | lattice length of a segment L w.r.t. lattice M |
| $\text{length}(P, p, v)$ | relative length of a polytope P at vertex p w.r.t. direction v |
| $P_v(m)$ | feasible region of a polytope P w.r.t. direction v given $m \in P$ |
| $\text{width}_u(P)$ | width of a polytope $P \subseteq M_{\mathbb{R}}$ w.r.t. linear functional $u \in N$ |

NOTATION

| | |
|-----------------------------|--|
| $MV(P, Q)$ | mixed volume of polytopes P, Q |
| $\text{sun}(P, v)$ | sunny side of a polytope P w.r.t. direction v |
| $\text{wedge}_F(P)$ | wedge of a polytope P over a face F |
| $P^{\text{FA}(c)}$ | fine adjoint of a polytope P and a parameter $c > 0$ |
| $\eta(D)$ | codegree of a polytope associated to the divisor D |
| $\eta^{\text{F}}(P)$ | fine codegree of a polytope P |
| $\text{core}(P)$ | core of a polytope P |
| $\text{core}^{\text{F}}(P)$ | fine core of a polytope P |
| (Π, \leq_{Π}) | poset |
| $\mathcal{O}(\Pi)$ | order polytope of a poset Π |
| $\mathcal{K}(\Pi)$ | order cone of a poset Π |

(TORIC) VARIETIES

| | |
|--------------------------|--|
| X | variety |
| z | a point in X |
| R | a general point in X |
| Z | a subvariety of X |
| M, χ^m | character lattice of a torus and a character of $m \in M$ |
| N | lattice of one-parameter subgroups of a torus |
| \mathbb{T} | torus $N \otimes_{\mathbb{Z}} \mathbb{C}^* = \text{hom}_{\mathbb{Z}}(M, \mathbb{C}^*)$ associated to N and M |
| $M_{\mathbb{R}}$ | vector space $M \otimes_{\mathbb{Z}} \mathbb{R}$ built from M |
| $N_{\mathbb{R}}$ | vector space $N \otimes_{\mathbb{Z}} \mathbb{R}$ built from N |
| $\langle m, u \rangle$ | pairing of $m \in M$ or $M_{\mathbb{R}}$ with $u \in N$ or $N_{\mathbb{R}}$ |
| S_{σ} | affine semigroup $\sigma^{\vee} \cap M$ |
| $\mathbb{C}[S_{\sigma}]$ | semigroup algebra |
| U_{σ} | affine toric variety of a cone $\sigma \subseteq N_{\mathbb{R}}$ |
| X_{Σ} | toric variety of a fan Σ in $N_{\mathbb{R}}$ |
| X_P | projective toric variety of a polytope or polyhedron P |
| \mathcal{H}_d | d -th Hirzebruch surface |
| S | Cox ring of X_{Σ} |
| x_{ρ} | variable in S corresponding to $\rho \in \Sigma(1)$ |
| S_d | graded piece of S in degree $d \in \text{Cl}(X_{\Sigma})$ |

DIVISORS

| | |
|---------------------------------------|---|
| D | divisor |
| $\operatorname{div}(f)$ | principal divisor of a rational function f |
| $D \sim D'$ | linear equivalence of divisors D and D' |
| $\operatorname{CDiv}(X)$ | group of Cartier divisors |
| $\operatorname{Cl}(X)$ | divisor class group of a normal variety X |
| $\operatorname{Pic}(X)$ | Picard group of a normal variety X |
| $D _U$ | restriction of a divisor to an open set U |
| $ D $ | complete linear system of D |
| D_ρ | torus-invariant prime divisor on X_Σ of ray $\rho \in \Sigma(1)$ |
| $\{m_\sigma\}_{\sigma \in \Sigma}$ | Cartier data of a torus-invariant Cartier divisor on X_Σ |
| P_D | polyhedron of a torus-invariant divisor D |
| \mathcal{O}_X | structure sheaf of a variety X |
| SF_D | support function of a Cartier divisor D |
| $\mathcal{O}_X(D)$ | sheaf of a Weil divisor D on X |
| s | global section |
| $H^0(X, \mathcal{O}_X(D))$ | global sections of the sheaf $\mathcal{O}_X(D)$ on X |
| $h^0(X, \mathcal{O}_X(D))$ | dimension of $H^0(X, \mathcal{O}_X(D))$ |
| \mathcal{L} | line bundle (invertible sheaf) |
| $\pi : V_{\mathcal{L}} \rightarrow X$ | rank 1 vector bundle of an invertible sheaf \mathcal{L} |
| C | curve |
| $D.C$ | intersection product of Cartier divisor D and complete curve C |
| $D \equiv D'$ | numerically equivalent Cartier divisors D and D' |
| $N^1(X)$ | Néron–Severi group |
| $N^1(X)_{\mathbb{R}}$ | Néron–Severi space |
| $\operatorname{Nef}(X)$ | cone in $N^1(X)_{\mathbb{R}}$ generated by nef divisor classes |
| $\operatorname{Amp}(X)$ | cone in $N^1(X)_{\mathbb{R}}$ generated by ample divisor classes |
| $\operatorname{Big}(X)$ | cone in $N^1(X)_{\mathbb{R}}$ generated by big divisor classes |
| $\overline{\operatorname{Eff}}(X)$ | closure of the cone in $N^1(X)_{\mathbb{R}}$ generated by effective divisor classes |
| D^+ | positive part of the Zariski decomposition of a divisor D |
| D^- | negative part of the Zariski decomposition of a divisor D |

NOTATION

NEWTON–OKOUNKOV BODIES AND SESHADRI CONSTANTS

| | |
|--------------------------------|--|
| val | valuation-like map |
| Val_{Y_\bullet} | set of valuative point associated to a flag Y_\bullet |
| $\Gamma_{Y_\bullet}(D)$ | valuation semigroup associated to a divisor D and a flag Y_\bullet |
| $\text{ord}_Z(s)$ | order of vanishing of a global section s along a subvariety Z |
| Y_\bullet | full flag of subvarieties |
| $\Delta_{Y_\bullet}(D)$ | Newton–Okounkov body of a big divisor D w.r.t. the flag Y_\bullet |
| φ_Z | Newton–Okounkov function coming from the geometric valuation ord_Z |
| $\mu_C(D)$ | pseudo-effective threshold of a divisor D and a curve C |
| $\varepsilon(X, D; z)$ | Seshadri constant of a divisor D at a point $z \in X$ |
| $\mathfrak{s}(\mathcal{L}, z)$ | degree of jet separation of a line bundle \mathcal{L} at a point $z \in X$ |

POPULATION GENETICS

| | |
|----------------------------|--|
| $\mathcal{P}(\mathcal{E})$ | probability of an event \mathcal{E} |
| Var | variance |
| ρ | density function |
| π | partition |
| \mathcal{P}_n | set of all set partitions of $[n]$ |
| \mathcal{R}_k^n | equivalence class of set partitions of $[n]$ after k coalescent events |
| t' | waiting time measured in generations |
| t | waiting time measured in coalescent units |
| T | tree |
| V | set of vertices of a tree |
| E | set of edges of a tree |
| r | root of a rooted tree |
| $\ell(e)$ | length of an edge e |
| L | set of leaves |
| $[[T]]$ | tree topology (of a tree T) |
| $[T]$ | ranked tree topology (of a tree T) |
| g | gene |
| T_g | gene tree |
| C | coalescent event |

| | |
|-----------------------|---|
| \mathfrak{C} | set of all coalescent events |
| DTM_n | space of dissimilarity maps that are tree metrics on n leaves |
| DUM_n | space of dissimilarity maps that are ultrametrics on n leaves |
| MTM_n | space of metrics that are tree metrics on n leaves |
| MUM_n | space of metrics that are ultrametrics on n leaves |
| S | species |
| T_S | species tree |
| τ_S | species divergence time of a species S |
| \mathfrak{S} | set of all species |
| \mathcal{C}_n | set of compatible species and gene trees on n leaves |
| h | (pre-)history |
| H | set of all histories |
| $R_{T_S}([[T_g]], h)$ | history region of a gene tree topology $[[T_g]]$ and history h , given a species tree T_S |

MATROIDS AND TROPICAL GEOMETRY

| | |
|--------------------------------|--|
| M | matroid |
| E | ground set |
| \mathcal{I} | independent sets |
| c | circuit |
| (c_+, c_-) | signed circuit |
| trop | tropicalization |
| $G(2, n)$ | Grassmannian of 2-planes in n -space |
| K_n | complete graph on n vertices |
| $\mathcal{M}_{0,n}$ | moduli space of n distinct labeled points on \mathbb{P}^1 |
| $\overline{\mathcal{M}}_{0,n}$ | moduli space of stable genus zero curves with n distinct marked points |

MIXED SUBDIVISIONS

| | |
|---------------|---------------------|
| A | point configuration |
| ω | weight vector |
| S | subdivision |
| \mathcal{T} | triangulation |

NOTATION

| | |
|----------------------------------|--|
| C | cell |
| $\text{Cayley}(P_1, \dots, P_n)$ | Cayley embedding of the polytopes P_1, \dots, P_n |
| $\Phi_A(\mathcal{T})$ | GKZ-vector of a triangulation \mathcal{T} of a point configuration A |
| $\Sigma\text{-poly}(A)$ | secondary polytope of a point configuration A |
| $\Sigma\text{-fan}(A)$ | secondary fan of a point configuration A |
| γ_n | moment curve |

INTRODUCTION

GEOMETRY IS THE ART
OF REASONING WELL FROM
BADLY DRAWN FIGURES.

— Henri Poincaré

When asked what I am doing all day long, my family has been known to say ‘Drawing parallelograms into trapezoids’, which is not entirely false, compare Figure 2.23. However, this thesis has 69 additional figures and beyond that a lot of reasoning to offer. Here, Poincaré’s quote applies quite accurately. On the one hand, we are studying objects originating from discrete geometry, and on the other hand, we are looking for polyhedral structures in settings that originate from (toric or numerical) algebraic geometry or mathematical population genetics.

Discrete structures such as convex polytopes, polyhedra, and polyhedral fans are relevant for various areas of mathematical research, pure and applied: Combinatorial optimization, combinatorics, commutative algebra, (toric) algebraic geometry, tropical geometry, statistics, and mathematical biology, to name just some of them.

In Chapter 2 we develop combinatorial tools to determine Newton–Okounkov bodies and Newton–Okounkov functions in the case of toric varieties. In analogy to the enriching dictionary of toric geometry, Newton–Okounkov bodies are convex bodies that encode information about the underlying line bundle on a projective variety, such as its positivity in the form of the Seshadri constant. Going back to [LM09; KK12], a lot of structural results have been obtained over the past decade, see among others [BC11a; Wit12; KMS13; Wit14; Bou+15; MR15; Dum+16b; Fuj16; KL18; KMR19]. However, concrete computations have remained very difficult. Motivated by this, we provide a combinatorial version of Zariski decomposition on toric surfaces, see Theorem 2.3.3. As a corollary we derive a piecewise linear isomorphism between the associated Newton–Okounkov body when the flag is centered at a general point, and the toric moment polytope, compare Corollary 2.3.8. This is reminiscent of the recently described ‘geometric wall-crossing maps’ in [EH19]. In 2.4.15, we conjecture that the valuation at a general point also transforms according to our map.

Our main contribution is the development of combinatorial tools to determine Newton–Okounkov functions concretely. This applies to a completely toric setting, where we even obtain a linear function (Proposition 2.4.1). The focus of our studies are functions that stem from valuations at a general point. In the latter case we can determine the

function for polytopes that we call ‘zonotopally well-covered’ (see Definition 2.4.16, and Theorem 2.4.17) and prove that Corollary 2.3.8 holds in these cases. The result of Theorem 2.4.9 holds in particular for anti-blocking polytopes.

One of the main open questions about Seshadri constants is that of their rationality. A positive answer on surfaces would imply the failure of Nagata’s conjecture [Dum+16a]. Existing criteria include Ito’s width bound [Ito14], Lundman’s core criterion [Lun20], and Sano’s anti-canonical pencil [San14]. Applying our methods, we deduce rationality on toric surfaces in the case of what we call ‘weakly zonotopally well-covered’ polytopes, see Definition 2.5.12 and Theorem 2.5.13, and for a class of polytopes for which none of the above criteria apply, compare Theorem 2.5.16.

In Chapter 3 we study spaces of phylogenetic trees and models stemming from mathematical population genetics from a polyhedral point of view. In order to do that we analyse polyhedral structures on the underlying spaces of trees. Billera and Holmes started to investigate the geometry of a space of trees in [BHV01] and its connection to objects from tropical geometry has been examined in [SS04; AK06]. This has led to recent progress regarding the establishment of tropical methods for probability and statistics on the space of phylogenetic trees, see for instance [Lin+17; Nye+17; Mon+20]. We define a coarse and a fine structure on our space of trees that recover the tropical connection and also link the geometry to certain order cones from discrete geometry, compare Propositions 3.3.9 and 3.3.12.

These considerations form the basis for considering two stochastic processes which are fundamental to mathematical population genetics, namely the Kingman coalescent [Kin82a; Kin82b; Kin82c] and the multispecies coalescent process [Tak89; RY03; Liu+09]. We show that the former is given as a density on a space of trees in Proposition 3.4.1. Motivated by the tropical connection we also define a forgetful map and examine how densities are related when increasing the sample size, compare Proposition 3.5.3.

Finally, we examine the multispecies coalescent model from a polyhedral point of view. We first describe compatibility of the involved gene and species trees in combinatorial terms in Proposition 3.6.5. A very relevant question for real world applications is the question of identifiability of the underlying species tree from a given distribution of observed gene trees. This is a highly active area of research, see for instance [DR06; ADR11; DRS12a; DRS12b]. The first step towards an answer is describing the conditional probability distribution. Based on fundamental results in [RY03; DS05; DR09], we provide a density on our space of trees, see Theorem 3.6.14.

Chapter 4 is dedicated to the study of the tropical version of Smale’s famous 17th problem. At the end of the 20th century he asked whether ‘a zero of n complex polynomial equations in n unknowns could be found approximately, on average, in polynomial time with a uniform algorithm’. This question was progressively answered by Beltrán and Pardo [BP08a; BP08b], Bürgisser and Chucker [BC11b] and Lairez [Lai17] over the past decade.

With regard to real world applications, it makes sense to investigate sparse polynomial systems. The link to discrete geometry is given by the BKK-Theorem [Ber79], which relates the number of finite solutions to the mixed volume of the involved Newton polytopes. This link is the foundation for (polyhedral) homotopy methods, see [Stu02, Chapter 3] and [VVC94; HS95] or [Mal17; Mal19; Mal20] for recent developments.

Furthermore, from the perspective of tropical geometry, a fully mixed cell in a regular fine mixed subdivision of the Minkowski sum (or a triangulation of the Cayley, respectively) corresponds to an intersection of the associated tropical hypersurfaces. Solving tropical analogues of polynomial systems is an active area of research, see for instance [Jen16].

Based on the above relation we investigate the tropical version of Smale’s problem: ‘Given n Newton polytopes in \mathbb{R}^n and a random weight vector, can we find one fully mixed cell in the induced subdivision in expected polynomial time?’ In Section 4.2 we fix notation and introduce the objects of interest and their correspondences. Our main contribution to this area is the construction of Example 4.3.2 in Section 4.3, which might lead to a lower exponential bound on the running time of a homotopy continuation approach.

1.1 POLYHEDRAL GEOMETRY: BACKGROUND AND NOTATION

In this section we introduce the reader to the main players of this thesis. To fix notation, we recall the definitions of the main discrete structures that we will work with, following the presentation in [Zie95], [LRS10], and [HNP12]. For more details we refer to these books which give a broad introduction.

1.1.1 Polyhedra and Polytopes

A *half space* is a set of the form

$$H^+ := \{x \in \mathbb{R}^n : \alpha(x) \geq b\},$$

where $\alpha \in (\mathbb{R}^n)^*$ is a linear functional and $b \in \mathbb{R}$ is some constant. An intersection of finitely many half spaces is called a *polyhedron* and is denoted by P . We often refer to the defining inequalities using matrix notation, i.e.,

$$P := \{x \in \mathbb{R}^n : Ax \geq b\},$$

where the rows of the $(d \times n)$ matrix A stand for the linear functionals $\alpha_1, \dots, \alpha_d \in (\mathbb{R}^n)^*$ and $b \in \mathbb{R}^d$ is the vector of the respective constants b_1, \dots, b_d .

The *dimension* of P is defined to be the dimension of its affine hull and is denoted by $\dim(P)$. A linear inequality $\alpha(x) \geq b$ is *valid* for P , if it is satisfied for all $x \in P$. For

INTRODUCTION

a valid inequality $\alpha(x) \geq b$, we call a set of the form

$$F := P \cap \{x \in \mathbb{R}^n : \alpha(x) = b\}$$

a *face* of the polyhedron P , denoted by $F \preceq P$. By $P(i)$ we denote the set of i -dimensional faces. The elements of the set $\text{vert}(P)$ of 0-dimensional faces of an n -dimensional polyhedron are called *vertices*, and the $(n - 1)$ -dimensional faces are called *facets*.

A *polyhedral complex* \mathcal{P} is a finite collection of polyhedra in \mathbb{R}^n such that

1. the empty polyhedron is in \mathcal{P} .
2. if $P \in \mathcal{P}$, then all faces of P are also in \mathcal{P} .
3. the intersection $P \cap Q$ of two polyhedra $P, Q \in \mathcal{P}$ is a face of both, P and Q .

A *polytope* P is the convex hull of a finite number of points in \mathbb{R}^n , i.e.,

$$P = \text{conv}(x_1, \dots, x_d) := \left\{ \sum_{i=1}^d \lambda_i x_i : \sum_{i=1}^d \lambda_i = 1 \text{ and } \lambda_i \geq 0 \text{ for } 1 \leq i \leq d \right\}.$$

Due to Weyl–Minkowski-Duality a bounded set $P \subseteq \mathbb{R}^n$ is a polytope if and only if it is the bounded intersection of a finite number of affine half spaces, compare [HNP12, Theorem 1.2.3]. A polytope P is called a *lattice polytope*, if all its vertices lie in a common lattice Λ .

For a full-dimensional polytope $P \subseteq \mathbb{R}^n$ with $0 \in P$ its *dual polytope* or the *polar dual* of P is defined as

$$P^\vee := \{\alpha \in (\mathbb{R}^n)^* : \alpha(x) \geq -1 \text{ for all } x \in P\}.$$

Given a Laurent polynomial $f \in \mathbb{C}[x_1^{\pm 1}, \dots, x_n^{\pm 1}]$, one can associate a polytope to it. The *support* $\text{supp}(f)$ of f is the set of all monomials that appear with non-zero coefficient. Each monomial is regarded as an exponent vector in \mathbb{Z}^n . Then the *Newton polytope* of f , denoted by $\text{NP}(f)$, is the convex hull of the exponent vectors of the monomials in the support of f .

Let $P \subseteq \mathbb{R}^n$ be an n -dimensional polytope and $F \preceq P$ a face that is defined by $\alpha(x) \geq b$ for some $\alpha \in (\mathbb{R}^n)^*$ and some $b \in \mathbb{R}$. Then the *wedge of P over F* is the polytope defined as

$$\text{wedge}_F(P) := \{(x, x_{n+1}) \in \mathbb{R}^{n+1} : x \in P, 0 \geq \alpha(x) - x_{n+1} \geq b\}.$$

The *Minkowski sum* of two sets $P, Q \subseteq \mathbb{R}^n$ is defined to be

$$P + Q := \{x + x' : x \in P, x' \in Q\}.$$

There are different ways to ‘measure’ polytopes. Let $P \subseteq \mathbb{R}^n$ be a polytope. The *width* of P with respect to a linear functional $\alpha \in (\mathbb{R}^n)^*$ is defined as

$$\text{width}_\alpha(P) := \max_{p,q \in P} |\alpha(p) - \alpha(q)|.$$

For a rational line segment $L \subset \mathbb{R}^n$ with respect to a lattice Λ there is the notion of *lattice length*, denoted by $\text{length}_\Lambda(L)$. Let for that L be the segment connecting two rational points $p, q \in \mathbb{Q}^n$ and denote by $u \in \Lambda$ the shortest lattice vector on the ray spanned by $p - q$. Then we define $\text{length}_\Lambda(L) := |j|$, where $j \in \mathbb{Q}$ such that $p - q = ju$.

Given n polytopes P_1, \dots, P_n in \mathbb{R}^n , their *mixed volume* $\text{MV}(P_1, \dots, P_n)$ equals the following sum of ordinary volumes

$$\sum_{I \subseteq \{1, \dots, n\}} (-1)^{|I|} \text{vol}\left(\sum_{i \in I} P_i\right).$$

1.1.2 Cones and Fans

A subset $\sigma \subseteq \mathbb{R}^n$ is a *cone* if for all $x, y \in \sigma$ and $\lambda, \mu \in \mathbb{R}_{\geq 0}$ also $\lambda x + \mu y \in \sigma$. A cone is *polyhedral* if there are linear functionals $\alpha_1, \dots, \alpha_m \in (\mathbb{R}^n)^*$ such that

$$\sigma = \{x \in \mathbb{R}^n : \alpha_i(x) \geq 0 \text{ for } 1 \leq i \leq m\}.$$

A cone is called *finitely generated* by vectors $x_1, \dots, x_d \in \mathbb{R}^n$ if

$$\sigma = \text{cone}(x_1, \dots, x_d) := \left\{ \sum_{i=1}^d \lambda_i x_i : \lambda_i \geq 0 \text{ for } 1 \leq i \leq d \right\}.$$

By the Weyl-Minkowski-Duality for cones, a cone is polyhedral if and only if it is finitely generated, see [HNP12, Theorem 1.1.3]. We call a polyhedral cone *pointed* if its *lineality space* $\text{lineal}(\sigma) := \{y \in \mathbb{R}^n : x + \lambda y \in \sigma \text{ for all } x \in \sigma, \lambda \in \mathbb{R}\}$ equals $\{0\}$. The afore mentioned notion of dimension and faces translates to the cone setting. An $(n - 1)$ -dimensional face of an n -dimensional cone is called *facet*, and a 1-dimensional face $\rho \preceq \sigma$ is called *ray*. If a ray $\rho \preceq \sigma$ is spanned by a rational vector, then there exists a shortest integer vector $u_\rho \in \rho$, which we call the *primitive ray generator* of ρ . If the primitive ray generators of an n -dimensional cone form a lattice basis of the underlying lattice Λ , then the cone is called *unimodular*. If the primitive ray generators form part of a lattice basis, then the corresponding cone is called *smooth*.

Given a polyhedral cone $\sigma \subseteq \mathbb{R}^n$, its *dual cone* is defined by

$$\sigma^\vee := \{\alpha \in (\mathbb{R}^n)^* : \alpha(x) \geq 0 \text{ for all } x \in \sigma\}.$$

INTRODUCTION

A *fan* Σ in \mathbb{R}^n is a collection of non-empty polyhedral cones with the following two properties:

1. Every non-empty face of a cone in Σ is also a cone in Σ .
2. The intersection of any two cones in Σ is a face of both.

If all cones of a fan are unimodular, then the fan itself is called *unimodular* and similarly, a fan is called *smooth* if all of its cones are smooth. A fan Σ in \mathbb{R}^n is called *complete* if for its *support* $|\Sigma| := \cup_{\sigma \in \Sigma} \sigma$, we have that $|\Sigma| = \mathbb{R}^n$.

We can associate a certain fan to a given polyhedron (or a polytope). Let P be a polyhedron in \mathbb{R}^n . For a point $x \in P$ we define the *inner normal cone* of x in P in \mathbb{R}^n as

$$N_P(x) := \{\alpha \in (\mathbb{R}^n)^* : \alpha(x) \leq \alpha(y) \text{ for all } y \in P\},$$

i.e., $N_P(x)$ consists of all linear functionals whose minimum on P is achieved at x . Similarly, for a face $F \preceq P$, we say $N_F(x)$ equals the cone $N_P(x)$ for any x in the relative interior of F . The set

$$\mathcal{N}_P := \{N_F(x) : F \preceq P\} = \{N_P(x) : x \in P\}$$

is called the *inner normal fan* of P .

TORIC NEWTON–OKOUNKOV FUNCTIONS

This chapter is joint work with Christian Haase and Alex Küronya and is based on [HKW20].

2.1 INTRODUCTION

In the present chapter, we start to develop methods to determine Newton–Okounkov functions in the case of toric varieties. As a by-product, we can show rationality of Seshadri constants for many new examples of toric surfaces.

Newton–Okounkov bodies are convex bodies which encode various facets of algebraic and symplectic geometry, such as the local positivity of line bundles on varieties and going as far as geometric quantization [HHK16]. To be more specific, it is possible to gain information on asymptotic invariants (Seshadri constants, pseudo-effective thresholds, Diophantine approximation constants) from well-chosen Newton–Okounkov bodies and concave (Newton–Okounkov) functions on them.

Over the past decade, Newton–Okounkov theory has attracted a lot of attention. Many deep structural results have been proven, extracting information about varieties and their line bundles from Newton–Okounkov bodies. At the same time it also became apparent that it is often very difficult to obtain precise information about Newton–Okounkov bodies and Newton–Okounkov functions in concrete cases.

Newton–Okounkov Functions

Newton–Okounkov functions are concave functions on Newton–Okounkov bodies arising from multiplicative filtrations on the section ring of a line bundle. They have proven to be even more evasive than Newton–Okounkov bodies themselves.

The first definition of Newton–Okounkov functions (in other terminology, concave transforms of multiplicative filtrations) in print is due to Boucksom–Chen [BC11a]. These functions on the Newton–Okounkov body yield refined information [Bou+15; Dum+16b; Fuj16; KMS13; KMR19; MR15] about the arithmetic and the geometry of the underlying variety.

Already the most basic invariants of Newton–Okounkov functions contain highly non-trivial information. Perhaps the most notable example is the average of such a function — called the β -invariant of the line bundle and the filtration —, which is closely related to Diophantine approximation [MR15], and K-stability [Fuj16]. By the connection of the β -invariant to Seshadri constants [KMR19], its rationality could decide Nagata’s conjecture [Dum+16a]. Not surprisingly, concrete descriptions of these functions are very hard to obtain.

A structure theorem of [KMR19] identifies the subgraph of a Newton–Okounkov function coming from a geometric situation as the Newton–Okounkov body of a projective bundle over the variety in question. (Compare Section 2.4.2 below.)

Based on earlier work of Donaldson [Don02], Witt–Nyström [Wit12] made the observation that the Newton–Okounkov function coming from a fully toric situation (meaning all of the line bundle, admissible flag, and filtration are torus-invariant) is piecewise affine linear with rational coefficients on the underlying Newton–Okounkov body, which happens to coincide with the appropriate moment polytope. In this very special situation, the function is in fact linear. (Compare Proposition 2.4.1 below.)

The next interesting case arises when we keep the toric polytope (that is, we work with a torus-invariant line bundle and a torus-invariant admissible flag), but we consider the order of vanishing at a general point to define the function. To our knowledge, no such function has been computed for toric varieties other than projective space.

While the usual dictionary between geometry and combinatorics is very effective in explaining torus-invariant geometry, when it comes to non-torus-invariant phenomena, one does need the more general framework of Newton–Okounkov theory. Broadly speaking Newton–Okounkov theory would be toric geometry without a torus action; in more technical terms Newton–Okounkov theory replaces the natural gradings on cohomology spaces by filtrations.

In determining Newton–Okounkov functions in a not completely toric setting, our first goal is to devise a strategy to determine Newton–Okounkov functions associated to orders of vanishing on toric surfaces, and to apply it to interesting examples. The trick is to avoid blowing up the valuation point, which could result in losing control of the Mori cone.

Instead, we change the flag defining the Newton–Okounkov polytope to one which contains the valuation point and show that there is a piecewise linear transformation of the moment polytope into the new Newton–Okounkov polytope (see Corollary 2.3.8). This is reminiscent of the transformation constructed in [EH19]. But the connection is, as of yet, unclear. It is worth mentioning at this point that certain pairs of subgraphs of Newton–Okounkov functions associated to torus-invariant and non-torus-invariant

flags happen to be equidecomposable (compare Remark 2.4.14). This is an exciting and unexpected phenomenon with possible ties to the mutations studied in [Cil+17]. We offer a conjectural explanation for this phenomenon.

We can then employ arguments from convex geometry to provide upper and lower bounds for the desired function. We study combinatorial conditions which guarantee that the obtained upper and lower bounds agree.

In the case of anti-blocking polyhedra in the sense of Fulkerson [Ful71; Ful72] we obtain a particularly easy answer. Nevertheless, the strategy works much more generally.

THEOREM (Newton–Okounkov functions on toric surfaces, Theorem 2.4.9, Corollary 2.4.11). Let X be a smooth projective toric surface, D an ample divisor, and Y_\bullet an admissible torus-invariant flag on X so that the Newton–Okounkov body $\Delta_{Y_\bullet}(D)$ is anti-blocking.

Let Y'_\bullet be a torus-invariant flag opposite to the origin. Then the Newton–Okounkov function φ_R on $\Delta_{Y'_\bullet}(D)$ coming from the geometric valuation ord_R in a general point $R \in X$ is linear with integral slope.

Along the way, we formulate and prove existence and uniqueness of Zariski decomposition on toric surfaces in the language of polyhedra. One can ‘see’ the decomposition in terms of the polygons, compare Theorem 2.3.3.

Local Positivity

Newton–Okounkov theory reveals a lot about positivity properties of line bundles. Just like in the toric case, one can use convex geometric information to decide, for instance, if the underlying line bundle is ample or nef [KL17a; KL17b]. One can even obtain localized information. A line bundle is called positive or ample at a point of our variety if global sections of a high enough multiple yield an embedding of an open neighborhood of the point. Local positivity can be decided and measured via Newton–Okounkov bodies [KL17a; KL17b; Roé16].

Local positivity is traditionally measured by Seshadri constants [KL18; Lazo04]. Originally invented by Demailly [Dem92] to attack Fujita’s conjecture on global generation, Seshadri constants have become the main numerical asymptotic positivity invariant (compare [Lazo04, Chapter 5], [Bau99]). While there has been considerable interest in this invariant’s behavior, many of its properties are still shrouded in mystery [Sze12].

One interesting question about Seshadri constants is if they are always rational numbers. This is widely believed to be false, but there has only been sporadic progress towards this issue. On surfaces, the rationality of Seshadri constants would imply the failure of Nagata’s conjecture [Dum+16a].

The rationality of Seshadri constants and related asymptotic invariants often follows from finite generation of an appropriate multi-graded ring or semigroup [Ein+06; CL12]. However, finite generation questions tend to be wide open, and are typically skew to the major finite generation theorems of birational geometry.

In the literature around Newton–Okounkov bodies the involved valuation semigroups are frequently assumed, from the outset, to be finitely generated (see [HK15; KM19], this is to obtain a toric degeneration as in [And13]). However, deciding finite generation of multigraded algebras or semigroups arising from a geometric setting is an utterly hard question.

We obtain results on the rationality of Seshadri constants in general points of toric surfaces using asymptotic considerations and convexity to circumvent some of these difficulties.

Previously, Ito [Ito13; Ito14], Lundman [Lun20], and Sano [San14] have verified rationality of these same Seshadri constants for restricted classes of (line bundles on) toric surfaces. As it turns out, a condition we call ‘weakly zonotopally well-covered’, is sufficient to guarantee rationality of the Seshadri constant.

THEOREM (Rationality of certain Seshadri constants, Theorem 2.5.13). Let X be a smooth projective toric surface and D an ample torus-invariant divisor on X with associated Newton–Okounkov body $\Delta_{Y_\bullet}(D)$ for an admissible torus-invariant flag Y_\bullet . If the polytope $\Delta_{Y_\bullet}(D)$ is weakly zonotopally well-covered, then

1. we can determine $\int_{\Delta_{Y_\bullet}(D)} \varphi_R$.
2. the Seshadri constant $\varepsilon(X, D; R)$ is rational.
3. the maximum $\max_{\Delta_{Y_\bullet}(D)} \varphi_R$ is attained at the boundary of $\Delta_{Y_\bullet}(D)$.

This theorem reproves some of the cases covered in [Ito13; Ito14; Lun20; San14] and adds many new cases, even some, where we can only conjecture what the Newton–Okounkov function looks like. We construct specific examples where the methods of Ito, Sano, or Lundman do not apply, see Theorem 2.5.16.

Organization of the Chapter

This chapter is structured as follows. We start in Section 2.2 by fixing notation and giving necessary background information. Since our work sits on the fence between two areas, we give ample information on both. Section 2.3 is devoted to a self-contained combinatorial proof of Zariski decomposition on toric surfaces and the existence of the ‘tilting isomorphism’ between certain Newton–Okounkov bodies. In Section 2.4 we give a description of Newton–Okounkov functions/concave transforms in the two relevant

cases: when every actor is torus-invariant (Subsection 2.4.1) and when we are looking at the order of vanishing filtration coming from a general point (Subsection 2.4.3). The latter part contains the outline of our general strategy. Moreover, we give a polyhedral description of the interpretation of a subgraph as a Newton–Okounkov body (Subsection 2.4.2). Section 2.5 contains the application of our results on Newton–Okounkov functions to the rationality of Seshadri constants. Finally, we formulate further research questions in Section 2.6.

2.2 BACKGROUND AND NOTATION

This section provides the necessary background and also fixes notation. At first we will recall basic properties of divisors and state associated criteria in Subsection 2.2.1. Since we will mostly consider toric varieties, we recall relevant facts in Subsection 2.2.2. Hereby we focus on the behaviour of divisors and their positivity in the toric case. In Subsection 2.2.3 we introduce the main player of our study, namely Newton–Okounkov bodies. We will review some properties, in particular in the surface case. We will finally define Newton–Okounkov functions in Subsection 2.2.4 and list some of their properties.

We work over an algebraically closed field K . Although no arguments depend on characteristic zero, for convenience we will assume $K = \mathbb{C}$.

2.2.1 Positivity

In this section we will recall basic facts about positivity of divisors and associated criteria and fix notation. For more details and proofs see for example [Lazo04, Chapters 1 and 2], [Har77, Chapter II.6] or [Smi+04].

Let X be a projective variety of dimension n with function field $\mathbb{C}(X)$. A divisor D on X will always be assumed to be a Cartier divisor if not mentioned otherwise and the group of Cartier divisors is denoted by $\text{CDiv}(X)$. To a Cartier divisor D one can associate the sheaf $\mathcal{L} = \mathcal{O}_X(D)$ which is the sheaf of sections of a line bundle $V_{\mathcal{L}} \rightarrow X$, which we will denote by \mathcal{L} for short. Let $h^0(X, \mathcal{O}_X(D))$ for that denote the dimension of $H^0(X, \mathcal{O}_X(D))$ which is the vector space of global sections.

We will often consider divisors with rational or real coefficients, meaning elements of

$$\text{CDiv}(X)_{\mathbb{Q}} := \text{CDiv}(X) \otimes_{\mathbb{Z}} \mathbb{Q}, \text{ and } \text{CDiv}(X)_{\mathbb{R}} := \text{CDiv}(X) \otimes_{\mathbb{Z}} \mathbb{R}.$$

The properties of divisors with \mathbb{Z} -coefficients, that we are interested in, extend in a natural way. Two divisors D and D' are called *linearly equivalent*, denoted by $D \sim D'$, if their difference is a principal divisor and *numerically equivalent*, written $D \equiv D'$, if $D \cdot C = D' \cdot C$ for all irreducible curves $C \subseteq X$. Note, that linear equivalence implies numerical equivalence. The group of numerical equivalence classes of integral Cartier divisors is called the *Néron–Severi group* and is denoted by $N^1(X) := \text{CDiv}(X) / \equiv$. The associated real vector space $N^1(X)_{\mathbb{R}} := (\text{CDiv}(X) / \equiv) \otimes_{\mathbb{Z}} \mathbb{R}$ is called the *Néron–Severi*

space. Inside this space there exist some interesting subsets of divisors with certain properties which we will define in the following.

Let \mathcal{L} be a line bundle on X . Then the set of global sections $H^0(X, \mathcal{L})$ is a finite dimensional K -vector space. Let $\{s_0, \dots, s_d\}$ be a basis of the complete linear system $|\mathcal{L}|$. This determines a rational map

$$\begin{aligned} X &\rightarrow \mathbb{P}^d \\ x &\mapsto [s_0(x) : \dots : s_d(x)]. \end{aligned} \tag{2.2.1}$$

Definition 2.2.1. Let X be a projective variety. A line bundle \mathcal{L} on X is called

1. *very ample* if the map defined in (2.2.1) is an everywhere defined morphism that defines an isomorphism onto its image, and
2. *ample* if $\mathcal{L}^{\otimes k}$ is very ample for some multiple $k > 0$.

A Cartier divisor D on X is called (very) ample if the associated line bundle $\mathcal{O}_X(D)$ is (very) ample.

The definition suggests to consider global sections of all multiples of a line bundle at the same time. The construction of Newton–Okounkov bodies will take this idea into account. There are several criteria to decide whether a given divisor is (very) ample.

THEOREM 2.2.2 ([Laz04, Nakai–Moishezon–Kleinman criterion, Theorem 1.2.23]). Let D be a Cartier divisor on a projective variety X . Then D is ample if and only if

$$D^{\dim(Z)} \cdot Z > 0$$

for every positive-dimensional irreducible subvariety $Z \subseteq X$.

In particular, this means that ampleness is a numerical property, saying that if D and D' are numerically equivalent Cartier divisors on X , then D is ample if and only if D' is [Laz04, Corollary 1.2.24].

In the case of surfaces this criterion becomes easier to check.

THEOREM 2.2.3 ([Har77, Chapter V, Theorem 1.10]). Let D be a divisor on a surface X . Then D is ample if and only if

$$D \cdot D > 0 \text{ and } D \cdot C > 0$$

for all irreducible curves C in X .

Another important definition is the following.

Definition 2.2.4. Let X be a complete variety. A Cartier divisor D on X is called *numerically effective* or *nef*, if for all irreducible curves $C \subseteq X$ we have

$$D.C \geq 0.$$

Note, that being nef is again a numerical property. By definition, any ample class is nef and the sum of two nef classes is again nef. The construction of Newton–Okounkov bodies requires that the given divisor has ‘many global sections’. This is made precise in the next definition.

Definition 2.2.5. Let X be an irreducible projective variety of dimension n , and let \mathcal{L} be a line bundle on X . The *volume* of \mathcal{L} is defined to be the non-negative real number

$$\mathrm{vol}(\mathcal{L}) = \mathrm{vol}_X(\mathcal{L}) := \limsup_{k \rightarrow \infty} \frac{h^0(X, \mathcal{L}^{\otimes k})}{k^n/n!}. \quad (2.2.2)$$

The volume $\mathrm{vol}(D)$ of a Cartier divisor is defined by passing to $\mathcal{O}_X(D)$. A divisor is called *big* if $\mathrm{vol}(D) > 0$.

It turns out that bigness also only depends on the numerical equivalence class [Lazo4, Corollary 2.2.8]. For nef divisors it has a particularly nice characterization. If D is nef, then $\mathrm{vol}(D)$ is its top-self-intersection [Lazo4, Equation (2.9)].

THEOREM 2.2.6 ([Lazo4, Theorem 2.2.16]). Let D be a nef divisor on an irreducible projective variety X of dimension n . Then D is big if and only if for its top self-intersection we have $(D^n) > 0$.

The criteria that involve the intersection product justify to consider the respective properties inside Néron–Severi space. This is captured by the following definition.

Definition 2.2.7. Let X be a complete variety. The *ample cone*

$$\mathrm{Amp}(X) \subseteq N^1(X)_{\mathbb{R}}$$

of X is the convex cone of all ample \mathbb{R} -divisor classes on X . The *nef cone*

$$\mathrm{Nef}(X) \subseteq N^1(X)_{\mathbb{R}}$$

of X is the convex cone of all nef \mathbb{R} -divisor classes. The *big cone*

$$\mathrm{Big}(X) \subseteq N^1(X)_{\mathbb{R}}$$

of X is the convex cone of all big \mathbb{R} -divisor classes on X . The *pseudo-effective cone*

$$\overline{\mathrm{Eff}}(X) \subseteq N^1(X)_{\mathbb{R}}$$

is the closure of the convex cone spanned by the classes of all effective \mathbb{R} -divisors. A divisor is called *pseudo-effective* if its class lies in the pseudo-effective cone.

2.2.2 Toric Varieties

Since we will mostly consider the case of toric varieties, we review some basic results and fix notation regarding toric varieties and divisors, in particular on the interplay between algebraic geometry and combinatorics. We will mainly follow the conventions used in [CLS11] which gives a broad introduction to toric varieties.

A *toric variety* is an irreducible variety X containing a torus $\mathbb{T} \cong (\mathbb{C}^*)^n$ as a Zariski open subset such that the action of \mathbb{T} on itself extends to an algebraic action of \mathbb{T} on X , that is a morphism $\mathbb{T} \times X \rightarrow X$. We want X to be an n -dimensional smooth projective toric variety. Then $X = X_\Sigma$ is determined by a complete unimodular fan Σ in $N_{\mathbb{R}} = N \otimes_{\mathbb{Z}} \mathbb{R} \cong \mathbb{R}^n$, where $N \cong \mathbb{Z}^n$ denotes the underlying lattice of one-parameter subgroups. Its dual, the lattice of characters χ , is denoted by $M = \text{Hom}_{\mathbb{Z}}(N, \mathbb{Z})$ and the associated vector space by $M_{\mathbb{R}} = M \otimes_{\mathbb{Z}} \mathbb{R}$.

Let $\Sigma(i)$ denote the set of i -dimensional cones of Σ . Each ray $\rho \in \Sigma(1)$ is determined by a primitive ray generator $u_\rho \in N$. Since Σ is unimodular, the primitive ray generators of each maximal cone $\sigma \in \Sigma$ form a basis of N . The affine toric patches will be denoted by U_σ for $\sigma \in \Sigma$. There is a bijective correspondence between cones $\sigma \in \Sigma$ and \mathbb{T} -orbits in X . For a cone $\sigma \in \Sigma$ we denote its corresponding orbit closure by $V(\sigma)$.

For a strongly convex rational polyhedral cone τ in $N_{\mathbb{R}}$, let N_τ be the sublattice of N spanned by points in $N \cap \tau$, then we denote the quotient lattice by $N(\tau) = N/N_\tau$. Let Σ be a fan in $N_{\mathbb{R}}$ and $\tau \in \Sigma$. We consider the quotient map $N_{\mathbb{R}} \rightarrow N(\tau)_{\mathbb{R}}$ and denote by $\bar{\sigma}$ the image of a cone $\sigma \in \Sigma$ containing τ . Then

$$\text{star}(\tau) := \{\bar{\sigma} \subseteq N(\tau)_{\mathbb{R}} : \tau \preceq \sigma \in \Sigma\}$$

is a fan in $N(\tau)_{\mathbb{R}}$.

There is again a toric variety associated to this fan. Let $P \subseteq M_{\mathbb{R}}$ be a full-dimensional lattice polytope with normal fan Σ_P and associated toric variety X_P . Then each face $F \preceq P$ corresponds to a cone $\sigma_F \in \Sigma_P$. According to Propositions 3.2.7 and 3.2.9 in [CLS11] we obtain the isomorphisms

$$X_{\text{star}(\sigma_F)} \cong V(\sigma_F) \cong X_F$$

between the resulting varieties, where X_F is the variety that is associated to the lattice polytope F .

2.2.2.1 Divisors on Toric Varieties

Since X is smooth, a divisor D is a Weil divisor if and only if it is a Cartier divisor, i.e., $\text{Pic}(X) = \text{Cl}(X)$. Due to the orbit-cone-correspondence, a ray $\rho \in \Sigma(1)$ gives a codimension 1 orbit whose closure $V(\rho)$ is a torus-invariant prime divisor on X

which we denote by D_ρ . Let $K_X = -\sum_{\rho \in \Sigma(1)} D_\rho$ denote the canonical divisor on X . A torus-invariant divisor $D = \sum_{\rho \in \Sigma(1)} a_\rho D_\rho$ on X determines a polyhedron

$$P_D := \{m \in M_{\mathbb{R}} : \langle m, u_\rho \rangle \geq -a_\rho \text{ for all } \rho \in \Sigma(1)\}, \quad (2.2.3)$$

which is actually a polytope, since Σ is complete.

Furthermore, we can describe a Cartier divisor $D = \sum_{\rho \in \Sigma(1)} a_\rho D_\rho$ in terms of its support function $\text{SF}_D: |\Sigma| \rightarrow \mathbb{R}$, which is linear on each $\sigma \in \Sigma$ and satisfies $\text{SF}_D(u_\rho) = -a_\rho$ for all $\rho \in \Sigma(1)$. Additionally, a Cartier divisor is determined by its Cartier data $\{m_\sigma\}_{\sigma \in \Sigma}$, where the $m_\sigma \in M$ satisfy $D|_{U_\sigma} = \text{div}(\chi^{-m_\sigma})|_{U_\sigma}$ for all $\sigma \in \Sigma$. The vector space of global sections arises from the characters for the lattice points inside the polytope, namely

$$H^0(X, \mathcal{O}_X(D)) = \bigoplus_{m \in P_D \cap M} \mathbb{C} \cdot \chi^m. \quad (2.2.4)$$

2.2.2.2 Intersection Product and Positivity on Toric Varieties

Intersection products on toric varieties are given in combinatorial terms if the curve is torus-invariant, according to Proposition 6.3.8 in [CLS11]. More precisely, let $C = V(\tau)$ be the complete torus-invariant curve in X_Σ , coming from the wall $\tau = \sigma \cap \sigma' \in \Sigma(n-1)$ with $\sigma, \sigma' \in \Sigma(n)$. Let D be a Cartier divisor with Cartier data $m_\sigma, m_{\sigma'} \in M$ corresponding to σ, σ' . Also pick $u \in \sigma' \cap N$ that maps to the minimal generator of $\bar{\sigma}' \subseteq N(\tau)_{\mathbb{R}}$. Then

$$D.C = \langle m_\sigma - m_{\sigma'}, u \rangle \in \mathbb{Z}. \quad (2.2.5)$$

For a smooth complete toric surface X_Σ the intersection number $D.C$ is defined for all divisors D, C . Let D_ρ be the divisor corresponding to the ray $\rho = \text{cone}(u_\rho)$ which is the intersection of two 2-dimensional cones $\text{cone}(u_\rho, u_1)$ and $\text{cone}(u_\rho, u_2)$ in Σ . Then due to Theorem 10.4.4 in [CLS11] we have

1. $D_\rho.D_\rho = -\lambda$, where $u_1 + u_2 = \lambda u_\rho$.
2. For a divisor $D_{\rho'} \neq D_\rho$, we have

$$D_{\rho'}.D_\rho = \begin{cases} 1 & \text{if } \rho' = \text{cone}(u_i) \text{ with } i \in \{1, 2\} \\ 0 & \text{otherwise.} \end{cases} \quad (2.2.6)$$

A lot of properties of the divisor D can be read off the polytope P_D in the following sense. Let $D = \sum_{\rho \in \Sigma(1)} a_\rho D_\rho$ be a Cartier divisor on a complete toric variety X of dimension n . Then D is big if and only if the polytope P_D is full-dimensional, i.e., $\dim(P_D) = n$.

THEOREM 2.2.8 ([CLS11, Proposition 6.1.10, Theorem 6.1.15, and Theorem 6.3.13]). Let X_Σ be a complete toric variety associated to the fan Σ and let D be a Cartier divisor on X . Then the following holds.

1. Let Σ be smooth. Then D is ample if and only if it is very ample.
2. (Toric Kleinman criterion) D is ample if and only if $D.C > 0$ for all torus-invariant irreducible curves $C \subseteq X_\Sigma$.
3. D is ample if and only if the normal fan Σ_{P_D} coincides with the fan Σ .

Let D be an ample divisor on X with corresponding polytope P_D . Then for each vertex $p \in \text{vert}(P_D)$ the primitive vectors m_1^p, \dots, m_n^p in its adjacent edge directions are a lattice basis for the lattice M and therefore specify an associated coordinate system of the space $M_{\mathbb{R}}$.

There is again a criterion in terms of the corresponding polytope to decide, whether a given divisor is nef.

THEOREM 2.2.9 ([CLS11, Theorem 6.3.12]). Let D be a Cartier divisor on a toric variety X_Σ whose fan Σ has convex support of full dimension. Then we have the following.

1. D is nef if and only if $D.C \geq 0$ for all torus-invariant irreducible complete curves $C \subseteq X$.
2. Let $D = \sum_{\rho \in \Sigma(1)} a_\rho D_\rho$ and P_D the corresponding polytope. Then D is nef if and only if the fan Σ refines the normal fan Σ_{P_D} of the polytope P_D and if all inequalities are tight, i.e., for all $\rho \in \Sigma(1)$ there exists a point $m \in P_D$ such that $\langle m, u_\rho \rangle = -a_\rho$.

Note that the characterization of tight inequalities for nefness is sufficient for surfaces but does not apply in higher dimensions in general.

2.2.3 Newton–Okounkov Bodies

The rich theory of toric varieties provides a very useful dictionary between algebraic geometry and convex geometry. It turns out that there is a one-to-one correspondence between the following sets, see Theorem 6.2.1 in [CLS11].

$$\begin{aligned} & \{P \subseteq M_{\mathbb{R}} : P \text{ is a full-dimensional lattice polytope}\} \\ & \quad \updownarrow \\ & \{(X_\Sigma, D) : \Sigma \text{ is a complete fan in } N_{\mathbb{R}}, D \text{ a torus-invariant ample divisor on } X_\Sigma\} \end{aligned}$$

This allows us to translate questions about algebro-geometric properties of the pair (X_Σ, D) into questions about P_D on the polytopal side and the other way round. In the

90's in [Ok09], Okounkov laid the groundwork to generalize this idea to arbitrary projective varieties motivated by questions coming from representation theory. Based on that, Lazarsfeld–Mustață [LM09] and Kaveh–Khovanskii [KK12] independently developed a systematic theory of Newton–Okounkov bodies about ten years later. It lets us assign a convex body to a given pair (X, D) that captures much of the asymptotic information about its geometry.

We review the construction of Newton–Okounkov bodies and will hereby mostly follow the approach and notation in [LM09].

Let X be an irreducible projective variety of dimension n . We fix an admissible flag

$$Y_\bullet: X = Y_0 \supseteq Y_1 \supseteq \cdots \supseteq Y_n$$

of irreducible subvarieties, where *admissible* requires that $\text{codim}_X(Y_i) = i$ for all $0 \leq i \leq n$, and that Y_i is smooth at the point Y_n for all $0 \leq i \leq n$.

Additionally, let D be a big Cartier divisor on X and $\mathcal{L} = \mathcal{O}_X(D)$ the associated big line bundle.

We define a valuation-like map

$$\begin{aligned} \text{val} = \text{val}_{Y_\bullet}: H^0(X, \mathcal{O}_X(kD)) \setminus \{0\} &\rightarrow \mathbb{Z}^n \\ s &\mapsto (\text{val}_1(s), \dots, \text{val}_n(s)) \end{aligned}$$

for any $k \in \mathbb{Z}_{\geq 1}$ in the following way. Given a global section $s \in H^0(X, \mathcal{O}_X(kD)) \setminus \{0\}$ set

$$\text{val}_1 = \text{val}_1(s) := \text{ord}_{Y_1}(s).$$

More explicitly, since $Y_0 = X$ is smooth at Y_n , there exists an open neighborhood B_0 of Y_n in which Y_1 is a Cartier divisor. Let f_1 denote its locally defining regular function and let g_1 be the regular function that locally defines s . Then $\text{ord}_{Y_1}(s)$ is the maximal integer j such that f_1^j divides g_1 . This determines a section

$$\tilde{s}_1 \in H^0(X, \mathcal{O}_X(kD - \text{val}_1 Y_1))$$

which does not vanish identically along Y_1 . Therefore its restriction yields a non-zero section

$$s_1 \in H^0(Y_1, \mathcal{O}_{Y_1}(kD - \text{val}_1 Y_1)) \tag{2.2.7}$$

that is locally given as $\frac{g_1}{f_1^{\text{val}_1}}|_{Y_1}$ in terms of regular functions. Next, choose a suitable open set B_1 on Y_1 and define

$$\text{val}_2(s) := \text{ord}_{Y_2}(s_1)$$

in the same manner. Proceed iteratively to determine val by the successive orders of vanishing along the subvarieties Y_i , i.e.,

$$\text{val}_i(s) := \text{ord}_{Y_i}(s_{i-1}).$$

Having this map, we want to associate a convex body to the given data.

Definition 2.2.10. The *Newton–Okounkov body* $\Delta_{Y_\bullet}(D)$ of D (with respect to the flag Y_\bullet) is defined to be the set

$$\Delta_{Y_\bullet}(D) := \overline{\bigcup_{k \geq 1} \frac{1}{k} \{\text{val}_{Y_\bullet}(s) : s \in H^0(X, \mathcal{O}_X(kD)) \setminus \{0\}\} \subseteq \mathbb{R}^n}.$$

An equivalent way of defining the Newton–Okounkov body is in terms of semigroups. Given the above data, we can associate the following semigroup to it

$$\Gamma_{Y_\bullet}(D) := \{(\text{val}_{Y_\bullet}(s), k) : s \in H^0(X, \mathcal{O}_X(kD)) \setminus \{0\}, k \in \mathbb{Z}_{\geq 1}\} \subseteq \mathbb{Z}_{\geq 1}^{n+1}.$$

Then the Newton–Okounkov body of D with respect to the flag Y_\bullet is given by the level-1-slice of the following cone

$$\Delta_{Y_\bullet}(D) := \overline{\text{cone}(\Gamma_{Y_\bullet}(D))} \cap (\mathbb{R}^n \times \{1\}).$$

Example 2.2.11. We consider the Hirzebruch surface $X = \mathcal{H}_1$ associated to the fan in Figure 2.1, where the torus-invariant prime divisor D_i corresponds to the ray $\rho_i \in \Sigma(1)$ for $1 \leq i \leq 4$.

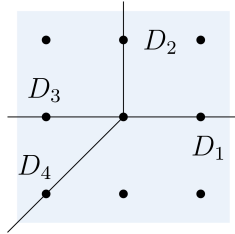


Figure 2.1: The fan Σ of the first Hirzebruch surface $X_\Sigma = \mathcal{H}_1$.

As an admissible flag Y_\bullet choose the curve $Y_1 = D_1$ and $Y_2 = D_1 \cap D_2$ as a smooth point on it. Then we have a local system of coordinates x, y such that $Y_1 = \{x = 0\}$ and $Y_2 = (0, 0)$. The ample divisor $D = D_3 + 2D_4$ determines a polytope P_D and, due to (2.2.4), the global sections of $H^0(X, \mathcal{O}_X(D))$ involve the monomials $1, x, y, xy$, and y^2 , given in local coordinates as depicted in Figure 2.2. The global section $s(x, y) = 2x + 8xy$ for instance gets mapped to $(1, 0)$ by the map val_{Y_\bullet} , because its divisible by x , but $s_1(x, y) = 2 + 8y$ is not divisible by y . Altogether, computing the Newton–Okounkov body $\Delta_{Y_\bullet}(D)$ recovers the polytope P_D , which is not a coincidence.

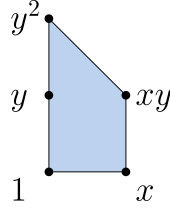


Figure 2.2: The polytope P_D with the monomials corresponding to its lattice points.

2.2.3.1 Properties of Newton–Okounkov Bodies

By definition, the Newton–Okounkov body $\Delta_{Y_\bullet}(D)$ is a convex set. Lemma 1.11 in [LM09] states that it is also bounded and therefore compact. The construction preserves an important invariant.

THEOREM 2.2.12 ([LM09, Theorem 2.3]). Let D be a big divisor on a projective variety X of dimension n . Then

$$n! \cdot \text{vol}_{\mathbb{R}^n}(\Delta_{Y_\bullet}(D)) = \text{vol}(D), \quad (2.2.8)$$

in particular, the volume of the Newton–Okounkov body is independent of the flag Y_\bullet .

Moreover, we will make use of the following properties.

PROPOSITION 2.2.13 ([LM09, Proposition 4.1]). Let X be an irreducible projective variety of dimension n , and fix any admissible flag Y_\bullet . Let D be a big divisor on X .

1. The Newton–Okounkov body $\Delta_{Y_\bullet}(D)$ depends only on the numerical equivalence class of D .
2. For any integer $k > 0$, one has

$$\Delta_{Y_\bullet}(kD) = k \cdot \Delta_{Y_\bullet}(D).$$

Note, that 2. justifies to extend to definition of Newton–Okounkov bodies to \mathbb{Q} -divisors and combined with 1. to also have the notion of $\Delta_{Y_\bullet}([D])$ for a divisor class from $N^1(X)_{\mathbb{Q}}$. Using a continuity argument, the definition is extended even further to $N^1(X)_{\mathbb{R}}$ in [LM09].

2.2.3.2 Newton–Okounkov Bodies on Surfaces

Given the data X , Y_\bullet , and D , there is no straight forward way to compute the corresponding Newton–Okounkov body that works in general. For the case of surfaces, the existence of Zariski decomposition plays the key role for a promising approach. In its original form it goes back to Zariski [Zar62], where he gave a way to uniquely

decompose a given effective \mathbb{Q} -divisor D into a positive part D^+ and a negative part D^- . This result was reproved by Bauer [Bau09] and also Fujita provided an alternative proof in [Fuj79] which also extends to pseudo-effective \mathbb{R} -divisors. Here we review the statement in its most general form.

THEOREM 2.2.14 ([KMM87, Theorem 7.3.1]). Let D be a pseudo-effective \mathbb{R} -divisor on a smooth projective surface X . Then there exists a unique effective \mathbb{R} -divisor

$$D^- = \sum_{i=1}^{\ell} a_i N_i$$

such that

1. $D^+ = D - D^-$ is nef,
2. D^- is either zero or its intersection matrix $(N_i \cdot N_j)_{i,j}$ is negative definite,
3. $D^+ \cdot N_i = 0$ for $i \in \{1, \dots, \ell\}$.

Furthermore, D^- is uniquely determined as a cycle by the numerical equivalence class of D ; if D is a \mathbb{Q} -divisor, then so are D^+ and D^- . The decomposition

$$D = D^+ + D^-$$

is called the *Zariski decomposition* of D .

The above theorem provides a decomposition $D = D^+ + D^-$ for a given divisor D . To receive information about the shape of the resulting Newton–Okounkov body, it is important to know how that decomposition varies once we perturb the divisor. This variation of Zariski decomposition has for instance been explored in [BKS04], see also [KL18, Chapter 2]. It turns out that the big cone $\text{Big}(X)$ has a locally finite decomposition into locally rational polyhedral chambers such that the support of the negative part D^- is constant on each individual chamber.

Let $C = Y_1$ denote the curve in the flag. Start at D , move in direction of $-C$ towards the boundary of the big cone $\text{Big}(X)$ and keep track of the variation of the Zariski decomposition of $D_t := D - tC$, when increasing $t \geq 0$. The next theorem is a fundamental result that applies this procedure in order to compute the Newton–Okounkov body $\Delta_{Y_\bullet}(D)$.

THEOREM 2.2.15 ([LM09, Theorem 6.4]). Let X be a smooth projective surface, D a big divisor (or more generally, a big divisor class), and $Y_\bullet: X \supseteq C \supseteq \{z\}$ an admissible flag on X . Then there exist continuous functions $\alpha, \beta: [\nu, \mu] \rightarrow \mathbb{R}_{\geq 0}$ such that $0 \leq \nu \leq \mu =: \mu_C(D)$ are real numbers,

1. ν is the coefficient of C in D^- ,
2. $\alpha(t) = \text{ord}_z(D_t^-|_C)$,
3. $\beta(t) = \alpha(t) + (D_t^+ \cdot C)$.

Then the associated Newton–Okounkov body is given by

$$\Delta_{Y_\bullet}(D) = \{(t, m) \in \mathbb{R}^2 : \nu \leq t \leq \mu, \alpha(t) \leq m \leq \beta(t)\}.$$

Moreover, α is convex, β is concave, and both are piecewise linear.

As an immediate consequence, the Newton–Okounkov body will always be a polytope in \mathbb{R}^2 . Note, that this is not true in general. In Section 6.3 in [LM09] the authors give an example of a non-polyhedral Newton–Okounkov body living in \mathbb{R}^4 .

2.2.4 Functions on Newton–Okounkov Bodies Coming from Geometric Valuations

The construction of Newton–Okounkov functions in the sense of concave transforms of filtrations goes back to Boucksom–Chen [BC11a] and Witt–Nyström [Wit14] who introduced them from different perspectives and in a more general way than considered in the following. We will focus on functions coming from geometric valuations as dealt with in [KMS13] and recall the definition restricted to that case.

Given an irreducible projective variety X , an admissible flag Y_\bullet , and a big divisor D , let $\Delta_{Y_\bullet}(D)$ be the corresponding Newton–Okounkov body. Let $Z \subseteq X$ be a smooth irreducible subvariety. Then we define a Newton–Okounkov function φ_Z in a two-step process. A point $m \in \Delta_{Y_\bullet}(D)$ is called a *valuative point* if

$$m \in \text{Val}_{Y_\bullet} := \bigcup_{k \geq 1} \frac{1}{k} \{\text{val}_{Y_\bullet}(s) : s \in H^0(X, \mathcal{O}_X(kD)) \setminus \{0\}\}.$$

For a valuative point $m \in \Delta_{Y_\bullet}(D)$ set

$$\begin{aligned} \tilde{\varphi}_Z: \text{Val}_{Y_\bullet} &\rightarrow \mathbb{R} \\ m &\mapsto \lim_{k \rightarrow \infty} \frac{1}{k} \sup\{t \in \mathbb{R} : \text{it exists } s \in H^0(X, \mathcal{O}_X(kD)) \\ &\quad \text{with } \text{val}_{Y_\bullet}(s) = km, \text{ord}_Z(s) \geq t\}. \end{aligned}$$

Due to Lemma 2.6 in [KMS13], the set of valuative points Val_{Y_\bullet} is dense in $\Delta_{Y_\bullet}(D)$. For all non-valuative points $m \in \Delta_{Y_\bullet}(D) \setminus \text{Val}_{Y_\bullet}$ set $\tilde{\varphi}_Z(m) := 0$. To define a meaningful function on the whole Newton–Okounkov body, we use the concave envelope.

Definition 2.2.16. Let $\Delta \subseteq \mathbb{R}^n$ be a compact convex set and $f: \Delta \rightarrow \mathbb{R}$ a bounded real-valued function on Δ . The *closed convex envelope* f^c of f is defined as

$$f^c := \inf\{g(x) : g \geq f \text{ and } g: \Delta \rightarrow \mathbb{R} \text{ is concave and upper-semicontinuous}\}.$$

Definition 2.2.17. Define the *Newton–Okounkov function* φ_Z coming from the geometric valuation associated to Z as

$$\begin{aligned} \varphi_Z: \Delta_{Y_\bullet}(D) &\rightarrow \mathbb{R} \\ m &\mapsto \tilde{\varphi}_Z^c(m). \end{aligned}$$

Due to Lemma 4.4 in [KMS13], taking the concave envelope does not effect the values of the underlying function $\tilde{\varphi}_Z(m)$ for valuative points $m \in \text{Val}_{Y_\bullet}$.

Computing the actual values of a Newton–Okounkov function φ_Z becomes extremely difficult and thus the functions are not well-known even in some of the easiest cases. In general, regarding the formal properties of φ_Z , we will make use of the following known facts.

- φ_Z is non-negative and concave [Wit14] or [BC11a, Lemma 1.6, 1.7].
- φ_Z depends only on the numerical equivalence class of D [KMS13, Proposition 5.6].
- φ_Z is continuous if $\Delta_{Y_\bullet}(D)$ is a polytope [KMS13, Theorem 1.1]. Note, that in general, concavity only yields continuity on the interior and not on the boundary of the Newton–Okounkov body.
- Since the Newton–Okounkov body $\Delta_{Y_\bullet}(D)$ varies heavily under changing the flag Y_\bullet , one is always interested in properties that stay invariant. The numbers

$$\max_{\Delta_{Y_\bullet}(D)} \varphi_Z \quad \text{and} \quad \int_{\Delta_{Y_\bullet}(D)} \varphi_Z$$

are independent of the choice of Y_\bullet [Dum+16b, Theorem 3.4] and [BC11a, Corollary 1.13].

- Let $\pi: X' \rightarrow X$ be a proper birational morphism. Then

$$\int_{\Delta_{Y_\bullet}(D)} \varphi_Z = \int_{\Delta_{Y'_\bullet}(\pi^*D)} \varphi_Z,$$

where Y_\bullet and Y'_\bullet are arbitrary admissible flags on X and X' , respectively [KMR19, Lemma 4.2].

A fairly easy but important observation for our considerations is the following.

LEMMA 2.2.18 ([KL18, Lemma 1.4.10]). Let D be an integral Cartier divisor on a projective (not necessarily smooth) variety X and let $s \in H^0(X, \mathcal{O}_X(D))$ be a non-zero global section. Then

$$\text{ord}_{Y_n}(s) \leq \sum_{i=1}^n \text{val}_i(s), \quad (2.2.9)$$

for any admissible flag $Y_\bullet: X = Y_0 \supseteq \cdots \supseteq Y_n$, where $\text{val}_{Y_\bullet} = (\text{val}_1, \dots, \text{val}_n)$ is the valuation map arising from Y_\bullet .

Note, that it might happen that the zero locus of the section s does not intersect an element of the flag transversely and therefore we do not have equality in (2.2.9) in general. In [KL18, Remark 1.4.11] the authors give an easy example of this fact. Consider the projective plane $X = \mathbb{P}^2$ and the admissible flag $Y_\bullet: X \supseteq Y_1 = \overline{\{x=0\}} \supseteq Y_2 = [0:0:1]$. Take $s(x, y) = xz - y^2$ as a section of $H^0(\mathbb{P}^2, \mathcal{O}_{\mathbb{P}^2}(2))$. Then we have

$$\text{ord}_{Y_2}(s) = 1 < 0 + 2 = \text{val}_1(s) + \text{val}_2(-y^2),$$

since Y_2 is a smooth point of the zero set of s .

In our setting, Lemma 2.2.18 has the following immediate consequence. Consider the Newton–Okounkov body $\Delta_{Y_\bullet}(D)$ with respect to the big divisor D and the admissible flag $Y_\bullet: X \supseteq Y_1 \supseteq \cdots \supseteq Y_n$. Whenever we consider the function φ_{Y_n} coming from the geometric valuation ord_{Y_n} of the point Y_n in the flag Y_\bullet , then it is bounded from above by the sum of coordinates, i.e.,

$$\begin{aligned} \varphi_{Y_n}: \Delta_{Y_\bullet}(D) &\rightarrow \mathbb{R} \\ (m_1, \dots, m_n) &\mapsto \varphi_{Y_n}(m_1, \dots, m_n) \leq m_1 + \cdots + m_n. \end{aligned} \quad (2.2.10)$$

There are plenty of examples for which the inequality in (2.2.10) is strict.

Example 2.2.19. Consider for instance the situation from Example 2.2.11, namely the Hirzebruch surface $X = \mathcal{H}_1$ with big divisor $D = D_3 + 2D_4$ on X . Choose the flag $Y_\bullet: X \supseteq Y_1 \supseteq Y_2$, where Y_1 is the curve given by the binomial $Y_1 = \overline{\{xy^{-2} - 1 = 0\}}$ in local coordinates and Y_2 is a generic point on Y_1 . Similar computations to the ones in Example 2.2.11 show that the Newton–Okounkov body $\Delta_{Y_\bullet}(D)$ is the polytope depicted in Figure 2.3. We are interested in the function φ coming from ord_{Y_2} on $\Delta_{Y_\bullet}(D)$ that measures the maximal order of vanishing in the center Y_2 of the flag. Assuming that $\varphi(a, b) = a + b$ for all $(a, b) \in \Delta_{Y_\bullet}(D)$ yields $\int_{\Delta_{Y_\bullet}(D)} \varphi = 2$ for its integral. But we will see later in Example 2.4.13, that we actually have $\int_{\Delta_{Y_\bullet}(D)} \varphi = \frac{11}{6} < 2$. This implies $\varphi(a, b) < a + b$ for some $(a, b) \in \Delta_{Y_\bullet}(D)$.

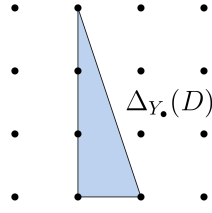


Figure 2.3: The Newton–Okounkov body $\Delta_{Y_\bullet}(D)$ for the choice $Y_1 = \overline{\{xy^{-2} - 1 = 0\}}$.

2.3 ZARISKI DECOMPOSITION FOR TORIC VARIETIES IN COMBINATORIAL TERMS

The focus of this section is the determination of Newton–Okounkov bodies in the toric case. For that we will first review the key-correspondence between the Newton–Okounkov body and the polytope associated to a torus-invariant divisor and give an interpretation in terms of Newton polytopes. Then we give a combinatorial way to find a torus-invariant representative for a class of certain divisors, see Proposition 2.3.1. This leads to a combinatorial version of Zariski decomposition for the toric case, see Theorem 2.3.3. Building on this, we illustrate a combinatorial way to define a piecewise linear isomorphism between the involved Newton Okounkov bodies, when changing to a non-invariant flag on a toric surface, see Subsection 2.3.1, in particular Corollary 2.3.8.

Given a smooth projective toric variety X of dimension n , a torus-invariant flag Y_\bullet , and a big divisor D , then the construction of the Newton–Okounkov body $\Delta_{Y_\bullet}(D)$ recovers the polytope P_D by Proposition 6.1 in [LM09]. This can be seen as follows.

Let $D_{\rho_1}, \dots, D_{\rho_d}$ denote the torus-invariant prime divisors. Since the flag Y_\bullet is torus-invariant, we can assume an ordering of the divisors such that the subvarieties in the flag are given as $Y_i = D_{\rho_1} \cap \dots \cap D_{\rho_i}$ for $1 \leq i \leq n$. The divisor $\sum_{i=1}^d D_{\rho_i}$ has simple normal crossings, hence the orders of vanishing of a section $s \in H^0(X, \mathcal{O}_X(D))$ that has $\sum_{i=1}^d a_{\rho_i} D_{\rho_i}$ as its divisor of zeros can be directly read off as $\text{val}_{Y_\bullet}(s) = (a_{\rho_1}, \dots, a_{\rho_n})$.

The underlying fan Σ is smooth and thus the primitive ray generators $u_{\rho_1}, \dots, u_{\rho_n} \in N$ span a maximal cone σ and form a basis of the lattice N . This gives an isomorphism $N \cong \mathbb{Z}^n$ and the dual isomorphism is given by

$$\begin{aligned} \Phi: M &\rightarrow \mathbb{Z}^n \\ m &\mapsto (\langle m, u_{\rho_i} \rangle)_{1 \leq i \leq n}, \end{aligned} \tag{2.3.1}$$

which extends linearly to the map $\Phi_{\mathbb{R}}: M_{\mathbb{R}} \xrightarrow{\cong} \mathbb{R}^n$.

The Newton–Okounkov body remains the same if one changes the divisor D within its linear equivalence class. Hence we can assume $D|_{U_\sigma} = 0$, i.e., if the divisor is given as $D = \sum_{\rho \in \Sigma(1)} a_\rho D_\rho$, then we have $a_\rho = 0$ for all $\rho \in \sigma(1)$.

The characters χ^m of points m in P_D are exactly the characters of \mathbb{T} that extend to sections of $\mathcal{O}_X(D)$ on X and according to (2.2.4) the characters associated to the lattice points of P_D form a basis of the vector space of global sections. Given a lattice point $m \in P_D \cap M$ its associated character χ^m has divisor of zeros $D + \sum_{i=1}^d \langle m, u_{\rho_i} \rangle D_{\rho_i}$. Thus for $\rho \in \Sigma(1)$ the inequality $\langle m, u_{\rho} \rangle \geq -a_{\rho}$ reflects the condition that χ^m is regular at the generic point of the divisor D_{ρ} . Since we assumed $D|_{U_{\sigma}} = 0$ this yields

$$\text{val}_{Y_{\bullet}}(\chi^m) = (\langle m, u_{\rho_1} \rangle, \dots, \langle m, u_{\rho_n} \rangle) = \Phi(m).$$

Thus

$$\text{conv}(\{\text{val}_{Y_{\bullet}}(s) : s \in H^0(X, \mathcal{O}_X(D)) \setminus \{0\}\}) = \Phi(P_D \cap M). \quad (2.3.2)$$

We have $\dim(\mathcal{O}_X(D)) = |P_D \cap M|$. For all $k \geq 1$ it holds that $P_{kD} = kP_D$. This gives $\Delta_{Y_{\bullet}}(D) = \Phi_{\mathbb{R}}(P_D)$.

We interpret this identification in terms of Newton polytopes. This approach will play a key role for ‘guessing’ suitable global sections in Section 2.4. For convenience, we assume D to be ample. Each divisor D_{ρ} corresponds to a facet F_{ρ} of P_D and all facets $F_{\rho_1}, \dots, F_{\rho_n}$ intersect in a vertex p_{σ} that is associated to σ . Assuming $D|_{U_{\sigma}} = 0$ on the polytope side means to embed the polytope P_D in \mathbb{R}^n such that the vertex p_{σ} is translated to the origin.

Let $s \in H^0(X, \mathcal{O}_X(D))$ be a global section with Newton polytope $\text{NP}(s) \subseteq P_D$. Then the order of vanishing of s along $Y_1 = D_{\rho_1}$ is given by the minimal lattice distance to F_{ρ_1} , that is

$$\text{ord}_{Y_1}(s) = \min_{m \in \text{NP}(s)} \langle u_{\rho_1}, m \rangle. \quad (2.3.3)$$

Let $F_1 \preceq \text{NP}(s)$ denote the face of the Newton polytope $\text{NP}(s)$ that has minimal lattice distance to F_{ρ_1} . Then $\text{ord}_{Y_2}(s_1) = \min_{m \in F_1} \langle u_{\rho_2}, m \rangle$ and in general we have

$$\text{ord}_{Y_{i+1}}(s_i) = \min_{m \in F_i} \langle u_{\rho_{i+1}}, m \rangle \quad (2.3.4)$$

for $1 \leq i \leq n-1$. Thus the map val sends the section s to the point $m \in \text{NP}(s)$ whose coordinates are lexicographically the smallest among all points of the Newton polytope. A similar argument applies to $k > 1$. Thus we obtain $\Delta_{Y_{\bullet}}(D) \subseteq P_D$. Since in particular all the vertices $p \preceq P_D$ correspond to respective global sections extending characters χ^p , this yields $P_D \subseteq \Delta_{Y_{\bullet}}(D)$ and therefore $P_D \cong \Delta_{Y_{\bullet}}(D)$. For our convenience we identify P_D with its image under $\Phi_{\mathbb{R}}$.

As the Newton–Okounkov bodies only depend on the numerical equivalence class of D , we can and often want to choose a torus-invariant representative. If D is given by a defining local equation, then there is a combinatorial way to find one.

PROPOSITION 2.3.1. Let X be a smooth projective toric variety with associated fan Σ , and D a divisor on X that is given by the local equation f in the torus for some $f \in \mathbb{C}(X) \setminus \{0\}$. Then $D' := \sum_{\rho \in \Sigma(1)} -a_\rho D_\rho$ with coefficients

$$a_\rho := \min_{m \in \text{supp}(f)} \langle m, u_\rho \rangle \quad (2.3.5)$$

is a torus-invariant divisor that is linearly equivalent to D .

Proof. Consider the Cox ring $S = \mathbb{C}[x_\rho : \rho \in \Sigma(1)]$ which is graded by the class group $\text{Cl}(X)$, see Chapter 5 in [CLS11] for details. For a cone $\sigma \in \Sigma$ we denote by $x^{\hat{\sigma}} = \prod_{\rho \notin \sigma(1)} x_\rho$ the associated monomial in S and by $S_{x^{\hat{\sigma}}}$ the localization of S at $x^{\hat{\sigma}}$. Applying Lemma 2.2 in [Cox95] to the $\{0\}$ -cone $\sigma_0 \in \Sigma$ gives an isomorphism of rings

$$\mathbb{C}[M] = \mathbb{C}[\sigma_0^\vee \cap M] \cong (S_{x^{\hat{\sigma}_0}})_0,$$

where $x^{\hat{\sigma}_0} = \prod_\rho x_\rho$ and $(S_{x^{\hat{\sigma}_0}})_0$ is the graded piece of degree 0.

Given a lattice point $m \in M$, the character χ^m is homogenized to the monomial $x^{\langle m \rangle} = \prod_\rho x_\rho^{\langle m, u_\rho \rangle}$ by the corresponding map $\theta: \mathbb{C}[M] \rightarrow (S_{x^{\hat{\sigma}_0}})_0$. Thus homogenizing $f = \sum_{m \in \text{supp}(f)} b_m \chi^m \in \mathbb{C}[M]$ yields

$$\tilde{f} = \theta(f) = \theta \left(\sum_{m \in \text{supp}(f)} b_m \chi^m \right) = \sum_{m \in \text{supp}(f)} b_m \prod_\rho x_\rho^{\langle m, u_\rho \rangle} = \frac{g}{\left(\prod_\rho x_\rho \right)^k}$$

for some homogeneous $g \in S$ and some $k \in \mathbb{Z}_{\geq 1}$. We can rewrite this as

$$\tilde{f} = \frac{g}{\left(\prod_\rho x_\rho \right)^k} = \prod_\rho x_\rho^{a_\rho} \cdot h \quad (2.3.6)$$

for $h \in S$ coprime with $\prod_\rho x_\rho$ and uniquely determined $a_\rho \in \mathbb{Z}$.

Since \tilde{f} is homogeneous of degree 0, it gives a rational function on X and we have $0 \sim \text{div}(\tilde{f}) = \text{div} \left(\prod_\rho x_\rho^{a_\rho} \right) + \text{div}(h)$. On the torus the zero sets of f and h agree. Since h is coprime with x_ρ for all $\rho \in \Sigma(1)$, it has no zeros or poles along the boundary components. Altogether we have

$$D = \text{div}(h) \sim \text{div} \left(\prod_\rho x_\rho^{-a_\rho} \right) =: D'.$$

Then D' is torus-invariant by construction. It remains to show, that the coefficients a_ρ from Equation (2.3.6) satisfy Equation (2.3.5). To see that, note, that the homogenization

of f consists of summands of the form $b_m \prod_{\rho} x_{\rho}^{\langle m, u_{\rho} \rangle}$, where we sum over $m \in \text{supp}(f)$. But h is an element of the Cox ring and it is supposed to be coprime with $\prod_{\rho} x_{\rho}$. Therefore, to obtain the expression in Equation (2.3.6), we have to bracket the factor x_{ρ}^j for j maximal that is a common factor of all the summands for each $\rho \in \Sigma(1)$. The maximal j is precisely

$$a_{\rho} = \min_{m \in \text{supp}(f)} \langle m, u_{\rho} \rangle$$

as claimed. \square

We give an example to illustrate the proof of Proposition 2.3.1.

Example 2.3.2. We consider the Hirzebruch surface $X = \mathcal{H}_1$ as in Example 2.2.11 and work with the divisor

$$D = \overline{\{(x, y) \in \mathbb{T} : f(x, y) = xy^{-2} - 1 = 0\}}.$$

Then the Cox ring is given by $S = \mathbb{C}[x_1, x_2, x_3, x_4] = \mathbb{C}[x, y, x^{-1}, x^{-1}y^{-1}]$, where we write x_i for x_{ρ_i} . Homogenizing f yields

$$\begin{aligned} \theta(f) &= \sum_{m \in \text{supp}(f)} b_m \prod_{\rho} x_{\rho}^{\langle m, u_{\rho} \rangle} = x_1^1 x_2^{-2} x_3^{-1} x_4^1 - 1 \\ &= \frac{g}{\left(\prod_{\rho} x_{\rho}\right)^k} = \frac{x_1^3 x_3 x_4^3 - x_1^2 x_2^2 x_3^2 x_4^2}{(x_1 x_2 x_3 x_4)^2} \\ &= \prod_{\rho} x_{\rho}^{a_{\rho}} \cdot h = x_2^{-2} x_3^{-1} \cdot (x_1 x_4 - x_2^2 x_3) \end{aligned}$$

with exponents $a_{\rho_1} = a_{\rho_4} = 0$, $a_{\rho_2} = -2$, and $a_{\rho_3} = -1$ and $h = x_1 x_4 - x_2^2 x_3$ is coprime with $x_1 x_2 x_3 x_4$. The same coefficients are obtained using Proposition 2.3.1.

$$\begin{aligned} a_{\rho_1} &= \min(\langle (0, 0), (1, 0) \rangle, \langle (1, -2), (1, 0) \rangle) = 0, \\ a_{\rho_2} &= \min(\langle (0, 0), (0, 1) \rangle, \langle (1, -2), (0, 1) \rangle) = -2, \\ a_{\rho_3} &= \min(\langle (0, 0), (-1, 0) \rangle, \langle (1, -2), (-1, 0) \rangle) = -1, \\ a_{\rho_4} &= \min(\langle (0, 0), (-1, -1) \rangle, \langle (1, -2), (-1, -1) \rangle) = 0. \end{aligned}$$

Thus $D' = \sum_{\rho \in \Sigma(1)} -a_{\rho} D_{\rho} = 2D_2 + D_3$ is a torus-invariant divisor which is linearly equivalent to D .

With Proposition 2.3.1 in hand, we can provide a combinatorial proof for the existence and uniqueness of Zariski decomposition for smooth toric surfaces independently of Theorem 2.2.14.

THEOREM 2.3.3. Let X be a smooth projective toric surface associated to the fan Σ and let D be a pseudo-effective torus-invariant \mathbb{R} -divisor on X . Then there exists a unique effective \mathbb{R} -divisor

$$D^- = \sum_{i=1}^{\ell} c_i N_i$$

such that

1. $D^+ = D - D^-$ is nef,
2. D^- is either zero or its intersection matrix $(N_i \cdot N_j)_{i,j}$ is negative definite, and
3. $D^+ \cdot N_i = 0$ for $i \in \{1, \dots, \ell\}$.

If D is a \mathbb{Q} -divisor, then so are D^+ and D^- .

For the proof we will need the following Lemma.

LEMMA 2.3.4. Let X be the toric surface associated to the fan Σ . Let D_0, \dots, D_{k+1} be torus-invariant prime divisors with adjacent associated primitive ray generators $u_0, \dots, u_{k+1} \in \mathbb{R}^2$ such that $\text{cone}(u_0, u_{k+1})$ is pointed and $u_1, \dots, u_k \in \text{cone}(u_0, u_{k+1})$. Then

$$\det((-D_i \cdot D_j)_{1 \leq i, j \leq k}) = \det(u_0, u_{k+1}). \quad (2.3.7)$$

Proof. By (2.2.6) the intersection numbers of the torus-invariant prime divisors D_1, \dots, D_k are given as

- $D_i \cdot D_i = -\lambda_i$, where $u_{i-1} + u_{i+1} = \lambda_i u_i$
- and for $i \neq j$ as

$$D_i \cdot D_j = \begin{cases} 1 & \text{if } \rho_i \text{ and } \rho_j \text{ are adjacent} \\ 0 & \text{otherwise.} \end{cases}$$

Thus the intersection matrix is of the form

$$A_k := (-D_i \cdot D_j)_{1 \leq i, j \leq k} = \begin{pmatrix} \lambda_1 & -1 & 0 & \cdots & \cdots & 0 \\ -1 & \lambda_2 & -1 & 0 & \cdots & 0 \\ 0 & \ddots & \ddots & \ddots & \cdots & 0 \\ 0 & \cdots & \ddots & \ddots & \ddots & 0 \\ 0 & \cdots & 0 & -1 & \lambda_{k-1} & -1 \\ 0 & \cdots & \cdots & 0 & -1 & \lambda_k \end{pmatrix}. \quad (2.3.8)$$

We will prove by induction on k that (2.3.7) holds.

Base case: For $k = 1$ we have

$$\begin{aligned} \det(u_0, u_2) &= u_0^{(1)} u_2^{(2)} - u_0^{(2)} u_2^{(1)} \\ &= \lambda_1 \left(u_0^{(1)} u_1^{(2)} - u_0^{(2)} u_1^{(1)} \right) \\ &= \lambda_1, \end{aligned}$$

since Σ is smooth. A similar computation applies to $k = 2$.

Induction step: Let $k \geq 3$ be given and suppose (2.3.7) is true for all integers smaller than k . Note that the determinant of the tridiagonal matrix A_k fulfills a particular recurrence relation, since it is an extended continuant. The recurrence relation is given by

$$\det(A_0) = 0, \det(A_1) = 1, \text{ and } \det(A_k) = \lambda_k \det(A_{k-1}) - \det(A_{k-2}).$$

Thus we have

$$\begin{aligned} \det(A_k) &= \lambda_k \det(A_{k-1}) - \det(A_{k-2}) \\ &\stackrel{\text{IH}}{=} \lambda_k \det(u_0, u_k) - \det(u_0, u_{k-1}) \\ &= \det(u_0, \lambda_k u_k - u_{k-1}) \\ &= \det(u_0, u_{k+1}) \end{aligned}$$

as claimed. □

Proof of Theorem 2.3.3. Since D is torus-invariant, it is given as $D = \sum_{\rho \in \Sigma(1)} a_\rho D_\rho$. We can assume, that D is effective, i.e., $a_\rho \geq 0$ for all $\rho \in \Sigma(1)$. This defines the polygon

$$P_D = \{m \in M_{\mathbb{R}} : \langle m, u_\rho \rangle \geq -a_\rho \text{ for all } \rho \in \Sigma(1)\}.$$

Let $\tilde{a}_\rho \in \mathbb{R}$ be the coefficients such that

$$P_D = \{m \in M_{\mathbb{R}} : \langle m, u_\rho \rangle \geq -\tilde{a}_\rho \text{ for all } \rho \in \Sigma(1)\}$$

and all the inequalities are tight on P_D , i.e., for every $\rho \in \Sigma(1)$ there exists some point $m \in P_D$ such that $\langle m, u_\rho \rangle = -\tilde{a}_\rho$.

Set $D^+ := \sum_{\rho \in \Sigma(1)} \tilde{a}_\rho D_\rho$ and $D^- := \sum_{\rho \in \Sigma(1)} (a_\rho - \tilde{a}_\rho) D_\rho$. Then

$$D = \sum_{\rho \in \Sigma(1)} a_\rho D_\rho = D^+ + D^-$$

and $(a_\rho - \tilde{a}_\rho) \geq 0$ by definition. We now show that the divisors satisfy 1.-3.

1. Since X is a surface, the divisor D^+ is nef by construction due to Theorem 2.2.9.

2. Let D_ρ be a curve with $D_\rho \cdot D_\rho \geq 0$ for some $\rho \in \Sigma(1)$. There exists a vector $v \in M$ such that v is orthogonal to $u_{\rho'}$ and $\langle v, u_\rho \rangle < 0$, where ρ' is a ray adjacent to ρ . Then the inequality corresponding to ρ is tight on P_D , i.e., $a_\rho = \tilde{a}_\rho$, because otherwise the polytope P_D would be unbounded in the direction of v . Thus only negative curves will appear in D^- .

The matrix $(N_i \cdot N_j)_{i,j}$ is negative definite if all leading principal minors of $(-N_i \cdot N_j)_{i,j}$ are positive. Label the negative curves that appear in the negative part D^- as $\{N_1, \dots, N_\ell\}$ in such a way that adjacent rays are given consecutive indices counter-clockwise. Then the intersection matrix $(N_i \cdot N_j)_{i,j}$ is a block matrix, where each block is of the form (2.3.8) as in Lemma 2.3.4. Let $\{N_1, \dots, N_k\} \subseteq \{N_1, \dots, N_\ell\}$ be adjacent negative curves that form a sub block $(-N_i \cdot N_j)_{1 \leq i,j \leq k}$ of the matrix $(-N_i \cdot N_j)_{1 \leq i,j \leq \ell}$ and denote by C_0 and C_{k+1} the remaining curves whose rays are adjacent to ρ_1 and ρ_k as indicated in Figure 2.4.

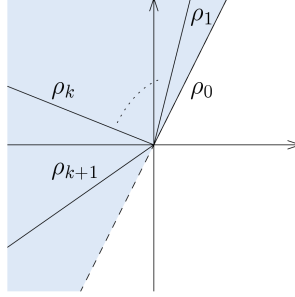


Figure 2.4: Adjacent rays $\rho_0, \dots, \rho_{k+1}$ of the prime divisors C_0, \dots, C_{k+1} .

For the ray generators we have $u_1, \dots, u_k \in \text{cone}(u_0, u_{k+1})$ and that $\text{cone}(u_0, u_{k+1})$ is convex, for otherwise the polytope P_D would be unbounded in the direction of v' , where $v' \in M$ is chosen to be orthogonal to u_0 and fulfill $\langle v', u_{k+1} \rangle > 0$.

Thus it remains to show that the determinant of each such sub block matrix is positive. According to Lemma 2.3.4 we have

$$\det(-N_i \cdot N_j)_{1 \leq i,j \leq k} = \det(u_0, u_{k+1}).$$

Let $u_0 = (m_1, m_2)$ and $u_{k+1} = (m'_1, m'_2)$, and assume without loss of generality that $m_1 > 0$. Since $\text{cone}(u_0, u_{k+1})$ is convex and $u_1, \dots, u_k \in \text{cone}(u_0, u_{k+1})$, we have $m'_2 > \frac{m_2}{m_1} m'_1$, because otherwise the polytope P_D would be unbounded. It follows that

$$\det(u_0, u_{k+1}) = \det \begin{pmatrix} m_1 & m'_1 \\ m_2 & m'_2 \end{pmatrix} = m_1 m'_2 - m'_1 m_2 > 0.$$

A similar argument works for $m_1 \leq 0$. Thus altogether, we have that $(N_i.N_j)_{i,j}$ is negative definite, since all sub block matrices of $(-N_i.N_j)_{i,j}$ have a positive determinant.

3. Let $\rho \in \Sigma(1)$ be a ray for which D_ρ appears in the negative part D^- of the decomposition. Then by construction of D^+ its corresponding face $F_\rho \preceq P_{D^+}$ is a vertex. Using (2.2.5) it follows that

$$D^+.D_\rho = |F_\rho \cap M| - 1 = 0,$$

when P_D is a lattice polytope. A similar argument works in the non-integral case using $\text{length}_M(F_\rho)$.

The above gives the existence of a Zariski decomposition. It remains to show uniqueness of D^- . Assume we have a decomposition

$$D = \bar{D}^+ + \bar{D}^- = \sum_{\rho \in \Sigma(1)} \bar{a}_\rho D_\rho + \sum_{\rho \in \Sigma(1)} (a_\rho - \bar{a}_\rho) D_\rho.$$

Since \bar{D}^- is supposed to be effective and \bar{D}^+ is supposed to be nef which translates into only tight inequalities for $P_{\bar{D}^+}$, we have $\bar{a}_\rho \leq \tilde{a}_\rho$ for all $\rho \in \Sigma(1)$. Let $\rho \in \Sigma(1)$ be the ray of a divisor D_ρ that appears in the negative part \bar{D}^- . Then as argued before this has to be a negative curve. But due to 3. the corresponding face F_ρ of $P_{\bar{D}^+}$ has to be a vertex and therefore it follows that $\bar{a}_\rho = \tilde{a}_\rho$. This yields uniqueness of \bar{D}^- . \square

2.3.1 The 'Tilting-Isomorphism' for Newton-Okounkov Bodies

Although, we can always assume the divisor D to be torus-invariant, the shape of the Newton-Okounkov body $\Delta_{Y_\bullet}(D)$ will heavily depend on the flag Y_\bullet which on the other hand is not necessarily torus-invariant. If the curve Y_1 in the flag is determined by an equation of the form $x^v - 1 = 0$ for some primitive $v \in \mathbb{Z}^2$, then we can give a combinatorial way to compute $\Delta_{Y_\bullet}(D)$.

PROPOSITION 2.3.5. Let X be a smooth projective toric surface, D a big divisor, and $Y_\bullet: X \supseteq C \supseteq \{z\}$ an admissible flag on X , where the curve is $C = \overline{\{x \in \mathbb{T} : x^v = 1\}}$ for some primitive $v \in \mathbb{Z}^2$ and z a general smooth point on C . Then the associated function $\beta(t)$ in Theorem 2.2.15 is given by

$$\beta(t) = (D - tC)^+.C \tag{2.3.9}$$

$$= (D - tC')^+.C \tag{2.3.10}$$

$$= \text{MV} \left(P_{(D-tC')^+}, \text{NP}(x^v - 1) \right) \tag{2.3.11}$$

$$= \text{MV} (P_D \cap (P_D + tv), \text{NP}(x^v - 1)) \tag{2.3.12}$$

for $0 \leq t \leq \mu$, where C' is a torus-invariant curve that is linearly equivalent to C .

Proof. Since the Newton–Okounkov body only depends on the numerical equivalence class, we may assume that the divisor D is torus-invariant, i.e., $D = \sum_{\rho \in \Sigma(1)} a_\rho D_\rho$, where Σ is the fan associated to X .

From Theorem 2.2.15 we know that $\beta(t) = (D - tC)^+ \cdot C$ for $v \leq t \leq \mu$, where $(D - tC)^+$ is the positive part of the Zariski decomposition of $D - tC$ and for C not part of $(D - tC)^-$ we have $v = 0$. Theorem 2.2.14 states that the decomposition is unique up to the numerical equivalence class of the given divisor. Let

$$C' = \sum_{\rho \in \Sigma(1)} - \min_{m \in \text{supp}(x^v - 1)} \langle m, u_\rho \rangle D_\rho$$

be the torus-invariant curve given in Proposition 2.3.1. This means $C' \sim C$ and the curves are in particular numerically equivalent which yields (2.3.10). Due to Sections 5.4/5.5 in [Ful93] the intersection product of two curves equals the mixed volume of the associated Newton polytopes and therefore we have (2.3.11).

To verify the remaining equality, we show that

$$P_{(D-tC)^+} = P_D \cap (P_D + tv)$$

holds up to translation. For the torus-invariant curve $D - tC'$ the construction of its Zariski decomposition as in Theorem 2.3.3 guarantees the equality

$$P_{(D-tC')^+} = P_{(D-tC')}$$

for the corresponding polytopes. Consider its translation by tv , this gives

$$\begin{aligned} & P_{(D-tC')^+} + tv \\ &= \{m + tv \in M_{\mathbb{R}} : \langle m, u_\rho \rangle \geq - (a_\rho + t \cdot \min(0, \langle v, u_\rho \rangle)) \text{ for all } \rho \in \Sigma(1)\} \\ &= \{m \in M_{\mathbb{R}} : \langle m - tv, u_\rho \rangle \geq - (a_\rho + t \cdot \min(0, \langle v, u_\rho \rangle)) \text{ for all } \rho \in \Sigma(1)\} \\ &= \{m \in M_{\mathbb{R}} : \langle m, u_\rho \rangle \geq -a_\rho - t \cdot \min(0, \langle v, u_\rho \rangle) + t \langle v, u_\rho \rangle \text{ for all } \rho \in \Sigma(1)\} \\ &= \{m \in M_{\mathbb{R}} : \langle m, u_\rho \rangle \geq -a_\rho + \max(0, t \langle v, u_\rho \rangle) \text{ for all } \rho \in \Sigma(1)\}. \end{aligned}$$

On the other hand, we have

$$P_D = \{m \in M_{\mathbb{R}} : \langle m, u_\rho \rangle \geq -a_\rho \text{ for all } \rho \in \Sigma(1)\}$$

and

$$P_D + tv = \{m \in M_{\mathbb{R}} : \langle m, u_\rho \rangle \geq -a_\rho + t \langle v, u_\rho \rangle \text{ for all } \rho \in \Sigma(1)\}.$$

Thus their intersection is the set

$$\begin{aligned} & P_D \cap (P_D + tv) \\ &= \{m \in M_{\mathbb{R}} : \langle m, u_{\rho} \rangle \geq -a_{\rho} \text{ and } \langle m, u_{\rho} \rangle \geq -a_{\rho} + t\langle v, u_{\rho} \rangle \text{ for all } \rho \in \Sigma(1)\} \\ &= \{m \in M_{\mathbb{R}} : \langle m, u_{\rho} \rangle \geq -a_{\rho} + \max(0, t\langle v, u_{\rho} \rangle) \text{ for all } \rho \in \Sigma(1)\}. \end{aligned}$$

This verifies equality in (2.3.12). \square

Example 2.3.6. We return to the Hirzebruch surface $X = \mathcal{H}_1$ from Example 2.2.11, and consider the big divisor $D = D_3 + 2D_4$ on X . Then for any admissible torus-invariant flag Y'_{\bullet} the associated Newton–Okounkov body $\Delta_{Y'_{\bullet}}(D)$ coincides with a translate of the polytope P_D which can be seen in Figure 2.5.

We wish to determine the Newton–Okounkov body $\Delta_{Y_{\bullet}}(D)$ given by a different flag $Y_{\bullet}: X \supseteq C \supseteq \{z\}$, where $C = \overline{\{(x, y) \in \mathbb{T} : y^{-1} - 1 = 0\}}$ is a non-invariant curve, and z is a general smooth point on C . In local coordinates the curve C is given by the binomial $y^{-1} - 1$ for $v = (0, -1)$ and has the line segment $\text{NP}(C) = \text{conv}((0, 0), (0, -1))$ as its Newton polytope. Using Proposition 2.3.1 we obtain the torus-invariant curve $C' = D_2$ which is linearly equivalent to C .

To determine the Newton–Okounkov body we use variation of Zariski decomposition for the divisor $D_t = D - tC$. To compute the upper part of the Newton–Okounkov body in terms of the piecewise linear function β , we move a copy of the polytope P_D in the direction of v as indicated in Figure 2.5.

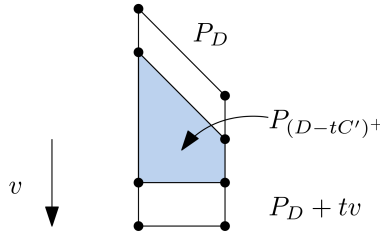


Figure 2.5: Moving a copy of P_D in the direction of v to obtain $P_D \cap (P_D + tv) = P_{(D-tC)^+}$.

The intersection $P_D \cap (P_D + tv)$ gives the polytope associated to $P_{(D-tC)^+}$. By Proposition 2.3.5 the function β is then given as

$$\begin{aligned} \beta(t) &= D_t^+ \cdot C = \text{MV} \left(P_D \cap (P_D + t \cdot (0, -1)), \text{NP}(y^{-1} - 1) \right) \\ &= \begin{cases} 1 & \text{if } 0 \leq t \leq 1 \\ 2 - t & \text{if } 1 \leq t \leq 2, \end{cases} \end{aligned}$$

where the mixed volume $MV(P_D \cap (P_D + t \cdot (0, -1)), NP(y^{-1} - 1))$ can be seen as the area of the shaded region in Figure 2.6.

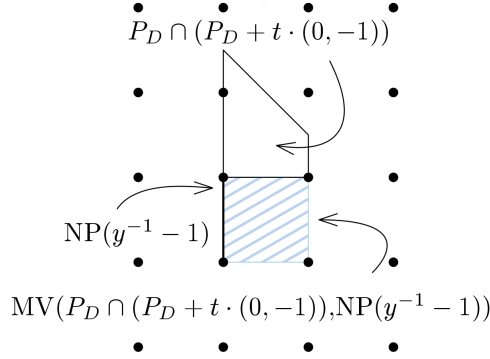


Figure 2.6: The mixed volume $MV(P_D \cap (P_D + t \cdot (0, -1)), NP(y^{-1} - 1))$.

Since D is nef, we have $\nu = 0$ and since z can be chosen general enough on C , we also have $\alpha(t) \equiv 0$. Therefore the Newton–Okounkov body $\Delta_{Y_\bullet}(D)$ is the polytope shown in Figure 2.7.

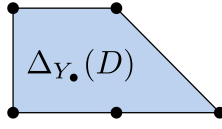


Figure 2.7: The Newton–Okounkov body $\Delta_{Y_\bullet}(D)$.

Let us for simplicity assume that $\nu = 0$ and that $\alpha \equiv 0$. Then the Newton–Okounkov body $\Delta_{Y_\bullet}(D)$ is completely determined by β .

Given the polytope P_D and the vector v , the procedure described in Proposition 2.3.5 to compute the function β divides the polytope P_D into chambers. In the following we consider this process in detail. For that we introduce the following definition.

Definition 2.3.7. Let $P \subseteq \mathbb{R}^2$ be a 2-dimensional polytope and let $v \in \mathbb{R}^2$ be a direction. Then we call a facet $F \preceq P$ *sunny* with respect to v if $\langle v, u_F \rangle > 0$, where u_F is the inner facet normal of F . We call the set of all sunny facets of P with respect to v the *sunny side* of P with respect to v and denote it by $\text{sun}(P, v)$.

Let $\text{sun}(P_D, v)$ be the sunny side of P_D with respect to v . By construction the function β is piecewise linear. There is a break point at time $\tilde{t} \geq 0$ if and only if there exists a vertex $p \in \text{vert}(P_D)$ such that

$$p \in P_D \cap (\text{sun}(P_D, v) + \tilde{t}v).$$

Thus we move the sunny side $\text{sun}(P_D, v)$ along the polytope P_D in the direction of v . We start at time $t_0 = 0$. Whenever we hit a vertex $p_i \in \text{vert}(P_D)$ at time t_i , we enter a new chamber as indicated in Figure 2.8.

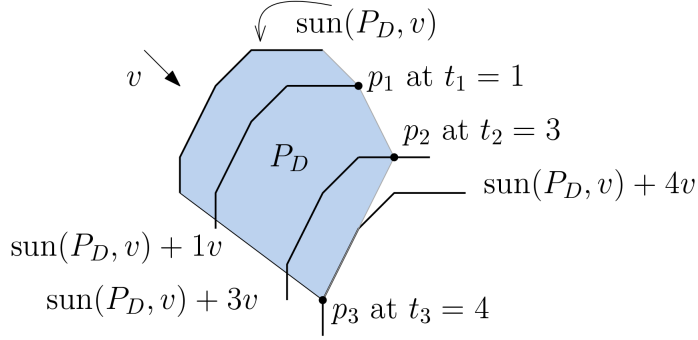


Figure 2.8: Break points p_1, p_2 , and p_3 of shifting the sunny side $\text{sun}(P_D, v)$ through P_D in the direction of v .

Then $\beta(t)$ is linear in each time interval $[t_i, t_{i+1}]$ for $i \in \mathbb{Z}_{\geq 0}$.

The other part of the chamber structure comes from inserting a wall in the direction of v for each vertex $p \in \text{sun}(P_D, v)$ and in the direction of $-v$ for each vertex $p \in \text{sun}(P_D, -v)$ as it can be seen in Figure 2.9.

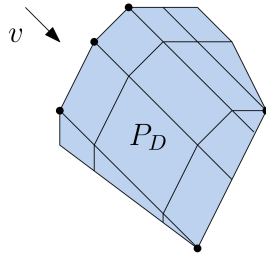


Figure 2.9: The chamber structure on P_D induced by the shifting process.

In the following, we verify that for this particular chamber structure there exists a map between P_D and $\Delta_{Y_\bullet}(D)$ that is linear on each of the chambers.

For that, we choose a coordinate system m_1, m_2 for $M_{\mathbb{R}} \cong \mathbb{R}^2$ such that $v = (1, 0)$ without loss of generality. Consider the polytope $P_D \subseteq \mathbb{R}^2$ in (m_1, m_2) -coordinates, and assume without loss of generality that P_D lies in the positive orthant. We can write it as

$$P_D = \{(m_1, m_2) \in \mathbb{R}^2 : \gamma \leq m_2 \leq \delta, \ell(m_2) \leq m_1 \leq r(m_2)\},$$

for some $\gamma, \delta \in \mathbb{R}$ and some piecewise linear functions ℓ and r that determine the sunny sides $\text{sun}(P_D, v)$ and $\text{sun}(P_D, -v)$, respectively. To determine the function β using the combinatorial approach from Proposition 2.3.5, we shift the sunny side $\text{sun}(P_D, v)$ through the polytope as depicted in Figure 2.8. Now we want to ‘tilt the polytope leftwards’ such that the m_1 -coordinate of each point in the image expresses exactly the time at which the point in the original polytope is visited in the shifting process. This is shown in Figure 2.10. To make this precise, map the polytope P_D via

$$\begin{aligned} \Psi_{\text{left}}: P_D \subseteq \mathbb{R}^2 &\rightarrow \mathbb{R}^2 \\ (m_1, m_2) &\mapsto (m_1 - \ell(m_2), m_2). \end{aligned}$$

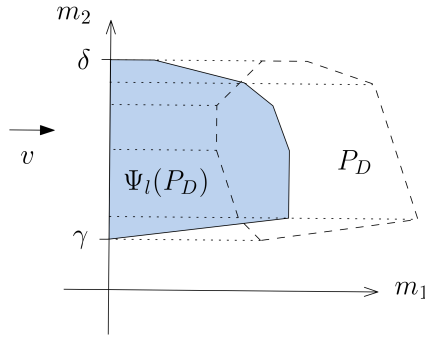


Figure 2.10: Tilting the polytope P_D leftwards via the map Ψ_{left} .

By construction, the map Ψ_{left} is a piecewise shearing of the original polytope and therefore volume-preserving. Additionally, $\Psi_{\text{left}}(P_D) \cap \{m_1 = t\}$ are exactly the images of the points of P_D that are visited at time t . Given $m_1 = t$ we now want to determine $\beta(t)$. According to (2.3.12) it is given by

$$\begin{aligned} \beta(t) &= \text{MV}(P_D \cap (P_D + tv), \text{NP}(x^v - 1)) \\ &= \text{MV}(P_D \cap (\text{sun}(P_D, v) + tv), \text{NP}(x^v - 1)) \\ &= \text{MV}(\Psi_{\text{left}}(P_D) \cap \{m_1 = t\}, \text{NP}(x^v - 1)) \\ &= \text{length}_M(\Psi_{\text{left}}(P_D) \cap \{m_1 = t\}). \end{aligned}$$

The last equation holds, since v was chosen to be $(1, 0)$. In the last step we want to ‘tilt the polytope downwards’ similarly to the previous process as can be seen in Figure 2.11. Therefore we can describe the polytope $\Psi_{\text{left}}(P_D)$ as

$$\begin{aligned} \Psi_{\text{left}}(P_D) &= \{(m_1, m_2) \in \mathbb{R}^2 : \gamma \leq m_2 \leq \delta, 0 \leq m_1 \leq r(m_2) - \ell(m_2)\} \\ &= \{(m_1, m_2) \in \mathbb{R}^2 : 0 \leq m_1 \leq \hat{\delta}, \hat{\ell}(m_1) \leq m_2 \leq \hat{r}(m_2)\}, \end{aligned}$$

for some $\hat{\delta} \in \mathbb{R}$ and some piecewise linear functions $\hat{\ell}$ and \hat{r} that determine the bottom and top of the polytope.

So set

$$\begin{aligned} \Psi_{\text{down}}: \Psi_{\text{left}}(P_D) \subseteq \mathbb{R}^2 &\rightarrow \mathbb{R}^2 \\ (m_1, m_2) &\mapsto (m_1, m_2 - \hat{\ell}(m_1)). \end{aligned}$$

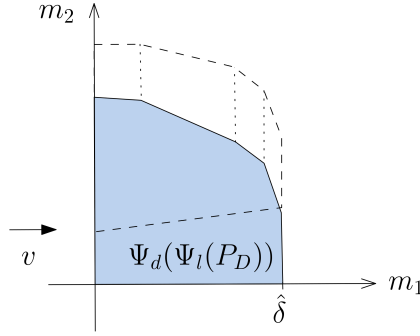


Figure 2.11: Tilting the polytope $\Psi_{\text{left}}(P_D)$ downwards via the map Ψ_{down} .

By construction this is again a piecewise shearing of the polytope and therefore volume-preserving. The image $\Psi_{\text{down}}(\Psi_{\text{left}}(P_D))$ is the subgraph of β and thus it coincides with the Newton–Okounkov body $\Delta_{Y_\bullet}(D)$ with respect to the new flag Y_\bullet .

The above shows the following.

COROLLARY 2.3.8. Let X be a smooth projective toric surface, D a big divisor, and $Y_\bullet: X \supseteq C \supseteq \{z\}$ an admissible flag on X , where the curve C is given by a binomial $x^v - 1$ for a primitive $v \in \mathbb{Z}^2$ and z is a general smooth point on C . Then there exists a piecewise linear, volume-preserving isomorphism $\Psi = \Psi_{\text{down}} \circ \Psi_{\text{left}}$ between the two Newton–Okounkov bodies P_D and $\Delta_{Y_\bullet}(D)$.

Moreover, the image under Ψ can explicitly be described in terms of measurements of the polytope. For that we need to introduce more terminology.

Definition 2.3.9. Let $P \subseteq \mathbb{R}^n$ be a polytope, $v \in \mathbb{Z}^n$ a primitive vector, and $u \in v^\perp$ a primitive integral functional.

For a point $m \in P$ we define the *length of P at m with respect to v* to be

$$\text{length}(P, m, v) := \max \{t \in \mathbb{R} : m - tv \in P\},$$

and $\text{length}(P, v)$ is the maximal length over all $m \in P$.

Further, we denote by $P_v(m)$ the intersection of

$$P \cap (P + \text{length}(P, m, v) \cdot v)$$

with the half plane given by $\langle u, \cdot \rangle \geq \langle u, m \rangle$.

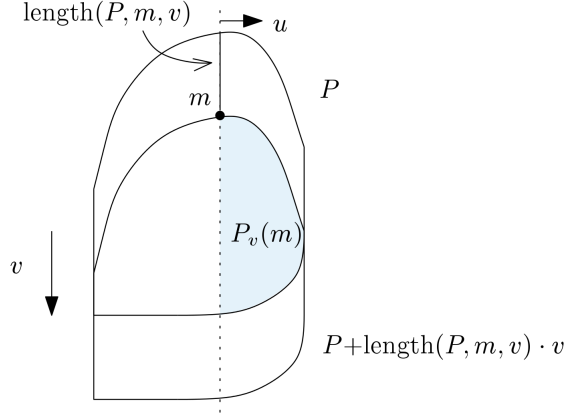


Figure 2.12: The feasible region in P with respect to v and u , given $m \in P$.

Observe that with the above notation $\Psi(m) = (\text{length}(P, m, v), \text{width}_u(P_v(m)))$ for $v = (1, 0)$ and $u = (0, -1)$.

Remark 2.3.10. Note, that the piecewise linear, volume-preserving isomorphism Ψ is reminiscent of the transformation constructed in [EH19]. The authors give geometric maps between the Newton–Okounkov bodies corresponding to two adjacent maximal-dimensional prime cones in the tropicalization of the variety X . This can also be studied from the perspective of complexity-one T-varieties.

2.4 NEWTON–OKOUNKOV FUNCTIONS ON TORIC VARIETIES

This section examines Newton–Okounkov functions in three settings. To start with, we consider the completely toric case in Subsection 2.4.1 and show that in this case the resulting function will be linear, see Proposition 2.4.1. This is related to a result that identifies the subgraph of a Newton–Okounkov function as a certain Newton–Okounkov body. We translate this relation into polyhedral language in Subsection 2.4.2. Eventually, we return to the surface case in Subsection 2.4.3 and examine Newton–Okounkov functions coming from the geometric valuation at a general point and give combinatorial criteria for when we can fully determine the function, see Theorem 2.4.9, Corollary 2.4.11 and Theorem 2.4.17.

2.4.1 The Completely Toric Case

Whenever we determine the value of a Newton–Okounkov function $\varphi(m)$ for a point $m \in \Delta_{Y_\bullet}(D)$, we will often assume that m is a valuative point if not mentioned otherwise.

In the case, when all the given data is toric, we can completely describe the function φ_Z , and it even has a nice geometric interpretation.

By ‘all data toric’ we mean that X is a smooth toric variety, Y_\bullet is a flag consisting of torus-invariant subvarieties, D is a big torus-invariant divisor on X , and $Z \subseteq X$ a torus-invariant subvariety.

In order to formulate and prove Proposition 2.4.1 below, we recall the combinatorics of the blow-up $\pi_Z: X^* \rightarrow X$ of Z . As Z is torus-invariant, it corresponds to a cone $\tau \in \Sigma$ of the fan. According to [CLS11, Definition 3.3.17] the fan Σ^* in $N_{\mathbb{R}}$ of the variety X^* is given by the star subdivision of Σ relative to τ . Set $u_\tau = \sum_{\rho \in \tau(1)} u_\rho$, $\rho_Z = \text{cone}(u_\tau)$, and for each cone $\sigma \in \Sigma$ containing τ , set

$$\Sigma_\sigma^*(\tau) = \{\sigma' + \rho_Z : \tau \not\subseteq \sigma' \subset \sigma\}$$

and the star subdivision of Σ relative to τ is the fan

$$\Sigma^* = \Sigma^*(\tau) = \{\sigma \in \Sigma : \tau \not\subseteq \sigma\} \cup \bigcup_{\sigma \supseteq \tau} \Sigma_\sigma^*(\tau).$$

Then the exceptional divisor E of the blow-up π_Z corresponds to the ray $\rho_Z \in \Sigma^*$, and the order of vanishing of a section s along Z is, by definition, the order of vanishing of $\pi_Z^*(s)$ along E .

The Cartier data $\{m_{\sigma^*}^*\}_{\sigma^* \in \Sigma^*(n)}$ of π_Z^*D is given by $m_{\sigma^*}^* = m_{\sigma^*}$ for $\sigma^* \in \Sigma(n)$ (i.e., $\sigma^* \not\supseteq \rho_Z$), and $m_{\sigma^*}^* = m_\sigma$ for $\sigma^* \in \Sigma_\sigma^*(\tau)(n)$.

PROPOSITION 2.4.1. Let X be an n -dimensional smooth projective toric variety associated to the unimodular fan Σ in $N_{\mathbb{R}}$. Furthermore, let Y_\bullet be an admissible torus-invariant flag and D a big torus-invariant divisor on X with resulting Newton–Okounkov body $\Delta_{Y_\bullet}(D)$.

Let $Z \subseteq X$ be an irreducible torus-invariant subvariety. Then the geometric valuation ord_Z yields a linear function φ_Z on $\Delta_{Y_\bullet}(D)$. More explicitly, it is given by

$$\begin{aligned} \varphi_Z: \Delta_{Y_\bullet}(D) &\rightarrow \mathbb{R} \\ m &\mapsto \langle m - m_\tau, u_\tau \rangle, \end{aligned}$$

where $m_\tau := m_\sigma$ is part of the Cartier data $\{m_\sigma\}_{\sigma \in \Sigma(n)}$ of D for any cone $\sigma \in \Sigma$ containing τ .

This function φ_Z measures the lattice distance of a given point m in the Newton–Okounkov body to the hyperplane with equation $\langle m, u_\tau \rangle = \langle m_\tau, u_\tau \rangle$. If D is ample this is the lattice distance to a face of $\Delta_{Y_\bullet}(D)$.

Proof. Since the flag Y_\bullet and the divisor D are torus-invariant, the resulting Newton–Okounkov body $\Delta_{Y_\bullet}(D)$ coincides with a translate of the polytope P_D .

We consider the blow-up $\pi_Z: X^* \rightarrow X$ of Z . Let Y_\bullet^* denote the proper transform of Y_\bullet on X^* . The pullback π_Z^*D of the given divisor D determines a polytope $P_{\pi_Z^*D}$ and by construction we have $P_D \cong P_{\pi_Z^*D}$. To embed the Newton–Okounkov body $\Delta_{Y_\bullet^*}(\pi_Z^*D) \cong P_{\pi_Z^*D}$ in \mathbb{R}^n we have to fix a trivialization of the line bundle. Fix the origin $\mathbf{0}$ of \mathbb{R}^n to be m_τ . If $m_\tau \in P_{\pi_Z^*D}$, this means that the corresponding character $\chi^{\mathbf{0}}$ is identified with a global section s of $\mathcal{O}_{X^*}(\pi_Z^*D)$ that does not vanish along Z .

Then according to [CLS11, Proposition 4.1.1] the order of vanishing of a character χ^m along Z is given as

$$\text{ord}_Z(\chi^m) = \text{ord}_E(\chi^m) = \langle m, u_\tau \rangle$$

for $m \in \Delta_{Y_\bullet^*}(\pi_Z^*D)$.

For a given point $m \in \Delta_{Y_\bullet^*}(\pi_Z^*D)$ let $s \in H^0(X^*, \mathcal{O}_{X^*}(k\pi_Z^*D))$ be an arbitrary global section that gets mapped to m by the flag valuation associated to Y_\bullet^* for some suitable $k \in \mathbb{Z}_{\geq 1}$. Write s in local coordinates x_i with respect to the flag Y_\bullet^* , that is, Y_i^* is given by $x_1 = \dots = x_i = 0$ and in particular $\mathbf{0} = Y_n^*$.

The change of coordinates is obtained by multiplication by the monomial χ^{m_τ} on the level of functions and by a respective translation by the vector $m_\tau \in M$ on the level of points. This yields

$$\text{ord}_Z(\chi^m) = \langle m - m_\tau, u_\tau \rangle.$$

The section s is identified with a linear combination of characters, in which χ^m appears with non-zero coefficient. This gives the upper bound

$$\text{ord}_Z(s) = \min_{m' \in \text{supp}(s)} \text{ord}_Z(\chi^{m'}) \leq \text{ord}_Z(\chi^m).$$

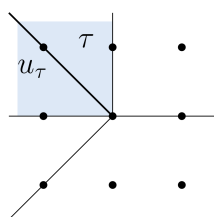
The lower bound is realized by the monomial χ^m itself. Hence, the function that comes from the geometric valuation along the subvariety Z is given as

$$\varphi_Z(m) = \text{ord}_Z(\chi^m) = \langle m - m_\tau, u_\tau \rangle$$

for $m \in \Delta_{Y_\bullet^*}(\pi_Z^*D) = \Delta_{Y_\bullet}(D)$. □

We give an example to illustrate the proof.

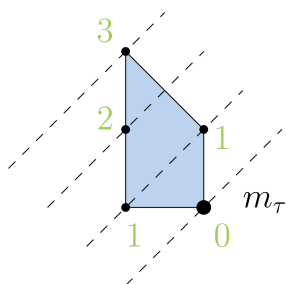
Example 2.4.2. As in Example 2.3.6 we consider the Hirzebruch surface $X = \mathcal{H}_1$, an admissible torus-invariant flag Y_\bullet , and the big divisor $D = D_3 + 2D_4$. As a torus-invariant subvariety $Z \subseteq X$ consider the torus fixed point associated to the cone $\tau = \text{cone}((-1, 0), (0, 1))$.


 Figure 2.13: Star subdivision of the fan Σ relative to τ .

Then the additional primitive ray generator $u_\tau = (-1, 1) = (-1, 0) + (0, 1)$ for the fan Σ^* comes from the star subdivision of the fan Σ relative to the cone τ as indicated in Figure 2.13. The Newton–Okounkov function φ_Z on the Newton–Okounkov body $\Delta_{Y_\bullet}(\pi_Z^* D)$ is given by

$$\varphi_Z(m) = \langle m - m_\tau, u_\tau \rangle = \langle m - (1, 0), (-1, 1) \rangle,$$

which gives the values shown in Figure 2.14.


 Figure 2.14: Values of the Newton–Okounkov function φ_Z associated to the distance to m_τ .

2.4.2 Interpretation of a Subgraph as a Newton–Okounkov Body

Let X be a smooth projective variety, Y_\bullet an admissible flag, and D a big \mathbb{Q} -Cartier divisor on X . This determines the Newton–Okounkov body $\Delta_{Y_\bullet}(D)$. Given a smooth subvariety $Z \subseteq X$ we consider the function φ_Z on $\Delta_{Y_\bullet}(D)$ that comes from the geometric valuation ord_Z .

In [KMR19] Küronya, Maclean, and Roé construct a variety \hat{X} , a flag \hat{Y}_\bullet , and a divisor \hat{D} on \hat{X} so that the resulting Newton–Okounkov body is the subgraph of φ_Z over $\Delta_{Y_\bullet}(D)$. We translate their construction into polyhedral language in the toric case.

2.4.2.1 The General Framework

THEOREM 2.4.3 ([KMR19, Theorem 4.1]). Let X be a smooth projective variety, Y_\bullet an admissible flag on X , and D a big divisor on X . Furthermore, let $Z \subseteq X$ be a smooth subvariety and φ_Z the Newton–Okounkov function associated to the geometric valuation ord_Z . Then there exists a projective variety \hat{X} , an admissible flag \hat{Y}_\bullet on \hat{X} , and a big divisor \hat{D} on \hat{X} such that

$$\Delta_{\hat{Y}_\bullet}(\hat{D}) = \hat{\Delta} := \text{subgraph of } \varphi_Z: \Delta_{Y_\bullet}(D) \rightarrow \mathbb{R}_{\geq 0}.$$

In particular,

$$\int_{\Delta_{Y_\bullet}(D)} \varphi_Z = \text{vol}_{\hat{X}}(\hat{D}).$$

According to Lemma 4.2 in [KMR19] we may assume that the geometric valuation ord_Z comes from a smooth effective Cartier divisor L on X , i.e., $\text{ord}_Z = \text{ord}_L$. This can always be guaranteed by possibly blowing up X (compare Section 2.4.1).

Set

$$\hat{X} := \mathbb{P}_X(\mathcal{O}_X \oplus \mathcal{O}_X(L)).$$

In other words, we consider the total space of the line bundle $\mathcal{O}_X(L)$ and compactify each fiber to a \mathbb{P}^1 . There exist two distinguished sections, namely the zero-section and the ∞ -section. The natural surjections $\mathcal{O}_X \oplus \mathcal{O}_X(L) \rightarrow \mathcal{O}_X(L)$ and $\mathcal{O}_X \oplus \mathcal{O}_X(L) \rightarrow \mathcal{O}_X$ yield embeddings $X \xrightarrow{\iota_0} \hat{X}$ and $X \xrightarrow{\iota_\infty} \hat{X}$. We denote the respective images by $X_0 := \iota_0(X)$ and $X_\infty := \iota_\infty(X)$ and by construction we have $X_0 \cap X_\infty = \emptyset$.

We can identify these with X , by restricting the natural projection $\hat{X} \xrightarrow{\pi} X$ to X_0 , X_∞ , respectively, i.e., $X_0 \cong X$ and $X_\infty \cong X$.

In addition, the construction gives rise to the linear equivalence $X_0 \sim X_\infty + \pi^*L$, when X_0 and X_∞ are considered as divisors on \hat{X} . Since X_0 and X_∞ intersect transversely this gives the following isomorphisms of sheaves of sections

$$\begin{aligned} \mathcal{O}_{\hat{X}}(X_0)|_{X_0} &\cong \mathcal{O}_{\hat{X}}(X_\infty + \pi^*L)|_{X_0} \cong \mathcal{O}_{\hat{X}}(\pi^*L)|_{X_0} \cong \mathcal{O}_{X_0}(L) \\ \mathcal{O}_{\hat{X}}(X_\infty)|_{X_\infty} &\cong \mathcal{O}_{\hat{X}}(X_0 - \pi^*L)|_{X_\infty} \cong \mathcal{O}_{\hat{X}}(-\pi^*L)|_{X_\infty} \cong \mathcal{O}_{X_\infty}(-L). \end{aligned}$$

For a suitable line bundle on \hat{X} we fix some rational number b such that

$$b > \sup\{t > 0 : D - tL \text{ is big}\}$$

and define $\hat{D} := \pi^*D + bX_\infty$. As an admissible flag \hat{Y}_\bullet we set

$$\hat{Y}_1 := X_0, \hat{Y}_i := \iota_0(Y_{i-1}) \text{ for all } i \geq 2.$$

In the proof of Theorem 2.4.3 Küronya, Maclean, and Roé show that \hat{X} and \hat{D} are the suitable objects to obtain the desired identification

$$\hat{\Delta} = \Delta_{\hat{Y}_\bullet}(\hat{D}).$$

2.4.2.2 The Toric Case on the Level of Fans and Polytopes

Let $X = X_\Sigma$ now be a smooth projective *toric* variety, Y_\bullet an admissible torus-invariant flag, and D a big torus-invariant divisor. Furthermore, let L be a smooth effective torus-invariant Cartier divisor on X .

In this case we can associate fans or polytopes to the given objects, respectively. We want to build the combinatorial objects that correspond to \hat{X} and \hat{D} in terms of this information.

GIVEN X AND D . WHICH FAN CORRESPONDS TO $V_{\mathcal{L}}$?

The Cartier divisor $D = \sum_{\rho \in \Sigma(1)} a_\rho D_\rho$ has an associated sheaf $\mathcal{L} = \mathcal{O}_X(D)$. This is the sheaf of sections of a rank 1 vector bundle $\psi: V_{\mathcal{L}} \rightarrow X$. According to Proposition 7.3.1 in [CLS11], $V_{\mathcal{L}}$ is again a toric variety and the associated fan $\Sigma \times D$ in $N_{\mathbb{R}} \times \mathbb{R}$ is constructed as follows.

Given $\sigma \in \Sigma$, set

$$\begin{aligned} \tilde{\sigma} &:= \{(u, h) \in N_{\mathbb{R}} \times \mathbb{R} : u \in \sigma, h \geq \text{SF}_D(u)\} \\ &= \text{cone}((0, 1), (u_\rho, -a_\rho) : \rho \in \sigma(1)), \end{aligned} \tag{2.4.1}$$

where $\text{SF}_D: |\Sigma| \rightarrow \mathbb{R}$ is the support function associated to D . Define $\Sigma \times D$ to be the fan consisting of the cones $\tilde{\sigma}$ for $\sigma \in \Sigma$ and their faces.

The projection $\tilde{\psi}: N \times \mathbb{Z} \rightarrow N$ gives a toric morphism $\psi: X_{\Sigma \times D} = V_{\mathcal{L}} \rightarrow X$ and a rank 1 vector bundle whose sheaf of sections is $\mathcal{O}_X(D)$.

Example 2.4.4. Let $X = \mathbb{P}^1$ be the projective line. Its corresponding fan Σ in \mathbb{R} is depicted in Figure 2.15, where the torus-invariant prime divisors D_0 and D_1 correspond to $\sigma_0 = \mathbb{R}_{\geq 0}$ and $\sigma_1 = \mathbb{R}_{\leq 0}$ with primitive ray generators $u_0 = 1$ and $u_1 = -1$.

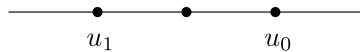


Figure 2.15: The fan Σ of the projective line $X = \mathbb{P}^1$.

Consider the divisor $D = 2D_0$. Then $\Sigma \times D$ is a fan in \mathbb{R}^2 and its two top-dimensional cones are spanned by

$$\begin{aligned}\tilde{\sigma}_0 &= \text{cone}((0, 1), (1, -2)) \text{ and} \\ \tilde{\sigma}_1 &= \text{cone}((0, 1), (-1, 0))\end{aligned}$$

as depicted in Figure 2.16.

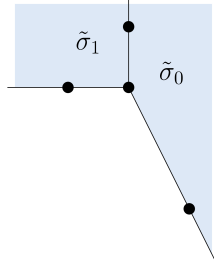


Figure 2.16: The fan $\Sigma \times D$.

GIVEN X AND L . WHICH FAN CORRESPONDS TO \hat{X} ?

In our toric situation, $\hat{X} = \mathbb{P}_X(\mathcal{O}_X \oplus \mathcal{O}_X(L))$ is again toric, and its fan is described in Proposition 7.3.3 in [CLS11] as follows. The local equation of L as a Cartier divisor along a toric patch U_σ is a torus character which corresponds to a linear function on σ . These linear functions glue to the support function $\text{SF}_L: |\Sigma| \rightarrow \mathbb{R}$ of L (see Definition 4.2.11 & Theorem 4.2.12 in [CLS11]). Using SF_L , we define an upper and a lower cone in $N_{\mathbb{R}} \times \mathbb{R}$ for every $\sigma \in \Sigma$:

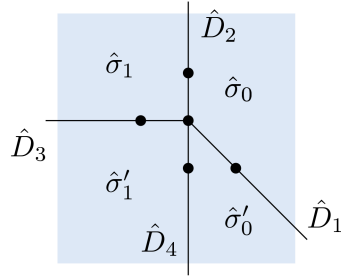
$$\begin{aligned}\hat{\sigma} &:= \{(u, h) \in N_{\mathbb{R}} \times \mathbb{R} : u \in \sigma, h \geq \text{SF}_L(u)\} \\ \hat{\sigma}' &:= \{(u, h) \in N_{\mathbb{R}} \times \mathbb{R} : u \in \sigma, h \leq \text{SF}_L(u)\}.\end{aligned}\tag{2.4.2}$$

Together with their faces, these cones form a fan $\hat{\Sigma}$ which determines our \hat{X} .

Example 2.4.5. We continue with Example 2.4.4. Hence $X = \mathbb{P}^1$ and the corresponding fan Σ has maximal cones $\sigma_0 = \text{cone}(u_0)$ and $\sigma_1 = \text{cone}(u_1)$. Consider the divisor $L = D_0$. Then $\hat{\Sigma}$ is a fan in \mathbb{R}^2 and its top-dimensional cones are

$$\begin{aligned}\hat{\sigma}_0 &= \text{cone}((0, 1), (1, -1)), \\ \hat{\sigma}'_0 &= \text{cone}((0, -1), (1, -1)), \\ \hat{\sigma}_1 &= \text{cone}((0, 1), (-1, 0)), \text{ and} \\ \hat{\sigma}'_1 &= \text{cone}((0, -1), (-1, 0)).\end{aligned}$$

We obtain the fan of the Hirzebruch surface \mathcal{H}_1 as depicted in Figure 2.17.


 Figure 2.17: The fan $\hat{\Sigma}$ of $\mathbb{P}_{\mathbb{P}^1}(\mathcal{O}_{\mathbb{P}^1} \oplus \mathcal{O}_{\mathbb{P}^1}(1))$.

GIVEN \hat{X} AND D . WHICH DIVISOR CORRESPONDS TO π^*D ?

In general, the pullback of a divisor is explicitly given in terms of support functions. For the divisor $D = \sum_{\rho \in \Sigma(1)} a_{\rho} D_{\rho}$ we have $\text{SF}_D(u_{\rho}) = -a_{\rho}$ for all $\rho \in \Sigma(1)$ for its corresponding support function. According to the construction of $\hat{\Sigma}$, the morphism $\pi: \hat{X} \rightarrow X$ is induced by the homomorphism of lattices $\bar{\pi}: N \times \mathbb{Z} \rightarrow N$ that sends (u, h) to u .

We denote by $\hat{D}_{\hat{\rho}}$ the torus-invariant prime divisor that corresponds to the ray $\hat{\rho}$ of the fan $\hat{\Sigma}$ having primitive ray generator $u_{\hat{\rho}}$. Applying Theorem 4.2.12 and Proposition 6.2.7 in [CLS11] yields $\pi^*D = \sum_{\hat{\rho} \in \hat{\Sigma}(1)} a_{\hat{\rho}}^* \hat{D}_{\hat{\rho}}$, where the coefficients are given as

$$a_{\hat{\rho}}^* = -\text{SF}_{\pi^*D}(u_{\hat{\rho}}) = -\text{SF}_D(\bar{\pi}(u_{\hat{\rho}})).$$

Example 2.4.6. As in Examples 2.4.4 and 2.4.5, we consider $X = \mathbb{P}^1$, $D = 2D_0$, and $\hat{X} = \mathbb{P}_{\mathbb{P}^1}(\mathcal{O}_{\mathbb{P}^1} \oplus \mathcal{O}_{\mathbb{P}^1}(L))$ for $L = D_0$.

Let \hat{u}_i denote the primitive generator of the ray $\hat{\rho}_i$ that corresponds to the divisor \hat{D}_i , i.e., $\hat{u}_1 = (1, -1)$, $\hat{u}_2 = (0, 1)$, $\hat{u}_3 = (-1, 0)$, and $\hat{u}_4 = (0, -1)$. Under the lattice morphism $\bar{\pi}: \mathbb{Z}^2 \rightarrow \mathbb{Z}$ they map to $\bar{\pi}(\hat{u}_1) = 1$, $\bar{\pi}(\hat{u}_2) = 0$, $\bar{\pi}(\hat{u}_3) = -1$, and $\bar{\pi}(\hat{u}_4) = 0$. This means that $\bar{\pi}(\hat{\rho}_1) \subseteq \sigma_0$ and $\bar{\pi}(\hat{\rho}_3) \subseteq \sigma_1$. Hence for the divisor on \hat{X} we have

$$\pi^*D = -(\text{SF}_D(1)\hat{D}_1 + \text{SF}_D(-1)\hat{D}_3) = 2\hat{D}_1.$$

GIVEN \hat{X} . WHAT DO X_0 AND X_{∞} CORRESPOND TO?

In the general setup, we have defined $X_0 := \iota_0(X)$ and $X_{\infty} := \iota_{\infty}(X)$. As varieties, both are isomorphic to X , and considered as divisors on \hat{X} the linear equivalence $X_0 \sim X_{\infty} + \pi^*L$ holds.

We want to consider what this translates to in the combinatorial toric picture. Given the variety \hat{X} we have already seen how to construct the associated fan $\hat{\Sigma}$ in $N_{\mathbb{R}} \times \mathbb{R}$. The upper and lower cones of the origin $\mathbf{0} \in \Sigma$ are rays $\hat{\mathbf{0}}$ and $\hat{\mathbf{0}}'$ whose toric divisors in \hat{X} are X_0 and X_{∞} , respectively. The projection $N \times \mathbb{Z} \rightarrow N$ identifies both $\text{star}(\hat{\mathbf{0}})$ and $\text{star}(\hat{\mathbf{0}}')$ with Σ . This can be seen as follows.

By construction (2.4.2) each maximal cone $\hat{\sigma}$ of $\hat{\Sigma}$ contains exactly one of the rays $\hat{\mathbf{0}}$ and $\hat{\mathbf{0}}'$. We consider the quotient maps

$$\bar{\eta}_{\mathbb{R}}: N_{\mathbb{R}} \times \mathbb{R} \rightarrow N(\hat{\mathbf{0}})_{\mathbb{R}} \text{ and } \bar{\eta}'_{\mathbb{R}}: N_{\mathbb{R}} \times \mathbb{R} \rightarrow N(\hat{\mathbf{0}}')_{\mathbb{R}},$$

where $N(\hat{\mathbf{0}}) \cong N$ and $N(\hat{\mathbf{0}}') \cong N$ are the respective quotient lattices. More precisely, let $N_{\hat{\mathbf{0}}}$ be the sublattice of $N \times \mathbb{Z}$ spanned by the points in $\hat{\mathbf{0}} \cap (N \times \mathbb{Z})$, then we set $N(\hat{\mathbf{0}}) = (N \times \mathbb{Z})/N_{\hat{\mathbf{0}}}$. According to (2.4.2) the images of the cones $\hat{\sigma} \in \hat{\Sigma}$ can be identified with the cones $\sigma \in \Sigma$ and thus the fan Σ can be recovered as $\text{star}(\hat{\mathbf{0}})$ and $\text{star}(\hat{\mathbf{0}}')$. Thus as orbit closures $X_0 = V(\hat{\mathbf{0}})$ and $X_{\infty} = V(\hat{\mathbf{0}}')$ are isomorphic to the variety X by Proposition 3.2.7 in [CLS11].

If we consider X_0 and X_{∞} as divisors on \hat{X} , it remains to argue, that the desired linear equivalence holds. Since $L = \sum_{\rho \in \Sigma(1)} c_{\rho} D_{\rho}$ is an effective Cartier divisor on X , we have $c_{\rho} \geq 0$ for all $\rho \in \Sigma(1)$. The associated support function SF_{π^*L} of the pullback π^*L takes values $\text{SF}_{\pi^*L}(u_{\hat{\rho}}) = -c_{\rho}$ for the corresponding rays $\hat{\rho}$ in $\hat{\Sigma}$ with $\bar{\pi}(u_{\hat{\rho}}) = u_{\rho}$. Whereas $\text{SF}_{\pi^*L}(u_{\hat{\mathbf{0}}}) = \text{SF}_{\pi^*L}(u_{\hat{\mathbf{0}}'}) = 0$. Let SF_{X_0} denote the support function that corresponds to X_0 , i.e., $\text{SF}_{X_0}(u_{\hat{\mathbf{0}}}) = -1$ and it has value 0 on all the other primitive ray generators. Similarly, we define $\text{SF}_{X_{\infty}}$ to be the support function associated to X_{∞} . We consider the linear function $f: |\hat{\Sigma}| \rightarrow \mathbb{R}$ that gives the height, meaning the last coordinate of each primitive ray generator. This means $f(u_{\hat{\mathbf{0}}}) = 1$, $f(u_{\hat{\mathbf{0}}'}) = -1$ and $f(u_{\hat{\rho}}) = -c_{\rho}$ for all the other rays $\hat{\rho} \in \hat{\Sigma}(1)$. Thus we have $X_0 \sim X_{\infty} + \pi^*L$.

Example 2.4.7. As in our ongoing Example 2.4.5 we consider the variety $\hat{X} = \mathcal{H}_1$ for the divisor $L = D_0$ on $X = \mathbb{P}^1$. Then X_0 is the prime divisor of the ray spanned by $\hat{u}_2 = (0, 1)$ and X_{∞} the prime divisor of the ray spanned by $\hat{u}_4 = (0, -1)$.

GIVEN \hat{X} AND \hat{D} . WHAT IS THE RELATION BETWEEN THE NEWTON–OKOUNKOV BODY $\Delta_{\hat{Y}_{\bullet}}(\hat{D})$ AND THE SUBGRAPH $\hat{\Delta}$?

We are given the divisor $\hat{D} = \pi^*D + bX_{\infty}$ on \hat{X} . This means $\hat{D} = \sum_{\hat{\rho} \in \hat{\Sigma}(1)} a_{\hat{\rho}} \hat{D}_{\hat{\rho}}$, where $a_{\hat{\mathbf{0}}'} = b$ and $a_{\hat{\rho}} = a_{\hat{\rho}}^*$ for all other rays $\hat{\rho} \in \hat{\Sigma}(1) \setminus \{\hat{\mathbf{0}}'\}$. The associated fan $\hat{\Sigma} \times \hat{D}$ can be constructed as in (2.4.1). Now we are interested in the correspondence between the Newton–Okounkov body $\Delta_{\hat{Y}_{\bullet}}(\hat{D})$ and the subgraph $\hat{\Delta}$ on a geometric level.

Since D is a torus-invariant Cartier divisor on X , the divisor π^*D is torus-invariant on \hat{X} . In the previous section, we have seen that X_{∞} is torus-invariant as well and hence \hat{D} is a torus-invariant Cartier divisor on \hat{X} . Thus the Newton–Okounkov body $\Delta_{\hat{Y}_{\bullet}}(\hat{D})$ coincides with a translate of the rational polytope $P_{\hat{D}}$ that is determined by \hat{D} .

According to (2.2.3) this polytope is defined as

$$P_{\hat{D}} = \{(m, y) \in M_{\mathbb{R}} \times \mathbb{R} : \langle (m, y), u_{\hat{\rho}} \rangle \geq -a_{\hat{\rho}} \text{ for all } \hat{\rho} \in \hat{\Sigma}(1)\}.$$

Let us first consider the situation for the divisor π^*D . Since this is the pullback of a divisor on X , it has coefficients $-\text{SF}_{\pi^*D}(\mathbf{0}, 1) = -\text{SF}_{\pi^*D}(\mathbf{0}, -1) = 0$ for the corresponding divisors X_0 and X_∞ .

The resulting polyhedron P_{π^*D} in $M_{\mathbb{R}} \times \mathbb{R}$ is

$$P_{\pi^*D} = \{(m, y) \in M_{\mathbb{R}} \times \mathbb{R} : m \in \Delta_{Y_\bullet}(D), y \geq 0, y \leq 0\}.$$

If we now start adding tX_∞ to the divisor π^*D for small $t > 0$, the resulting polytope $P_{\pi^*D+tX_\infty}$ becomes full-dimensional and has P_{π^*D} as a facet that corresponds to the ray $\hat{\mathbf{0}}$. This means that P_{π^*D} determines a divisor on $X_0 \cong V(\hat{\mathbf{0}})$. Since $X_0 \cap X_\infty = \emptyset$, this is actually the divisor π^*D . In addition, we have $X_0 \cong X$ and hence $P_{\pi^*D} \cong P_D \cong \Delta_{Y_\bullet}(D)$.

Let us now consider the facet of $P_{\pi^*D+tX_\infty}$ that corresponds to the ray $\hat{\mathbf{0}}'$. Analogously, this polytope corresponds to a divisor on $X \cong X_\infty \cong V(\hat{\mathbf{0}}')$. Due to $\pi^*D + tX_\infty \sim \pi^*D + t(X_0 - \pi^*L) = \pi^*(D - tL) + tX_0$ and $X_0 \cap X_\infty = \emptyset$ this is the divisor $D - tL$ on X . For t small enough, this polytope appears as a facet and thus has codimension 1, meaning, that the divisor $D - tL$ is big on X . The required condition $b > \sup\{t > 0 : D - tL \text{ is big}\}$ means on the polytope side that we have $\langle m, u_{\hat{\mathbf{0}}'} \rangle > -a_{\hat{\mathbf{0}}'} = -b$ for all $m \in P_D$ and thus the facet disappears.

We claim that the polytope $\Delta_{\hat{Y}_\bullet}(\hat{D})$ is isomorphic to the wedge of P_D over its facet F_L associated to L if D is ample and the other divisor is $L = D_{\rho_L}$ for some ray $\rho_L \in \Sigma$.

To verify the claim, we must review the involved defining inequalities. For L its corresponding facet $F_L \preceq P_D$ in the polytope P_D is determined by an inequality of the form

$$\langle m, u_{\rho_L} \rangle \geq -a_{\rho_L},$$

for $m \in M_{\mathbb{R}}$. According to the construction of the fan $\hat{\Sigma}$ as in (2.4.2) there is a unique ray $\hat{\rho}_L \in \hat{\Sigma}(1)$ generated by $u_{\hat{\rho}_L} = (u_{\rho_L}, -1)$ that corresponds to ρ_L . The only other ray generators $u_{\hat{\rho}}$ for $\hat{\rho} \in \hat{\Sigma}(1)$ having a non-zero last coordinate are $u_{\hat{\mathbf{0}}} = (\mathbf{0}, 1)$ and $u_{\hat{\mathbf{0}}'} = (\mathbf{0}, -1)$.

In the new polytope $P_{\hat{D}}$ the ray $\hat{\rho}_L$ is associated to a facet $\hat{F}_L \preceq P_{\hat{D}}$ that is determined by the inequality

$$\langle m, u_{\rho_L} \rangle - y = \langle (m, y), u_{\hat{\rho}_L} \rangle \geq -a_{\hat{\rho}_L} = -a_{\rho_L},$$

for $(m, y) \in M_{\mathbb{R}} \times \mathbb{R}$.

This shows that

$$P_{\hat{D}} \cong \text{wedge}_{\hat{F}_L}(P_D).$$

According to Proposition 2.4.1 it follows that the Newton–Okounkov body $\Delta_{\hat{Y}_\bullet}(\hat{D}) = P_{\hat{D}}$ coincides with the subgraph of φ_L over $\Delta_{Y_\bullet}(D)$.

Example 2.4.8. We continue with Example 2.4.5. In addition to the data $X = \mathbb{P}^1$, $L = D_0$, we choose the toric flag $Y_1 = V(\sigma_0)$ and the big divisor $D = 2D_0$. Then the flag \hat{Y}_\bullet consists of $\hat{Y}_1 = V(\hat{\sigma}_0)$ and $\hat{Y}_2 = \iota_0(Y_1) = V(\hat{\sigma}_0)$. We have seen in Example 2.4.6 that $\pi^*D = 2\hat{D}_1$, where \hat{D}_1 is the prime divisor associated to the ray generator $\hat{u}_1 = (1, -1)$. Due to Example 2.4.7 the divisor X_∞ is \hat{D}_4 , associated to $\hat{u}_2 = (0, -1)$.

For the line segment P_D the facet F_L is determined by the inequality $m \geq -2$, for $m \in \mathbb{R}$. It turns into the facet-defining inequality $m - y \geq -2$ for $(m, y) \in \mathbb{R}^2$ for the polytope $P_{\hat{D}}$.

The left part of Figure 2.18 shows the polytope $P_{\pi^*D+tX_\infty}$ corresponding to the divisor $\pi^*D + tX_\infty = 2\hat{D}_1 + t\hat{D}_4$ for small $t > 0$ and the right part shows the polytope $P_{\hat{D}}$ for $t = b$.

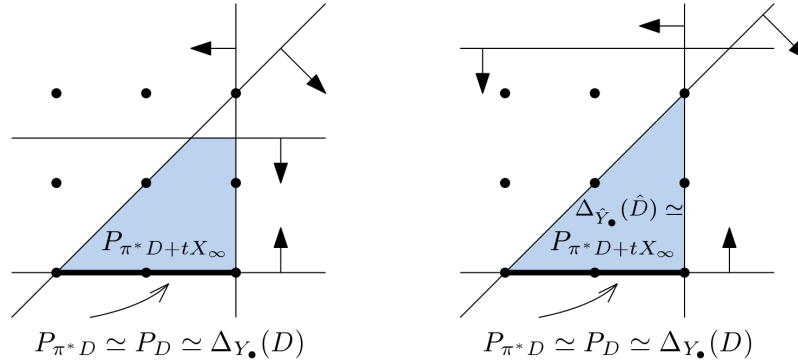


Figure 2.18: The polytope $P_{\pi^*D+tX_\infty}$ for small t on the left and for $t = b$ on the right.

2.4.3 Geometric Valuation Coming from a General Point

Let X be a smooth projective toric surface and D an ample divisor on X . In this section we relax the requirements in the sense that the function φ_R now comes from the geometric valuation ord_R at a general point R , not necessarily torus-invariant. Here we can determine the values of φ_R on parts of $\Delta_{Y_\bullet}(D)$ and give an upper bound on the entire Newton–Okounkov body.

In order to do so, we need to introduce some more terminology. We are given an admissible torus-invariant flag $Y_\bullet: X \supseteq Y_1 \supseteq Y_2$ on X . Since Y_\bullet is toric, the Newton–Okounkov body $\Delta_{Y_\bullet}(D) \subseteq \mathbb{R}^2$ is isomorphic to P_D and one of its facets corresponds to Y_1 . Let $u \in (\mathbb{R}^2)^*$ denote the defining linear functional that selects this face Y_1 , when minimized over the polytope $\Delta_{Y_\bullet}(D)$. We denote by $F \preceq \Delta_{Y_\bullet}(D)$ the face that

is selected, when maximizing u over $\Delta_{Y_\bullet}(D)$. Either this already is a vertex or if not, we maximize u' over F , where $u' \in (\mathbb{R}^2)^*$ is a linear functional selecting Y_2 , when minimized over $\Delta_{Y_\bullet}(D)$. Denote the resulting vertex in $\text{vert}(\Delta_{Y_\bullet}(D))$ by p_{Y_\bullet} . We say that the vertex p_{Y_\bullet} lies at the *opposite side* of the polytope $\Delta_{Y_\bullet}(D)$ with respect to the flag Y_\bullet .

THEOREM 2.4.9. Let X be a smooth projective toric surface, D an ample divisor, and Y_\bullet an admissible torus-invariant flag on X . Denote by $\Delta_{Y_\bullet}(D)$ the corresponding Newton–Okounkov body and by $p = p_{Y_\bullet}$ the vertex at the opposite side of $\Delta_{Y_\bullet}(D)$ with respect to Y_\bullet . Moreover let $R \in \mathbb{T}$ be a general point. Then for the Newton–Okounkov function φ_R coming from the geometric valuation ord_R we have

1.

$$\varphi_R(a, b) \leq a + b$$

for all $(a, b) \in \Delta_{Y_\bullet}(D)$, where (a, b) are the coordinates in the coordinate system associated to p .

2. Furthermore, we have

$$\varphi_R(a, b) = a + b$$

for all

$$(a, b) \in \{(a', b') \in \Delta_{Y_\bullet}(D) : \text{NP}((x-1)^{a'}(y-1)^{b'}) \subseteq \Delta_{Y_\bullet}(D)\}.$$

Proof. 1. Let $(a, b) \in \Delta_{Y_\bullet}(D)$ be a valutive point in the Newton–Okounkov body. We want to determine $\varphi_R(a, b)$, where φ_R is the function coming from the geometric valuation ord_R . Consider an arbitrary section $s \in H^0(X, \mathcal{O}_X(kD))$ that is mapped to $(a, b) = \frac{1}{k} \text{val}_{Y_\bullet}(s)$ for some $k \in \mathbb{Z}_{\geq 1}$. Let $u, u' \in (\mathbb{R}^2)^*$ be as above. Then, by construction, the rescaled exponent vectors of all monomials that can occur in s have to be an element of the set

$$H^+ := \{m \in \Delta_{Y_\bullet}(D) : u(m) > u(a, b) \text{ or } (u(m) = u(a, b) \text{ and } u'(m) \geq u'(a, b))\}.$$

As indicated in Figure 2.19, this region is obtained by intersecting $\Delta_{Y_\bullet}(D)$ with the positive halfspace associated to the hyperplane $H = \{m : u(m) = u(a, b)\}$.

Moreover, we can assume, without loss of generality that the general point R is given as $R = (1, 1)$. To determine the order of vanishing of s at R we substitute x by $x' + 1$ and y by $y' + 1$ and bound the order of vanishing of $s'(x', y') = s(x' + 1, y' + 1)$ at $(0, 0)$. Assuming, without loss of generality that the monomial $x^{ka}y^{kb}$ itself occurs in s with coefficient 1, multiplying out gives

$$\begin{aligned} s'(x', y') &= s(x' + 1, y' + 1) = (x' + 1)^{ka}(y' + 1)^{kb} + \dots \\ &= (x')^{ka}(y')^{kb} + \text{lower order terms} + \dots \end{aligned}$$

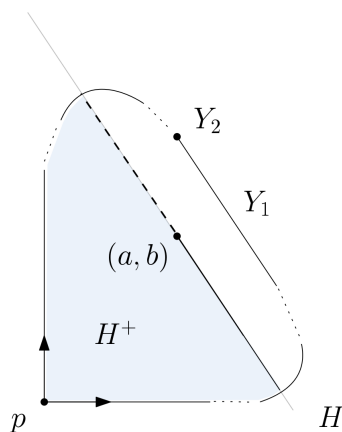


Figure 2.19: Admissible region H^+ of rescaled exponent vectors associated to monomials of s inside the Newton–Okounkov body $\Delta_{Y_\bullet}(D)$.

CLAIM: The monomial $(x')^{ka}(y')^{kb}$ cannot be canceled out by terms coming from ***.

Aiming at a contradiction, assume that *** contains a monomial $(x' + 1)^{kc}(y' + 1)^{kd}$ for some $kc, kd \in \mathbb{Z}_{\geq 1}$ that produces $(x')^{ka}(y')^{kb}$ when multiplied out. Observe that multiplying out $(x' + 1)^{kc}(y' + 1)^{kd}$ produces all monomials in $\{(x')^e(y')^f : e \leq kc \text{ and } f \leq kd\}$. Thus $kc \geq ka$ and $kd \geq kb$. In addition, as an exponent vector of a monomial in s , the point (c, d) is required to be an element of the set H^+ , which forces the hyperplane H to have positive slope as indicated in Figure 2.20.

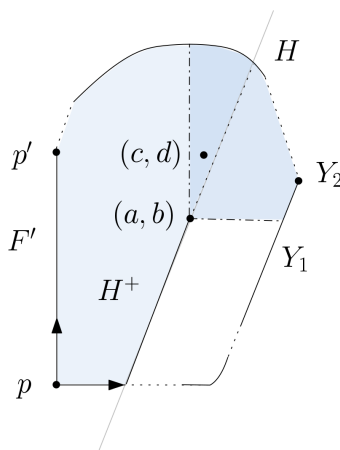


Figure 2.20: A non-empty region of points $(c, d) \in H^+$ that satisfy $c \geq a$ and $d \geq b$ forcing H to have positive slope.

Let $F' \preceq \Delta_{Y_\bullet}(D)$ denote the face that corresponds to $\{x = 0\}$ and let p' denote its second vertex. Then $u(p') > u(p)$ which contradicts the fact that u is maximized at p over $\Delta_{Y_\bullet}(D)$. Thus such a monomial $(x' + 1)^{kc}(y' + 1)^{kd}$ cannot exist and $(x')^{ka}(y')^{kb}$ does not cancel out.

Consequently, $k(a + b)$ is an upper bound for the order of vanishing of s' at $(0, 0)$ and thus for s at R . Since this is true for all sections s that get mapped to (a, b) , this yields $\varphi_R(a, b) \leq a + b$.

2. Consider a point

$$(a, b) \in \text{Par} := \{(a', b') \in \Delta_{Y_\bullet}(D) : \text{NP}((x - 1)^{a'}(y - 1)^{b'}) \subseteq \Delta_{Y_\bullet}(D)\},$$

and set $s(x, y) = (x - 1)^{ka}(y - 1)^{kb}$, for a $k \in \mathbb{Z}_{\geq 1}$ such that s is a global section of kD , whose Newton polytope can be seen in Figure 2.21. Then by construction, s is a section associated to the point (a, b) and its Newton polytope fits inside $k\Delta_{Y_\bullet}(D)$. We have $\text{ord}_R(s) = k(a + b)$ which gives the lower bound $\varphi_R(a, b) \geq \frac{1}{k} \text{ord}_R(s)$. Combined with 1. we obtain $\varphi_R(a, b) = a + b$.

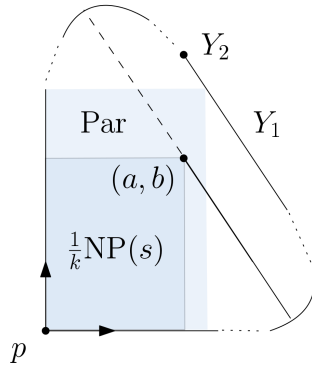


Figure 2.21: The scaled Newton polytope $\frac{1}{k} \text{NP}(s)$ of the section $s(x, y) = (x - 1)^{ka}(y - 1)^{kb}$.

□

We illustrate the use of Theorem 2.4.9 by the following example.

Example 2.4.10. We continue our running example of the Hirzebruch surface $X = \mathcal{H}_1$ and the ample divisor $D = D_3 + 2D_4$ as in Example 2.3.6. Furthermore, fix the torus-invariant flag $Y_\bullet: X \supseteq Y_1 \supseteq Y_2$, where $Y_1 = D_1$ and $Y_2 = D_1 \cap D_2$. Then the vertex $p = p_{Y_\bullet}$ of the Newton–Okounkov body $\Delta_{Y_\bullet}(D) \cong P_D$ that lies at the opposite side of the polytope P_D with respect to the flag Y_\bullet is the one indicated in Figure 2.22. The associated coordinate system specifies coordinates a, b for the plane \mathbb{R}^2 and local toric coordinates x, y .

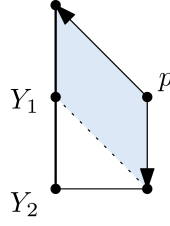


Figure 2.22: The coordinate system associated to the vertex p which lies at the opposite side of P_D with respect to the flag Y_\bullet .

We want to determine the Newton–Okounkov function coming from the geometric valuation at the point $R = (1, 1)$. Theorem 2.4.9 yields the upper bound $\varphi_R(a, b) \leq a + b$ on the entire Newton–Okounkov body $\Delta_{Y_\bullet}(D)$, and $\varphi_R(a, b) = a + b$ for (a, b) satisfying $a, b \leq 1$, as indicated by the shaded region in Figure 2.22. It will turn out in Example 2.4.13 that there exist points $(a, b) \in \Delta_{Y_\bullet}(D)$ for which we have $\varphi_R(a, b) < a + b$.

For a particularly nice class of polygons, Theorem 2.4.9 alone is enough to determine the function φ_R . A polytope $P \subseteq \mathbb{R}_{\geq 0}^n$ is called anti-blocking if $P = (P + \mathbb{R}_{\leq 0}^n) \cap \mathbb{R}_{\geq 0}^n$ (compare [Ful71; Ful72]). Observe that this coordinate dependent property implies (and for $n = 2$ is equivalent to) the fact that the parallelepiped spanned by the edges at the origin covers P .

COROLLARY 2.4.11. Let X, Y_\bullet, D and R be as in Theorem 2.4.9. Suppose $\Delta_{Y_\bullet}(D)$ is anti-blocking. Let Y'_\bullet be a torus-invariant flag opposite to the origin. Then the Newton–Okounkov function φ_R on $\Delta_{Y'_\bullet}(D)$ is given by

$$\varphi_R(a, b) = a + b$$

on the entire Newton–Okounkov body $\Delta_{Y'_\bullet}(D) \cong P_D$ in the coordinate system associated to Y'_\bullet .

Using the tools from Section 2.5, Corollary 2.4.11 implies that the Seshadri constant of D at R is rational. This can also be seen from Sano’s Theorem [San14] as $\dim | -K_X| \geq 3$ in the anti-blocking case.

If we are not in the lucky situation of Corollary 2.4.11, then things are getting more complicated and more interesting. We give an approach that works in numerous cases.

THE GENERAL STRATEGY

For the remainder of the chapter we will consider the following situation.

THE GENERAL SET-UP 2.4.12.

- X a smooth projective toric surface,
- D an ample torus-invariant divisor on X ,
- Y_\bullet an admissible torus-invariant flag,
- v the primitive direction of the edge of $P_D \cong \Delta_{Y_\bullet}(D)$ corresponding to Y_1 , towards the vertex corresponding to Y_2 ,
- u the primitive ray generator corresponding to Y_1 ,
- C the curve in X given by the binomial $x^v - 1$,
- R a general point on C ,
- Y'_\bullet the admissible flag $X \supseteq C \supseteq \{R\}$,
- Ψ the piecewise linear, volume-preserving isomorphism $\Delta_{Y_\bullet}(D) \rightarrow \Delta_{Y'_\bullet}(D)$ from Corollary 2.3.8,
- φ_R the function $\Delta_{Y_\bullet}(D) \rightarrow \mathbb{R}$ coming from the geometric valuation ord_R ,
- φ'_R the function $\Delta_{Y'_\bullet}(D) \rightarrow \mathbb{R}$ coming from the geometric valuation ord_R .

GOAL: Determine the function

$$\varphi_R: \Delta_{Y_\bullet}(D) \cong P_D \rightarrow \mathbb{R}.$$

APPROACH:

1. For each valiative point $(a, b) \in \Delta_{Y_\bullet}(D)$ ‘guess’ a Newton polytope $\frac{1}{k} \text{NP}(s) \subseteq P_D$ of a global section $s \in H^0(X, \mathcal{O}_X(kD))$ for some $k \in \mathbb{Z}_{\geq 1}$ to maximize the order of vanishing $\text{ord}_R(s)$ according to the following rules:
 - The section s has to correspond to the point (a, b) .
 - Choose a Newton polytope $\text{NP}(s)$ that is a zonotope whose edge directions all come from edges in P_D .
 - Try to maximize the perimeter of the Newton polytope $\frac{1}{k} \text{NP}(s)$ among the above.
2. Determine the values of the function $\varphi: \Delta_{Y_\bullet}(D) \rightarrow \mathbb{R}$ that takes $\frac{1}{k} \text{ord}_R(s)$ as a value with respect to the chosen sections s for a point $(a, b) \in \Delta_{Y_\bullet}(D)$ and compute the integral $\int_{\Delta_{Y_\bullet}(D)} \varphi$.

3. Compute the Newton–Okounkov body $\Delta_{Y'_\bullet}(D)$ with respect to the new flag Y'_\bullet using variation of Zariski decomposition or the combinatorial methods from Section 2.3.
4. Compute the integral $\int_{\Delta_{Y'_\bullet}(D)} \varphi'$, where we assume the function to be given by

$$\begin{aligned} \varphi' : \Delta_{Y'_\bullet}(D) &\rightarrow \mathbb{R} \\ (a', b') &\mapsto a' + b'. \end{aligned}$$

5. Compare the value of the integrals $\int_{\Delta_{Y_\bullet}(D)} \varphi$ and $\int_{\Delta_{Y'_\bullet}(D)} \varphi'$. It holds that

$$\int_{\Delta_{Y_\bullet}(D)} \varphi \leq \int_{\Delta_{Y_\bullet}(D)} \varphi_R = \int_{\Delta_{Y'_\bullet}(D)} \varphi'_R \leq \int_{\Delta_{Y'_\bullet}(D)} \varphi'. \quad (2.4.3)$$

- If $\int_{\Delta_{Y_\bullet}(D)} \varphi = \int_{\Delta_{Y'_\bullet}(D)} \varphi'$, then we have equality in (2.4.3) and therefore a certificate that the choices that we have made were valid and we are done.
- If $\int_{\Delta_{Y_\bullet}(D)} \varphi < \int_{\Delta_{Y'_\bullet}(D)} \varphi'$, then either we have chosen sections with non-maximal orders of vanishing at R in step 1 or for the chosen vector v the function φ'_R takes values smaller than $a' + b'$ somewhere on $\Delta_{Y'_\bullet}(D)$.

Example 2.4.13. We return to Example 2.4.10, and again consider the Hirzebruch surface $X = \mathcal{H}_1$ equipped with the torus-invariant flag $Y_\bullet : X \supseteq Y_1 \supseteq Y_2$, where $Y_1 = D_1$ and $Y_2 = D_1 \cap D_2$ and the ample divisor $D = D_3 + 2D_4$ on X . We want to determine the values of a function on $\Delta_{Y_\bullet}(D)$ coming from a geometric valuation at a general point, so let $R = (1, 1) \in X$ in local coordinates. More precisely, for the rational points in $\Delta_{Y_\bullet}(D)$ in the coordinate system associated to the flag Y_\bullet we study

$$\begin{aligned} \varphi_R : \Delta_{Y_\bullet}(D) &\rightarrow \mathbb{R} \\ (a, b) &\mapsto \lim_{k \rightarrow \infty} \frac{1}{k} \sup \{ t \in \mathbb{R} : \text{there exists } s \in H^0(X, \mathcal{O}_X(kD)) : \\ &\quad \text{val}_{Y_\bullet}(s) = k(a, b), \text{ord}_R(s) \geq t \} \\ &= \lim_{k \rightarrow \infty} \frac{1}{k} \sup \{ t \in \mathbb{R} : \text{there exists } s \in H^0(X, \mathcal{O}_X(kD)) : \\ &\quad \text{ord}_{Y_1}(s) = ka, \text{ord}_{Y_2}(s) = kb, \text{ord}_R(s) \geq t \}, \end{aligned}$$

where s_1 is given as in (2.2.7).

We claim that φ_R coincides with the function φ given by

$$\varphi(a, b) = \begin{cases} 2 - a & \text{if } 0 \leq a + b \leq 1 \\ 3 - 2a - b & \text{if } 1 \leq a + b \leq 2 \end{cases}$$

at a point $(a, b) \in \Delta_{Y_\bullet}(D)$.

To verify this claim, we will give explicit respective sections and argue that the maximal value of ord_R is achieved for these particular sections. We treat the two cases individually.

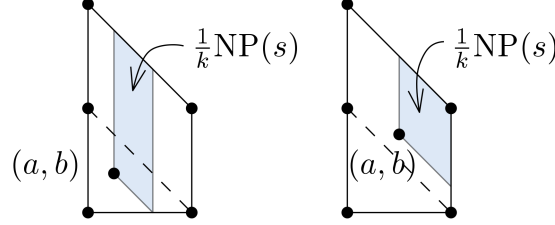


Figure 2.23: Newton polytopes $\frac{1}{k} \text{NP}(s)$ of the respective sections s .

$$0 \leq a + b \leq 1:$$

Set

$$s(x, y) = (x^a(y-1)^{2-a-b}(x-y)^b)^k$$

in local coordinates x, y for suitable $k \in \mathbb{Z}_{\geq 1}$. The corresponding Newton polytope $\frac{1}{k} \text{NP}(s)$ is depicted in Figure 2.23. Since the leftmost part of it has coordinates (a, \cdot) , we have $\text{ord}_{Y_1}(s) = ka$. If we restrict to the line (a, \cdot) , then the lowest point of the Newton polytope is (a, b) and thus $\text{ord}_{Y_2}(s_1) = kb$. Together with the fact that the Newton polytope $\frac{1}{k} \text{NP}(s)$ fits inside the Newton–Okounkov body $\Delta_{Y_\bullet}(D)$, this guarantees that the section s is actually mapped to the point (a, b) when computing $\Delta_{Y_\bullet}(D)$.

For the order of vanishing of interest we obtain

$$\text{ord}_R(s) = k((2 - a - b) + b) = k(2 - a).$$

$$1 \leq a + b \leq 2:$$

Set

$$s(x, y) = (x^a y^{a+b-1} (y-1)^{2-a-b} (x-y)^{1-a})^k.$$

That all the requirements are fulfilled by s follows by using the same arguments as in the previous case. For the order of vanishing of interest we obtain

$$\text{ord}_R(s) = k((2 - a - b) + (1 - a)) = k(3 - 2a - b).$$

The values of the resulting piecewise linear function are depicted in Figure 2.24.

If we integrate φ over $\Delta_{Y_\bullet}(D)$, we obtain

$$\int_{\Delta_{Y_\bullet}(D)} \varphi = \frac{11}{6}.$$

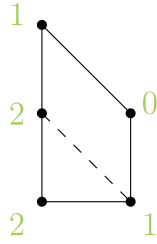


Figure 2.24: The values of the function φ on $\Delta_{Y_\bullet}(D)$.

Now it remains to show that these values are actually the maximal ones that can be realized. In order to do this, we make use of the fact that the integral of our function φ over the Newton–Okounkov body $\Delta_{Y_\bullet}(D)$ is independent of the flag Y_\bullet .

We keep the underlying variety X and the ample divisor D . Choose a new admissible flag $Y'_\bullet: X \supseteq Y'_1 \supseteq Y'_2$, where Y'_1 is the curve defined by the local equation $y^{-1} - 1 = 0$ and $Y'_2 = R = (1, 1)$ is the point of the geometric valuation. Since this flag is no longer torus-invariant, the corresponding Newton–Okounkov body $\Delta_{Y'_\bullet}(D)$ will differ from the polytope P_D . As shown in Example 2.3.6, we obtain the new Newton–Okounkov body $\Delta_{Y'_\bullet}(D)$ depicted in Figure 2.7.

For the function φ'_R on $\Delta_{Y'_\bullet}(D)$, we are still working with the geometric valuation associated to ord_R . Thus, set

$$\begin{aligned} \varphi' : \Delta_{Y'_\bullet}(D) &\rightarrow \mathbb{R} \\ (a', b') &\mapsto a' + b'. \end{aligned}$$

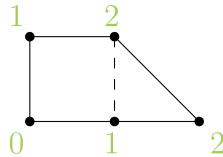


Figure 2.25: The values of the function φ' on $\Delta_{Y'_\bullet}(D)$.

The values of φ' are depicted in Figure 2.25. If we integrate φ' over $\Delta_{Y'_\bullet}(D)$, we obtain

$$\int_{\Delta_{Y'_\bullet}(D)} \varphi' = \frac{11}{6}.$$

Overall, we have $\int_{\Delta_{Y_\bullet}(D)} \varphi = \int_{\Delta_{Y'_\bullet}(D)} \varphi'$. This shows that our choice for the section s was indeed maximal with respect to $\text{ord}_R(s)$ and thus determines the value of $\varphi_R = \varphi$.

Remark 2.4.14. In the previous example the integrals $\int_{\Delta_{Y_\bullet}(D)} \varphi$ and $\int_{\Delta_{Y'_\bullet}(D)} \varphi'$ coincide. Observe that even more is true. Let

$$G(\varphi) = \{(a, b, \varphi(a, b)) : (a, b) \in \Delta_{Y_\bullet}(D)\}$$

denote the graph of φ . Since φ is a concave and piecewise linear function, the set

$$\Delta_{Y_\bullet}(D)_\varphi := \text{conv}((\Delta_{Y_\bullet}(D) \times \{0\}) \cup G(\varphi)) \subseteq \mathbb{R}^3$$

is a 3-dimensional polytope. If we compare $\Delta_{Y_\bullet}(D)_\varphi$ and $\Delta_{Y'_\bullet}(D)_{\varphi'}$, it turns out that they are $\text{SL}_3(\mathbb{Q})$ -equidecomposable, where the respective maps are volume-preserving. To see this, we give the explicit maps, where ψ_1 and ψ_2 come from the piecewise linear pieces of Ψ on the respective domains of linearity. Use

$$\begin{aligned} \psi_1: \mathbb{R}^3 &\rightarrow \mathbb{R}^3 \\ \begin{pmatrix} a \\ b \\ c \end{pmatrix} &\mapsto \begin{pmatrix} -1 & -1 & 0 \\ -1 & 0 & 0 \\ 0 & 0 & 1 \end{pmatrix} \cdot \begin{pmatrix} a \\ b \\ c \end{pmatrix} + \begin{pmatrix} 2 \\ 1 \\ 0 \end{pmatrix} \end{aligned}$$

to map the parallelogram in $\Delta_{Y_\bullet}(D)$ with its corresponding heights, and use

$$\begin{aligned} \psi_2: \mathbb{R}^3 &\rightarrow \mathbb{R}^3 \\ \begin{pmatrix} a \\ b \\ c \end{pmatrix} &\mapsto \begin{pmatrix} -1 & -1 & 0 \\ 0 & 1 & 0 \\ 0 & 0 & 1 \end{pmatrix} \cdot \begin{pmatrix} a \\ b \\ c \end{pmatrix} + \begin{pmatrix} 2 \\ 0 \\ 0 \end{pmatrix} \end{aligned}$$

for mapping the triangle in $\Delta_{Y'_\bullet}(D)$ with its corresponding heights. This is illustrated in Figure 2.26, where the respective heights are given in green.

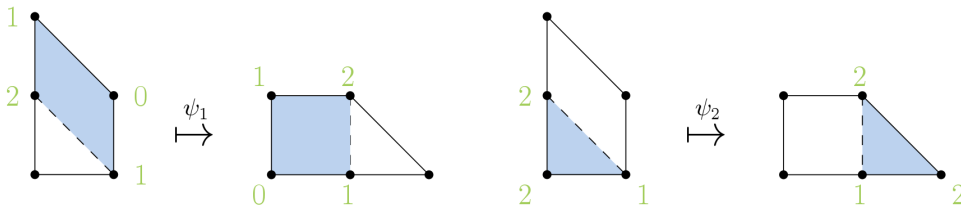


Figure 2.26: $\text{SL}_3(\mathbb{Q})$ -equidecomposable pieces of the Newton–Okounkov bodies $\Delta_{Y_\bullet}(D)$ on the left and $\Delta_{Y'_\bullet}(D)$ on the right.

We conjecture that this is not a coincidence but holds in our general set-up.

CONJECTURE 2.4.15. In the situation of our general set-up 2.4.12, $\varphi_R = \varphi'_R \circ \Psi$.

The approach for determining the Newton–Okounkov function via Ψ applies to a certain class of polytopes. To describe this class we need to introduce the following term.

Definition 2.4.16. Let $P \subseteq \mathbb{R}^2$ be a polygon. Let $v \in \mathbb{Z}^2$ be a primitive vector, and $u \in v^\perp$ a primitive integral functional.

We call P *zonotopally well-covered with respect to (v, u)* if for all points $m \in P$ the set $P_v(m)$ contains a zonotope $L_1 + \dots + L_\ell$ with none of the L_i parallel to v , such that

$$\sum_{i=1}^{\ell} \text{length}_{\mathbb{Z}^2}(L_i) = \text{width}_u(P_v(m)).$$

The polygon P is *zonotopally well-covered* if it is so with respect to some (v, u) .

In fact, it is enough to check the condition for the finitely many vertices of domains of linearity of Ψ .

THEOREM 2.4.17. In the situation of our general set-up 2.4.12, if the polytope $\Delta_{Y_\bullet}(D)$ is zonotopally well-covered with respect to (v, u) , then $\varphi_R = \varphi'_R \circ \Psi$ and $\varphi'_R(a', b') = a' + b'$.

In particular, Conjecture 2.4.15 holds in this case.

Proof. According to our general strategy, it is sufficient to certify, for every valuat-
ive point $m \in \Delta_{Y_\bullet}(D) \cap \mathbb{Q}^2$, the existence of a section $s \in H^0(X, \mathcal{O}_X(kD))$ for some
 $k \in \mathbb{Z}_{\geq 1}$ with $\frac{1}{k} \text{val}_{Y_\bullet}(s) = m$ and with order of vanishing $\text{ord}_R(s) = k(a' + b')$ where
 $\Psi(m) =: (a', b')$.

To this end, let $L_1 + \dots + L_\ell$ be the zonotope inside $P_v(m)$ which must exist because
 $\Delta_{Y_\bullet}(D)$ is zonotopally well-covered. Add the segment L_0 from $\mathbf{0}$ to $\text{length}(P, m, v) \cdot v$
to obtain a rational zonotope

$$L_0 + L_1 + \dots + L_\ell \subseteq L_0 + P_v(m) \subseteq \Delta_{Y_\bullet}(D)$$

inside $\Delta_{Y_\bullet}(D)$ with valuation vertex m . If k is a common denominator of its vertices, the
 k -th dilate is the Newton polytope of a product of binomials which vanishes to order

$$k \cdot \sum_{i=0}^{\ell} \text{length}_M(L_i) = k \cdot (\text{length}(P, m, v) + \text{width}_u(P_v(m))) = k \cdot (a' + b')$$

as required. □

Remark 2.4.18. The property of being centrally-symmetric is not sufficient for being zonotopally well-covered. Consider for instance the polytope

$$P = \text{conv}((0,0), (2,1), (1,3), (-1,2)) \subseteq \mathbb{R}^2$$

in Figure 2.27 and the direction $v = (-1,0)$ with $u = (0,1)$. Then for the point $m = (-\frac{1}{2}, 1)$ the polygon has length $\text{length}(P, m, v) = \frac{5}{2}$ at m with respect to v . The intersection $P_v(m) = P \cap (P + \frac{5}{2} \cdot (-1,0))$ is just a line segment L whose lattice length is $\text{length}_{\mathbb{Z}^2}(L) = \frac{1}{2}$. But on the other hand, we have $\text{width}_u(P_v(m)) = 1 > \frac{1}{2}$.

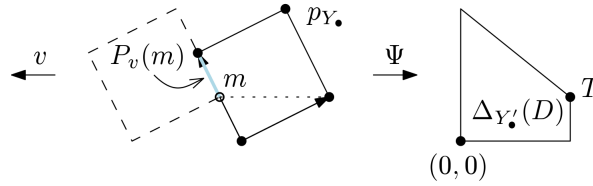


Figure 2.27: An instance of a centrally-symmetric polytope P that is not zonotopally well-covered.

It remains to argue, why any other direction $v \in \mathbb{Z}^2$ will also fail. If we interpret P as the Newton–Okounkov body $\Delta_{Y_\bullet}(D)$ for some completely toric situation X, D, Y_\bullet , then the shifting process by the vector $v = (-1,0)$ yields the polytope on right in Figure 2.27 as the Newton–Okounkov body $\Delta_{Y'_\bullet}(D)$ for the adjusted flag Y'_\bullet , where Y'_1 is the curve determined by v and $Y'_2 = R = (1,1)$. Consider the Newton–Okounkov function $\varphi'_R: \Delta_{Y'_\bullet}(D) \rightarrow \mathbb{R}$. Since $\varphi'_R(a', b') \leq a' + b'$ and $\max_{(a', b') \in \Delta_{Y'_\bullet}(D)} \varphi'_R(a', b')$ is independent of the flag, this yields that $\max \varphi'_R \leq \frac{7}{2}$. A straight forward computation shows that any primitive direction $v \in \mathbb{Z}^2$ with $\|v\| > 1$ results in a vertex $(0, b') \in \Delta_{Y'_\bullet}(D)$ with $b' > \frac{7}{2}$ which is a contradiction to the above.

Although P is not the polytope of an ample divisor on a smooth surface, it can be used as a starting point to construct such an example: The minimal resolution $\pi: X_p^* \rightarrow X_p$ has a centrally-symmetric fan. There is a ‘centrally-symmetric’ ample \mathbb{Q} -divisor on X_p^* near the nef divisor π^*D . Now scale up the resulting rational polygon to a lattice polygon.

A similar argument applies to the polygon from Example 4.6 in [Cas+20], which is depicted in Figure 2.28. The authors construct examples of projective toric surfaces whose blow-up at a general point has a non-polyhedral pseudo-effective cone. In this context they introduce, what they call *good* polytopes. For our particular instance of a good polytope the authors argue, that all sections $s \in H^0(X, \mathcal{O}_X(kD))$ will have order of vanishing at most $7k$ at the general point. However, all primitive directions $v \in \mathbb{Z}^2$ will produce a vertex of $\Psi(P)$ with coordinate sum > 7 .

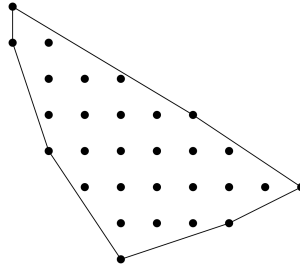


Figure 2.28: A polygon for which our approach does not work.

We give another example for which our strategy works.

Example 2.4.19. Let $\pi : X \rightarrow \mathbb{P}^2$ be the blow-up of the projective plane in the three torus fixed points with corresponding exceptional divisors E_1, E_2 and E_3 . We denote by H the pullback of the hyperplane class and by $E_{ij} := H - E_i - E_j$ the strict transforms of the lines through two distinct blown-up points z_i and z_j for $i, j \in \{1, 2, 3\}$ and $i \neq j$, respectively. The corresponding fan is shown in Figure 2.29.

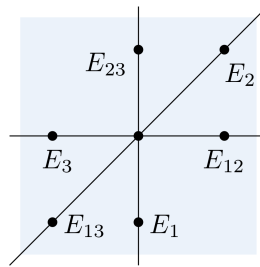


Figure 2.29: The fan Σ with prime divisors E_1, \dots, E_{23} .

We fix an admissible torus-invariant flag $Y_\bullet : X = Y_0 \supseteq Y_1 \supseteq Y_2$ such that $Y_1 = \overline{\{x = 0\}}$ and $Y_2 = (0, 0)$ for the local coordinates as in Figure 2.30. As a big Cartier divisor we choose $D = 3H - E_1 - E_2 - E_3$. Since we are again in a toric situation, the Newton–Okounkov body $\Delta_{Y_\bullet}(D)$ is given by a translate of the polytope P_D as depicted in Figure 2.30.

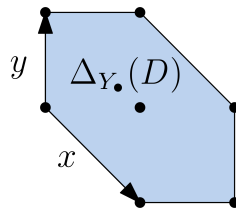


Figure 2.30: Local toric coordinates x, y for the Newton–Okounkov body $\Delta_{Y_\bullet}(D)$.

We now want to study the function φ_R on $\Delta_{Y_\bullet}(D)$ coming from the geometric valuation associated to the order of vanishing of a section at the general point $R = (1, 1)$. We claim, that the following sections achieve the maximal order of vanishing at R for suitable $k \in \mathbb{Z}_{\geq 1}$. The fact that they fulfill the required conditions follows as in Example 2.4.13.

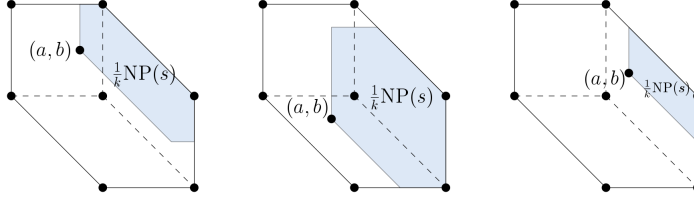


Figure 2.31: Newton polytopes $\frac{1}{k} \text{NP}(s)$ of the respective sections s inside $\Delta_{Y_\bullet}(D)$.

$$\boxed{a \leq 1, a \leq b:}$$

Set

$$s(x, y) = (x^a y^b (x-1)(y-1)^{1+a-b} (1-xy)^{1-a})^k.$$

For the order of vanishing of interest we obtain

$$\text{ord}_R(s) = k(1 + (1 + a - b) + (1 - a)) = k(3 - b).$$

$$\boxed{b \leq 1, b \leq a:}$$

Set

$$s(x, y) = (x^a y^b (x-1)^{1-a+b} (y-1)(1-xy)^{1-b})^k.$$

For the order of vanishing of interest we obtain

$$\text{ord}_R(s) = k((1 - a + b) + 1 + (1 - b)) = k(3 - a).$$

$$\boxed{a \geq 1, b \geq 1:}$$

Set

$$s(x, y) = (x^a y^b (x-1)^{2-a} (y-1)^{2-b})^k.$$

For the order of vanishing of interest we obtain

$$\text{ord}_R(s) = k((2 - a) + (2 - b)) = k(4 - a - b).$$

This determines a function

$$\varphi(a,b) = \begin{cases} 3-b & \text{if } a \leq 1, a \leq b \\ 3-a & \text{if } b \leq 1, b \leq a \\ 4-a-b & \text{if } a \geq 1, b \geq 1 \end{cases}$$

at a point $(a,b) \in \Delta_{Y_\bullet}(D)$.

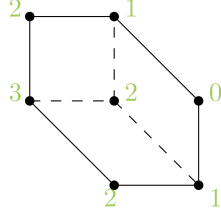


Figure 2.32: The values of the function φ on the Newton–Okounkov body $\Delta_{Y_\bullet}(D)$.

The integral of φ over $\Delta_{Y_\bullet}(D)$ can be easily computed by computing the volume over the square and the two parallelogramms, which are depicted in Figure 2.32, with the respective values of φ in green.

$$\int_{\Delta_{Y_\bullet}(D)} \varphi = 1 \cdot \frac{1}{4}(0 + 1 + 1 + 2) + 1 \cdot \frac{1}{4}(1 + 2 + 2 + 3) + 1 \cdot \frac{1}{4}(1 + 2 + 2 + 3) = 5.$$

It remains to show that it is not possible to find sections, having higher orders of vanishing at R . In order to do that, we consider the toric variety X with another flag $Y'_\bullet : X \supseteq Y'_1 \supseteq Y'_2$, where the curve is chosen as $Y'_1 = \overline{\{y^{-1} = 1\}}$ and $Y'_2 = (1, 1)$ in local coordinates, i.e., the point of the flag is the valuation point R of the function.

Thus, what remains to be determined, is the shape of the Newton–Okounkov body $\Delta_{Y'_\bullet}(D)$. Since the flag is no longer torus-invariant, this is not immediate from the divisor. Although our methods from Section 2.3 can be used here, we want to give an explicit example of how to compute the Newton–Okounkov body via variation of Zariski decomposition. By Proposition 2.3.1 the curve $C = Y'_1$ is linearly equivalent to the torus-invariant divisor $H - E_3$. We apply Theorems 2.2.14 and 2.2.15 by using variation of the Zariski-decomposition for $D_t := D - t(H - E_3)$ for $t \geq 0$.

We first give the intersection numbers that will be needed in the computations. The Picard group of X is generated by H and the exceptional curves. The only irreducible curves having negative self-intersection are $E_1, E_2, E_3, E_{12}, E_{13}$ and E_{23} . Note, that we are lacking this information about negative curves in general.

Their intersection numbers are

$$H.H = 1, \quad H.E_i = 0, \quad E_i.E_j = -\delta_{ij}$$

and therefore for $i, j, k, l \in \{1, 2, 3\}$ we obtain $H.E_{ij} = 1$,

$$E_i.E_{jk} = \begin{cases} 1 & \text{if } i \in \{j, k\} \\ 0 & \text{if } i \notin \{j, k\} \end{cases}, \quad E_{ij}.E_{kl} = \begin{cases} -1 & \text{if } \{i, j\} = \{k, l\} \\ 0 & \text{if } |\{i, j\} \cap \{k, l\}| = 1 \\ 1 & \text{if } |\{i, j\} \cap \{k, l\}| = 0 \end{cases}$$

Since D is nef, we obtain $D^+ = D$ for $t = 0$ and thus the coefficient of C in D^- is $\nu = 0$. Thus for small $t > 0$, the Zariski decomposition is given by $D_t^+ = D_t$ and $D_t^- = 0$.

If we assume R to be chosen general enough on Y'_1 , then $\alpha(t) \equiv 0$, and we will only have to deal with the computation of $\beta(t)$.

By the openness of ampleness in the Néron–Severi space, D_t is still nef for small $t > 0$. By the Kleiman–Nakai–Moishezon criterion 2.2.8, this stays true if and only if D_t has a non-negative intersection number with all irreducible torus-invariant curves on X . This yields

$$D_t.E_i = \begin{cases} 1 & \text{if } i \neq 3 \\ 1 - t & \text{if } i = 3 \end{cases}, \quad D_t.E_{ij} = \begin{cases} 1 - t & \text{if } \{i, j\} = \{1, 2\} \\ 1 & \text{otherwise} \end{cases} \quad (2.4.4)$$

and hereby the bound is $t = 1$. For $0 \leq t \leq 1$ we have $D_t^+ = D_t$ and thus the upper part of the Newton–Okounkov body is then given by

$$\beta(t) = \alpha(t) + (D_t^+.(H - E_3)) = 0 + D_t.(H - E_3) = 3 - t - (1 - t) = 2.$$

In the case $t > 1$, negative curves will appear in the Zariski decomposition. According to (2.4.4), the curves that can appear in D_t^- are E_3 and E_{12} , which gives

$$D_t^+ = D_t - D_t^- = D_t - \gamma_3(t)E_3 - \gamma_{12}(t)E_{12}$$

for certain $\gamma_3, \gamma_{12} \in \mathbb{R}[t]$. On the one hand we have $D_t.E_1 = D_t.E_{23} = 1 - t$ and on the other hand, we have

$$\begin{aligned} D_t.E_3 &= (D_t^+ + D_t^-).E_3 = 0 + D_t^-.E_3 = -\gamma_3(t) \\ D_t.E_{12} &= (D_t^+ + D_t^-).E_{12} = 0 + D_t^-.E_{12} = -\gamma_{12}(t). \end{aligned}$$

It follows that $\gamma_3(t) = \gamma_{12}(t) = t - 1$ and therefore

$$\beta(t) = \alpha(t) + D_t^+.(H - E_3) = 0 + D_t.(H - E_3) = (3 - t) + (1 - t) = 4 - 2t.$$

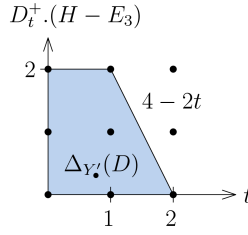


Figure 2.33: The Newton–Okounkov body $\Delta_{Y_\bullet}(D)$.

We have to determine the Zariski decomposition of D_t , while D_t stays in the pseudo-effective cone. We claim that this bound is given by $t = 2$ and that we do not cross various chambers for $t > 1$. For verifying that claim, we compare certain volumes. On the one hand, since D is nef, $\text{vol}(D) = D \cdot D = 6$ by Theorem 2.2.6. On the other hand, consider the volume of the resulting Newton–Okounkov body. Under our assumption, $\Delta_{Y_\bullet}(D)$ is the polygon depicted in Figure 2.33 and consequently $\text{vol}_{\mathbb{R}^2}(\Delta_{Y_\bullet}(D)) = 3$. Now Theorem 2.2.12 tells us that for any big divisor D

$$\text{vol}_{\mathbb{R}^2}(\Delta_{Y_\bullet}(D)) = \frac{1}{2!} \text{vol}(D)$$

which in our case means that $\text{vol}_{\mathbb{R}^2}(\Delta_{Y_\bullet}(D))$ is $\frac{6}{2!} = 3$. Together with the fact, that β is concave by Theorem 2.2.15 it follows, that we have determined the Newton–Okounkov body $\Delta_{Y_\bullet}(D)$.

We consider the function

$$\begin{aligned} \varphi' : \Delta_{Y_\bullet}(D) &\rightarrow \mathbb{R} \\ (a', b') &\mapsto a' + b' \geq \varphi'_R(a', b'). \end{aligned}$$

We can read the respective values at the vertices of the Newton–Okounkov body off Figure 2.34.

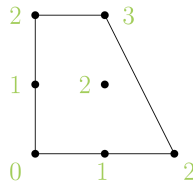


Figure 2.34: The values of the function φ' on the Newton–Okounkov body $\Delta_{Y_\bullet}(D)$.

This gives

$$\int_{\Delta_{Y_\bullet}(D)} \varphi' = 2 \cdot \frac{1}{4} (0 + 1 + 2 + 3) + 1 \cdot \frac{1}{3} (1 + 2 + 3) = 5.$$

Comparing the integrals of the functions φ and φ' over the respective Newton–Okounkov bodies yields

$$\int_{\Delta_{Y'_\bullet}(D)} \varphi' = \int_{\Delta_{Y_\bullet}(D)} \varphi$$

and this shows again, that the choices made for the sections in Figure 2.31 yield the maximal orders of vanishing.

2.5 RATIONALITY OF CERTAIN SESHADRI CONSTANTS ON TORIC SURFACES

Finally, in this section we apply our methods to deduce the rationality of certain invariants. We first recover the rationality of Newton–Okounkov bodies on toric surfaces, by considering the invariant $\mu_C(D)$, see Lemma 2.5.2. Then we recall known criteria for the rationality of another important invariant, namely the Seshadri constant $\varepsilon(X, D; z)$. We prove that we can guarantee rationality, given a combinatorial property, that we call *weakly zonotopally well-covered*, see Theorem 2.5.13. Moreover we construct a class of polytopes for which the other above criteria do not apply and prove rationality in these cases, see Theorem 2.5.16.

Given a smooth projective surface X , a big divisor D , and an admissible flag $Y_\bullet: X \supseteq C \supseteq \{z\}$, one can use Zariski decomposition of $D_t = D - tC$ to determine the corresponding Newton–Okounkov body $\Delta_{Y_\bullet}(D)$. According to Theorem 2.2.15, the coordinates of some of the vertices involve the *pseudo-effective threshold* invariant

$$\mu_C(D) = \sup\{t > 0 : D - tC \text{ is big}\}.$$

Due to Theorem 2.2.12, we have

$$(D - tC)^2 = \text{vol}(D - tC) = 2 \cdot \text{vol}_{\mathbb{R}^2}(\Delta_{Y_\bullet}(D - tC)) \quad (2.5.1)$$

and therefore $\mu_C(D)$ is in general determined by a quadratic equation and thus not necessarily rational. The following proposition states that the rationality of $\mu_C(D)$ is the crucial criterion that determines the rationality of the whole Newton–Okounkov body.

PROPOSITION 2.5.1 ([KLM12, Proposition 2.2]). Let X be a smooth projective surface, D a big rational divisor on X , and Y_\bullet an admissible flag on X . Then the following holds.

1. All the vertices of the polygon $\Delta_{Y_\bullet}(D)$ contained in the set $\{[v, \mu) \times \mathbb{R}\}$ have rational coordinates.
2. $\mu_C(D)$ is either rational or satisfies a quadratic equation over \mathbb{Q} .

In the toric case we can guarantee rationality.

LEMMA 2.5.2. Let X be a smooth projective toric surface, D a big \mathbb{Q} -divisor on X and $Y_\bullet: X \supseteq C \supseteq \{z\}$ an admissible flag. Then $\mu_C(D)$ is rational.

Proof. Due to (2.5.1) the value $\mu_C(D)$ is a root of an equation that is invariant under linear equivalence of the involved divisors. Hence let $D' = \sum_{\rho \in \Sigma(1)} a_\rho D_\rho$ be a torus-invariant divisor such that $D' \sim D$. Moreover fix an admissible torus-invariant flag Y'_\bullet , since the volume of the Newton–Okounkov body is independent of the flag. In particular, there exists a torus-invariant curve $C' = \sum_{\rho \in \Sigma(1)} a'_\rho D_\rho$ that is linearly equivalent to C and whose coefficients a'_ρ are rational for all rays $\rho \in \Sigma(1)$.

Then the Newton–Okounkov body $\Delta_{Y'_\bullet}(D')$ coincides with a translate of the polytope $P_{D'}$. This polytope can be described in terms of the intersection of finitely many half spaces, i.e.,

$$P_{D'} = \{m \in M_{\mathbb{R}} : A \cdot m \geq b\} \quad (2.5.2)$$

for some matrix $A \in \mathbb{Z}^{r \times 2}$ and vector $b \in \mathbb{Q}^r$, where r is the number of rays.

The polytope $P_{C'}$ associated to C' is given as $P_{C'} = \{m \in M_{\mathbb{R}} : A \cdot m \geq b'\}$ for some vector $b' \in \mathbb{Q}^r$.

We consider the polytope

$$P_t = P_{D' - tC'} = \{m \in M_{\mathbb{R}} : A \cdot m \geq b - tb'\}$$

for $t \geq 0$. Then being big on the divisorial side translates into being full-dimensional on the polytopal side, i.e.,

$$\begin{aligned} \mu_C(D) = \mu_{C'}(D') &= \sup\{t > 0 : D' - tC' \text{ is big}\} \\ &= \sup\{t > 0 : P_t \text{ full-dimensional}\}. \end{aligned}$$

Thus for $t = \mu_C(D)$ the polytope P_t is lower-dimensional. Let p be a vertex of $P_{\mu_C(D)}$. Let A_i denote the i -th row of the matrix A . There are two possible cases.

1. $\dim(P_{\mu_C(D)}) = 1$:

Then there exist two parallel defining hyperplanes of $P_{D'}$ whose translates are defining hyperplanes for $P_{\mu_C(D)}$. This yields $A_i = -A_j$ for some $i \neq j \in \{1, \dots, r\}$ and

$$\begin{aligned} A_i p &= b_i - \mu_C(D) b'_i \\ -A_i p &= b_j - \mu_C(D) b'_j. \end{aligned}$$

Since $\mu_C(D)$ is then determined by a linear equation with rational coefficients, it follows that $\mu_C(D)$ itself is rational.

2. $\dim(P_{\mu_C(D)}) = 0$:

Then $P_{\mu_C(D)} = p$ and there exist three defining hyperplanes of $P_{D'}$ whose translates

are defining hyperplanes for $P_{\mu_C(D)}$. This yields

$$\begin{aligned} A_i p &= b_i - \mu_C(D) b'_i \\ A_j p &= b_j - \mu_C(D) b'_j \\ A_k p &= b_k - \mu_C(D) b'_k \end{aligned}$$

for some pairwise different $i, j, k \in \{1, \dots, r\}$. This again determines rational p and $\mu_C(D)$. □

As a corollary we recover the following.

COROLLARY 2.5.3. Let X be a smooth projective toric surface, D a big \mathbb{Q} -divisor, and Y_\bullet an admissible flag. Then the Newton–Okounkov body $\Delta_{Y_\bullet}(D)$ is a rational polygon.

The invariant μ is closely related to another invariant. Let X be a smooth projective surface, D an ample divisor, and $z \in X$ a point. We denote the blow-up of z with exceptional divisor E by $\pi: X' \rightarrow X$. The *Seshadri constant* is the invariant

$$\varepsilon(X, D; z) := \sup\{t > 0 : \pi^*D - tE \text{ is nef}\}. \quad (2.5.3)$$

According to Remark 3.1 in [Dum+16b] $\varepsilon(X, D; z)$ is rational if the invariant $\mu_E(\pi^*D)$ is. The problem is that we have to consider the blown-up situation here, in which things can get out of hand.

The Seshadri constant measures the local positivity of D at the point z . Seshadri constants provide information on the shape of the nef and effective cones of the surface X' in the direction of $-E$. Although they have been studied for over thirty years, several basic questions about them remain unanswered. One of the main questions is the rationality of $\varepsilon(X, D; z)$. It is expected that there will be instances (even in dimension two) when irrational Seshadri constants occur (in fact, this would be consistent with Nagata’s conjecture [Dum+16a]), at the same time, no irrational example has been found so far. In particular, it is known that Seshadri constants on del Pezzo, Enriques [Sze01], abelian [Bau98] and certain K3 surfaces [Bau97; GK13; Knu08] are rational. Certainly, if the blow-up of X at z has a finite rational polyhedral effective cone, then $\varepsilon(X, D; z)$ is forced to be rational.

Our lack of knowledge about the rationality of Seshadri constants on surfaces is all the more mysterious, since in dimension two there is one way in which $\varepsilon(X, D; z)$ can be irrational: if it is equal to $\sqrt{(D^2)}$ [Laz04, Section 5.1] and (D^2) is not a square. If the latter arithmetic condition does not hold, then the rationality of $\varepsilon(X, D; z)$ is equivalent to the existence of a (necessarily negative) curve C on the blow-up of X at z orthogonal to $\pi^*D - tE$ for some $t < \sqrt{(D^2)}$. In this sense the irrationality of $\varepsilon(X, D; z)$ is evidence

for the non-existence of certain irreducible curves of negative self-intersection on the blow-up.

Remark 2.5.4. By the duality between the nef and effective cones on a surface, if $\varepsilon(X, D; z) < \mu_E(\pi^*D)$ then both numbers are rational. As a consequence, if one can find an effective divisor of the form $\pi^*D - tE$ with $\sqrt{(D^2)} < t$ then $\varepsilon(X, D; z) \in \mathbb{Q}$. As the first known rationality criterion we adjust Theorem 3.6 and Remark 3.7 from [Ito14] to our situation.

THEOREM 2.5.5. In the situation of our general set-up 2.4.12, if the width $\text{width}_u(P) \leq \text{length}(P, v)$ then $\varepsilon(X, D; R) = \text{width}_u(P)$.

In particular, in this case, $\varepsilon(X, D; R)$ is rational.

In [San14] Sano studies Seshadri constants on rational surfaces with anti-canonical pencils. More precisely, he considers a smooth rational surface X that is either a composition of blow-ups of \mathbb{P}^2 or of a Hirzebruch surface \mathcal{H}_d such that $\dim | -K_X| \geq 1$. In terms of the corresponding polytope this means that P_{-K_X} contains at least two lattice points. In these cases, he gives explicit formulas for the Seshadri constant $\varepsilon(X, D; R)$ of an ample divisor D at a general point $R \in X$ in [San14, Theorem 3.3 and Corollary 4.12]. As a consequence he obtains rationality in the cases above as observed in Remark 4.2.

In [Lun20] Lundman computes Seshadri constants at a general point R for some classes of smooth projective toric surfaces. It follows in particular that the Seshadri constant is rational in these cases. The characterization of the classes involve the following definitions.

Definition 2.5.6. Let \mathcal{L} be a line bundle on a smooth variety X and $z \in X$ a smooth point with maximal ideal $\mathfrak{m}_z \subseteq \mathcal{O}_X$. For a $k \in \mathbb{Z}_{\geq 1}$ consider the map

$$\begin{aligned} j_z^k: H^0(X, \mathcal{L}) &\rightarrow H^0(X, \mathcal{L} \otimes \mathcal{O}_X/\mathfrak{m}_z^{k+1}) \\ s &\mapsto \left(s(z), \dots, \frac{\partial^t s}{\partial \underline{z}^t}(z), \dots \right)_{t \leq k}, \end{aligned}$$

where $\underline{z} = (z_1, \dots, z_n)$ is a local system of coordinates around z . We say that \mathcal{L} is k -jet spanned at z if the map j_z^k is surjective. We denote by $\mathfrak{s}(\mathcal{L}, z)$ the largest k such that X is k -jet spanned at z and call it the *degree of jet separation* of \mathcal{L} at z .

So the map j_z^k takes s to the terms of degree at most k in the Taylor expansion of s around z . For X a projective toric variety let s_0, \dots, s_d be a basis for $H^0(X, \mathcal{L})$. Then \mathcal{L} is k -jet spanned at $z \in X$ if and only if the *matrix of k -jets*

$$J_k(\mathcal{L}) := (J_k(\mathcal{L}))_{i,j} := \left(\frac{\partial^{|\underline{t}|}}{\partial z_{t_1} \partial z_{t_2} \cdots \partial z_{t_n}}(s_i) \right)_{0 \leq i \leq d, 0 \leq |\underline{t}| \leq k}$$

has maximal rank when evaluated at the point z , where $\underline{t} = (t_1, \dots, t_n) \in \mathbb{Z}_{\geq 1}^n$ and $|\underline{t}| = |t_1 + \cdots + t_n|$.

Definition 2.5.7 ([Di +13, compare Definition 1.15]). Let X be a smooth projective toric variety and D a torus-invariant divisor on X . We define the *codegree* $\eta(D)$ as

$$\eta(D) := (\sup\{t > 0 : P_{tK_X+D} \text{ is non-empty}\})^{-1}$$

and call the polytope $\text{core}(P_D) := P_{\eta(D)^{-1}K_X+D}$ the *core* of P_D .

THEOREM 2.5.8 ([Lun20, Theorem 1]). Let X be a smooth toric surface and \mathcal{L} an ample line bundle. If X is a projective bundle or $\mathfrak{s}(\mathcal{L}, R) \leq 2$, then $\varepsilon(X, \mathcal{L}; R) = \mathfrak{s}(\mathcal{L}, R)$.

The other Theorems in [Lun20] that yield rationality of Seshadri constants both require $\text{core}(P_D)$ to be a line segment.

Just as the rationality of Seshadri constants follows from that of the corresponding pseudo-effective thresholds, it can also be deduced from the rationality of the associated integral in the following way.

COROLLARY 2.5.9 ([KMR19, Corollary 4.5]). Let X be a smooth projective surface, $z \in X$, and D an ample Cartier divisor on X . Then $\varepsilon(X, D; z)$ is rational if $\int_{\Delta_{Y_\bullet}(D)} \varphi_z$ is rational, where φ_z is the Newton–Okounkov function coming from the geometric valuation associated to z and Y_\bullet any admissible flag.

We apply this criterion to an example for which Lundman’s and Sano’s criteria do not apply.

Example 2.5.10. We consider a blow-up $\pi: X \rightarrow \mathbb{P}^2$ of the projective plane in 13 points, namely the toric variety X whose associated fan Σ is depicted in Figure 2.35.

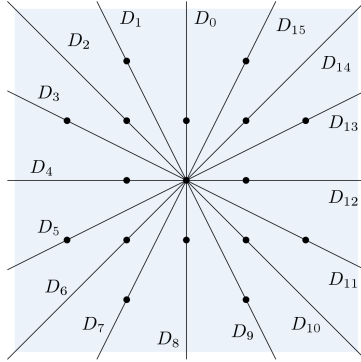


Figure 2.35: The fan Σ with associated torus-invariant prime divisors D_0, \dots, D_{15} .

The torus-invariant prime divisors are denoted by D_0, \dots, D_{15} and choose $D = D_1 + 2D_2 + 6D_3 + 5D_4 + 15D_5 + 11D_6 + 19D_7 + 9D_8 + 18D_9 + 10D_{10} + 13D_{11} + 4D_{12} + 4D_{13} + D_{14}$ as an ample divisor on X . For the torus-invariant flag $Y_\bullet: X \supseteq Y_1 \supseteq Y_2$ with $Y_1 = \{y = 0\}$ and $Y_2 = (0, 0)$ this gives the polytope P_D in Figure 2.36 as the

Newton–Okounkov body $\Delta_{Y_\bullet}(D)$. We have $\dim | -K_X| = 0$, $\text{core}(P_D)$ is a point and the degree of jet separation is $\mathfrak{s}(\mathcal{L}, R) = 9$. Thus this example does not fall in any of the classes covered by Sano or Lundman.

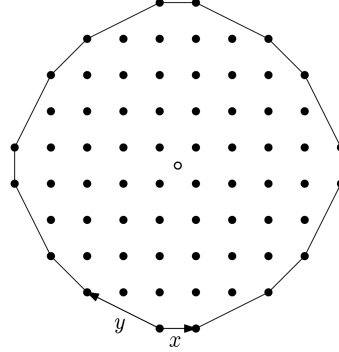


Figure 2.36: The Newton–Okounkov body $\Delta_{Y_\bullet}(D) \cong P_D$ with $\text{core}(P_D)$ highlighted.

We claim that the Seshadri constant $\varepsilon(X, D; R)$ is rational. To verify this claim we consider the Newton–Okounkov function φ'_R on $\Delta_{Y'_\bullet}(D)$ coming from the geometric valuation ord_R at the general point $R = (1, 1)$ and argue that its integral takes a rational value. In order to do this, consider the flag $Y'_\bullet: X \supseteq Y'_1 \supseteq Y'_2$, where Y'_1 is the curve given by the local equation $x^{-1} - 1 = 0$ and $Y'_2 = R$. Thus we obtain the Newton–Okounkov body $\Delta_{Y'_\bullet}(D)$ with respect to this flag by the shifting process via the vector $v = (-1, 0)$ as explained in Section 2.3. This gives the polytope $\Delta_{Y'_\bullet}(D)$ shown in Figure 2.37.

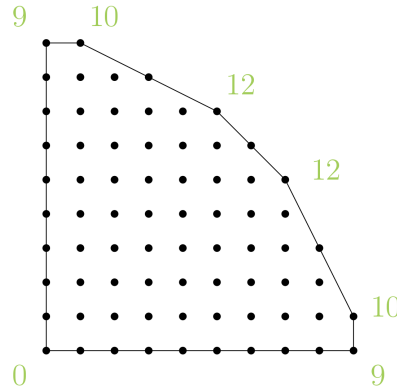


Figure 2.37: The Newton–Okounkov body $\Delta_{Y'_\bullet}(D)$ with respective values of φ'_R .

We claim that the Newton–Okounkov function φ'_R on $\Delta_{Y'_\bullet}(D)$ that comes from the geometric valuation ord_R is given as $\varphi'_R(a', b') = a' + b'$ for all $(a', b') \in \Delta_{Y'_\bullet}(D)$. To prove this, we consider the following global sections of $H^0(X, \mathcal{O}_X(D))$ as in Table 2.1. The sections are chosen in a way such that they get mapped to the vertices, when building the new Newton–Okounkov body $\Delta_{Y'_\bullet}(D)$ and a such that the order of vanishing is $\text{ord}_R(s) = a' + b'$ for a section s that gets mapped to the point $(a', b') \in \Delta_{Y'_\bullet}(D)$. For the vertices in $\text{vert}(\Delta_{Y'_\bullet}(D))$ these values realize a lower bound for the function φ'_R .

| global section s | image in $\Delta_{Y_\bullet}(D)$ | image in $\Delta_{Y'_\bullet}(D)$ | $\text{ord}_R(s)$ |
|---|----------------------------------|-----------------------------------|-------------------|
| $s_1(x, y) = (x - 1)(x^2y - 1)^9$ | (0, 0) | (1, 9) | 10 |
| $s_2(x, y) = x(x^2y - 1)^9$ | (1, 0) | (0, 9) | 9 |
| $s_3(x, y) = x^4y^4(x - 1)^9(x^2y - 1)$ | (4, 4) | (9, 1) | 10 |
| $s_4(x, y) = x^6y^5(x - 1)^9$ | (6, 5) | (9, 0) | 9 |
| $s_5(x, y) = y(x - 1)^5(x^2y - 1)^7$ | (0, 1) | (5, 7) | 12 |
| $s_6(x, y) = xy^2(x - 1)^7(x^2y - 1)^5$ | (1, 2) | (7, 5) | 12 |
| $s_7(x, y) = x^{19}y^9$ | (19, 9) | (0, 0) | 0 |

Table 2.1: Global sections of $\mathcal{O}_X(D)$ that realize lower bounds for the order of vanishing ord_R .

Since the function φ'_R has to be concave, this yields $\varphi'_R(a', b') = a' + b'$ on the entire Newton–Okounkov body. For the integral we obtain

$$\int_{\Delta_{Y'_\bullet}(D)} \varphi'_R = \frac{1295}{3},$$

which is rational and therefore the Seshadri constant $\varepsilon(X, D; R)$ is rational.

Although proving rationality of the Seshadri constant did not require knowing the values of the function φ_R on the Newton–Okounkov body $\Delta_{Y_\bullet}(D)$, determining these values in this particular example is of independent interest. It turns out that the approach of choosing sections whose Newton polytopes are zonotopes with prescribed edge directions is not always sufficient to maximize the order of vanishing at the general point R . For the function φ_R we expect 22 domains of linearity as shown in Figure 2.38 that arise from the shifting process in the direction of $v = (-1, 0)$.

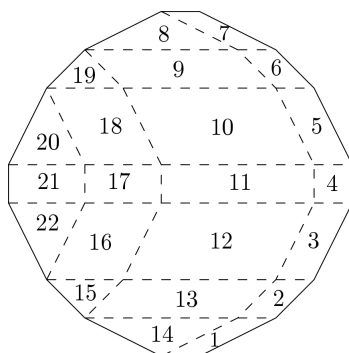


Figure 2.38: Expected domains of linearity of the function φ_R on the Newton–Okounkov body $\Delta_{Y_\bullet}(D)$.

As seen in the Appendix in Table A.1 for the domains 1, . . . , 9, 13, 14, 15, and 19 zonotopes using only edge directions of $\Delta_{Y_\bullet}(D)$ are sufficient. For the domains 10, 11, and

12 we need a Minkowski sum of those edge directions and ‘small’ triangles that have a high order of vanishing at $(1, 1)$. The section $s(x, y) = x^3y^2 - 3xy + y + 1$ for instance has order of vanishing $\text{ord}_R(s) = 2$ and its Newton polytope $\text{NP}(s)$ is depicted in Figure 2.39.

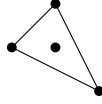


Figure 2.39: The Newton polytope $\text{NP}(s)$ of the section $s(x, y) = x^3y^2 - 3xy + y + 1$.

For the remaining regions 16, 17, 18, 20, 21, and 22 global sections with the desired order of vanishing at R could not be found via computations up to $k = 12$. We expect φ to take the values shown in Figure 2.40.

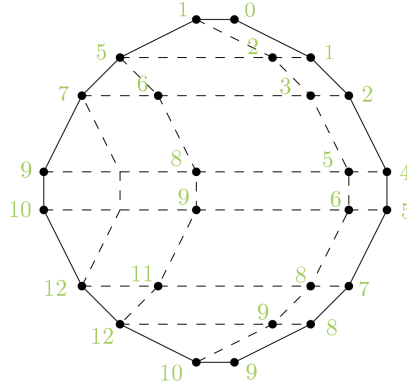


Figure 2.40: The values of φ on the Newton–Okounkov body $\Delta_{Y_*}(D)$.

The approach for proving rationality of the Seshadri constant applies to a certain class of polytopes. To describe this class we need to introduce the following terms.

Definition 2.5.11. Let $P \subseteq \mathbb{R}^2$ be a polygon and $v \in \mathbb{Z}^2$ a primitive direction. Set $\text{vert}(P, v) := \Psi^{-1}(\text{vert}(\Psi(P)))$ for the piecewise linear isomorphism from Section 2.3.1 and call it the *relevant vertex set of P with respect to v* .

Definition 2.5.12. Let $P \subseteq \mathbb{R}^2$ be a polygon. Let $v \in \mathbb{Z}^2$ be a primitive vector, and $u \in v^\perp$ a primitive integral functional. We call P *weakly zonotopally well-covered with respect to (v, u)* if for all points $m \in \text{vert}(P, v)$ the set $P_v(m)$ contains a zonotope $L_1 + \dots + L_\ell$ with none of the L_i parallel to v , such that

$$\sum_{i=1}^{\ell} \text{length}_{\mathbb{Z}^2}(L_i) = \text{width}_u(P_v(m)).$$

The polygon P is *weakly zonotopally well-covered* if it is with respect to some (v, u) .

THEOREM 2.5.13. Let X be a smooth projective toric surface and D an ample torus-invariant divisor on X with associated Newton–Okounkov body $\Delta_{Y_\bullet}(D)$ for an admissible torus-invariant flag Y_\bullet . If the polytope $\Delta_{Y_\bullet}(D)$ is weakly zonotopally well-covered, then

1. we can determine $\int_{\Delta_{Y_\bullet}(D)} \varphi_R$.
2. the Seshadri constant $\varepsilon(X, D; R)$ is rational.
3. the maximum $\max_{\Delta_{Y_\bullet}(D)} \varphi_R$ is attained at the boundary of $\Delta_{Y_\bullet}(D)$.

Proof. Since all input data is torus-invariant, the Newton–Okounkov body $\Delta_{Y_\bullet}(D)$ is isomorphic to the polytope P_D for any admissible torus-invariant flag Y_\bullet . By assumption, this polytope is weakly zonotopally well-covered, so let $v = (v_1, v_2) \in \mathbb{Z}^2$ be its associated primitive direction. Consider the flag $Y'_\bullet: X \supseteq C \supseteq \{R\}$, where C is the curve given by the local equation $x^{v_1}y^{v_2} - 1 = 0$ and $R = (1, 1)$ is a general point on C . Then the shifting process explained in Section 2.3 yields the Newton–Okounkov body $\Delta_{Y'_\bullet}(D)$ with respect to this new flag. By Corollary 2.3.8 this process relates the Newton–Okounkov bodies via a piecewise linear isomorphism $\Psi: \Delta_{Y_\bullet}(D) \xrightarrow{\sim} \Delta_{Y'_\bullet}(D)$.

We show that the Newton–Okounkov function $\varphi'_R: \Delta_{Y'_\bullet}(D) \rightarrow \mathbb{R}$, that comes from ord_R , satisfies $\varphi'_R(a', b') = a' + b'$ for all vertices $T = (a', b') \in \text{vert}(\Delta_{Y'_\bullet}(D))$. In order to do so, apply the arguments of the proof of Theorem 2.4.17 to all $m \in \text{vert}(\Delta_{Y_\bullet}(D), v)$. Together with the facts that φ'_R is concave and has $a' + b'$ as an upper bound it follows that $\varphi'_R(a', b') = a' + b'$ on the entire Newton–Okounkov body. Rationality of the integral $\int_{\Delta_{Y'_\bullet}(D)} \varphi'_R$ yields rationality of the Seshadri constant $\varepsilon(X, D; R)$. Since the maximum is independent of the flag, and φ'_R is linear, it is attained at the boundary of $\Delta_{Y_\bullet}(D)$. □

Note, that zonotopally well-covered implies weakly zonotopally well-covered.

Example 2.5.14. To illustrate the proof we stick to Example 2.5.10. The polytope $\Delta_{Y_\bullet}(D)$ is weakly zonotopally well-covered with respect to $(v, u) = ((-1, 0), (0, 1))$. Consider, for instance, the vertex $T = (7, 5) \in \Delta_{Y'_\bullet}(D)$. Its preimage under the piecewise linear isomorphism Ψ is $m = (1, 2) \in \Delta_{Y_\bullet}(D)$ and $\text{length}(\Delta_{Y_\bullet}(D), m, v) = 7$. A global section which is mapped to m and T respectively, is

$$s(x, y) = xy^2 \cdot (x - 1)^7 \cdot (x^2y - 1)^5$$

as seen in Figure 2.41 with $\text{ord}_R(s) = 7 + 5 = 12$.

We can construct classes of polarized toric surfaces for which our method of guessing sections using convex geometry yields rationality of the Seshadri constant while other methods like Ito’s width bound, Lundman’s core criterion or Sano’s anti-canonical

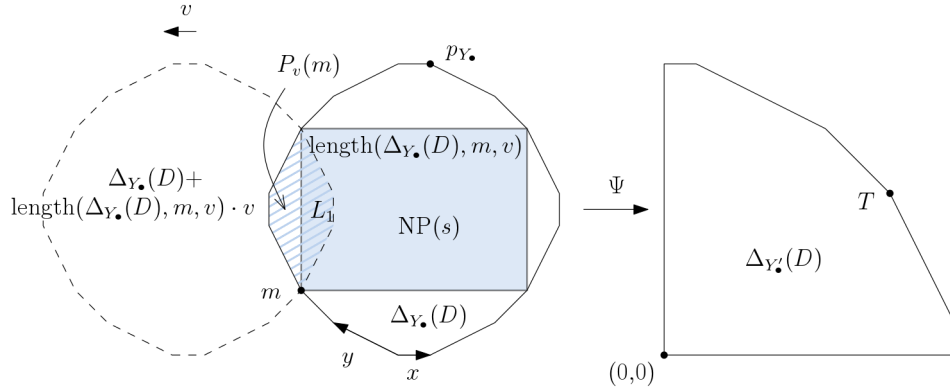


Figure 2.41: The setup of the proof of Theorem 2.5.13 in the context of Example 2.5.10.

pencil do not apply. We explain the general method and illustrate it with an explicit example. (The hard part is to find polygons for which the above methods do not work.)

In order to ensure that the core of our polygons is a point, we need to introduce some machinery which might be of independent interest. In analogy with the Fine interior of a rational polytope (compare [Fin83, §4.2], [BKS20]) we define the *Fine adjoint* $P^{\text{FA}(c)}$ of a convex body $P \subseteq M_{\mathbb{R}}$ and a parameter $c > 0$ as follows.

$$P^{\text{FA}(c)} := \bigcap_{u \in N \setminus \{0\}} \{m \in M_{\mathbb{R}} : \langle u, m \rangle \geq \min \langle u, P \rangle + c\}$$

If P is a rational polytope and $c \in \mathbb{Q}_{>0}$, this is again a rational polytope; $P^{\text{FA}(1)}$ is called *Fine interior* in [BKS20]. If the toric variety X_P associated with P has at most canonical singularities, this agrees with the standard adjoint $P^{(c)}$ where the intersection is taken only over facet defining u 's (see [Di +13]).

The *Fine codegree* $\eta^{\text{F}}(P)$ of P is then the minimal c for which $P^{\text{FA}(1/c)} \neq \emptyset$. Finally, we call the last non-empty Fine adjoint $P^{\text{FA}(1/\eta^{\text{F}}(P))}$ of P its *Fine core* $\text{core}^{\text{F}}(P)$.

If $m \in \text{relint}(\text{core}^{\text{F}}(P))$, call those $u \in N \setminus \{0\}$ for which $\langle u, m \rangle = \min \langle u, P \rangle + 1/\eta^{\text{F}}(P)$ *essential* for P (compare [Di +13, Lemma 2.2]).

For rational P the Fine codegree will be a rational number and hence the Fine core will be a rational polytope of positive codimension. Figure 2.42 illustrates that in the case of non-canonical singularities, the dimensions of core and Fine core can differ, and even if both are points, they need not agree.

LEMMA 2.5.15. Suppose P and Q are polytopes in $M_{\mathbb{R}}$ whose Fine cores are points $\text{core}^{\text{F}}(P) = \{m_P\}$ and $\text{core}^{\text{F}}(Q) = \{m_Q\}$, respectively. Suppose further that the $u \in N \setminus \{0\}$ which are essential for both P and Q positively span $N_{\mathbb{R}}$.

Then the Fine core of $kP + Q$ is the point $km_P + m_Q$ for all $k \geq 1$.

In particular, if X_{P+Q} has at most canonical singularities, then the (usual) core of $kP + Q$ is this point.

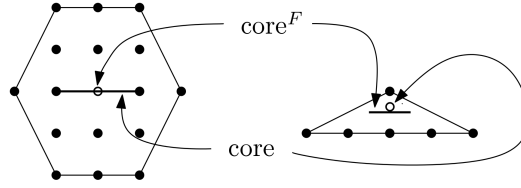


Figure 2.42: Core versus Fine core.

With these preparations, we can describe our construction. We write $\deg(P) = 2 \text{ area}(P)$ for the normalized volume of P .

THEOREM 2.5.16. Suppose P is a lattice polygon whose Fine core is a point such that $\text{width}(P) > \sqrt{\deg(P)}$ and P supports a Laurent polynomial s which vanishes to order $> \sqrt{\deg(P)}$ at R .

Then there is a lattice polygon Q so that for $k \gg 0$ the polygon $kP + Q$ satisfies

1. X_{kP+Q} is smooth,
2. $\text{core}(kP + Q)$ is a point,
3. $\mathfrak{s}(D_{kP+Q}, R) \geq k + 1$,
4. $h^0(-K_{X_{kP+Q}}) = 1$,
5. $\text{width}(kP + Q) > \sqrt{\deg(kP + Q)}$
6. $kP + Q$ supports a Laurent polynomial which vanishes to order $> \sqrt{\deg(kP + Q)}$ at R .

In particular, $\varepsilon(X_{kP+Q}, D_{kP+Q}; R) \in \mathbb{Q}$.

Example 2.5.17. Specific examples of such polygons P are the triangles

$$\Delta^{(d)} = \text{conv}(d \cdot \Delta \cup \{(-1, -1)\}),$$

where Δ denotes the standard triangle $\text{conv}((0, 0), (1, 0), (0, 1))$ from Figure 2.43. Their parameters are $\deg(\Delta^{(d)}) = d^2 + 2d$, $\text{width}(\Delta^{(d)}) = d + 1$, and they support a section which vanishes to order $\geq d + 1$ at R simply because they contain more than $\dim_{\mathbb{C}} \mathbb{C}[x, y] / \langle x, y \rangle^d = \binom{d+1}{2}$ lattice points so that the linear map

$$\begin{aligned} \{s \in \mathbb{C}[x, y] : \text{supp}(s) \subseteq P + (1, 1)\} &\rightarrow \mathbb{C}[x, y] / \langle x, y \rangle^d \\ s(x, y) &\mapsto s(x + 1, y + 1) \end{aligned}$$

must have a kernel. Specifically, for $P = \Delta^{(1)}$, we have $\deg(P) = 3$, $\text{width}(P) = 2$, and $s = x + y + 1/xy - 3$ is a section which vanishes to order 2 at R .

For our specific $P = \Delta^{(1)}$, the polygon Q in Figure 2.44 does the job.

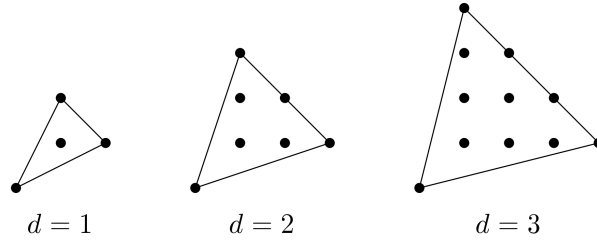


Figure 2.43: Examples of wide polygons $\Delta^{(d)}$ with small area for $d = 1, 2, 3$.

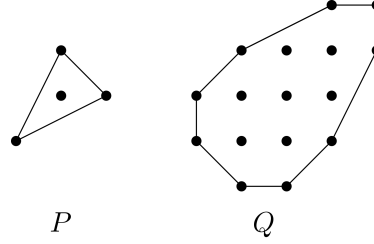


Figure 2.44: Resolving $\Delta^{(1)}$, eliminating anti-canonical sections, and ensuring that the core is a point.

In order to prove the theorem, we need another lemma.

LEMMA 2.5.18. Let P be a polygon whose Fine core is a point. Then the origin is the only lattice point in the interior of

$$\text{Ess} := \text{conv}(\{u \in N \setminus \{0\} : u \text{ is primitive and essential for } P\}).$$

Proof. Assume there exists a lattice point $u_0 \in N \setminus \{0\}$ in the interior of Ess . Then there exist adjacent vertices $u_1, u_2 \in N$ of Ess and coefficients $\lambda_1, \lambda_2 > 0$, such that $u_0 = \lambda_1 u_1 + \lambda_2 u_2$ with $\lambda_1 + \lambda_2 < 1$. For the essential vertices it holds that $\langle u_1, \text{core}^F(P) \rangle = \min \langle u_1, P \rangle + 1/\eta^F(P)$ and $\langle u_2, \text{core}^F(P) \rangle = \min \langle u_2, P \rangle + 1/\eta^F(P)$, respectively. Thus for u_0 we have

$$\begin{aligned} \langle u_0, \text{core}^F(P) \rangle &= \langle \lambda_1 u_1 + \lambda_2 u_2, \text{core}^F(P) \rangle \\ &= (\lambda_1 + \lambda_2) \cdot 1/\eta^F(P) + \lambda_1 \cdot \min \langle u_1, P \rangle + \lambda_2 \cdot \min \langle u_2, P \rangle \\ &\leq (\lambda_1 + \lambda_2) \cdot 1/\eta^F(P) + \min \langle u_0, P \rangle \\ &< 1/\eta^F(P) + \min \langle u_0, P \rangle. \end{aligned}$$

This is a contradiction to the definition of $\text{core}^F(P)$. Thus, such a lattice point cannot exist and therefore the origin is the only interior lattice point. \square

Proof of Theorem 2.5.16. The inequalities 5 and 6 hold by assumption for large k , no matter what Q is. Inequality 3 holds for all k because $kP + Q$ will contain a $k + 1$ fold dilate of a unimodular triangle.

Toric resolution of singularities is a standard procedure, see [CLS11, Chapters 10 & 11]. If necessary, we blow up further torus fixed points until only one anti-canonical section is left. This determines the normal fan of Q .

It remains to pick Q with the given fan so that the Fine core is a point and so that we can apply Lemma 2.5.15. To this end, consider the set of primitive ray generators which are essential for the given P . As $\text{core}^F(P)$ is a point, the origin is the only lattice point in the interior of their convex hull $Q_1^\vee \subset N_{\mathbb{R}}$ due to Lemma 2.5.18. Denote E the set of vertices of Q_1^\vee and denote $Q_1 \subset M_{\mathbb{R}}$ the polar dual of Q_1^\vee . As Q_1 is a simple polytope, we can pick a large $J \in \mathbb{Z}_{>0}$ so that for every $u_0 \in E$ there is a polygon Q_{u_0} with the same normal fan as Q_1 such that $\min\langle u_0, Q_{u_0} \rangle = -1 + 1/J$ while $\min\langle u, Q_u \rangle = -1$ for all other $u \in E \setminus \{u_0\}$. By adding appropriate multiples of the JQ_u for $u \in E$ to Q_1 , we can assure that all $u \in E$ are essential for the resulting Q . \square

2.6 OUTLOOK

A lot of question remain open and require further examination and also new questions arise from our studies. We will mention a few concrete ones.

- What is the connection between our tilting isomorphism Ψ and the geometric wall-crossing maps from [EH19], compare Remark 2.3.10?
- Does Conjecture 2.4.15 hold, that is, does the function transform according to Ψ ?
- (When) is the maximum $\max_{\Delta_{Y_\bullet}(D)} \varphi_R$ always attained at the boundary of $\Delta_{Y_\bullet}(D)$?
- Can we extend our general strategy to a larger class of polytopes?
- Is there an invariant in analogy to the Seshadri constant in terms of the corresponding polytope and what properties does it have?
- Do all polytopes fall into a class for which we have a rationality criterion, i.e., are Seshadri constants rational on all toric surfaces?

THE KINGMAN COALESCENT AND THE MULTISPECIES COALESCENT AS DENSITIES ON A SPACE OF TREES

This chapter is joint work with Christian Haase.

3.1 INTRODUCTION

The graph-theoretical concept of a tree has been used as a mathematical tool to describe numerous hierarchical relationships appearing in real world settings. One famous example that dates back to the beginning of the nineteenth century is the idea of the existence of a *tree of life*. Tree-like diagrams were already being used in the medieval era. Figure 3.1 shows a page from Darwin's notebook dating from around 1837, displaying his first attempt to conceptualize an evolutionary tree. Although research in population genetics has moved far beyond that stage today, trees are still omnipresent when it comes to modeling genealogical relationships.

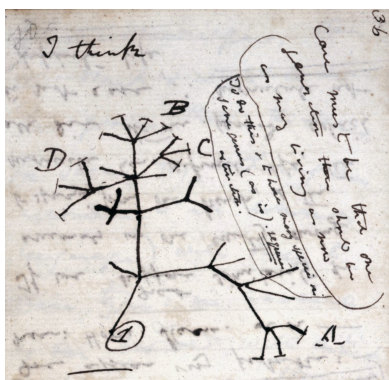


Figure 3.1: Darwin's tree of life.

Against this background, spaces of phylogenetic trees have been studied from various perspectives. In 2001 Billera, Holmes, and Vogtmann [BHV01] laid the groundwork for also studying the geometry of such spaces of trees and provided a fundamentally new perspective. In this light, we approach models from mathematical population genetics in terms of polyhedral geometry.

There are interesting links to objects coming from tropical geometry. Speyer and Sturmfels proved a first formal connection by identifying the space of phylogenetic trees with the tropical Grassmannian, compare [SS04]. Ardila and Klivans relate it to the tropicalization of the graphical matroid of a complete graph, see [AK06]. Thus,

there is also a connection to the tropicalization of the moduli space of marked genus zero curves. Consequently, efforts have recently been made to establish foundations of tropical methods for probability and statistics on the space of phylogenetic trees, see for instance [Lin+17; Nye+17; Mon+20].

The two models at the center of our studies are the Kingman coalescent process [Kin82a; Kin82b; Kin82c] and the multispecies coalescent process [Tak89; RY03; Liu+09]. The former models the gene divergence of a sample within a population. This is extended by the latter model, in the sense that it deals with the evolution of genes within multiple species. Although these models require major simplifications regarding the corresponding real world situation, they are the foundation which many current research questions are based on.

Apart from the extreme technical advances that have been made throughout the last decades, a lot of theoretical progress has been achieved with regard to phylogenetic inference. One of the main lines of research that we follow tries to answer the question of identifiability of the underlying species tree from a given distribution of observed gene trees. This is a very active area of research, see for instance [DR06; ADR11; DRS12a; DRS12b]. The first step towards an answer is to describe the conditional probability distribution. This was done in [DS05; DR09; RY03].

Our objects of interest have been studied from very different perspectives, meaning that problems have been approached from the viewpoint of biology, population genetics, medicine, mathematics, computer science, or statistics. This has resulted in a wide range of models, notations, and conventions in the existing literature. One aim of ours is to bring order into this situation and to furthermore bring together the different inner mathematical perspectives.

This chapter is organized as follows. Section 3.2 provides the necessary background on the underlying models, namely the Fisher–Wright model and the Kingman n -coalescent, and fixes notation. The focus of Section 3.3 is to define the spaces of trees that our work is based on and examine their geometry. This lays the groundwork for proving that the Kingman n -coalescent is given as a density on one of these spaces of trees, see Proposition 3.4.1 in Section 3.4. In Section 3.5, we discuss how the respective densities are related once we increase n , compare Proposition 3.5.3. We conclude in Section 3.6 by applying our methods to the multispecies coalescent.

3.2 THE FISHER–WRIGHT MODEL AND THE KINGMAN n -COALESCENT

In this section we present the population genealogical models that our studies are based on. We give an introduction that focuses on the aspects relevant to our setting. We follow [Yan14, in particular Chapter 9], which offers a more detailed discussion, as does [Wak09]. For readability, we will mostly omit proofs and point the reader to the referenced literature. To begin with, we review the Fisher–Wright model in Subsec-

tion 3.2.1. In order to do so, we focus on tree topology in 3.2.2 and on waiting times in 3.2.3. Based on that, we can describe the Kingman n -coalescent in Subsection 3.2.4.

The coalescent models gene divergence within a genealogy. Here, ‘to coalesce’ means ‘to merge’ or ‘to join’. Thus as the term ‘coalesce’ suggests, our study focuses on a given population for which we are tracing their genealogy backwards in time. So, we make historical rather than predictive statements.

3.2.1 The Fisher–Wright Model

To get to these statements, we have to make several assumptions that simplify the real world situation. The underlying population genetic model that is used here is called the *Fisher–Wright model*. It was established in the ‘30s first by Fisher in [Fis23] and Wright in [Wri31]. Its characteristics are

- a constant population size,
- non-overlapping generations,
- random mating,
- no selection,
- no mutation, and
- no recombination.

This means that we start with a finite population, consisting of $N \in \mathbb{Z}_{\geq 1}$ individuals, respectively lineages or genes. These terms will be used interchangeably. The model refers to a haploid organism, but the same model also works for diploid organisms, for which N would be replaced by $2N$ genes. If we visualize the process, one generation is usually depicted as a row as it can be seen on the left in Figure 3.2. Each dot represents one individual. In every generation, each individual chooses at random a parent of the previous generation, as indicated by the arrows.

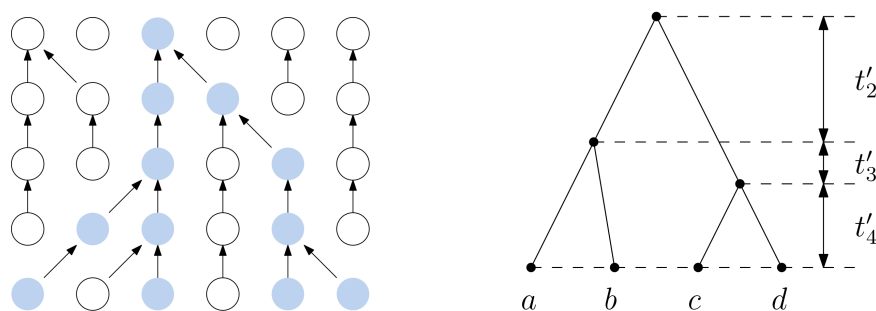


Figure 3.2: The Fisher–Wright model with $n = 4$.

In coalescent theory, we consider a sample of size $n \in \mathbb{Z}_{\geq 1}$ with $n \ll N$ from the current population and trace its ancestry backwards in time, indicated by the colored dots. We keep going until we reach the sample's MRCA, which stands for *Most Recent Common Ancestor*. This process consists of at most $n - 1$ coalescent events. Each time a coalescent event takes place, at least two lineages are merged — they coalesce — and the number of considered lineages is reduced. When the MRCA of the entire sample is reached, there is only one lineage left. If we only consider the genes that are involved in the process, this yields a tree as a result, as indicated by the dark-shaded dots on the left in Figure 3.2. The resulting tree is depicted on the right. It consists of two kinds of information. One is the branching pattern of the tree, which in general is often referred to as the *topology* or the *combinatorial type* of the tree. There are different levels of detail in which this topology is described. The second part of information is the *waiting times* t'_2, \dots, t'_n , where t'_j denotes the time, during which there are exactly j lineages in the sample. We will formalize these terms in the following.

3.2.2 Tree Topology

Let us focus on the topology first. In the literature, the term *phylogenetic tree* which emphasizes the connection to population genetics is used for diverse objects. Thus, we specify which kind of trees we are considering. For us a (*phylogenetic*) n -tree $T = (V, E)$ with set of vertices V and set of edges E , has at most one vertex of degree 2, and is required to have exactly n vertices of degree 1, the leaves $L \subset V$, which we label with $L = [n] := \{1, \dots, n\}$ or with letters a, b, c, \dots . If not mentioned otherwise, we will also require it to be *non-degenerate*, meaning that

- it is *rooted*, i.e., has a distinguished vertex of degree two, its root, denoted by r ,
- it is *binary*, i.e., every vertex $v \in V$ has at most two children.

Biologists often use the terms *node* for vertex and *branch* for edge. The leaves are also called *external nodes* in contrast to the other *internal nodes*. Similarly, the edges adjacent to the leaves are called *external edges* and the others *internal edges*.

The combinatorial information, meaning the vertex-edge adjacencies of a tree T together with the labeling of the leaves, is encapsulated in the term *tree topology* of T , which is denoted by $[[T]]$. If we want to refer to a tree topology independent of the representative of the equivalence class, we often write $[[T^*]]$. There are $(2n - 3)!!$ different tree topologies for a non-degenerate n -tree, see for example [BHV01]. Figure 3.3 shows all 15 tree topologies for $n = 4$ leaves. Since the topology has to be representable for the use of computer programs, it is often represented by the *Newick format*, also called the *nested parentheses format*. As the name suggests, it is iteratively built by grouping both children (leaves or subtrees) of an internal vertex $v \in V$ inside a pair of parentheses, separated by a comma. Here the outermost parentheses represent the root. For instance, the upper left tree topology in Figure 3.3 is represented by $[[T]] = (a, (b, (c, d)))$. Note, that this representation is not unique. For a tree T or a tree topology, respectively, we

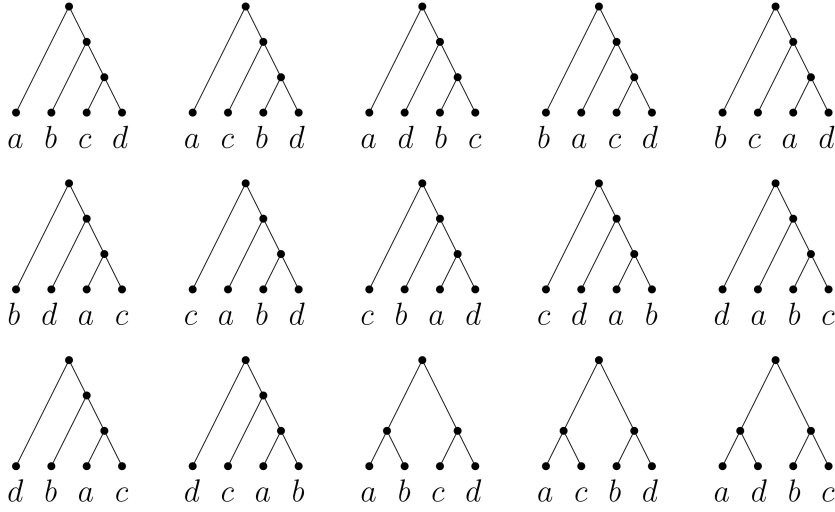


Figure 3.3: All 15 tree topologies of 4-trees.

denote a *coalescent event* C by the segment of the Newick representation that is involved in the coalescent event. For instance the merging of the leaf b with the subtree (c, d) in the first tree in Figure 3.3, is represented by $C = (b, (c, d))$. The set of coalescent events is denoted by \mathfrak{C} or by $\mathfrak{C}([T])$ if we want to refer to the underlying tree topology.

In our model it sometimes plays a role in which order the associated coalescent events take place. This information is not entirely captured by the tree topology of an n -tree. Thus, we introduce the *ranked tree topology* $[T]$ of T , that in addition keeps track of this order. In the literature, the ranked tree topology is sometimes referred to as the concept of *labeled histories*, first introduced by Edwards in [Edw70]. This term can be thought of as an n -tree with its internal nodes ranked according to the order in which the coalescent events took place. For a given $n \in \mathbb{Z}_{\geq 1}$, there are $\frac{n!(n-1)!}{2^{n-1}}$ different ranked tree topologies: Initially, there used to be n lineages in the sample. At each of the $n - 1$ coalescent events $C \in \mathfrak{C}$, two random lineages are merged. For the first coalescent event, there are $\binom{n}{2}$ potential pairs in the sample. For the next one we have $\binom{n-1}{2}$ and so on. For the number of all different combinations of pairings, in total this gives

$$\# \text{ ranked tree topologies} = \binom{n}{2} \binom{n-1}{2} \cdots \binom{2}{2} = \frac{n!(n-1)!}{2^{n-1}}. \quad (3.2.1)$$

Since the coalescing pairs are chosen at random in the Fisher–Wright model, all ranked tree topologies appear with the same probability, namely

$$\mathcal{P}([T] = [T^*]) = \frac{1}{\# \text{ ranked tree topologies}} = \frac{2^{n-1}}{n!(n-1)!} \quad (3.2.2)$$

for a specific ranked tree topology $[T^*]$.

Example 3.2.1. In our running example for $n = 4$ leaves, the tree topology $[[T]] = [[T']] = ((a, b), (c, d))$ cannot distinguish between the two 4-trees T and T' depicted in Figure 3.4, whereas their ranked tree topologies are different.

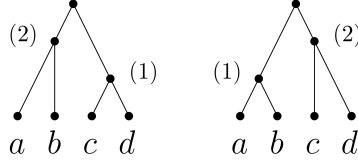


Figure 3.4: Two 4-trees T and T' of the same tree topology, but different ranked tree topology.

In order to indicate the order of coalescent events, one can add this information to the Newick format by using the respective orders in the index of the internal parentheses. For the two trees given in Figure 3.4 this gives $[T] = ((a, b)_2, (c, d)_1)$ for the tree on the left and $[T'] = ((a, b)_1, (c, d)_2)$ for the one on the right.

3.2.3 Waiting Times

The combinatorial type does not give precise information about the actual lengths of the edges of a tree T , so we assign an edge length $\ell(e) \in \mathbb{R}$ to each edge $e \in E$. For a tree coming from a coalescent process, these lengths are just given as the sum of the respective waiting times.

Let us now focus on the waiting times. How many generations does it take to reach the MRCA in the Fisher–Wright model? Let t'_j denote the time during which there are exactly j lineages in the sample, measured in generations. For a sample size of $n = 2$ individuals, the probability that they coalesce in the immediately previous generation is the probability that they choose the same parent. Having N potential parents present within the population, this probability is $\frac{1}{N}$. Similarly, the probability that they do not coalesce is $1 - \frac{1}{N}$. Thus, the coalescent waiting time t'_2 is geometrically distributed with parameter $\frac{1}{N}$, meaning that the probability that the MRCA of two lineages can be found exactly i generations ago is

$$\mathcal{P}(t'_2 = i) = \left(1 - \frac{1}{N}\right)^{i-1} \frac{1}{N}. \quad (3.2.3)$$

What happens if our population size N is large? To get a meaningful answer, we need to change our time scale. So far, time was measured discretely in generations. Let t_2 be the rescaled time such that one time unit equates to N generations, i.e., $t_2 = t'_2/N$. This means replacing the discrete time scale by a continuous one. As a consequence of the large population size approximation, this yields an exponentially distributed waiting

time variable t_2 with parameter 1 and density function $\rho_2(t_2) = \exp(-t_2)$, since

$$\mathcal{P} \left(t_2 > \frac{i}{N} \right) = \mathcal{P} (t'_2 > i) = \left(1 - \frac{1}{N} \right)^i \approx \exp \left(-\frac{i}{N} \right) \quad (3.2.4)$$

as N goes to infinity.

The arguments generalize to the case of considering a sample of $n \in \mathbb{Z}_{\geq 1}$ individuals. Since we assume $n \ll N$, the probability that more than two lineages coalesce simultaneously is negligibly small, and these terms are not taken into account in the computations. This means, the probability that all n individuals choose pairwise different parents in the previous generation is

$$\begin{aligned} \left(1 - \frac{1}{N} \right) \left(1 - \frac{2}{N} \right) \cdots \left(1 - \frac{n-1}{N} \right) &= 1 - \binom{n}{2} \frac{1}{N} + \mathcal{O} \left(\frac{1}{N^2} \right) \\ &\approx 1 - \binom{n}{2} \frac{1}{N}. \end{aligned}$$

In general, let t_j denote the time during which there are exactly j lineages present in the sample, measured in time units of N generations. Each pair coalesces with rate $\frac{1}{N}$ per generation, this means rate 1 per N generations, and there are $\binom{j}{2}$ pairs present in the sample. Consequently, j genes coalesce with rate $\binom{j}{2} \frac{1}{N}$ per generation and t_j has an exponential distribution with parameter $\binom{j}{2}$. Its density is given by

$$\rho_j(t_j) = \binom{j}{2} \exp \left(-\binom{j}{2} t_j \right) \quad (3.2.5)$$

and being exponentially distributed yields

$$\mathbb{E} [t_j] = \frac{1}{\binom{j}{2}} \quad \text{and} \quad \text{Var} [t_j] = \left(\frac{1}{\binom{j}{2}} \right)^2 \quad (3.2.6)$$

for its mean and variance. Given a certain ranked tree topology $[T^*]$, the waiting times t_j are independent random variables for all $j = n, \dots, 2$ because the exponential is memoryless. Therefore for the density we have

$$\rho_{[n]}(t_n, \dots, t_2 \mid [T^*]) = \prod_{j=2}^n \rho_j(t_j). \quad (3.2.7)$$

For the joint distribution of the ranked tree topology $[T^*]$ and the waiting times this yields

$$\rho_{[n]}([T^*], t_n, \dots, t_2) = \rho_{[n]}([T^*]) \rho_{[n]}(t_n, \dots, t_2 \mid [T^*]) = \prod_{j=2}^n \exp \left(-\binom{j}{2} t_j \right), \quad (3.2.8)$$

since we have (3.2.2) and since the waiting times are independent of the tree topology.

Remark 3.2.2. For further considerations we will mostly not take the population size N into account. Therefore, we just assume that the time t is measured in what is called *coalescent units*, where this continuous time scale is defined such that the rate of coalescence is equal to 1. So indirect information about the population size is hidden in the rescaling.

3.2.4 The Kingman n -Coalescent

So far, we have described the two kinds of information that we got out of a large population size approximation of the Fisher–Wright model. On the one hand, we have discrete information about the tree topology, and on the other hand, we have information about the waiting times. Here the two kinds of information are independent of each other.

If we take both into account, this yields a stochastic process. One common way of describing it is as a continuous-time Markov-chain process. We will explain this interpretation in more detail in Section 3.5. This stochastic process was first described by Kingman and is therefore often called the *Kingman n -coalescent* or just *n -coalescent*. In [Kin82a; Kin82b; Kin82c] he formally proved what we have roughly argued above. Namely, that in the limit, as N tends to infinity, the ancestral process under the Fisher–Wright model converges to the Kingman n -coalescent. This does not only apply to the Fisher–Wright model but for the larger class of Cannings models, of which the Fisher–Wright model is a particular case [Can74; Can75].

3.3 SPACES OF TREES

Having described the n -coalescent, our goal is to identify the Kingman n -coalescent as a density on a space of trees. In order to do that, we want to build a space of trees, where each point in the space corresponds to one particular tree, specified by its combinatorial type and its edge lengths. The focus of this section is to establish suitable spaces of trees as a basis of our studies. One additional aim is to bring order into the various notions from existing literature. We define the spaces DTM_n , DUM_n , MTM_n and in particular MUM_n , the space of metrics that are ultrametrics. In Subsection 3.3.1 we examine the geometry of this space. It turns out, that it carries a fine structure, see Proposition 3.3.9, and a coarse structure, see Proposition 3.3.12. Finally, we discuss the relation to objects coming from tropical geometry in Subsection 3.3.2.

There are several ways to parametrize a tree. In [BHV01], internal edge lengths are used for this purpose. Here, we use the approach of pairwise distance functions, compare for instance [SS03].

Definition 3.3.1. A *dissimilarity map* on $[n]$ is a map $\delta : [n] \times [n] \rightarrow \mathbb{R}$ such that $\delta(i, i) = 0$ for all $i \in [n]$, and $\delta(i, j) = \delta(j, i)$ for all $i, j \in [n]$.

Given a tree T , we assign a dissimilarity map δ_T to it, where $\delta_T(i, j)$ measures the distance between leaves $i, j \in L$. The *distance* is given by the sum of the edge lengths

of the unique path connecting the leaves i and j . It will be convenient to also consider negative lengths. We call δ_T the *distance function* of the tree T .

Remark 3.3.2. We drop the index T if it is clear from the context, or if it is not relevant for the context, which particular tree we are considering. To shorten notation, we also often write $d_T \in \mathbb{R}^{\binom{n}{2}}$ for the associated *distance vector* if we refer to a distance function δ_T . This enables us to associate a point in the vector space $\mathbb{R}^{\binom{n}{2}}$ to a given tree. The coordinate giving the distance between leaves i and j is denoted by $d_{ij} := \delta_T(i, j)$, and the coordinates are ordered lexicographically.

Example 3.3.3. For the tree T in Figure 3.2, we obtain the distance vector

$$\begin{aligned} d_T &= (d_{ab}, d_{ac}, d_{ad}, d_{bc}, d_{bd}, d_{cd}) \\ &= (2(t'_3 + t'_4), 2(t'_2 + t'_3 + t'_4), 2(t'_2 + t'_3 + t'_4), \\ &\quad 2(t'_2 + t'_3 + t'_4), 2(t'_2 + t'_3 + t'_4), 2t'_4). \end{aligned}$$

We call a dissimilarity map δ on $[n]$ a *tree metric* if it is the distance function of an unrooted n -tree with non-negative internal edge lengths. There is a criterion to decide whether a given dissimilarity map can be realized as a distance function of such a tree. This condition is often referred to as the *four-point-condition*.

THEOREM 3.3.4 ([SS03, Theorem 7.2.6]). A dissimilarity map δ on $[n]$ is a tree metric, that is, it is the distance function of an unrooted n -tree with non-negative edge lengths, if and only if for all pairwise different $i, j, k, l \in [n]$

$$\max(\delta(i, j) + \delta(k, l), \delta(i, k) + \delta(j, l), \delta(i, l) + \delta(j, k))$$

is attained at least twice.

Therefore, the space of all tree metrics can be characterized as

$$\text{DTM}_n := \{d \in \mathbb{R}^{\binom{n}{2}} : \max(d_{ij} + d_{kl}, d_{ik} + d_{jl}, d_{il} + d_{jk}) \text{ is attained at least twice for all pairwise different } i, j, k, l \in [n]\},$$

where DTM is short for *Dissimilarity maps that are Tree Metrics*.

When we track the history of a sample of genes, we start at the leaves until we reach the MRCA, which becomes the root of our tree. By construction all leaves will have the same distance from this root in the resulting tree. We call such a tree an *equidistant tree*. There is also a corresponding property in terms of distance functions, which is also referred to as the *three-point-condition*.

Definition 3.3.5. An *ultrametric* δ on $[n]$ is a dissimilarity map such that for all pairwise different $i, j, k \in [n]$

$$\max(\delta(i, j), \delta(i, k), \delta(j, k))$$

is attained at least twice.

The terms are related in the following sense.

THEOREM 3.3.6 ([SS03, Theorem 7.2.5]). A dissimilarity map δ on $[n]$ is an ultrametric if and only if it is the distance function of an equidistant n -tree with non-negative internal edge lengths.

We set

$$\text{DUM}_n := \{d \in \mathbb{R}^{\binom{n}{2}} : \max(d_{ij}, d_{ik}, d_{jk}) \text{ is attained at least twice for all pairwise different } i, j, k \in [n]\},$$

where DUM_n is short for *Dissimilarity maps that are UltraMetrics*.

The two spaces DTM_n and DUM_n and some of their geometric properties have been studied before. We introduce two additional spaces of trees that fit our biological context better. Since the edges of a tree are meant to model amounts of time, we want *all* edge lengths to be non-negative. Then the associated distance function δ is a *metric*, which requires the triangle inequality

$$\delta(i, j) \leq \delta(i, k) + \delta(k, j) \text{ to hold for all } i, j, k \in [n],$$

which implies non-negativity, i.e., $\delta(i, j) \geq 0$ for all $i, j \in [n]$.

The space of all such distance vectors is denoted by MTM_n , which is short for *Metrics that are Tree Metrics*, i.e.,

$$\text{MTM}_n := \{d \in \mathbb{R}^{\binom{n}{2}} : \max(d_{ij} + d_{kl}, d_{ik} + d_{jl}, d_{il} + d_{jk}) \text{ is attained at least twice for all } i, j, k, l \in [n]\}.$$

Note, that since the leaves i, j, k, l are not required to be pairwise different, the four-point-condition implies the triangle inequality and therefore non-negativity. This can be seen as follows. For $k = l \in [n]$ we have that the maximum of

$$\max(d_{ij} + d_{kl}, d_{ik} + d_{jl}, d_{il} + d_{jk}) = \max(d_{ij}, d_{ik} + d_{jk}, d_{ik} + d_{jk})$$

is attained at least twice. This implies $d_{ij} \leq d_{ik} + d_{jk}$.

Thus, elements in MTM_n correspond to unrooted n -trees with non-negative distances d_{ij} for all pairs $i, j \in [n]$.

Similarly, we define

$$\text{MUM}_n := \left\{d \in \mathbb{R}^{\binom{n}{2}} : \max(d_{ij}, d_{ik}, d_{jk}) \text{ is attained at least twice for all } i, j, k \in [n]\right\},$$

where MUM_n is short for *Metrics that are UltraMetrics*. This space represents the equidistant n -trees with non-negative edge lengths $\ell(e)$ for all $e \in E$. Here, non-negativity is also implied by the three-point-condition, since the triple is not required to have

pairwise different indices. Even more is true, for an ultrametric δ_T , we have $\delta_T(i, j) \geq 0$ for all $i, j \in [n]$ if and only if $\ell(e) \geq 0$ for all $e \in E$. Thus $\text{MUM}_n = \text{DUM}_n \cap \mathbb{R}_{\geq 0}^{\binom{n}{2}}$. If a dissimilarity map δ on $[n]$ is an ultrametric, this implies that it is in particular a tree metric.

The four spaces of trees are closely related in the following sense. Let

$$\mathcal{L}_n := \text{span} \left(\sum_{j \in [n]: j \neq i} e_{ij} : 1 \leq i \leq n \right),$$

where $e_{ij} = (0, \dots, 0, 1, 0, \dots, 0)$ is the standard basis vector for the distance d_{ij} between the leaves $i, j \in L$. Given a tree distance d_T and $i \in [n]$, then $d_T + \lambda \sum_{j \in [n]: j \neq i} e_{ij}$ is again a tree distance, for all constants $\lambda \in \mathbb{R}$. The corresponding tree is obtained by adding the constant λ to the external branch of the i -th leaf in the tree T . As a consequence, \mathcal{L}_n is contained in the lineality space of DTM_n . On the other hand, by keeping the internal branch lengths, every element in DTM_n can be obtained by adjusting the external branch lengths of a tree of DUM_n or MUM_n . When the resulting tree is supposed to be equidistant as well, then it is sufficient to vary the external edges simultaneously. This gives the following result.

LEMMA 3.3.7.

$$\begin{aligned} \text{DTM}_n &= \text{DUM}_n + \mathcal{L}_n = \text{MUM}_n + \mathcal{L}_n \\ \text{DUM}_n &= \text{MUM}_n + \mathbb{R} \cdot \mathbf{1}. \end{aligned}$$

3.3.1 The Geometry of the Space of Trees MUM_n

For describing the coalescent process, the resulting tree T is an equidistant rooted n -tree having only non-negative edge lengths, or equivalently, the associated distance vector d_T is an element of MUM_n . Thus, we take a closer look at the geometry of this space as a subspace of $\mathbb{R}^{\binom{n}{2}}$. The space DUM_n is known to carry a fine and a coarse combinatorial structure, as discovered in [AKo6] in the context of tropical geometry.

3.3.1.1 The Ranked Tree Topology Cones

Example 3.3.8. Let us consider the case $n = 3$, because then $\binom{n}{2} = \binom{3}{2} = 3$ and the space MUM_3 is still depictable in 3-space. The pairwise distances between the leaves $L = \{a, b, c\}$ yield three global coordinates $(d_{ab}, d_{ac}, d_{bc}) \in \mathbb{R}_{\geq 0}^3$ in the non-negative orthant. There are three different tree topologies of 3-trees which can be seen in Figure 3.5. Here, tree topologies and ranked tree topologies are the same. Let us fix the ranked tree topology $[T^*] = (a, (b, c))$, the one on the left in Figure 3.5. Which distance vectors $d_T \in \mathbb{R}^3$ correspond to this topology? For trees of the given type $[T^*]$, the distance d_{ab} will always equal d_{ac} , and thus, all points corresponding to

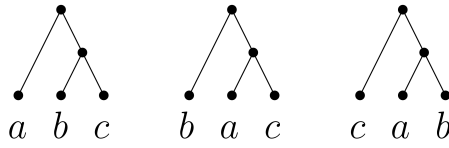
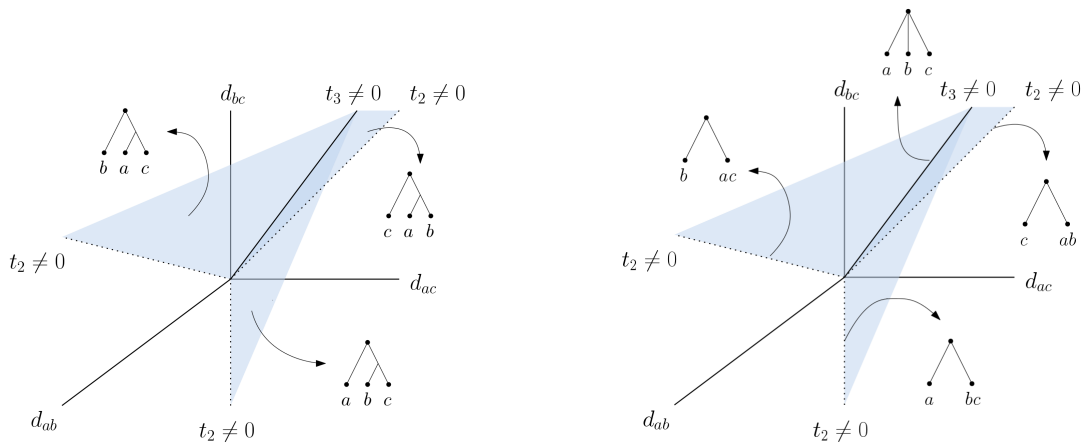


Figure 3.5: The (ranked) tree topologies of 3-trees.

trees having this (ranked) tree topology $[T^*]$ will lie in the hyperplane given by the equation $d_{ab} = d_{ac}$. Because the tree has to be equidistant, we also have $d_{ab} = d_{ac} \geq d_{bc}$. Consequently, we obtain a 2-dimensional cone $\sigma_{[T^*]}$ associated to the given ranked tree topology $[T^*]$ which is spanned by the vectors $(1, 1, 0)$ and $(1, 1, 1)$. The same holds analogously for the other ranked tree topologies. The three cones intersect nicely in lower-dimensional cones, and thus yield a polyhedral fan Σ_3 , which can be seen in Figure 3.6. We want to examine what the lower-dimensional cones correspond to.

- The three 2-dimensional cones intersect in a 1-dimensional ray, given by the equation $d_{ab} = d_{ac} = d_{bc}$. Hence, for trees on that ray we have $t_2 = 0$, and the edge lengths are fully described by $t_3 \neq 0$.
- If we consider the 1-dimensional rays lying in the coordinate hyperplanes, one respective distance is equal to 0 in the corresponding tree. For instance, if $d_{bc} = 0$, this means that we cannot distinguish anymore between the leaves b and c and thus $t_3 = 0$. In this case, the edge lengths are just determined in terms of $t_2 \neq 0$.


 Figure 3.6: Full- and lower-dimensional cones in the space MUM_3 .

In the general case, where we start with a sample of size n , the space MUM_n can be described in a similar way. For a given equidistant n -tree T that arose from the n -coalescent process, its corresponding distance vector d_T has $\binom{n}{2}$ entries. How many different entries may it have? If one expresses the entries in terms of the waiting times t_j for $j = 2, \dots, n$, the distances that can occur are of the form $2 \sum_{j=k}^n t_j$ for

$k = 2, \dots, n$. Thus, independent of the tree topology, the coordinates of a distance vector are contained in subset of cardinality at most $n - 1$. For a fixed ranked tree topology, the subsets of the respective coordinate indices that coincide will always be the same. Thus, all the corresponding distance vectors lie in a common subspace of dimension $n - 1$. The intersection with MUM_n is cut out by linear inequalities that come from the tree's property of being equidistant, and that are determined by its ranked tree topology. As a result, we obtain an $(n - 1)$ -dimensional *ranked topology cone* $\sigma_{[T^*]}$ that corresponds to the fixed ranked tree topology $[T^*]$. As in Example 3.3.8, considering all possible ranked tree topologies, these cones intersect nicely, and we obtain a polyhedral fan Σ_n , whose support is MUM_n . This can also be verified using a result of Ardila and Klivans. In Theorem 3 and Proposition 3 of [AK06] they showed that DUM_n is the support of a fan, where the top-dimensional cones correspond to ranked tree topologies. Both spaces MUM_n and DUM_n have the same combinatorics by definition, and $\text{MUM}_n = \text{DUM}_n \cap \mathbb{R}_{\geq 0}^{\binom{n}{2}}$. Altogether, this leads to the following proposition.

PROPOSITION 3.3.9. Let $n \in \mathbb{Z}_{\geq 1}$. The space $\text{MUM}_n \subset \mathbb{R}^{\binom{n}{2}}$ is the support of a polyhedral fan Σ_n , whose top-dimensional cones are in one-to-one-correspondence with ranked tree topologies.

In general, this means that in order to interpolate between n -trees, we will also need to consider non-binary trees or trees with multiple leaf labels. Let us make this more precise. Let T be an equidistant n -tree that arose from an n -coalescent process. We have observed earlier that its edge lengths can be expressed in terms of the waiting times t_j . An edge $e \in E$ always has a length of the form $\ell(e) = \sum_{j=i}^k t_j$ for some $i \leq k \in \{2, \dots, n\}$. We will call a tree T a *degenerate n -tree* if it arose from an n -tree by setting $t_j = 0$ for some $j \in \{2, \dots, n\}$. Thus for a degenerate n -tree it holds that

- it has between 2 and n leaves, some of them may have multiple labels.
- its root has degree between 2 and n .
- all of its other internal vertices have degree between 3 and n .
- all leaves have the same distance to the root.

For a fixed ranked tree topology $[T^*]$, the corresponding cone $\sigma_{[T^*]} \in \Sigma_n$ is an $(n - 1)$ -dimensional unimodular cone with respect to the lattice $\mathbb{Z}^{\binom{n}{2}}$, see Section 3.3.1.2. Thus, a face of codimension k for $k \in \{1, \dots, n - 2\}$ consists of distance vectors of degenerate n -trees which arose by setting k of the waiting times equal to zero. In particular, this means that for each of the $n - 1$ rays, exactly one waiting time t_j for a $j \in \{2, \dots, n\}$ remains non-zero. Thus we can give local coordinates in terms of t_2, \dots, t_n to this specific cone.

3.3.1.2 The Tree Topology Cones

Also the subsets of MUM_n corresponding to an unranked tree topology $[[T^*]]$ have a nice geometric interpretation that relates to known objects from discrete geometry. We did not find this interpretation in the literature. To make this more precise, we recall the necessary definitions.

A *partially ordered set* (Π, \leq_Π) , or *poset* for short, is a set Π together with a *partial order*, which is a binary relation \leq_Π , that is reflexive, antisymmetric, and transitive. A finite poset can be represented via its *Hasse diagram*. A *linear extension* of \leq_Π is a total order that refines \leq_Π .

Given a tree topology $[[T^*]]$, this can be interpreted as a poset

$$(\mathfrak{C}, \leq) := (\Pi([[T^*]]), \leq_{\Pi([[T^*]])}), \quad (3.3.1)$$

where the partial order \leq on the set of coalescent events $\mathfrak{C} = \mathfrak{C}([[T^*]])$ is determined by the topology of the tree in the natural way: More precisely, let $v_C \in V$ denote the internal vertex at which the coalescent event $C \in \mathfrak{C}$ takes place. Two coalescent events $C_1, C_2 \in \mathfrak{C}$ are in relation $C_1 \leq C_2$ if and only if the subtree descending from the internal vertex $v_{C_2} \in V$ associated to C_2 contains the internal vertex $v_{C_1} \in V$ associated to C_1 . Note, that the Hasse diagram coincides with the tree without external edges.

Example 3.3.10. In our running example the tree topology $[[T^*]] = ((a, b), (c, d))$ involves the three coalescent events $\mathfrak{C} = \{(a, b), (c, d), ((a, b), (c, d))\}$. For the associated poset (\mathfrak{C}, \leq) we have the partial order \leq given by $(a, b) \leq ((a, b), (c, d))$ and $(c, d) \leq ((a, b), (c, d))$.

To every finite poset, Stanley associates two geometric objects.

Definition 3.3.11 ([Sta86, Definition 1.1]). The *order polytope* $\mathcal{O}(\Pi)$ of a finite poset (Π, \leq_Π) is the subset of $\mathbb{R}^\Pi = \{f: \Pi \rightarrow \mathbb{R}\}$ defined by the conditions

$$0 \leq f(i) \leq 1, \quad \text{for all } i \in \Pi, \quad (3.3.2)$$

$$f(i) \leq f(j), \quad \text{if } i \leq_\Pi j \text{ in } \Pi. \quad (3.3.3)$$

In [Sta86], Stanley also states that there exists a unimodular triangulation of $\mathcal{O}(\Pi)$ such that the maximal simplices are in bijection to the linear extensions of the partial order \leq_Π . Every simplex in the triangulation also comes from some monotone path from $(0, \dots, 0)$ to $(1, \dots, 1)$ in the unit cube $[0, 1]^\Pi$.

If we relax the upper bound condition $f(i) \leq 1$ in (3.3.2), then the resulting object will be a pointed polyhedral cone, which is called the *order cone* and denoted by $\mathcal{K}(\Pi)$. It captures all order-preserving functions from Π to $\mathbb{R}_{\geq 0}$. The unimodular triangulation of $\mathcal{O}(\Pi)$ induces a unimodular triangulation of $\mathcal{K}(\Pi)$.

This relates to our space of trees in the following sense. Given a coalescent event $C \in \mathfrak{C}$, we denote by d_C the point in time at which the coalescent event takes place and call it its *coalescent time*.

PROPOSITION 3.3.12. Let $[[T^*]]$ be a tree topology for MUM_n . Then the subset

$$\sigma_{[[T^*]]} := \{d_T \in \text{MUM}_n : [[T]] = [[T^*]]\} \quad (3.3.4)$$

is isomorphic to the order cone $\mathcal{K}(\mathfrak{C}([[T^*]]))$ of the poset $(\mathfrak{C}([[T^*]]), \leq)$ given as in (3.3.1) and is therefore called a *tree topology cone*. The unimodular subcones of $\mathcal{K}(\mathfrak{C}([[T^*]]))$, that are in bijection to linear extensions of \leq , correspond to the respective ranked tree topologies that refine $[[T^*]]$.

Proof. We fix a tree topology $[[T^*]]$. As argued in Section 3.3.1.1, a distance vector $d_T \in \text{MUM}_n$ can have at most $(n-1)$ pairwise different entries, namely $\sum_{j=k}^n t_j$ for $k \in \{2, \dots, n\}$. For the fixed tree topology $[[T^*]]$, the indices of the coordinates that coincide respectively, for all trees with tree topology $[[T^*]]$, are determined by the tree topology. Thus, we fix a maximal index set $I \subseteq \binom{[n]}{2}$ with $|I| = n-1$ of pairwise different coordinates. Then, we consider the subset $\mathbb{R}_{\geq 0}^I \cong \mathbb{R}_{\geq 0}^{n-1}$. Within that orthant, the restriction to the subset $\{d_T \in \text{MUM}_n : [[T]] = [[T^*]]\} |_I$ is cut out by hyperplanes. The hyperplanes are determined by linear inequalities of the form $d_{ij} \leq d_{kl}$ for $i, j, k, l \in L$, that are determined by the tree topology.

Let $\mathfrak{C} = \mathfrak{C}([[T^*]])$ be the set of coalescent events associated to $[[T^*]]$. The tree topology determines the poset (\mathfrak{C}, \leq) as explained in (3.3.1). This yields the associated order cone $\mathcal{K}(\mathfrak{C})$ with coordinates $(d_C)_{C \in \mathfrak{C}}$, where d_C is the coalescent time of the coalescent event $C \in \mathfrak{C}$. It is an $(n-1)$ -dimensional cone, where each coordinate represents one coalescent event $C \in \mathfrak{C}$. Let $C \in \mathfrak{C}$ be a coalescent event, that merges the subtrees T_1 and T_2 of T . Then for a tree distance in (3.3.4), we have $d_C = \frac{1}{2}d_{ij}$, for all leaves i of T_1 and j of T_2 , respectively. This yields a change of coordinates, that identifies $\mathbb{R}^{\mathfrak{C}}$ with \mathbb{R}^I . By (3.3.3), in the definition of the order polytope, the defining inequalities cut out the same half spaces and therefore we have the identification of cones $\sigma_{[[T^*]]} \cong \mathcal{K}(\mathfrak{C})$.

A linear extension of the poset (\mathfrak{C}, \leq) is a total order that refines \leq . In our context this means, that we obtain a total order of all coalescent events $C \in \mathfrak{C}$. This exactly determines a ranked tree topology $[T^*]$ that is coarsened by the tree topology $[[T^*]]$. Thus, the unimodular cones in the triangulation of the order cone are in bijection with the ranked tree topologies that refine $[[T^*]]$. \square

We illustrate the proposition for our running example.

Example 3.3.13. We continue with Example 3.3.10 and consider the tree topology $[[T^*]] = ((a, b), (c, d))$ for $n = 4$. Then MUM_4 is $\binom{4}{2} = 6$ -dimensional and the considered subspace is given by the equalities $d_{ac} = d_{ad} = d_{bc} = d_{bd}$. This gives a 3-dimensional orthant with local coordinates (d_{ab}, d_{ac}, d_{cd}) or $(d_{(a,b)}, d_{((a,b),(c,d))}, d_{(c,d)})$

in terms of coalescent events, respectively. The cone $\sigma_{((a,b),(c,d))} \cong \mathcal{K}(\mathfrak{C})$ is depicted in Figure 3.7. It is triangulated into two unimodular cones, corresponding to the ranked tree topologies $((a,b)_1, (c,d)_2)$ (green) and $((a,b)_2, (c,d)_1)$ (blue).

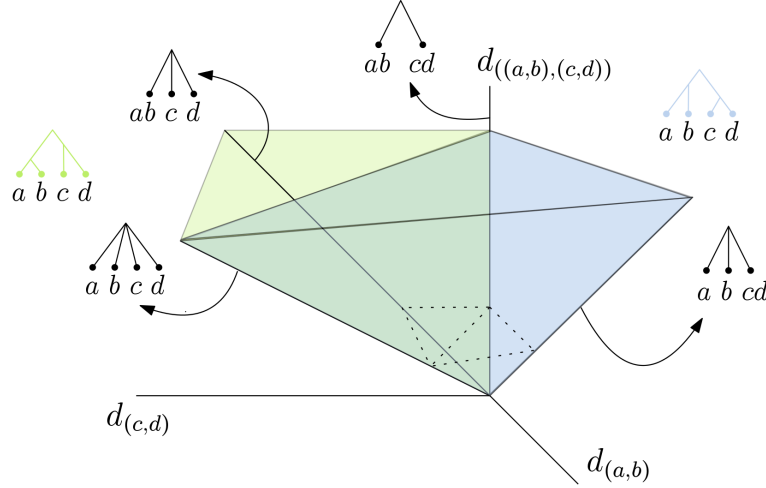


Figure 3.7: The tree topology cone $\sigma_{((a,b),(c,d))}$ triangulated into two unimodular ranked tree topology cones $\sigma_{((a,b)_1,(c,d)_2)}$ (green) and $\sigma_{((a,b)_2,(c,d)_1)}$ (blue).

3.3.2 The Connection to Tropical Geometry

The spaces of trees that we are considering in Section 3.3 have an important connection to objects coming from tropical geometry. We give a brief summary of these relations, following the presentation in [MS15, Chapter 3.5] and [PS05, Chapters 4.2 and 4.3]. See there, for detailed definitions, statements, proofs, and a broad introduction into tropical geometry.

The Grassmannian $G(2, n) \subseteq \mathbb{P}^{\binom{n}{2}-1}$ is the smooth projective variety of dimension $2(n-2)$ that parametrizes the family of 2-planes containing the origin in \mathbb{R}^n . By $G^0(2, n) = G(2, n) \cap \mathbb{T}^{\binom{n}{2}-1}$, we denote the open variety which corresponds to removing the coordinate hyperplanes. Then the tropical Grassmannian $\text{trop}(G^0(2, n))$ can be thought of as follows. Let $A = (a_{ij})_{i,j}$ be a symmetric $(n \times n)$ -matrix with zeros on the diagonal. The remaining $\binom{n}{2}$ distinct entries are unknown. Each quadruple $\{i, j, k, l\} \subseteq [n]$ with $|\{i, j, k, l\}| = 4$ gives a tropical polynomial

$$p_{ijkl}(A) = \max(a_{ij} + a_{kl}, a_{ik} + a_{jl}, a_{il} + a_{jk}) \quad (3.3.5)$$

which defines a tropical hypersurface in $\mathbb{R}^{\binom{n}{2}}$. It consists of the points, for which the maximum is attained at least twice. Then, the tropical Grassmannian is the intersection of these $\binom{n}{4}$ hypersurfaces. It is a pure $2(n-2)$ -dimensional rational polyhedral fan

in $\mathbb{R}^{\binom{n}{2}-1} \cong \mathbb{R}^{\binom{n}{2}}/\mathbb{R}\mathbf{1}$. The polynomials in (3.3.5) are reminiscent of the four-point-condition, which is not a coincidence.

THEOREM 3.3.14 ([SS04, Theorem 4.2]). The tropical Grassmannian $\text{trop}(G^0(2, n))$ coincides with the space of trees $\text{DTM}_n/\mathbb{R}\mathbf{1}$, up to sign.

Let K_n denote the complete graph on n vertices. We consider the associated *graphical matroid* $M(K_n)$, where the ground set is given by the set of edges of K_n labeled by $\binom{[n]}{2}$. The smallest circuits c of the matroid are given by the triangles in the graph K_n . The *linear tropical space* $\text{trop}(M(K_n))$ is the set of vectors $\omega \in \mathbb{R}^{\binom{n}{2}}$ such that for any circuit c of $M(K_n)$, the maximum of the numbers ω_{ij} is attained at least twice, when ij ranges over c [MS15, compare Definition 4.2.5]. For triangles this condition describes the set of all weights $\omega \in \mathbb{R}^{\binom{n}{2}}$ such that $\max(\omega_{ij}, \omega_{ik}, \omega_{jk})$ is attained at least twice for all pairwise different $i, j, k \in \{1, \dots, \binom{n}{2}\}$. If the condition is fulfilled for all triangles, then it holds for all bigger circuits as well. Therefore we have the following connection.

THEOREM 3.3.15 ([AK06, Theorem 3]). The space of trees DUM_n coincides with $\text{trop}(M(K_n))$.

For $\omega \in \text{trop}(M(K_n))$, we have $\omega + \lambda\mathbf{1} \in \text{trop}(M(K_n))$ for any $\lambda \in \mathbb{R}$. Thus $\text{trop}(M(K_n))$ is often regarded as a subset of the quotient space $\mathbb{R}^{\binom{n}{2}-1}$. If we divide out its lineality space, the set carries a fan structure that comes out of the combinatorics of the underlying matroid. This fan is called the *Bergman fan*. It has a coarse and a fine fan structure. In Proposition 3 in [AK06], Ardila and Klivans show that these correspond to (ranked) tree topologies, respectively, compare Sections 3.3.1.1 and 3.3.1.2

The above yields another insightful connection. Consider the moduli space $\mathcal{M}_{0,n}$ of n distinct labeled points on the projective line \mathbb{P}^1 up to an automorphisms of \mathbb{P}^1 . This can be thought of as

$$\begin{aligned} \mathcal{M}_{0,n} &= (\mathbb{P}^1 \setminus \{0, 1, \infty\})^{n-3} \setminus \text{diagonals} \\ &= \mathbb{P}^{n-3} \setminus \{x_i = 0, x_i = x_j \text{ for all } 0 \leq i, j \leq n-3\}. \end{aligned}$$

Since this realizes $\mathcal{M}_{0,n}$ as the complement of $\binom{n-1}{2}$ hyperplanes in \mathbb{P}^{n-3} , it defines a closed embedding into a suitable torus $\mathbb{T}^{\binom{n-1}{2}-1}$. It can be read off the defining linear equalities that the tropicalization $\text{trop}(\mathcal{M}_{0,n}) \subseteq \mathbb{R}^{\binom{n-1}{2}-1}$ coincides with the tropicalization of the graphical matroid $\text{trop}(M(K_{n-1}))$ and by Theorem 3.3.15 therefore with the space of trees DUM_{n-1} . Hence, it carries a fan structure, which determines a toric variety. Actually, the closure of $\mathcal{M}_{0,n}$ in the corresponding toric variety equals the Deligne–Mumford compactification $\overline{\mathcal{M}}_{0,n}$. Here, $\overline{\mathcal{M}}_{0,n}$ is the moduli space of stable genus zero curves with n distinct marked points. See [MS15, Chapter 6.4], [Tev07, Theorem 5.5], or [GM10, Theorem 5.7] for more details.

Moduli spaces carry universal families. In the case of $\mathcal{M}_{0,n}$, the universal family arises via the so called *forgetful maps*. In [FH13], the authors introduce a tropical counterpart by giving a suitable definition of a family of tropical curves and prove that the forgetful map between the moduli spaces of tropical curves

$$\text{ft}_n : \mathcal{M}_{0,n}^{\text{trop}} \rightarrow \mathcal{M}_{0,n-1}^{\text{trop}}, \quad (3.3.6)$$

is then indeed a universal family. This map can be thought of as *forgetting* the n -th marked point. We will come back to this in Section 3.5.2, when we consider a forgetful-like map in the context of spaces of trees.

3.4 THE KINGMAN n -COALESCENT AS A DENSITY ON A SPACE OF TREES

The discussion of Sections 3.2 and 3.3 enables us to describe the Kingman n -coalescent by a density on MUM_n with respect to a well defined Lebesgue-measure.

PROPOSITION 3.4.1. The Kingman n -coalescent is locally given by the continuous density

$$\rho_{[n]}(t_n, \dots, t_2) = \prod_{j=2}^n \exp\left(-\binom{j}{2} t_j\right), \quad (3.4.1)$$

where t_2, \dots, t_n are waiting times and local coordinates for each top-dimensional cone $\sigma_{[T^*]} \in \Sigma_n$ on MUM_n corresponding to a ranked tree topology $[T^*]$. On the lower-dimensional intersections the densities coming from different top-dimensional cones agree, and thus, this yields a global continuous density on MUM_n .

Proof. We consider the fan Σ_n . Let $\sigma_{[T^*]}$ be a top-dimensional cone, corresponding to the ranked tree topology $[T^*]$. Then, as argued before, $\sigma_{[T^*]}$ is an $(n-1)$ -dimensional unimodular cone, whose rays correspond to the local coordinates t_2, \dots, t_n . Since the cone is unimodular, we can map it to the positive $(n-1)$ -dimensional orthant in \mathbb{R}^{n-1} , such that the primitive ray generators of $\sigma_{[T^*]}$ are mapped to the standard basis vectors of \mathbb{R}^{n-1} via a unimodular transformation. On \mathbb{R}^{n-1} we have the Lebesgue-measure which we pull back. By (3.2.5) and (3.2.7), given a fixed ranked tree topology $[T^*]$, the coalescent process is described by the density

$$\rho_{[n]}(t_n, \dots, t_2 \mid [T^*]) = \prod_{j=2}^n \rho_j(t_j) = \prod_{j=2}^n \binom{j}{2} \exp\left(-\binom{j}{2} t_j\right) \quad (3.4.2)$$

with respect to this Lebesgue-measure. Since tree topology and waiting times are independent and all ranked tree topologies are equally likely to appear, we have to divide by the total number of ranked tree topologies which yields

$$\rho_{[n]}(t_n, \dots, t_2) = \prod_{j=2}^n \exp\left(-\binom{j}{2} t_j\right) \quad (3.4.3)$$

as in (3.2.8). The t_j are uniquely determined by T for all $j \in [n]$, even if some are 0. Therefore we obtain a unique value also for degenerate trees in the relative interior of lower-dimensional cones. Thus, (3.4.3) yields a well-defined global density. \square

3.5 THE KINGMAN COALESCENT

In Section 3.2.4 we have already mentioned that the Kingman n -coalescent is often described as a continuous Markov-chain process on partitions of $[n]$. We provide the necessary background for this approach in Subsection 3.5.1. This enables us to consider the Kingman coalescent as a limiting process. Against this background we define a forgetful map in Subsection 3.5.2 and discuss the relation of the respective densities for increasing n , compare Proposition 3.5.3.

3.5.1 The Kingman n -Coalescent as a Markov-Chain Process

We will explain the basics of this description following [Kin82a; Kin82b; Kin82c]. For simplicity, we assume our n individuals to be labeled by $1, \dots, n$. Furthermore, let P_n denote the set of all set-partitions of $[n]$. At the beginning of the process all individuals are separated, which is modeled by the partition of $[n]$ into singletons $\{1\}, \dots, \{n\}$. Each time a coalescent event takes place in the n -coalescent process, two of the lineages present in the sample are merged. This can be interpreted as merging the corresponding blocks in the current partition. Thus, we define \sim_k as the equivalence relation on $[n]$ with $i \sim_k j$, if i and j are in the same block of the partition after k coalescent events. In our phylogenetic context this means that the respective lineages shared a common ancestor k generations/time units ago. We denote the equivalence classes by \mathcal{R}_k^n and call $\mathcal{R}^n = (\mathcal{R}_k^n)_{k \in \mathbb{Z}_{\geq 1}}$ the *ancestral process* of the sample of size n . This process is a homogeneous Markov-chain with values in P_n . So the process starts in the state $\mathcal{R}_0^n = \{\{1\}, \dots, \{n\}\}$. The transition probability $\mathcal{P}(\pi \rightarrow \pi')$ that a partition π is turned into a partition π' is non-zero if and only if π' arises from π by merging two of its blocks.

If t denotes the rescaled time in our large population size approximation, as in Section 3.2.3, Kingman [Kin82a; Kin82b; Kin82c] and Möhle and Sagitov [MS01] showed that in the limit, this yields the Kingman n -coalescent $(\mathcal{R}_t^n)_{t \geq 0}$ as an continuous-time Markov-chain process with values in P_n starting at the partition into singletons and having the transition rates

$$q_{\pi, \pi'} = \begin{cases} 1 & \text{if } \pi' \text{ is obtained by merging two elements of } \pi, \\ 0 & \text{otherwise.} \end{cases} \quad (3.5.1)$$

for $\pi, \pi' \in P_n$. For $m > n$ we define $\mathcal{R}^{m,n}$ to be the restriction of \mathcal{R}^m to P_n . One important property of the n -coalescent is its consistency. This means that the restriction $\mathcal{R}^{m,n}$ has the same law as the n -coalescent process \mathcal{R}^n .

This property with the additional application of Kolmogorov's extension theorem enables us to define a more general process on P_∞ , which denotes the set of partitions of $\mathbb{Z}_{\geq 1}$.

PROPOSITION 3.5.1 (Kingman, Möhle-Sagitov). There is a unique Markov process on P_∞ , the set-partitions of $\mathbb{Z}_{\geq 1}$, such that for every $n \in \mathbb{Z}_{\geq 1}$ its restriction to the partitions of any subset of size n is an n -coalescent. This process is called the *Kingman coalescent*.

3.5.2 A Forgetful Map on the Space of Trees

The Kingman n -coalescent's property of being consistent can also be interpreted in terms of the involved trees. Let T be a tree resulting from an n -coalescent process and let $d_T \in \mathbb{R}^{\binom{n}{2}}$ be the corresponding distance vector. If we restrict T to an $(n-1)$ -subtree \hat{T} , this means that we just forget the $n-1$ entries of d_T that involve the n -th leaf. None of the leaves have a distinguishing property. Thus, for simplicity of presentation, we always assume the n -th leaf to be removed if not specified otherwise. This yields a new distance vector $d_{\hat{T}} \in \mathbb{R}^{\binom{n-1}{2}}$. We denote this linear projection by Φ_n , where

$$\begin{aligned} \Phi_n : \text{MUM}_n &\rightarrow \text{MUM}_{n-1} \\ d_T &\mapsto d_{\hat{T}}. \end{aligned} \tag{3.5.2}$$

Graphically, we can think of this restriction as removing the external branch adjacent to leaf n from the tree T . Consistency of the underlying process tells us that the tree \hat{T} can be interpreted as the resulting tree of an $(n-1)$ -coalescent process on the remaining $n-1$ leaves $L_{n-1} = L_n \setminus \{n\}$.

We are now interested in the preimage of a point under the map Φ_n . That is, given an $(n-1)$ -tree \hat{T} with $d_{\hat{T}} \in \text{MUM}_{n-1}$, where can we attach an n -th external branch to \hat{T} in such a way that \hat{T} is the image of the new tree T under the restriction map Φ_n ? Our answer can be understood as a tree version of Proposition 4.5 in [FH13], where they consider DUM_n from a tropical perspective.

PROPOSITION 3.5.2. Let \hat{T} be an equidistant $(n-1)$ -tree with distance vector $d_{\hat{T}} \in \text{MUM}_{n-1}$. Then the preimage Φ_n^{-1} can be identified with the tree \hat{T} with an additional infinitely long branch above the root.

Proof. Let $\hat{T} = (\hat{V}, \hat{E})$ be an equidistant $(n-1)$ -tree. We denote by \hat{T}_∞ the tree \hat{T} with an additional infinitely long branch above the root. Given a point \hat{v} on \hat{T}_∞ , we first construct a point in $\Phi_n^{-1}(\hat{T})$. As argued above, every tree T in the preimage of Φ_n arises from \hat{T} by adding an external branch adjacent to a new n -th leaf to the current tree \hat{T} . There are three cases, as depicted in Figure 3.8.

1. \hat{v} is not a vertex and lies on one of the finite edges $\hat{e} \in \hat{E}$. Split it into two edges by inserting \hat{v} as a new internal vertex. Attach an external edge \hat{e}_n to \hat{v} , that is

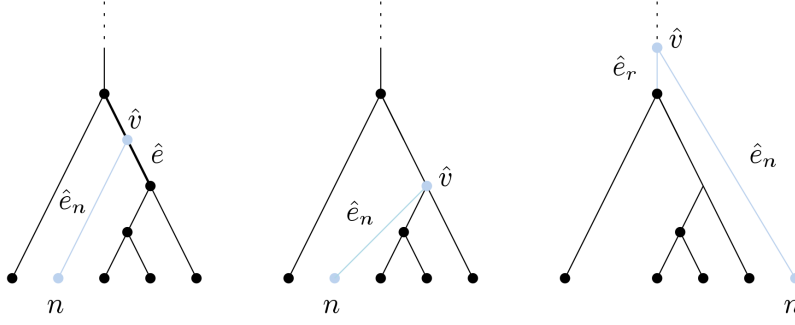


Figure 3.8: The different ways to insert an n -th leaf to obtain a tree T in the preimage $\Phi_n^{-1}(\hat{T})$.

adjacent to the new leaf n . The edge length of \hat{e}_n is determined by the required property of being equidistant.

2. \hat{v} is an internal vertex $\hat{v} \in \hat{V}$. Attach an external edge \hat{e}_n to \hat{v} that is adjacent to the new leaf n . The edge length of \hat{e}_n is determined by the required property of being equidistant. Note that the resulting tree T will be degenerate, since it involves multiple simultaneous coalescence. If \hat{v} is an existing leaf, then add n as a label to this leaf, which will then have multiple labels.
3. \hat{v} lies on the extra branch. Add \hat{v} to the set of vertices as a new root. Insert an internal edge \hat{e}_r joining \hat{v} and the old root of \hat{T} . Attach an external edge \hat{e}_n to \hat{v} , that is adjacent to the new leaf n . The edge length of \hat{e}_n is determined by the required property of being equidistant.

All these procedures give rise to an equidistant n -tree T and do not change the pairwise distances between the leaves $L_{n-1} = \{1, \dots, n-1\}$. Therefore, all trees obtained these ways lie in the preimage $\Phi_n^{-1}(\hat{T})$.

Conversely, let $T = (V, E)$ be an n -tree in the preimage $\Phi_n^{-1}(\hat{T})$. Then there exists a vertex $\hat{v} \in V$ which attaches the external branch adjacent to the n -th leaf to tree. Then either \hat{v} is already a point on \hat{T} or it is the root of T . In this case it can be identified with its corresponding point on the additional branch. The described procedures are mutual inverses and thus the preimage $\Phi_n^{-1}(\hat{T})$ can be identified with the tree \hat{T} with an additional infinitely long branch above the root. \square

After dividing out $\mathbb{R} \cdot \mathbb{1}$, this map Φ_n descends to the universal family described in [FH13].

In Proposition 3.4.1 we have shown that the Kingman n -coalescent is given as a density on the space of trees MUM_n . Let $d_{\hat{T}} \in \text{MUM}_{n-1}$ be the distance vector of an equidistant $(n-1)$ -tree \hat{T} . Moreover, let T be an equidistant n -tree with distance vector $d_T \in \text{MUM}_n$ with $\Phi_n(d_T) = d_{\hat{T}}$, where T arose from \hat{T} by attaching the additional external branch in the k -th time interval of \hat{T} for a $k \in \{1, \dots, n-1\}$ as in Figure 3.9, with t_{k+1} known.

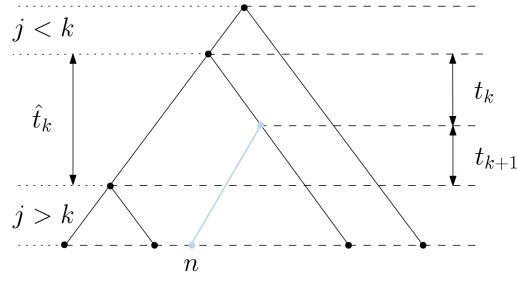


Figure 3.9: Adding an n -th external branch within the k -th time interval.

Since it is allowed to attach it above the root, we also have to take the time interval \hat{t}_1 into account, representing the time during which there is only one lineage present in \hat{T} . Having this information, we can recover the value of the density $\rho_{[n]}$ at d_T from the value of the density $\rho_{[n-1]}$ at $d_{\hat{T}}$.

PROPOSITION 3.5.3. Let $d_T \in \text{MUM}_n$ be the distance vector of an n -tree T that arose from an $(n-1)$ -tree \hat{T} with $d_{\hat{T}} \in \text{MUM}_{n-1}$ by attaching an external branch within the k -th time interval for some $k \in \{1, \dots, n-1\}$. Then the value of the density $\rho_{[n]}$ at d_T can be recovered from the value of the density $\rho_{[n-1]}$ at $d_{\hat{T}}$ via

$$\rho_{[n]}(d_T) = \exp\left(-\left(\sum_{j=k+2}^{n-1} j\hat{t}_j\right) - kt_{k+1}\right) \rho_{[n-1]}(d_{\hat{T}}),$$

where the \hat{t}_j denote the waiting times for \hat{T} for $j \in \{2, \dots, n-1\}$.

Proof. Let T and \hat{T} be trees as given in the proposition. We have already discussed that attaching a new external branch to \hat{T} in order to obtain T does not affect the entries of $d_{\hat{T}}$. The computation of the value $\rho_{[n]}(d_T)$ requires to know the values of the local coordinates t_2, \dots, t_n , i.e., the waiting times for T . In general it is not true that $t_k = \hat{t}_k$ holds for all $k \in \{2, \dots, n-1\}$. If the new branch is inserted during the k -th time interval of \hat{T} , then we consider the following cases.

1. All waiting times \hat{t}_j for $j < k$ are not affected and for those we have $t_j = \hat{t}_j$. They contribute the same respective factor $\rho_j(t_j) = \rho_j(\hat{t}_j) = \binom{j}{2} \exp\left(-\binom{j}{2}t_j\right)$ to $\rho_{[n]}(d_T)$ as they did to $\rho_{[n-1]}(d_{\hat{T}})$.
2. For all $j > k+1$, we have $t_j = \hat{t}_{j-1}$, since the number of lineages that are present in the sample is increased by one, respectively, and the values of the waiting times

are not affected. Since

$$\begin{aligned} \rho_j(t_j) &= \exp\left(-\binom{j}{2}t_j\right) = \exp\left(-\binom{j}{2}\hat{t}_{j-1}\right) \\ &= \exp\left(-(j-1)\hat{t}_{j-1}\right) \exp\left(-\binom{j-1}{2}\hat{t}_{j-1}\right), \end{aligned}$$

we have to multiply our original value $\rho_{j-1}(\hat{t}_{j-1})$ by $\exp\left(-(j-1)\hat{t}_{j-1}\right)$.

3. For $j = k$ and $j = k + 1$ the contribution to $\rho_{[n]}(d_T)$ are the two factors $\rho_k(t_k) = \exp\left(-\binom{k}{2}t_k\right)$ and $\rho_{k+1}(t_{k+1}) = \exp\left(-\binom{k+1}{2}t_{k+1}\right)$, where $t_k = \hat{t}_k - t_{k+1}$ and t_{k+1} are given. In $\rho_{[n-1]}(d_{\hat{T}})$ we already have the factor

$$\begin{aligned} \rho_k(\hat{t}_k) &= \exp\left(-\binom{k}{2}\hat{t}_k\right) = \exp\left(-\binom{k}{2}(\hat{t}_k - t_{k+1})\right) \exp\left(-\binom{k}{2}t_{k+1}\right) \\ &= \exp\left(-\binom{k}{2}t_k\right) \exp\left(-\binom{k}{2}t_{k+1}\right). \end{aligned}$$

Thus the remaining additional factor is $\exp\left(-kt_{k+1}\right)$.

Altogether this yields

$$\rho_{[n]}(d_T) = \exp\left(\left(\sum_{j=k+2}^{n-1} -j\hat{t}_j\right) - kt_{k+1}\right) \rho_{[n-1]}(d_{\hat{T}}).$$

□

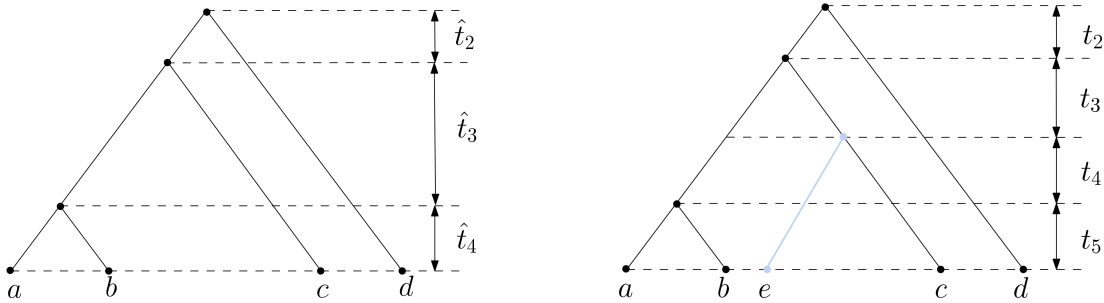


Figure 3.10: The 4-tree \hat{T} and the resulting 5-tree T after attaching an additional external branch during the third time interval.

Example 3.5.4. Let us apply Proposition 3.5.3 to the example depicted in Figure 3.10. For the 4-tree \hat{T} we have

$$\rho_{[4]}(d_{\hat{T}}) = \exp\left(-\hat{t}_2 - 3\hat{t}_3 - 6\hat{t}_4\right).$$

For getting from \hat{T} to T , the additional branch is attached during the third time interval, i.e., $k = 3$, and we are given the waiting time $t_{k+1} = t_4$. Furthermore, we have $t_3 = \hat{t}_3 - t_4$. To compute $\rho_{[5]}(d_T)$, we consider the three cases mentioned in the proof of Proposition 3.5.3.

1. $j = 2$: No additional factor is needed.
2. $j = 5$: This yields the additional factor $\exp(-4\hat{t}_4)$.
3. $j = 3, j = 4$: This yields the additional factor $\exp(-3t_4)$.

In total, having $t_2 = \hat{t}_2$ and $t_5 = \hat{t}_4$, this gives

$$\begin{aligned} \rho_{[5]}(d_T) &= \exp(-4\hat{t}_4 - 3t_4) \rho_{[4]}(d_{\hat{T}}) \\ &= \exp(-4\hat{t}_4 - 3t_4) \exp(-\hat{t}_2 - 3\hat{t}_3 - 6\hat{t}_4) \\ &= \exp(-t_2 - 3t_3 - 6t_4 - 10t_5). \end{aligned}$$

3.6 THE MULTISPECIES COALESCENT — SPECIES TREES AND GENE TREES

So far, we have examined the genealogical relationships for a sample of individuals coming from one single population or *species*. The terms population and species are used interchangeably. In the following, samples from multiple species will come into play. The corresponding model was described under different names, as the *interspecific coalescent* [Tak89], or *censored coalescent* [RY03], and is now often referred to as the *multispecies coalescent* [Liu+09]. This extends the Kingman n -coalescent process.

First, we will introduce the multispecies coalescent and fix our notation. Among other things, we introduce the notion of compatibility and describe the resulting set of compatible pairs in Subsection 3.6.1. We then explain approaches concerning the distribution of gene tree topologies in Subsection 3.6.2. Theorem 3.6.14 translates this into a density on our space of trees. We conclude in Subsection 3.6.2.2 with a brief outlook about an interesting identifiability question.

For our summary on the multispecies coalescent we follow the presentation in [Yan14, Chapter 9]. In the multispecies coalescent model, we keep track of how genes evolve within multiple species. Here, a species is denoted by S and the set of all involved species by \mathfrak{S} . These species are organized in a *species tree* $T_{\mathfrak{S}}$ which is an equidistant n -tree for some $n \in \mathbb{Z}_{\geq 1}$, where every branch represents a whole population, as it can be seen in Figure 3.11. In contrast to the trees considered so far, we always assume an additional non-ending species to be present above the root. To distinguish between species and gene trees, we denote the extant species by capital letters and the extinct species will recursively be given the names of their two children, e.g. the species that A and B coalesce to is denoted by AB . Such a merging is called a *specification event*. For each species $S \in \mathfrak{S}$, we are given the parameter τ_S which we call the *specification time*

of S , where we set $\tau_S = 0$ for all extant species S . Here, τ_S is measured in coalescent units which reflects on the assumption of a standardized population size throughout all populations.

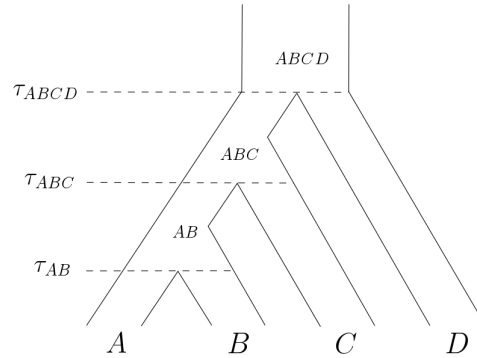


Figure 3.11: A species tree T_S with specification times τ_S .

For the multispecies coalescent, the phylogeny of the underlying species tree is assumed to be known, meaning, we fix a concrete species tree T_S with $d_{T_S} \in \text{MUM}_n$. We now consider a sample of size n , where we sample one gene per extant species. The model also applies to sampling multiple genes per species, but for our studies we concentrate on the single sample case. For each of the species $S \in \mathfrak{S}$, we run an independent Kingman k -coalescent process, where k is the number of lineages that enter the species and trace the genealogy of our sample backwards in time throughout all the species. Ignoring the individuals that are not ancestral to the individuals in our sample, we obtain an equidistant n -tree as a result, which we call the *gene tree* and denote it by T_g . By construction, the resulting gene tree always has to ‘fit’ into the given species tree, meaning, two genes cannot be merged until they are in a population that is a common ancestor of their associated species. We call a given gene tree T_g and a species tree T_S *compatible*, if T_g fits inside T_S and write $T_S \leq T_g$. This is the case if and only if each entry of the distance vector d_{T_S} of the species tree is a lower bound for the respective entry of the distance vector d_{T_g} of the gene tree. We write $d_{T_S} \leq d_{T_g}$ which is meant coordinate-wise.

Given enough time, all the lineages will coalesce with probability 1, at the latest in the population above the root. Note that, since the number of generations per species is prescribed, it may happen that the individuals that enter a species fail to completely coalesce within this population. So it is feasible that several individuals leave the current population without coalescing, because the Kingman j -coalescent process is terminated before they do. This occurrence is called *incomplete lineage sorting* and is also the origin of the term *censored coalescent*. Thus, it may happen that the combinatorics of the species tree and a resulting gene tree do not coincide.

Example 3.6.1. As an example for $n = 4$, we start out with the four extant species A, B, C , and D and we assume the species tree T_S to have tree topology $[T_S] = (((A, B), C), D)$

as depicted in Figure 3.12 on the left, where the relevant edge lengths are given by $x = \tau_{ABC} - \tau_{AB}$ and $y = \tau_{ABCD} - \tau_{ABC}$. From each of the extant species, we sample single genes and these will become the leaves $a, b, c,$ and d of the gene tree T_g . The four Kingman 1-coalescent processes within the extant species cannot cause any coalescent events. Since two genes enter species AB , we run a Kingman 2-coalescent. Tracing the genealogy of the genes backwards in time, one can observe that the two lineages a and b fail to coalesce within species AB . Therefore, three lineages enter the ancestral species ABC and this may cause an order of coalescence that differs from the one of the species tree. In this case, a and c merge first during the Kingman 3-coalescent process. Hence, the resulting gene tree T_g has different ranked tree topology, namely $[T_g] = ((a, c), b), d$ as can be seen on the right in Figure 3.12. The last coalescent event is the result of a Kingman 2-coalescent within species $ABCD$.

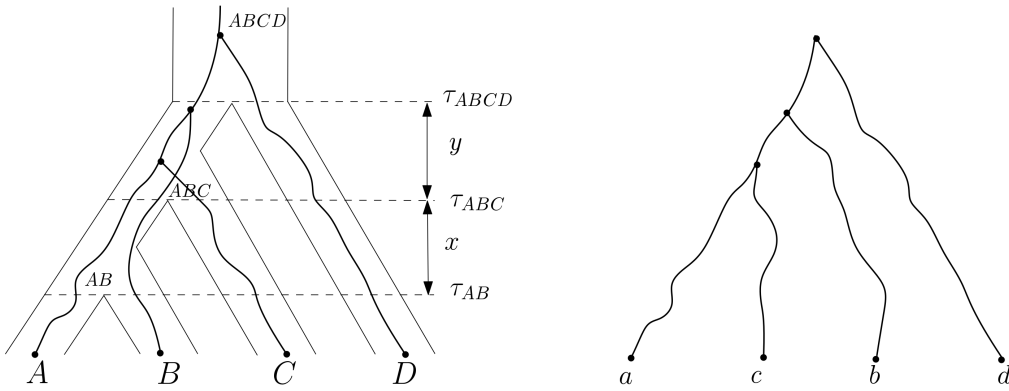


Figure 3.12: Non-matching species and gene tree topologies resulting from incomplete lineage sorting.

3.6.1 A Polyhedral Description of Compatibility

We are given a species tree T_S and a gene tree T_g with n leaves, respectively, where a is the gene that is sampled from species A and so on. Are these two trees compatible? Both can be interpreted as elements of MUM_n via the corresponding distance vectors d_{T_S} and d_{T_g} . Here, we ignore the species ancestral to the root, since it is assumed to have infinitely many generations for every species tree and, thus, does not give additional specific information in terms of compatibility. We now want to build a subset of MUM_n^2 that captures all the pairs of species and gene trees that are compatible. We use the convention that the first $\binom{n}{2}$ coordinates refer to the species tree and the last $\binom{n}{2}$ to the gene tree. When relevant, we denote the respective factors by MUM_n^S and MUM_n^g .

Definition 3.6.2. We define the *compatibility set*

$$\mathcal{C}_n := \left\{ (d_{T_S}, d_{T_g}) \in \text{MUM}_n^S \times \text{MUM}_n^g \cong \text{MUM}_n^2 : T_S \leq T_g \right\}$$

to be the set of all compatible pairs of species and gene trees for n extant species or respectively n sampled genes.

The two natural projections are denoted by $\pi^S: \mathcal{C}_n \rightarrow \text{MUM}_n^S$ and $\pi^g: \mathcal{C}_n \rightarrow \text{MUM}_n^g$. Let $\mathbb{1}_S := (1, \dots, 1, 0, \dots, 0) \in \text{MUM}_n^2$ and $\mathbb{1}_g := (0, \dots, 0, 1, \dots, 1) \in \text{MUM}_n^2$ denote the distance vectors corresponding to the degenerate species, respectively gene tree, for which all the distances coincide.

LEMMA 3.6.3. For the set of compatible pairs we have

$$\begin{aligned} \mathcal{C}_n &= \mathcal{C}_n + \mathbb{R}_{\geq 0} \cdot (\mathbb{1}_S + \mathbb{1}_g) \\ &= \mathcal{C}_n + \mathbb{R}_{\geq 0} \cdot (\mathbb{1}_S + \mathbb{1}_g) + \mathbb{R}_{\geq 0} \cdot \mathbb{1}_g. \end{aligned}$$

Proof. Let $(d_{T_S}, d_{T_g}) \in \mathcal{C}_n$ be a pair of distance vectors for compatible trees $T_S \leq T_g$. If we add $\lambda \cdot (\mathbb{1}_S + \mathbb{1}_g)$ for some $\lambda \in \mathbb{R}_{\geq 0}$ to the point, this can be interpreted as increasing all the edge lengths in T_S and T_g that are adjacent to a leaf simultaneously by $\frac{\lambda}{2}$. Thus, we still have $T_S \leq T_g$ which gives the first equality. The second equality holds, since an additional increasing of the external edge lengths of the gene tree preserves compatibility. \square

Since we have $\text{MUM}_n + \mathbb{R} \cdot \mathbb{1}_n = \text{DUM}_n$ by Lemma 3.3.7, the set of compatible pairs sits inside the space DUM_n^2 as follows.

LEMMA 3.6.4. For the set of compatible pairs we have

$$\mathcal{C}_n + \mathbb{R} \cdot \mathbb{1}_S + \mathbb{R} \cdot \mathbb{1}_g = \text{DUM}_n^2.$$

We have already observed that MUM_n has a nice combinatorial structure, namely, it is given as a fan glued together from cones that correspond to ranked tree topologies. The set of compatible pairs \mathcal{C}_n has a nice combinatorial structure as well. The product of the two fans Σ_n^S and Σ_n^g is again a fan, which is supported on MUM_n^2 and which we will denote by $\Sigma_n^S \times \Sigma_n^g$.

PROPOSITION 3.6.5. The set of compatible pairs $\mathcal{C}_n \subset \text{MUM}_n^2 \subset \mathbb{R}^{2 \cdot \binom{n}{2}}$ is the support of a fan $\Sigma_n^{\mathcal{C}}$.

1. Locally, each full-dimensional cone in $\sigma \in \Sigma_n^{\mathcal{C}}$ can be derived from a corresponding cone of the fan $\Sigma_n^S \times \Sigma_n^g$ by at most $(n-1)$ additional inequalities.
2. Globally, $\binom{n}{2}$ additional inequalities are needed for each ranked tree topology $[T_S^*]$ of a species tree to cut out the support of all cones in \mathcal{C}_n that involve species trees of type $[T_S^*]$.

Proof. Let us first consider the fan $\Sigma_n^S \times \Sigma_n^g$. Its cones are given as the product of the respective cones in Σ_n^S and Σ_n^g , i.e., $\sigma_{[T_S^*], [T_g^*]} := \sigma_{[T_S^*]} \times \sigma_{[T_g^*]}$ for $\sigma_{[T_S^*]} \in \Sigma_n^S$ and $\sigma_{[T_g^*]} \in \Sigma_n^g$ and the cones corresponding to fixed ranked tree topologies $[T_S^*]$ and $[T_g^*]$. If one adds

a large enough multiple of $\mathbb{1}_g$ to a given gene tree, it will be compatible with any given species tree. This is due to the fact that when all the coalescent events take place above the species tree's root, all combinatorial types of gene trees are possible. Thus, all cones $\sigma_{[T_S^*],[T_g^*]} \in \Sigma_n^S \times \Sigma_n^g$ contribute to \mathcal{C}_n .

1. Let us consider a fixed cone $\sigma_{[T_S^*],[T_g^*]}$ for given ranked tree topologies $[T_S^*]$ and $[T_g^*]$. We have observed earlier that the fitting condition can be interpreted as $d_{T_S} \leq d_{T_g}$ for the respective distance vectors of trees T_S and T_g . Thus each of the $\binom{n}{2}$ pairs of entries causes an additional linear inequality, requiring that

$$d_{T_S}(I, J) \leq d_{T_g}(i, j) \quad (3.6.1)$$

for leaves $I, J \in L_S$ from the species tree T_S and corresponding leaves $i, j \in L_g$ from the gene tree T_g . Since many of the distances agree, it is sufficient to have one for every internal vertex of the gene tree. Thus we need at most $(n - 1)$ additional inequalities. As a result they cut out a full-dimensional cone $\sigma_{[T_S^*],[T_g^*]}^C$ inside $\sigma_{[T_S^*],[T_g^*]}$.

2. Let us now fix a ranked tree topology $[T_S^*]$ of a species tree. Given a species tree T_S of this type and an arbitrary gene tree T_g , we obtain $\binom{n}{2}$ additional linear inequalities of the form $d_{T_S}(I, J) \leq d_{T_g}(i, j)$ for leaves $I, J \in L_S$ from the tree T_S and corresponding leaves $i, j \in L_g$ from the tree T_g , as explained above. In this case, all inequalities are necessary. Assume that one of the inequalities is redundant for a pair of leaves $I, J \in L_S$. Then there exists a ranked tree topology $[T_g]$ for which the pair (i, j) is the first pair that coalesces in the corresponding gene tree T_g . In this case, the inequality $d_{T_S}(I, J) \leq d_{T_g}(i, j)$ is not implied by any other inequality and is thus necessary. As a result, the additional inequalities cut out all the full-dimensional cones $\sigma_{[T_S^*],[T_g^*]}^C$ inside $\sigma_{[T_S^*],[T_g^*]}$ for each pair of ranked tree topologies $[T_S^*], [T_g^*]$.

□

Remark 3.6.6. The bound of necessary additional inequalities in the local situation as given in Proposition 3.6.5 (1.) is tight. If the ranked tree topologies of the species tree and the gene tree coincide, then all of them are needed. In the other extremal case, only one additional inequality is needed which implies all the other ones. This happens if and only if the following is true for the ranked tree topologies $[T_g]$ and $[T_S]$. Let $i, j \in L_g$ be the first two leaves that coalesce in the gene tree, while the corresponding leaves $I, J \in L_S$ in the species tree are not merged before its root. This forces all coalescent events of the gene tree to happen above this root if it wants to fit inside the species tree. This is guaranteed by the single inequality $d_{T_S}(I, J) \leq d_{T_g}(i, j)$ on the distance vectors.

3.6.2 The Distribution of Gene Tree Topologies

We start with the probabilist's point of view. In Section 3.6.2.2 we will then take the statistician's perspective. According to the properties of a given species tree, different compatible gene trees appear with certain probabilities, which are determined by the multispecies coalescent. Various aspects of these probabilities have been studied by many authors, starting with [Mad97]. To begin with, we will review the discrete results of Degnan and Salter in [DS05], [DR09] for one gene sampled per species. The concordance of gene and species tree topology for a bigger sample was studied in [Ros02]. In [DRS12b] similar considerations lead to a formula for ranked gene tree topologies.

Fix the phylogeny of a species tree T_S , meaning its ranked tree topology $[T_S]$ and the parameters τ_S for all its species $S \in \mathfrak{S}$ are given. Running the multispecies coalescent, one obtains a gene tree T_g that fits inside the species tree. We are interested in the conditional probability, that the gene tree has a certain tree topology $[[T_g^*]]$, i.e., $\mathcal{P} \left([[T_g^*]] \mid T_S \right)$.

For a given tree topology $[[T_g^*]]$, there are usually many different valid combinations of species, inside which the coalescent events of the gene tree can take place. The coalescent history keeps track of these species.

Definition 3.6.7. Let $[[T_S^*]]$ be a species tree topology and $[[T_g^*]]$ a gene tree topology. We call a map h from the set of coalescent events $\mathfrak{C} = \mathfrak{C}([[T_g^*]])$ to the set of species \mathfrak{S} a *pre-history*. Every compatible pair of a species tree T_S and a gene tree T_g defines a pre-history $h^{(T_S, T_g)}$, in the sense that a coalescent event is mapped to the species within which it takes place. A pre-history is called a *history*, if there exists a pair (T_S, T_g) inducing it. Given a species tree T_S and a gene tree topology $[[T_g^*]]$, we call a history h *valid* if there exists a compatible gene tree T_g with that topology, inducing h . We denote the set of all histories by H .

If we want to give a history explicitly, we will use a matrix notation, where the first row contains all the coalescent events $C \in \mathfrak{C}$ and the second row their respective images $S \in \mathfrak{S}$.

Example 3.6.8. In the case of Example 3.6.1 the history of the resulting gene tree T_g inside the species tree T_S is

$$h_1 = \begin{pmatrix} (a, c) & ((a, c), b) & (((a, c), b), d) \\ ABC & ABC & ABCD \end{pmatrix}.$$

If we require the gene tree topology to be $[[T_g^*]] = (((a, c), b), d)$, then there are two additional possible coalescent histories, namely

$$h_2 = \left(\begin{array}{ccc} (a, c) & ((a, c), b) & (((a, c), b), d) \\ ABC & ABCD & ABCD \end{array} \right) \text{ and } h_3 = \left(\begin{array}{ccc} (a, c) & ((a, c), b) & (((a, c), b), d) \\ ABCD & ABCD & ABCD \end{array} \right)$$

to realize this particular tree topology $[[T_g]]$ as depicted in Figure 3.13.

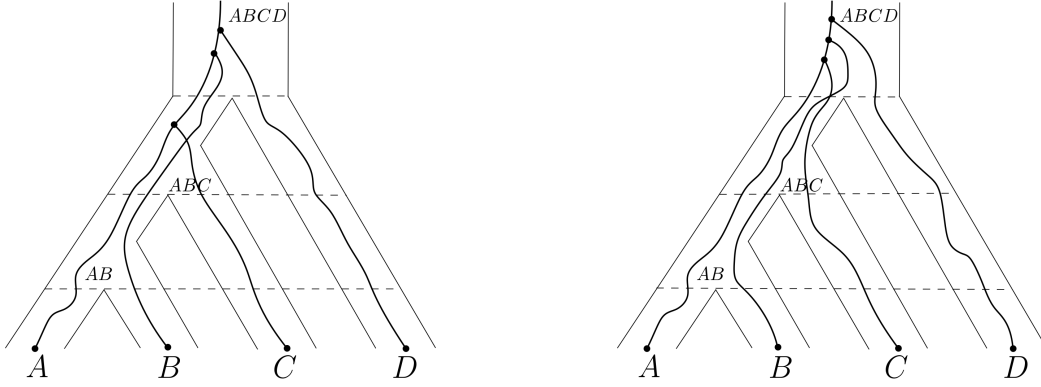


Figure 3.13: Coalescent histories h_2 and h_3 .

In [DS05] Degnan and Salter compute the desired probability $\mathcal{P} \left([[T_g^*]] \mid T_S \right)$ based on the following function that is due to Tavaré [Tav84]. Fix a population. Then $g_{k,m}(t)$ expresses the probability that k lineages will coalesce into m lineages in time t . It is given by

$$g_{k,m}(t) = \sum_{j=m}^k \exp \left(-\binom{j}{2} t \right) \frac{(2j-1)(-1)^{j-m}}{m!(j-m)!(m+j-1)} \prod_{l=0}^{j-1} \frac{(m+l)(k-l)}{k+l} \quad (3.6.2)$$

for $1 \leq m \leq k$.

The following values will be needed in the case of $n = 4$ leaves.

$$\begin{array}{ll} g_{1,1}(t) = 1 & g_{3,1}(t) = 1 - \frac{3}{2} \exp(-t) + \frac{1}{2} \exp(-3t) \\ g_{2,1}(t) = 1 - \exp(-t) & g_{3,2}(t) = \frac{3}{2} \exp(-t) - \frac{3}{2} \exp(-3t) \\ g_{2,2}(t) = \exp(-t) & g_{3,3}(t) = \exp(-3t) \end{array} \quad (3.6.3)$$

The respective Kingman k -coalescent processes in the multispecies coalescent model are independent processes. To compute the probability of a specific coalescent history, one applies the formula (3.6.2) to each species $S \in \mathfrak{S}$ and takes the product of the resulting probabilities over all species. Thus, conditioned on the underlying species

tree, a coalescent history $h \in H$ has a probability of the form

$$\mathcal{P}(h | T_S) = c(h) \prod_{S \in \mathfrak{S}} g_{k(h,S), m(h,S)}(\ell(S)), \quad (3.6.4)$$

where $\ell(S)$ is the duration of the species S (i.e., the branch length in T_S associated to S), $k(h, S)$ is the number of lineages that enter species S and $m(h, S)$ the number of lineages that leave the species with respect to the coalescent history h . Moreover, $c(h)$ is a combinatorial constant factor that comes from the specific order of the coalescent events within a species, more precisely

$$\frac{1}{c(h)} = \prod_{S \in \mathfrak{S}} \# \text{ ways to coalesce } k(h, S) \text{ into } m(h, S) \text{ lineages.}$$

We spell out the formula for our running example.

Example 3.6.9. We continue with Example 3.6.1 and consider the coalescent history

$h_1 = \begin{pmatrix} (a, c) & ((a, c), b) & (((a, c), b), d) \\ ABC & ABC & ABCD \end{pmatrix}$ as depicted in Figure 3.12. Since there is only one lineage present in each of the extant species A, B, C , and D , they are not taken into account in the computation, because they stay single lineages with probability 1, respectively. Because of incomplete lineage sorting, the two lineages that enter species AB fail to coalesce within time x and do both leave the species. Thus, this contributes

$$g_{2,2}(x) = \exp(-x)$$

to the probability of the given coalescent history. For the species ABC , three lineages enter the population, and after two coalescent events only one lineage leaves it. The first coalescent event merges the genes a and c . There are three potential pairs out of which this particular one is merged with probability $\frac{1}{3}$. Therefore species ABC contributes

$$\frac{1}{3} \cdot g_{3,1}(y) = \frac{1}{3} \left(1 - \frac{3}{2} \exp(-y) + \frac{1}{2} \exp(-3y) \right).$$

Finally, there is another coalescent event within species $ABCD$. Since we assume this species above the root to have infinitely many generations, the probability that the two remaining lineages will coalesce inside this species is 1.

Hence, in total, given T_S , the coalescent history h_1 appears with probability

$$\mathcal{P}(h_1 | T_S) = g_{2,2}(x) \cdot \frac{1}{3} \cdot g_{3,1}(y) = \exp(-x) \frac{1}{3} \left(1 - \frac{3}{2} \exp(-y) + \frac{1}{2} \exp(-3y) \right).$$

To obtain the probability that we are eventually interested in, we have to sum over all possible coalescent histories that are valid for the given tree topology $[[T_g^*]]$. Explicitly,

this gives

$$\mathcal{P} \left([[T_g^*]] \mid T_S \right) = \sum_{h \text{ valid for } [[T_g^*]]} \mathcal{P} (h \mid T_S). \quad (3.6.5)$$

Example 3.6.10. Since there are three valid coalescent histories in the case of our running example, all of the corresponding probabilities can be computed as in Example 3.6.9. Altogether, this gives

$$\begin{aligned} \mathcal{P} \left([[T_g^*]] \mid T_S \right) &= \mathcal{P} (h_1 \mid T_S) + \mathcal{P} (h_2 \mid T_S) + \mathcal{P} (h_3 \mid T_S) \\ &= g_{2,2}(x) \cdot \frac{1}{3} \cdot g_{3,1}(y) + g_{2,2}(x) \cdot \frac{1}{3} \cdot g_{3,2}(y) \cdot \frac{1}{3} + g_{2,2}(x) \cdot g_{33}(y) \cdot \frac{1}{18} \end{aligned}$$

for the probability that a compatible gene tree will have the tree topology $[[T_g^*]] = (((a, c), b), d)$, given the species tree T_S .

So far, we were only interested in the appearance of certain tree topologies and the edge lengths of the resulting gene trees did not play a role. This changes as soon as we leave the discrete setting and ask for probability distributions in terms of a continuous density on our space of trees. This general probability density was given by Rannala and Yang in [RY03] and will in the following be explained in our language.

Given a species tree T_S , we are now interested in the distribution $\rho(T_g \mid T_S)$, where T_g is a compatible gene tree with ranked tree topology $[T_g]$ and edge lengths in terms of t_2, \dots, t_n .

For a single population consisting of n individuals, we have already argued that the densities as stated in (3.2.5) and (3.2.7) describe the probability distribution of the waiting times t_2, \dots, t_n for the Kingman n -coalescent. In the multispecies coalescent model, we run a Kingman k -coalescent process for every species $S \in \mathfrak{S}$ for respective $k = k(h^{(T_S, T_g)}, S) \in \{1, \dots, n\}$. Thus, in a first step, we apply the densities given above to each species separately and in a second step, multiply them to a joint probability density.

In order to perform the first step, we need to introduce new waiting time variables for a compatible gene tree T_g and for each species. So let $t_j^{(S)}$ denote the time during which there are exactly j lineages present in species S .

Let us fix a species $S \in \mathfrak{S}$ in the species tree and let $k = k(h^{(T_S, T_g)}, S)$ be the number of lineages that enter the population and $m = m(h^{(T_S, T_g)}, S)$ be the number of lineages that leave it. By S' we denote the species immediately ancestral to the species S . Then (3.2.5) gives

$$\rho_j \left(t_j^{(S)} \right) = \binom{j}{2} \exp \left(- \binom{j}{2} t_j^{(S)} \right), \quad \text{for all } j = k, \dots, m+1 \quad (3.6.6)$$

for the density of the waiting time $t_j^{(S)}$ until the next coalescent event that reduces the number of lineages in the population from j to $j - 1$. To obtain the given gene tree, coalescing pairs are prescribed. Because all pairs are equally likely to coalesce, two particular lineages are merged with probability $\frac{1}{\binom{j}{2}}$.

In case of incomplete lineage sorting, i.e., $m > 1$, we also have to take the probability into account that these last m lineages do not coalesce within the remaining time $\tau_{S'} - \tau_S - (t_k^{(S)} + \dots + t_{m+1}^{(S)})$. Since the considered process is a Poisson-process with rate $\binom{m}{2}$, the probability of having no coalescent event is

$$\exp\left(-\binom{m}{2}\left(\tau_{S'} - \tau_S - (t_k^{(S)} + \dots + t_{m+1}^{(S)})\right)\right). \quad (3.6.7)$$

Altogether, for the contribution of species S this yields

$$\begin{aligned} \rho^{(S)}(T_g | T_S) &= \left(\prod_{j=m+1}^k \exp\left(-\binom{j}{2}t_j^{(S)}\right)\right) \\ &\quad \cdot \exp\left(-\binom{m}{2}\left(\tau_{S'} - \tau_S - (t_k^{(S)} + \dots + t_{m+1}^{(S)})\right)\right). \end{aligned} \quad (3.6.8)$$

After doing this for all species $S \in \mathfrak{S}$ in the species tree, we take the product over all the species and obtain

$$\rho(T_g | T_S) = \prod_{S \in \mathfrak{S}} \rho^{(S)}(T_g | T_S) \quad (3.6.9)$$

for the probability distribution.

Example 3.6.11. Let us reconsider what happens in population $S = ABC$ in Example 3.6.8. As indicated in Figure 3.14, this population has duration $y = \tau_{ACBD} - \tau_{ABC}$ and the considered gene tree T_g has coalescent history h_2 . Thus $k = 3$ lineages enter population ABC and $m = 2$ leave it. According to Equation (3.6.8) population ABC contributes

$$\rho^{(ABC)}(T_g | T_S) = \exp\left(-3t_3^{(ABC)}\right) \cdot \exp\left(-\left(\tau_{ACBD} - \tau_{ABC} - t_3^{(ABC)}\right)\right) \quad (3.6.10)$$

to the desired density. Overall, taking the product over all species yields

$$\begin{aligned} \rho(T_g | T_S) &= \rho^{(AB)}(T_g | T_S) \cdot \rho^{(ABC)}(T_g | T_S) \cdot \rho^{(ABCD)}(T_g | T_S) \\ &= \exp\left(-(\tau_{ABC} - \tau_{AB})\right) \\ &\quad \cdot \exp\left(-3t_3^{(ABC)}\right) \cdot \exp\left(-\left(\tau_{ACBD} - \tau_{ABC} - t_3^{(ABC)}\right)\right) \\ &\quad \cdot \exp\left(-3t_3^{(ABCD)}\right) \cdot \exp\left(-t_2^{(ABCD)}\right). \end{aligned}$$

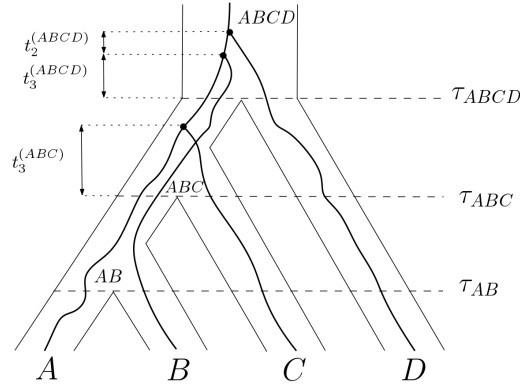


Figure 3.14: Waiting times $t_j^{(S)}$ within the species $S \in \mathfrak{S}$.

3.6.2.1 Density on the Space of Gene Trees

For defining the desired density on MUM_n^g , we need to introduce another type of subsets which MUM_n^g can be subdivided into.

Definition 3.6.12. Given a species tree T_S and a gene tree topology $[[T_g^*]]$, let h be a pre-history. The *history region* $R_{T_S}([[T_g^*]], h)$ is defined as

$$R_{T_S}([[T_g^*]], h) := \left\{ d_{T_g} \in \sigma_{[[T_g^*]]} \subseteq \text{MUM}_n^g : T_S \leq T_g \text{ and } h^{(T_S, T_g)} = h \right\}, \quad (3.6.11)$$

i.e., the subset of MUM_n^g within which all gene trees share the same history h with respect to T_S .

Note that, since a history contains the information of the tree topology $[[T_g^*]]$, a non-empty history region is always contained in a unique tree topology cone $\sigma_{[[T_g^*]]}$.

Another observation is that there is in general no inclusion relation between history regions and ranked tree topology cones.

By definition, a history region $R_{T_S}([[T_g^*]], h)$ is a polyhedron determined by the following inequalities: We are given a fixed species tree T_S , whose branch lengths are determined by the specification times τ_S for all $S \in \mathfrak{S}$. Let $C \in \mathfrak{C} = \mathfrak{C}([[T_g^*]])$ be a coalescent event that takes place within species $S \in \mathfrak{S}$ according to h and denote by S' the species right above S . This requires

$$\tau_S \leq d_C \leq \tau_{S'}, \quad (3.6.12)$$

where d_C is the coalescent time and local coordinate associated to C in the tree topology cone $\sigma_{[[T_g^*]]}$, compare Section 3.3.1.2. For each coalescent event $C \in \mathfrak{C}$, we obtain inequalities of the form (3.6.12) and these fully describe the history region $R_{T_S}([[T_g^*]], h)$ within $\sigma_{[[T_g^*]]}$. Note, that the resulting inequalities include all the compatibility requirements from Proposition 3.6.5. This gives the following lemma. Given a species tree T_S , we

can restrict the considerations to the part of MUM_n^g of compatible gene trees, that is to $\pi^g((\pi^S)^{-1}(T_S))$.

LEMMA 3.6.13. Given a species tree T_S and a gene tree topology $[[T_g^*]]$, the subdivision of the polyhedral complex $\pi^g((\pi^S)^{-1}(T_S)) \cap \sigma_{[[T_g^*]]}$ into history regions is a polyhedral subdivision.

With this notion in hand, we can now define the density on MUM_n^g in a suitable way. For a unimodular ranked tree topology cone $\sigma_{[[T_g^*]]} \subseteq \text{MUM}_n^g$, we have the Lebesgue-measure available, as argued in the proof of Proposition 3.4.1. Fix a tree topology $[[T_g^*]]$. Then by Proposition 3.3.12, the tree topology cone $\sigma_{[[T_g^*]]}$ is unimodularly triangulated into ranked tree topology cones, and therefore, we have recourse to the same measure on $\sigma_{[[T_g^*]]}$.

THEOREM 3.6.14. Given a species tree T_S , there exists a continuous density ρ on MUM_n^g that models the distribution $\rho(T_g | T_S)$ and is piecewise analytic on subsets of the form $R_{T_S}([[T_g^*]], h) \cap \sigma_{[[T_g^*]]}$, for all histories $h \in H$, gene tree topologies $[[T_g^*]]$ and ranked tree topology cones $\sigma_{[[T_g^*]]}$. Furthermore, we have

$$\int_{\sigma_{[[T_g^*]]}} \rho = \mathcal{P} \left([[T_g^*]] \mid T_S \right)$$

for all tree topologies $[[T_g^*]]$.

Proof. For a gene tree outside of $\pi^g((\pi^S)^{-1}(T_S))$, we set $\rho(T_g | T_S) = 0$.

Consider a history region $R_{T_S}([[T_g^*]], h)$ and a gene tree T_g with $d_{T_g} \in R_{T_S}([[T_g^*]], h)$. For this tree Rannala and Yang [RY03] give a formula for the desired density in terms of the specification times τ_S for $S \in \mathfrak{S}$ and the waiting times $t_j^{(S)}$ for the j -th coalescent event within species S , as in (3.6.8). The formula is a product that runs over all species $S \in \mathfrak{S}$. So, let us fix a species $S \in \mathfrak{S}$ and denote by S' the species right above S . We assume that $k = k(h, S)$ lineages enter the species S and $m = m(h, S)$ lineages leave it. Then we have to consider two cases:

- For $j = k$ we have $t_j^{(S)} = d_{C_1} - \tau_S$, where C_1 is the first coalescent event within species S according to h .
- For $j = k - 1, \dots, m + 1$ we have $t_j^{(S)} = d_{C'} - d_C$, where C is the coalescent at the beginning of $t_j^{(S)}$ and C' the one at the end.

The remaining time for the factor (3.6.7) is given as $\tau_{S'} - d_{C''}$, where C'' is the last coalescent event happening in species S . Thus, we have expressed the contribution

of species S in terms of specification times τ_S for $S \in \mathfrak{S}$ and coalescent times d_C for $C \in \mathfrak{C}$. For all trees sharing the same ranked tree topology, the above described change of coordinates is given by the same linear transformation. Since the contributions of the different species are independent, we obtain a density on MUM_n^g for the joint distribution $\rho(T_g | T_S)$, whose formula is piecewise analytic on subsets of the form $R_{T_S}([\![T_g^*]\!], h) \cap \sigma_{[\![T_g^*]\!]}$, where $R_{T_S}([\![T_g^*]\!], h)$ is a history region within a tree topology cone $\sigma_{[\![T_g^*]\!]}$ and $\sigma_{[\![T_g^*]\!]}$ is a ranked topology cone.

By definition of the tree topology cone $\sigma_{[\![T_g^*]\!]}$, integrating over such a cone yields

$$\int_{\sigma_{[\![T_g^*]\!]}} \rho = \mathcal{P}([\![T_g^*]\!] | T_S)$$

as in (3.6.5). □

3.6.2.2 Identifiability

Now we take the statistician's point of view. In the multispecies coalescent model our starting situation is a fixed species tree, and for a given gene tree, we are able to decide if it is compatible with this species tree. In the real world situation, one usually observes or derives gene trees from given data and wants to conclude information about the underlying species tree in the next step. Many approaches have been studied in terms of this question of indentifiability. For a long time, the working assumption that the species tree topology coincides with the most likely gene tree topology was not questioned. Starting with [Nei87] and [PN88], where the probability that the tree topologies of gene and species tree coincide was studied, a lot of similar questions were studied based on this.

For any species tree topology with five or more extant species, there exist branch lengths for which the most likely gene tree topology to evolve along the branches of a species tree differs from the species phylogeny, see [DR06]. The phenomenon of a mismatching ranked tree topology can also occur, when trying to identify it from the distribution of ranked tree topologies of gene trees, see [DRS12b]. In [DRS12a] the authors give a complete characterization of the set of species trees that give rise to anomalous ranked gene tree topologies. This is also called the *anomaly zone*.

Nevertheless, knowing the precise distribution of gene tree topologies as a whole is very insightful. In [ADR11] Allman, Degnan, and Rhodes show that for five or more species, the species tree topology and all its branch lengths can even be identified from the distribution of the unrooted gene tree topologies. This raises the question, of how precise this identification is. Further directions should investigate that question by giving some sort of condition number. For that the recent advances that have been made in tropical geometry could be applied to measure distances in our tree space, compare [Lin+17; Nye+17; Mon+20].

This chapter is joint work with Giulia Codenotti, Christian Haase, and Francisco Santos and is based on [CW19].

4.1 INTRODUCTION

At the end of the 20th century, Smale proposed his famous list of 18 unsolved problems in mathematics, the 17th of which was the following:

‘Can a zero of n complex polynomial equations in n unknowns be found approximately, on average, in polynomial time with a uniform algorithm?’ [Sma98]

Here, a *uniform algorithm* is understood as an algorithm that is supposed to work for all inputs. Its expected running time should be bounded by a polynomial in the input size. An *approximate* solution is a point from which Newton’s iteration converges quadratically. The term *on average* refers to the input being sampled from a certain probability distribution. Smale and Shub extensively studied a homotopy method in order to find a solution, starting with [SS93]. The problem has by now been solved. Beltrán and Pardo found a uniform probabilistic algorithm [BP08a; BP08b] in 2009. In 2011, Bürgisser and Chucker performed a smoothed analysis of the Beltrán-Pardo algorithm and described a deterministic algorithm with complexity $N^{O(\log \log N)}$, where N is the input size [BC11b]. Finally, Lairez was able to de-randomize the algorithm using an alternative method and thus found a deterministic algorithm with an average polynomial running time in 2017 [Lai17].

Even though this was an enormous breakthrough, assuming that the given system of polynomials is dense is unrealistic when it comes to real world applications. Thus, it makes sense to also consider systems carrying a certain sparsity structure. In a *sparse* polynomial system its zero coefficients are not explicitly stored.

The structure of a sparse system of polynomials (f_1, \dots, f_n) is modeled by an n -tuple of Newton polytopes (P_1, \dots, P_n) spanned by the support of the polynomial system $(A_1, \dots, A_n) = (\text{supp}(f_1), \dots, \text{supp}(f_n))$.

This connection is the foundation for the method of polyhedral homotopies for solving polynomial systems, see [Stu02, Chapter 3] and [HS95; VVC94] for more details. Recent progress in this direction has for instance been made by Malajovich [Mal17; Mal19; Mal20], where he investigates the cost of solving systems of sparse polynomial equations by homotopy continuation.

At times, we are only interested in the ‘finite’ roots of a sparse system, which are the roots in $(\mathbb{C}^*)^n$. The famous Bernstein-Khovanskii-Kushnirenko theorem gives a bound for the number of these roots and highlights an important connection to discrete geometry.

THEOREM 4.1.1 (BKK-Theorem [Ber79]). For a system of Laurent polynomials $f_1, \dots, f_n \in \mathbb{C}[x_1^{\pm 1}, \dots, x_n^{\pm 1}]$, the number of isolated solutions to $f_1 = \dots = f_n = 0$ in $(\mathbb{C}^*)^n$ is bounded from above by the mixed volume of the Newton polytopes $MV(\text{NP}(f_1), \dots, \text{NP}(f_n))$. For generic non-zero coefficients there exist exactly $MV(\text{NP}(f_1), \dots, \text{NP}(f_n))$ many solutions.

When working over a valued field, the valuation of the coefficients of the system can be interpreted as weights and induce a regular subdivision of the Minkowski sum $A_1 + \dots + A_n$. The so called ‘fully mixed cells’ of the subdivision correspond to the intersections of the tropical hypersurfaces $(\text{trop}(V(f_1)), \dots, \text{trop}(V(f_n)))$ of the associated tropical polynomial system, where the volume of such a cell represents the multiplicity of the intersection. For further details on this correspondence we refer the reader to [Stu02, Chapter 9] and [MS15, Chapter 4.6]. The correspondence has led to recent progress from the tropical perspective, see for instance [Jen16], where tropical homotopy continuation methods are developed.

This motivates us to consider the ‘tropical sparse 17th Smale’s problem’:

‘Given n Newton polytopes in \mathbb{R}^n with random weights, is there an algorithm to find a fully mixed cell in the induced mixed subdivision of their Minkowski sum in expected polynomial time?’

Computing the entire mixed subdivision would be the naive approach for finding one such fully mixed cell. Since we are only interested in a small part of the information, we want to avoid doing the whole expensive computation. Here, ‘polynomial time’ is understood to mean polynomial in the input A_1, \dots, A_n and ‘expected’ refers to the expected running time when varying the weights.

The Chapter is organized as follows. In Section 4.2 we set notation and explain the construction of the main objects of interest and the respective correspondences. In Section 4.3 we describe a homotopy continuation approach and construct an example that could lead to an exponential lower bound on the expected running time.

4.2 BACKGROUND AND NOTATION

In this section, we give all the definitions and constructions necessary to understand the statement of the problem, and state a few main theorems that we will need in the following. This is based on the presentation in [LRS10, in particular Chapters 2, 5 and 9.2]. We refer to this extensive introduction for further details and proofs.

4.2.1 Regular Subdivisions and Triangulations

A *point configuration* is a finite set of points $A \subseteq \mathbb{R}^n$ with labels. A *face* of a point configuration A is the set of all points of A which minimize the value of some linear functional among all points of A . A face which is not the whole configuration A is called a *proper face*. A face of maximal dimension among proper faces is called a *facet*. A (sub-)configuration A is a *simplex* if $|A| = \dim \text{aff}(\text{conv}(A)) + 1$.

We can now define a (*polyhedral*) *subdivision* of A as a collection \mathcal{S} of subsets $C \subseteq A$, called *cells*, such that

- if $C \in \mathcal{S}$ and F is a face of C , then $F \in \mathcal{S}$ as well,
- the union of the convex hulls of all cells of \mathcal{S} covers $\text{conv}(A)$,
- the intersection of any two cells of \mathcal{S} is a face of both cells.

A *triangulation* \mathcal{T} of A is a subdivision, where all of the cells are simplices.

We can also speak of a subdivision of a polytope P : given any point configuration A such that $\text{conv}(A) = P$ and any subdivision \mathcal{S} of A , we say that the collection of convex hulls of all cells of \mathcal{S} is a subdivision of P . A triangulation of P is a subdivision, where all the elements are simplices. In Example 4.2.1 we will see that there is a subtle difference between triangulations of the polytope and triangulations of the point configuration.

A *regular* subdivision of a full-dimensional point configuration $A \subseteq \mathbb{R}^n$ is a subdivision that can be obtained as the orthogonal projection of the lower facets of a lift of A . More precisely, given weights $\omega \in \mathbb{R}^A$, lift all points of A to \mathbb{R}^{n+1} using the given weights as the last coordinate, to define

$$\tilde{A} := \left\{ (a, \omega(a)) \in \mathbb{R}^{n+1} : a \in A \right\},$$

a point configuration in \mathbb{R}^{n+1} . Now consider the lower facets of \tilde{A} , that is, those facets whose outer normal has negative last coordinate. Their images in A via the projection which forgets the last coordinate form the cells of the *regular* subdivision \mathcal{S}_ω of A induced by the weights ω . We can then define a regular subdivision of a polytope P via a subdivision of A such that $P = \text{conv}(A)$ just as before.

Example 4.2.1. Consider five points on a line, that is the point configuration $A = \{1, 2, 3, 4, 5\}$, and let $P = \text{conv}(A) \subset \mathbb{R}$. Let $\omega = (4, 3, 2, 4, 3) \in \mathbb{R}^5$. (We abuse notation here and denote by ω also the corresponding weight vector in $\mathbb{R}^{|A|}$.) The regular subdivision \mathcal{S}_ω of A induced by ω has maximal cells $\{\{1, 2, 3\}, \{3, 5\}\}$ as depicted in Figure 4.1. Observe that although as a subdivision of the polytope P this is a triangulation, as a subdivision of the point configuration A it is not, since $\{1, 2, 3\}$ is not a simplex. The weight vector $\omega' = (4, 4, 2, 4, 3)$ instead does induce a triangulation $\mathcal{T}_{\omega'}$ with maximal cells $\{\{1, 3\}, \{3, 5\}\}$.

As subdivisions of the polytope P both vectors induce the same triangulation, as can be seen in Figure 4.1, which shows the subdivision induced by ω , consisting of the two full-dimensional cells $C_1 = \text{conv}(\{1, 2, 3\})$ and $C_2 = \text{conv}(\{3, 5\})$.

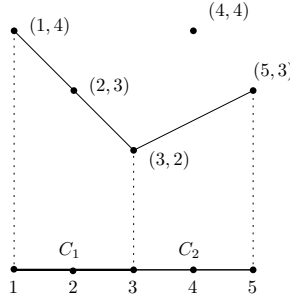


Figure 4.1: A regular subdivision of a line segment.

4.2.2 Minkowski Sums and Mixed Cells

In the introduction, we mentioned the term ‘fully mixed cell’; this only makes sense if several polytopes are considered. In our situation, we are given finite integer point configurations $A = (A_1, \dots, A_n)$ with $A_i \subseteq \mathbb{Z}^n$ for each $i = 1, \dots, n$, whose convex hull $P_i = \text{conv}(A_i)$ is a lattice polytope in \mathbb{R}^n such that $\dim(\text{aff}(\sum_{i=1}^n A_i)) = n$. We denote the number of points in A_i by d_i , so the total number of points is $d := \sum_{i=1}^n d_i$. Also given are weights $\omega_i \in \mathbb{R}^{A_i}$ for $i = 1, \dots, n$. For convenience we also define $\omega := (\omega_1, \dots, \omega_n) \in \mathbb{R}^A$.

The definition can be given by looking at two different constructions, the Minkowski sum and the Cayley embedding. We begin by introducing the former. The latter will be discussed in the next section. Recall that the *Minkowski sum* $\sum_{i=1}^n A_i$ of A_1, \dots, A_n is the configuration defined as

$$\sum_{i=1}^n A_i := \{a_1 + \dots + a_n : a_i \in A_i \text{ for } i = 1, \dots, n\}.$$

An example of a Minkowski sum consisting of a square and a triangle is shown in Figure 4.2. In the previous section we introduced subdivisions of a point configuration.

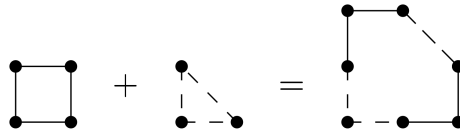


Figure 4.2: The Minkowski sum of a square and a triangle.

In the case of Minkowski sums, we can define a special kind of subdivisions, the *mixed*

subdivisions, which respect the structure of the summands. More precisely, a mixed subdivision of $\sum_{i=1}^n A_i$ is a subdivision, where all cells are of the form $C = \sum_{i=1}^n B_i$, for subsets $B_i \subseteq A_i$, and where all cells intersect properly, that is, if $\sum_{i=1}^n B_i$ and $\sum_{i=1}^n B'_i$ are two cells, then

$$\sum_{i=1}^n B_i \cap \sum_{i=1}^n B'_i = \sum_{i=1}^n (B_i \cap B'_i).$$

We call a cell $C = \sum_{i=1}^n B_i$ itself *mixed* if $\dim(B_i) \geq 1$ for at least two $i \in \{1, \dots, n\}$, and *fully mixed*, if $\dim(B_i) = 1$ for all $i \in \{1, \dots, n\}$, i.e., if it is the Minkowski sum of n segments, one coming from each of the configurations A_i .

To obtain a regular subdivision of the Minkowski sum $\sum_{i=1}^n A_i$, we apply a variation of the construction described in the previous section: we lift each of the configurations A_i to $\tilde{A}_i \in \mathbb{R}^{n+1}$ according to the given weights ω_i . Then we project the lower convex hull of the Minkowski sum $\sum_{i=1}^n \tilde{A}_i$. This yields a regular subdivision of the Minkowski sum $\sum_{i=1}^n A_i$, see [LRS10, Theorem 1.3.5]. Regular subdivisions of Minkowski sums obtained this way are by construction mixed. We obtain analogous notions for polytopes by passing over to the respective convex hulls.

Example 4.2.2. Let us continue with the example shown in Figure 4.2 and give coordinates in the plane to the triangle $P_1 = \text{conv}(A_1)$ and the square $P_2 = \text{conv}(A_2)$, where the point configurations are

$$A_1 = \begin{pmatrix} 0 & 1 & 0 \\ 0 & 0 & 1 \end{pmatrix} \text{ and } A_2 = \begin{pmatrix} 0 & 1 & 0 & 1 \\ 0 & 0 & 1 & 1 \end{pmatrix}.$$

We are slightly abusing notation here, since A_i is also used to denote the matrix having $a_{i_1}, \dots, a_{i_{d_i}}$ as columns. Choosing $\omega = (\omega_1, \omega_2) = (1, 2, 0, 0, 0, 0) \in \mathbb{R}^7$ as a weight vector, one obtains the regular mixed subdivision $\mathcal{S}_\omega(P_1 + P_2)$ in Figure 4.3. The induced subdivision contains two fully mixed cells, which are the unshaded ones.

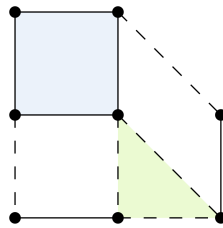


Figure 4.3: A regular mixed subdivision of the Minkowski sum of a square and a triangle.

4.2.3 The Cayley Trick

There is another way to look at mixed subdivisions and mixed cells, via the Cayley embedding of the point configurations A_1, \dots, A_n . We embed the configurations in

parallel affine subspaces in a higher-dimensional space: each A_i is embedded in the subspace of \mathbb{R}^{2n} defined by $x_{n+1} = 0, \dots, x_{n+i} = 1, \dots, x_{2n} = 0$. That is, the *Cayley embedding* $\text{Cayley}(A_1, \dots, A_n) \subseteq \mathbb{R}^n \times \mathbb{R}^n$ is the point configuration

$$\text{Cayley}(A_1, \dots, A_n) := (A_1 \times \{e_1\}) \cup \dots \cup (A_n \times \{e_n\}),$$

where e_1, \dots, e_n denote the standard basis vectors of \mathbb{R}^n .

For polytopes $P_1 = \text{conv}(A_1), \dots, P_n = \text{conv}(A_n)$, the *Cayley embedding* is given by

$$\text{Cayley}(P_1, \dots, P_n) := \text{conv}(\text{Cayley}(A_1, \dots, A_n)).$$

In the case of full-dimensional polytopes $P_1, \dots, P_n \subseteq \mathbb{R}^n$, the Cayley embedding will be a $(2n - 1)$ -dimensional polytope in \mathbb{R}^{2n} , with the unique affine relation being that the last n coordinates add up to 1.

Example 4.2.3. Applying the Cayley embedding to our running Example 4.2.2 yields the point configuration

$$\text{Cayley}(A_1, A_2) = \begin{pmatrix} 0 & 1 & 0 & 0 & 1 & 0 & 1 \\ 0 & 0 & 1 & 0 & 0 & 1 & 1 \\ 1 & 1 & 1 & 0 & 0 & 0 & 0 \\ 0 & 0 & 0 & 1 & 1 & 1 & 1 \end{pmatrix}.$$

The corresponding Cayley embedding $\text{Cayley}(P_1, P_2) \subseteq \mathbb{R}^4$ can be pictured by making use of the fact that it is contained in the 3-dimensional subspace given by the equation $x_3 + x_4 = 1$, as in Figure 4.4.

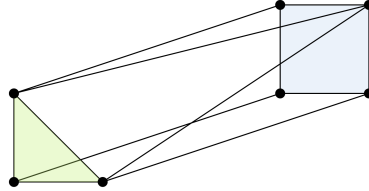


Figure 4.4: The Cayley embedding of a square and a triangle.

So far the two constructions, Minkowski sum and Cayley embedding, may seem unrelated. But they are far from it, since the Minkowski sum is the intersection of the Cayley embedding with the subspace $\{x \in \mathbb{R}^{2n} : x_{n+1} = \dots = x_{2n} = 1/n\}$, up to a scaling factor:

$$\sum_{i=1}^n P_i \times \{1\} = n \cdot (\text{Cayley}(P_1, \dots, P_n) \cap \{x \in \mathbb{R}^{2n} : x_{n+1} = \dots = x_{2n} = 1/n\}).$$

For our running Example 4.2.2 this is illustrated in Figure 4.5.

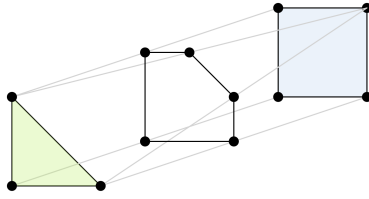


Figure 4.5: The connection between the Cayley embedding and the Minkowski sum.

By a *cell* C in the Cayley embedding, we mean a cell in some polyhedral subdivision of $\text{Cayley}(A_1, \dots, A_n)$. We will often write $C = (C_1, \dots, C_n)$, where $C_i = C \cap (A_i \times \{e_i\})$, to keep track of which points of the cell belong to which point configuration. Since the original point configurations A_1, \dots, A_n are embedded in parallel affine subspaces, a full-dimensional cell must always involve points of all original configurations A_1, \dots, A_n . A *fully mixed* cell will be a full-dimensional cell which involves exactly two points of each configuration. It is not a coincidence that this reminds us of the fully mixed cells appearing in regular subdivisions of Minkowski sums. Indeed, the following statement relating subdivisions of the Cayley embedding and mixed subdivisions of the Minkowski sum holds and it is referenced to as (combinatorial) Cayley trick.

THEOREM 4.2.4 ([LRS10, compare Theorem 9.2.16]). Let $A_1, \dots, A_n \subseteq \mathbb{R}^n$ be point configurations. Then (regular) polyhedral subdivisions of the Cayley embedding $\text{Cayley}(A_1, \dots, A_n)$ are in one-to-one correspondence with (regular) mixed subdivisions of the Minkowski sum $\sum_{i=1}^n A_i$.

Explicitly, given a polyhedral subdivision of the Cayley embedding, we can recover (a scaled version of) the corresponding mixed subdivision by intersecting the Cayley embedding as we did above with the subspace $\{x \in \mathbb{R}^{2n} : x_{n+1} = \dots = x_{2n} = 1/n\}$. In particular, fully mixed cells of the mixed subdivision are sections of fully mixed cells of the subdivision of the Cayley embedding. For more details on the Cayley trick, the reader is referred to [HRS00].

Example 4.2.5. We have already seen a mixed subdivision of the Minkowski sum $P_1 + P_2$ for our running example in Figure 4.3. Each cell corresponds to a cell in the Cayley embedding $\text{Cayley}(P_1, P_2)$ and all together they form a polyhedral subdivision of $\text{Cayley}(P_1, P_2)$. For one of the cells this correspondence is illustrated in Figure 4.6.

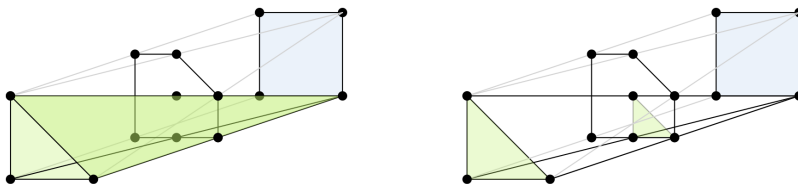


Figure 4.6: The correspondence between Minkowski cells and Cayley cells.

We call a mixed subdivision of the Minkowski sum a *fine mixed subdivision* if it corresponds to a triangulation of the Cayley embedding. The name ‘fine’ comes from the fact that it is impossible to have a mixed subdivision strictly refining it while keeping the vertex set.

We now have two ways of thinking of fully mixed cells, and we will often switch between the two. There should be no ambiguity since we have given an explicit bijection.

4.2.4 The Secondary Polytope and the Secondary Fan

If we assume the weight vector ω to be generic, the regular polyhedral subdivision of $\text{Cayley}(A_1, \dots, A_n)$ it induces will be a triangulation. In this section we introduce the secondary polytope, which captures useful information about all possible triangulations of a given point configuration. Before we can give a precise definition, we have to introduce some notation. We follow the construction of the secondary polytope presented in [LRS10, Chapters 2 and 5].

Consider a point configuration $A \subseteq \mathbb{R}^n$ consisting of d points. To each triangulation \mathcal{T} of A we associate a vector $\Phi_A(\mathcal{T}) \in \mathbb{R}^d$. The entry of this vector corresponding to the point $a \in A$ is defined as the sum of the volumes of all cells of the triangulation which contain the point a as a vertex, where the volume is understood to be the usual Euclidean volume of the convex hull of a cell.

Definition 4.2.6. Let $A \subseteq \mathbb{R}^n$ be a point configuration with $d = |A|$ and let \mathcal{T} be a triangulation of A . The vector

$$\Phi_A(\mathcal{T}) := \sum_{i \in [d]} \sum_{C \in \mathcal{T}: a_i \in C} \text{vol}(C) e_i \in \mathbb{R}^d$$

is called the *Gelfand-Kapranov-Zelevinsky* vector of \mathcal{T} , often referred to as GKZ-vector.

Example 4.2.7. Let us come back to the one-dimensional example of five points on a line which we studied in Example 4.2.1. The GKZ-vector for the triangulation $\mathcal{T}_{\omega'}$ is given by

$$\Phi_{\{1,2,3,4,5\}}(\mathcal{T}_{\omega'}) = \begin{pmatrix} \text{vol}(13) \\ 0 \\ \text{vol}(13) + \text{vol}(35) \\ 0 \\ \text{vol}(35) \end{pmatrix} = \begin{pmatrix} 2 \\ 0 \\ 4 \\ 0 \\ 2 \end{pmatrix}.$$

The convex hull of the GKZ-vectors of all triangulations is called the secondary polytope.

Definition 4.2.8. Let A be a point configuration. The *secondary polytope* $\Sigma\text{-poly}(A)$ of A is defined as

$$\Sigma\text{-poly}(A) := \text{conv} \{ \Phi_A(\mathcal{T}) : \mathcal{T} \text{ is a triangulation of } A \}.$$

Example 4.2.9. We continue with Example 4.2.7. The given point configuration $A = \{1, 2, 3, 4, 5\} \subseteq \mathbb{R}$ has eight different triangulations in total. For each of them one can compute the corresponding GKZ-vector as in the previous example. The resulting secondary polytope $\Sigma\text{-poly}(A)$ has the combinatorics of a cube as shown in Figure 4.7.

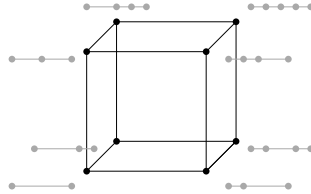


Figure 4.7: The combinatorics of the secondary polytope of five points on a line.

Let us revisit Example 4.2.5. In Figure 4.8, we have drawn fine mixed subdivisions of the Minkowski sum. The labeling $\mathcal{T}_1, \dots, \mathcal{T}_{16}$ refers to the corresponding triangulations of the Cayley embedding. Each of these fine mixed subdivisions corresponds to a vertex of the secondary polytope.

An important result about the secondary polytope is that, although we took the convex hull of GKZ-vectors of all triangulations, the vertices correspond only to the regular triangulations, see for example [LRS10, Theorem 5.1.9].

Not only vertices, but the whole face lattice of the secondary polytope encodes information about regular subdivisions of the original point configuration. In fact, if there is an edge connecting two vertices, the associated triangulations are similar. That is, they only differ by a local change, a so-called *flip*.

A point configuration $A \subseteq \mathbb{R}^n$ with $|A| = d$ is called a *corank 1* configuration if there is a non-trivial unique affine dependence relation among its points, $\sum_{i \in [d]} \lambda_i a_i = 0$, with $\sum_{i \in [d]} \lambda_i = 0$ for some $\lambda_i \in \mathbb{R}$. The *signed circuit*, denoted by $c = (c_+, c_-)$ keeps track of the labels of the points that are involved in the dependence relation, i.e., $c_+ = \{i \in [d] : \lambda_i > 0\}$ and $c_- = \{i \in [d] : \lambda_i < 0\}$. We refer to c_+ or c_- as one *side* of the signed circuit c . Since this describes a minimal affine dependence, the convex hulls of the points indexed by the two sides of the circuit intersect in a unique point, as can for instance be seen in Figure 4.9.

The important property of corank 1 configurations is that they only have two possible triangulations:

LEMMA 4.2.10 ([LRS10, Lemma 2.4.2]). Let A be a configuration of corank 1 and $c = (c_+, c_-)$ the associated circuit. Then the following are the only two triangulations of A :

$$\mathcal{T}_+ = \{C \subseteq [d] : c_+ \not\subseteq C\} \quad \text{and} \quad \mathcal{T}_- = \{C \subseteq [d] : c_- \not\subseteq C\}.$$

Both triangulations are regular.

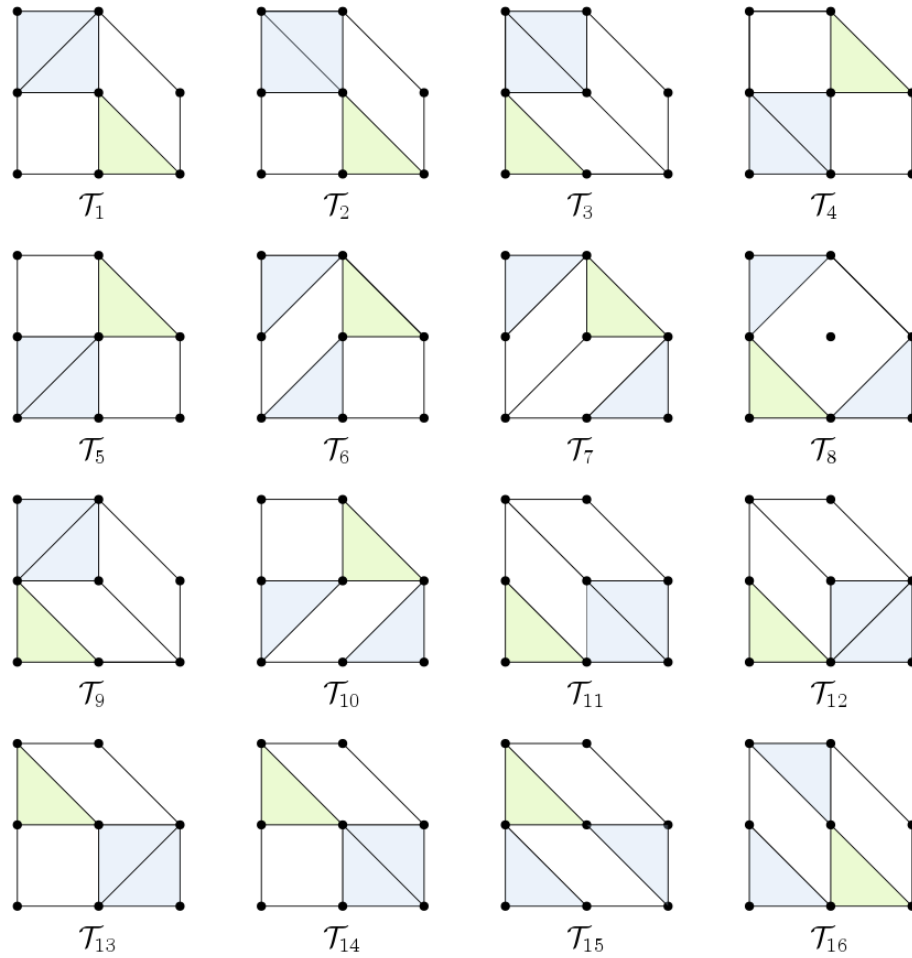


Figure 4.8: Fine mixed subdivisions of the Minkowski sum of triangle and square.

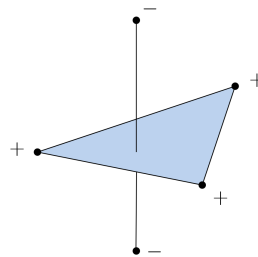


Figure 4.9: A signed circuit $c = (c_+, c_-)$.

An *almost triangulation* is a subdivision \mathcal{S} such that it itself is not a triangulation, but all its proper refinements are. Any cell of an almost triangulation is composed of points which are either affinely independent or form a configuration of corank 1, and all its cells of corank 1 contain the same circuit. Therefore by Lemma 4.2.10 it has exactly two

proper refinements, which are both triangulations. We say that two triangulations of the same point configuration are *connected by a flip supported on the almost triangulation \mathcal{S}* if they are the only two triangulations refining \mathcal{S} .

For the secondary polytope this means that two vertices are connected by an edge if the corresponding triangulations differ by a flip, and the edge corresponds to the involved almost triangulation. Figure 4.10 shows some flips in the plane.



Figure 4.10: Some flips in the plane.

In some contexts it is more useful to consider not the secondary polytope, but the secondary fan. The *secondary fan* is the inner normal fan of the secondary polytope and is denoted by $\Sigma\text{-fan}(A)$. Since each vertex of the secondary polytope corresponds to a regular triangulation, a full-dimensional cone in the secondary fan also does. It actually is the closure of the set of all the weight vectors $\omega \in \mathbb{R}^n$ inducing the regular triangulation \mathcal{T}_ω .

4.3 A LOWER BOUND ON THE RUNNING TIME OF A HOMOTOPY CONTINUATION APPROACH

Recall, that we are given the following problem.

INPUT: Point configurations $A = (A_1, \dots, A_n) \subseteq \mathbb{R}^n$, where $|A_i| = d_i$ and $d = \sum_{i=1}^n d_i$ with associated polytopes $P_i = \text{conv}(A_i)$ and random weights $\omega = (\omega_1, \dots, \omega_n) \in \mathbb{R}^A$.

GOAL: Finding a fully mixed cell in the regular fine mixed subdivision of $A_1 + \dots + A_n$, or alternatively the regular triangulation \mathcal{T}_ω of the Cayley embedding $\text{Cayley}(A_1, \dots, A_n)$, induced by ω , in expected polynomial time.

One way to approach our problem of finding a fully mixed cell is the following.

APPROACH:

1. Choose weights $\bar{\omega} \in \mathbb{R}^A$ for which we know how to compute a fully mixed cell in polynomial time.
2. Apply a homotopy continuation method, where $\bar{\omega}$ encodes the start system and ω the target system and track the fully mixed cell.

There already exists an algorithm to execute step 1 which we will discuss in the following.

4.3.1 A Matroid Intersection Algorithm

Given our point configuration $A = (A_1, \dots, A_n)$ there exists a way to find a fully mixed cell of *some* regular subdivision of $\text{Cayley}(A_1, \dots, A_n)$ in polynomial time. However, the weight vector is *not* part of the input here.

In order to find such a cell, we follow the approach used in the proof of [DGH98, Theorem 8]. This requires to translate the given problem to a matroidal setting. Background information and more details about matroid theory can be found in [Oxl11].

As a ground set we consider all segments, i.e., vectors that connect two points of a respective point configuration. More precisely, set

$$E_i = \{a - a' : a, a' \in A_i\} \text{ for } i = 1, \dots, n \text{ and } E = \bigsqcup_{i=1}^n E_i.$$

On this ground set we define two matroids $M_1 = (E, \mathcal{I}_1)$ and $M_2 = (E, \mathcal{I}_2)$. Here, M_1 is the *linear* matroid whose independent sets \mathcal{I}_1 are the linearly independent subsets of the vectors in E . For the matroid M_2 a subset of E is independent if it contains at most one element from E_i for all $i \in \{1, \dots, n\}$ and it is called the *transversal* matroid. By construction M_1 and M_2 have the same rank, namely n . Furthermore, a common basis \mathcal{B} chooses exactly one segment per configuration A_i for all $i \in \{1, \dots, n\}$. Since these segments are linearly independent, they determine a full-dimensional subset \bar{C} of the associated Cayley embedding $\text{Cayley}(A_1, \dots, A_n)$. We claim that there exists a weight vector $\bar{\omega} \in \mathbb{R}^d$ such that \bar{C} corresponds to a fully mixed cell in the regular subdivision $\mathcal{S}_{\bar{\omega}}$. For that we define the vector $\bar{\omega}$ such that points from \bar{C} receive weight 0 and give weight 1 to all other points.

Finding such a common basis \mathcal{B} — and hence a fully mixed cell — can be done in polynomial time by the matroid intersection algorithm of Edmonds [Edm70].

We can make $\bar{\omega}$ generic, by perturbing the weights a little bit. This perturbed vector then induces a triangulation that involves \bar{C} . This can also be done in polynomial time.

4.3.2 A Lower Bound on the Number of Flips

We now want to take a closer look at step 2 and give an example that suggests that it might be more promising to search for lower bounds than for upper bounds regarding the expected running time.

Recall that the given weight vectors ω and $\bar{\omega}$ can be thought of as elements in the support of the secondary fan $\Sigma\text{-fan}(\text{Cayley}(A_1, \dots, A_n))$. A full-dimensional cone in the secondary fan corresponds to a regular triangulation of the Cayley embedding, and the codimension 1 boundary between two such cones therefore corresponds to a flip. We now consider the segment $I \subseteq |\Sigma\text{-fan}(\text{Cayley}(A_1, \dots, A_n))|$, connecting $\bar{\omega}$ and our objective weight ω in the secondary fan as depicted in Figure 4.11. Since $\omega, \bar{\omega}$ corre-

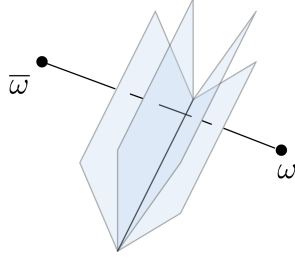


Figure 4.11: Wall-crossing for a homotopy continuation in the secondary fan with start system $\bar{\omega}$ and target system ω .

spond to triangulations, we can assume that I is generic in the sense that it intersects $\Sigma\text{-fan}(\text{Cayley}(A_1, \dots, A_n))$ only in the relative interior of d - and $(d-1)$ -dimensional cones. Starting at $\bar{\omega}$ and moving towards ω , the points on I induce the same triangulation $\mathcal{T}_{\bar{\omega}}$ until the segment meets the boundary of the full-dimensional cone corresponding to $\mathcal{T}_{\bar{\omega}}$. We will call these codimension 1 boundaries *walls*. The point of intersection of the segment I with a wall induces an almost triangulation \mathcal{S} , and points on the other side of the wall induce the other triangulation refining \mathcal{S} . Thus, intersections of I with walls correspond to a sequence of flips transforming the triangulation $\mathcal{T}_{\bar{\omega}}$ into \mathcal{T}_{ω} .

Therefore, the expected running time of step 2 can be bounded in terms of probabilities of the form

$$\sum_{\substack{\text{flips affecting} \\ \text{fully mixed cells}}} \mathcal{P}(I \text{ intersects the wall associated to the flip}). \quad (4.3.1)$$

Hence, one natural question that arises is, how many summands can this expression have, i.e., how many flips affect fully mixed cells?

For that we need to introduce the fine type of a cell.

Definition 4.3.1. For a subset $C = (C_1, \dots, C_n)$ of a configuration $A = (A_1, \dots, A_n)$, its *fine type* $\tau(C)$ is defined as the vector $(|C_1|, \dots, |C_n|) \in \mathbb{Z}_{\geq 0}^n$, which keeps track of the number of points of A_i that contribute to C . For a signed circuit $c = (c_+, c_-)$, the fine type $\tau(c)$ is a pair of integer vectors $((|C_1|_+, \dots, |C_n|_+), (|C_1|_-, \dots, |C_n|_-))$, with $|C_i|_+$ and $|C_i|_-$ recording the number of labels of A_i contributing to c_+ and c_- , respectively.

The only flips, affecting fully mixed cells, will be those supported on a signed circuit c of fine type $\tau(c) = ((1, \dots, 1), (1, \dots, 1))$ or $\tau(c) = ((2, 1, \dots, 1), (1, \dots, 1))$, up to permutation. This means that for the ‘smaller side’ c_- of the circuit, we have to choose a subconfiguration $C_- \subseteq \text{Cayley}(A_1, \dots, A_n)$ which consists of exactly one point per configuration $A_i \times \{e_i\}$ for all $i \in \{1, \dots, n\}$.

We give an example of a configuration A for which there exist exponentially many ‘smaller sides’ C_- of fine type $\tau(C_-) = (1, \dots, 1)$ in the interior of the Cayley embedding

that can be completed to a circuit c . This yields exponentially many summands in Equation (4.3.1).

Example 4.3.2. We define a point configuration $A = (A_1, \dots, A_n)$ with $A_i \subseteq \mathbb{R}^n$ and $|A_i| = m$ for an integer $m \geq 4$ and all $i \in \{1, \dots, n\}$ as follows.

Let a_i^j denote the j -th point of the configuration A_i and \mathbf{a}_i^j the respective point in $A_i \times \{e_i\}$. The points are chosen on the moment curve $\gamma_n(t): \mathbb{R} \rightarrow \mathbb{R}^n$, i.e., they are of the form (t, t^2, \dots, t^n) for some $t \in \mathbb{R}$. These t are chosen in a consecutive way as illustrated in Figure 4.12, meaning that $t_{a_i^j} < t_{a_i^k}$ for $j < k$ and $t_{a_i^j} < t_{a_k^l}$ for $i < k$ and any $j, l \in \{1, \dots, m\}$.

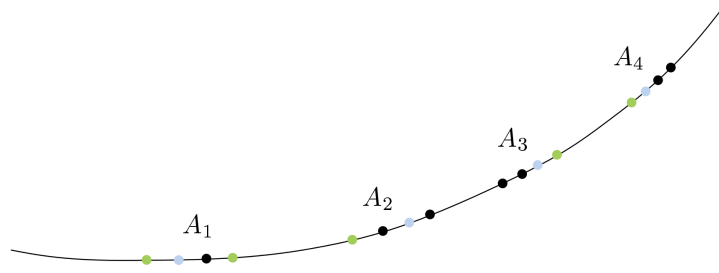


Figure 4.12: Point configurations on the moment curve for $n = 4$ and $m = 4$.

Consequently, our polytopes $P_i = \text{conv}(A_i)$ are cyclic polytopes. We will extend Gale's evenness criterion to our situation. More precisely, we will use the following facts about polynomials.

1. The derivative of a univariate polynomial of degree n can have at most $n - 1$ changes of sign.
2. Therefore a univariate polynomial of degree n can have at most $n - 1$ local extrema, hence at most $\frac{n}{2}$ local minima or maxima.

In total there are m^n possible ways to choose exactly one point per A_i for all $i \in \{1, \dots, n\}$ in order to form a subconfiguration $C_- = (\mathbf{a}_1^{j_1}, \dots, \mathbf{a}_n^{j_n})$ with $a_i^{j_i} \in A_i$ of fine type $\tau(C_-) = (1, \dots, 1)$. To ensure, that C_- actually corresponds to the smaller side of a circuit c we have to exclude all configurations on the boundary of the Cayley embedding, because for them we cannot guarantee, that they contribute to a desired circuit. We now show the following.

CLAIM 1: The convex hull of a configuration $C_- = (\mathbf{a}_1^{j_1}, \dots, \mathbf{a}_n^{j_n})$ with $j_i \notin \{1, m\}$ for all $i \in \{1, \dots, n\}$ will lie in the interior of the Cayley embedding.

We verify the claim via proof by contradiction. Assume, we pick a configuration C_- as above such that $\text{conv}(C_-)$ lies on the boundary of $\text{Cayley}(P_1, \dots, P_n)$. Then there exists a linear functional $\ell = (\alpha_1, \dots, \alpha_n, \beta_1, \dots, \beta_n) \in (\mathbb{R}^{2n})^*$, whose minimum is attained at C_- , when minimizing over the Cayley embedding. Consider the restriction of the

functional ℓ to the subspace $\{x \in \mathbb{R}^{2n} : x_{n+i} = 1, x_{n+j} = 0 \text{ for all } j \in \{1, \dots, n\} \setminus \{i\}\}$, where the point configuration $A_i \times \{e_i\}$ lives. Then the minimum among the points of $A_i \times \{e_i\}$ is still attained at $\mathbf{a}_i^{j_i}$, for each i , respectively.

We recall that the points $\mathbf{a}_i^{j_i}$ lie on the moment curve. Thus, restricting ℓ to the moment curve yields n local minima which is a contradiction to Fact 2. Hence, for C_- to belong to the boundary, the points of C_- have to be chosen as \mathbf{a}_i^1 or \mathbf{a}_i^m for at least half of the $i \in \{1, \dots, n\}$.

Conversely, this guarantees, that the convex hull associated to a configuration $C_- = (\mathbf{a}_1^{j_1}, \dots, \mathbf{a}_n^{j_n})$ with $j_i \notin \{1, m\}$ for all $i \in \{1, \dots, n\}$ will lie in the interior of the Cayley embedding. There are $(m-2)^n$ pairwise different such configurations.

CLAIM 2: All of these $(m-2)^n$ configurations C_- correspond to one side of a circuit.

Fix a configuration C_- , represented by the blue dots in Figure 4.12. Choose $n+1$ points C_+ to be the alternating endpoints as indicated by the green ones in Figure 4.12. Consider the configuration $C = C_- \cup C_+$. Since it consists of $2n+1$ points in \mathbb{R}^{2n} , there exists an affine dependence relation among the points. We claim that $\text{conv}(C_-)$ is not contained in the boundary of $\text{conv}(C)$. Assume that it was. Then there exists a linear functional that is minimized at $\text{conv}(C_-)$, when minimizing over $\text{conv}(C)$. Restricted to the moment curve, this results in n changes of sign of the derivative γ'_n . But this is a contradiction to Fact 1. Thus, $\text{conv}(C_-)$ is not contained in the boundary of $\text{conv}(C)$. Moreover, it is a minimal subset regarding this property. Because due to the Cayley structure, removing a point from C_- would force it to lie on the boundary. Consequently, C_- gives the smaller side of a circuit that corresponds to a flip affecting fully mixed cells. There are $(m-2)^n$ pairwise different such configurations. Thus, for this particular example, the number of summands in Equation (4.3.1) is exponential in the input size n .

This leads to the following further remarks and questions that should be examined.

- In order to obtain a lower bound we would need to answer the following question: Can we find a lower bound on the individual summands probability in Equation (4.3.1), for instance in terms of the volume of the respective walls?
- On the other hand the following considerations might reduce complexity: Since we are only interested in a single fully mixed cell, not in the whole triangulation, the secondary polytope captures more information than needed.

In [MCo0] Cools and Michiels introduce the so-called *mixed secondary polytope* which is related to the secondary polytope but which captures less information and is therefore less complicated. Roughly speaking, a vertex of such a polytope represents the collection of fully mixed cells that is involved in a given mixed subdivision and ignores all other cells of the subdivision. Thus two mixed

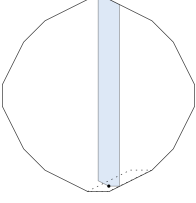
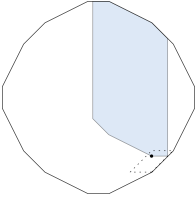
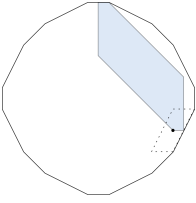
subdivisions that contain the same fully mixed cells are represented by the same vertex.

Does considering the mixed secondary fan instead of the secondary fan reduce the complexity?

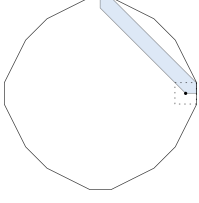
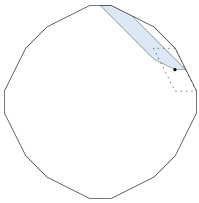
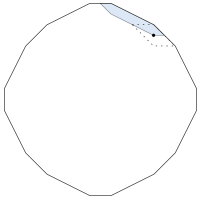
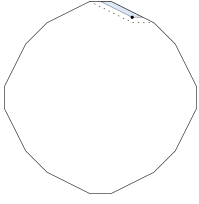
- Note, that considering only flips involving fully mixed cells might be too much, since not all flips will involve the specific fully mixed cell that we are tracking; it is possible that most of the flips do not change this mixed cell at all. Does this reduce the complexity?
- (How) can we lift the obtained tropical solution to one of the original system?

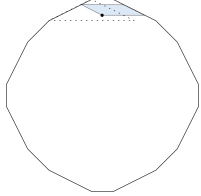
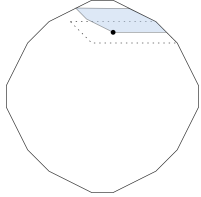
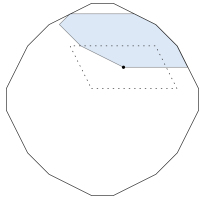
APPENDIX

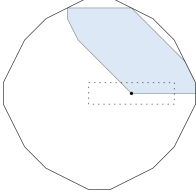
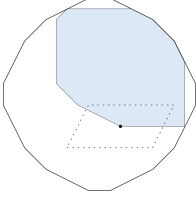
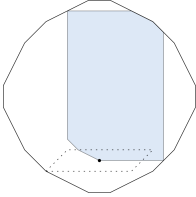
We give the respective global sections and Newton polytopes that realize a lower bound for the Newton–Okounkov function φ_R on the Newton–Okounkov body $\Delta_Y(D)$ from Example 2.5.10.

| Region | Inequalities | Newton Polytope | Section | $\text{ord}_R(s)$ |
|--------|---|---|--|-------------------------|
| 1 | $0 \leq b \leq 1,$ $0 \leq a - 4b \leq 1$ |  | $s(x, y) = x^a y^b$ $(x - 1)^{1-a+4b}$ $(y - 1)^b$ $(x^2 y - 1)^{9-2b}$ | $10 - a + 3b$ |
| 2 | $1 \leq b \leq 2,$ $1 \leq a - 3b \leq 2$ |  | $s(x, y) = x^a y^b$ $(x - 1)^{2-a+3b}$ $(y - 1)^{2-b}$ $(x^2 y - 1)^{10-3b}$ $(xy - 1)^{3b-3}$ | $11 - a + 2b$ |
| 3 | $2 \leq b \leq 4,$ $4 \leq 2a - 5b \leq 6$ |  | $s(x, y) = x^a y^b$ $(x - 1)^{3-a+\frac{5}{2}b}$ $(x^2 y - 1)^{7-\frac{3}{2}b}$ $(xy - 1)^{2+\frac{1}{2}b}$ | $12 - a + \frac{3}{2}b$ |

APPENDIX

| Region | Inequalities | Newton Polytope | Section | $\text{ord}_R(s)$ |
|--------|---|---|---|-----------------------------------|
| 4 | $4 \leq b \leq 5,$ $4 \leq a - 2b \leq 5$ |  | $s(x, y) = x^a y^b$ $(x - 1)^{5-a+2b}$ $(x^2 y - 1)^{5-b}$ $(xy - 1)^4$ | $14 - a + b$ |
| 5 | $1 \leq b \leq 2,$ $1 \leq a - 3b \leq 2$ |  | $s(x, y) = x^a y^b$ $(x - 1)^{\frac{15}{2}-a+\frac{3}{2}b}$ $(y - 1)^{-\frac{5}{2}+\frac{1}{2}b}$ $(xy - 1)^{\frac{23}{2}-\frac{3}{2}b}$ | $\frac{33}{2} - a + \frac{1}{2}b$ |
| 6 | $7 \leq b \leq 8,$ $10 \leq a - b \leq 11$ |  | $s(x, y) = x^a y^b$ $(x - 1)^{11-a+b}$ $(y - 1)$ $(xy - 1)^{8-b}$ | $20 - a$ |
| 7 | $8 \leq b \leq 9,$ $18 \leq a \leq 19$ |  | $s(x, y) = x^a y^b$ $(x - 1)^{19-a}$ $(y - 1)^{9-b}$ | $28 - a - b$ |

| Region | Inequalities | Newton Polytope | Section | $\text{ord}_R(s)$ |
|--------|---|---|---|---|
| 8 | $8 \leq b \leq 9,$ $a \leq 18,$ $-a + 4b \leq 18$ |  | $s(x, y) = x^a y^b$ $(x - 1)^{19-a}$ $(y - 1)^{\frac{9}{2} + \frac{1}{4}a - b}$ | $\frac{47}{2} - \frac{3}{4}a - b$ |
| 9 | $7 \leq b \leq 8,$ $6 \leq a - b \leq 10$ |  | $s(x, y) = x^a y^b$ $(x - 1)^{11-a+b}$ $(y - 1)^{-3 + \frac{1}{4}a - \frac{1}{4}b}$ $(xy - 1)^{8-b}$ | $\frac{35}{2} - \frac{3}{4}a - \frac{1}{4}b$ |
| 10 | $5 \leq b \leq 7,$ $5 \leq 2a - 3b \leq 13$ |  | $s(x, y) = x^a y^b$ $(x - 1)^{\frac{15}{2} - a + \frac{3}{2}b}$ $(y - 1)^{-\frac{5}{8} + \frac{1}{4}a - \frac{3}{8}b}$ $(xy - 1)$ $(x^3 y^2 - 3xy$ $+ y + 1)^{\frac{7}{2} - \frac{1}{2}b}$ | $\frac{119}{8} - \frac{3}{4}a + \frac{1}{8}b$ |

| Region | Inequalities | Newton Polytope | Section | $\text{ord}_R(s)$ |
|--------|--|---|---|--|
| 11 | $4 \leq b \leq 5,$ $0 \leq a - 2b \leq 4$ |  | $s(x, y) = x^a y^b$ $(x - 1)^{5-a+2b}$ $(x^2 y - 1)^{5-b}$ $(xy - 1)^{1+\frac{3}{4}a-\frac{3}{2}b}$ $(x^3 y^2 - 3xy + y + 1)^{1-\frac{1}{4}a+\frac{1}{2}b}$ | $13 - \frac{3}{4}a + \frac{1}{2}b$ |
| 12 | $2 \leq b \leq 4,$ $-4 \leq -2a + 5b,$ $-2a + 5b \leq 4$ |  | $s(x, y) = x^a y^b$ $(x - 1)^{3-a+\frac{5}{2}b}$ $(y - 1)^{\frac{1}{2}+\frac{1}{4}a-\frac{5}{8}b}$ $(x^2 y - 1)^{9-2b}$ $(xy - 1)$ $(x^3 y^2 - 3xy + y + 1)^{-1+\frac{1}{2}b}$ | $\frac{23}{2} - \frac{3}{4}a + \frac{7}{8}b$ |
| 13 | $1 \leq b \leq 2,$ $-3 \leq a - 3b \leq 1$ |  | $s(x, y) = x^a y^b$ $(x - 1)^{2-a+3b}$ $(y - 1)^{\frac{3}{4}+\frac{1}{4}a-\frac{3}{4}b}$ $(x^2 y - 1)^{9-2b}$ $(xy - 1)^{-1+b}$ | $\frac{43}{4} - \frac{3}{4}a + \frac{5}{4}b$ |

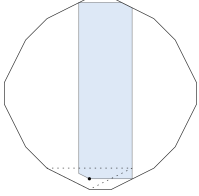
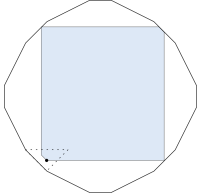
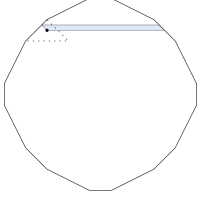
| Region | Inequalities | Newton Polytope | Section | $\text{ord}_R(s)$ |
|--------|--|---|---|--|
| 14 | $5 \leq b \leq 7,$ $5 \leq 2a - 3b \leq 13$ |  | $s(x, y) = x^a y^b$ $(x - 1)^{1-a+4b}$ $(y - 1)^{\frac{1}{4}a}$ $(x^2 y - 1)^{9-2b}$ $(xy - 1)^{-1+b}$ | $10 - \frac{3}{4}a + 2b$ |
| 15 | $1 \leq b \leq 2,$ $-a + b \leq 1,$ $-a + 3b \geq 3$ |  | $s(x, y) = x^a y^b$ $(x - 1)^{2-a+3b}$ $(x^2 y - 1)^{9-2b}$ $(xy - 1)^{\frac{1}{2} + \frac{1}{2}a - \frac{1}{2}b}$ | $\frac{23}{2} - \frac{1}{2}a + \frac{1}{2}b$ |
| 19 | $7 \leq b \leq 8,$ $a - b \leq 6,$ $-a + 3b \leq 10$ |  | $s(x, y) = x^a y^b$ $(x - 1)^{11-a+b}$ $(xy - 1)^{5 + \frac{1}{2}a - \frac{3}{2}b}$ | $16 - \frac{1}{2}a - \frac{1}{2}b$ |

Table A.1: Sections s such that s^k are global sections of $H^0(X, \mathcal{O}_X(kD))$ that realize lower bounds for the order of vanishing ord_R for respective $k \in \mathbb{Z}_{\geq 1}$.

BIBLIOGRAPHY

- [ADR11] Elizabeth S. Allman, James H. Degnan, and John A. Rhodes. „Identifying the rooted species tree from the distribution of unrooted gene trees under the coalescent.“ In: *J. Math. Biol.* 62.6 (2011), pp. 833–862. ISSN: 0303-6812. DOI: [10.1007/s00285-010-0355-7](https://doi.org/10.1007/s00285-010-0355-7).
- [AK06] Federico Ardila and Caroline J. Klivans. „The Bergman complex of a matroid and phylogenetic trees.“ In: *J. Comb. Theory, Ser. B* 96.1 (2006), pp. 38–49. ISSN: 0095-8956. DOI: [10.1016/j.jctb.2005.06.004](https://doi.org/10.1016/j.jctb.2005.06.004).
- [And13] Dave Anderson. „Okounkov bodies and toric degenerations.“ In: *Math. Ann.* 356.3 (2013), pp. 1183–1202. ISSN: 0025-5831. DOI: [10.1007/s00208-012-0880-3](https://doi.org/10.1007/s00208-012-0880-3).
- [Bau09] Thomas Bauer. „A simple proof for the existence of Zariski decompositions on surfaces.“ In: *J. Algebraic Geom.* 18.4 (2009), pp. 789–793. ISSN: 1056-3911. DOI: [10.1090/S1056-3911-08-00509-2](https://doi.org/10.1090/S1056-3911-08-00509-2).
- [Bau97] Thomas Bauer. „Seshadri constants of quartic surfaces.“ In: *Math. Ann.* 309.3 (1997), pp. 475–481. ISSN: 0025-5831. DOI: [10.1007/s002080050122](https://doi.org/10.1007/s002080050122).
- [Bau98] Thomas Bauer. „Seshadri constants and periods of polarized abelian varieties.“ In: *Math. Ann.* 312.4 (1998), pp. 607–623. ISSN: 0025-5831. DOI: [10.1007/s002080050238](https://doi.org/10.1007/s002080050238).
- [Bau99] Thomas Bauer. „Seshadri constants on algebraic surfaces.“ In: *Math. Ann.* 313.3 (1999), pp. 547–583. ISSN: 0025-5831. DOI: [10.1007/s002080050272](https://doi.org/10.1007/s002080050272).
- [BC11a] Sébastien Boucksom and Huayi Chen. „Okounkov bodies of filtered linear series.“ In: *Compos. Math.* 147.4 (2011), pp. 1205–1229. ISSN: 0010-437X. DOI: [10.1112/S0010437X11005355](https://doi.org/10.1112/S0010437X11005355).
- [BC11b] Peter Bürgisser and Felipe Cucker. „On a problem posed by Steve Smale.“ In: *Ann. Math. (2)* 174.3 (2011), pp. 1785–1836. ISSN: 0003-486X. DOI: [10.4007/annals.2011.174.3.8](https://doi.org/10.4007/annals.2011.174.3.8).
- [Ber79] David N. Bernstein. „The number of roots of a system of equations.“ In: *Funct. Anal. Appl.* 9.3 (1979), pp. 183–185. ISSN: 0016-2663. DOI: [10.1007/BF01075595](https://doi.org/10.1007/BF01075595).
- [BHV01] Louis J. Billera, Susan P. Holmes, and Karen Vogtmann. „Geometry of the Space of Phylogenetic Trees.“ In: *Adv. Appl. Math.* 27.4 (2001), pp. 733–767. ISSN: 0196-8858. DOI: [10.1006/aama.2001.0759](https://doi.org/10.1006/aama.2001.0759).

BIBLIOGRAPHY

- [BKS04] Thomas Bauer, Alex Küronya, and Tomasz Szemberg. „Zariski chambers, volumes, and stable base loci.“ In: *J. Reine Angew. Math.* 576 (2004), pp. 209–233. ISSN: 0075-4102. DOI: [10.1515/cr11.2004.090](https://doi.org/10.1515/cr11.2004.090).
- [BKS20] Victor Batyrev, Alexander M. Kasprzyk, and Karin Schaller. „On the Fine Interior of Three-dimensional Canonical Fano Polytopes.“ In: *Interactions with Lattice Polytopes*. Ed. by Alexander M. Kasprzyk and Benjamin Nill. Springer, 2020 (in press).
- [Bou+15] Sébastien Boucksom, Alex Küronya, Catriona Maclean, and Tomasz Szemberg. „Vanishing sequences and Okounkov bodies.“ In: *Math. Ann.* 361 (2015), pp. 811–834. ISSN: 0025-5831. DOI: [10.1007/s00208-014-1081-z](https://doi.org/10.1007/s00208-014-1081-z).
- [BPo8a] Carlos Beltrán and Luis M. Pardo. „On Smale’s 17th Problem: A Probabilistic Positive Solution.“ In: *Found. Comput. Math.* 8.1 (2008), pp. 1–43. ISSN: 1615-3375. DOI: [10.1007/s10208-005-0211-0](https://doi.org/10.1007/s10208-005-0211-0).
- [BPo8b] Carlos Beltrán and Luis M. Pardo. „Smale’s 17th problem: Average polynomial time to compute affine and projective solutions.“ In: *J. Amer. Math. Soc.* 22.2 (2008), pp. 363–385. ISSN: 0894-0347. DOI: [10.1090/S0894-0347-08-00630-9](https://doi.org/10.1090/S0894-0347-08-00630-9).
- [Can74] Chris Cannings. „The latent roots of certain Markov chains arising in genetics: A new approach, I. Haploid models.“ In: *Adv. Appl. Probab.* 6.2 (1974), pp. 260–290. ISSN: 0001-8678. DOI: [10.2307/1426293](https://doi.org/10.2307/1426293).
- [Can75] Chris Cannings. „The latent roots of certain Markov chains arising in genetics: A new approach, II. Further haploid models.“ In: *Adv. Appl. Probab.* 7.2 (1975), pp. 264–282. ISSN: 0001-8678. DOI: [10.2307/1426077](https://doi.org/10.2307/1426077).
- [Cas+20] Ana-Maria Castravet, Antonio Laface, Jenia Tevelev, and Luca Ugaglia. *Blown-up toric surfaces with non-polyhedral effective cone*. 2020. arXiv: [2009.14298](https://arxiv.org/abs/2009.14298).
- [Cil+17] Ciro Ciliberto, Michal Farnik, Alex Küronya, Victor Lozovanu, Joaquim Roé, and Constantin Shramov. „Newton-Okounkov bodies sprouting on the valuative tree.“ In: *Rend. Circ. Mat. Palermo II* 66.2 (2017), pp. 161–194. ISSN: 0009-725X. DOI: [10.1007/s12215-016-0285-3](https://doi.org/10.1007/s12215-016-0285-3).
- [CL12] Paolo Cascini and Vladimir Lazić. „New outlook on the minimal model program, I.“ In: *Duke Math. J.* 161.12 (2012), pp. 2415–2467. ISSN: 0012-7094. DOI: [10.1215/00127094-1723755](https://doi.org/10.1215/00127094-1723755).
- [CLS11] David A. Cox, John B. Little, and Henry K. Schenck. *Toric varieties*. Providence, RI: American Mathematical Society, 2011. ISBN: 978-0-8218-4819-7. DOI: [10.1090/gsm/124](https://doi.org/10.1090/gsm/124).
- [Cox95] David A. Cox. „The homogeneous coordinate ring of a toric variety.“ In: *J. Algebraic Geom.* 4.1 (1995), pp. 17–50. ISSN: 1056-3911.

- [CW19] Giulia Codenotti and Lena Walter. „Finding a fully mixed cell in a mixed subdivision of polytopes.“ In: *Algebraic and Geometric Combinatorics on Lattice Polytopes*. Ed. by Takayuki Hibi and Akiyoshi Tsuchiya. Singapore and Hackensack, NJ: World Scientific, 2019, pp. 147–164. ISBN: 978-981-12-0047-2. DOI: [10.1142/9789811200489_0009](https://doi.org/10.1142/9789811200489_0009).
- [Dem92] Jean-Pierre Demailly. „Singular hermitian metrics on positive line bundles.“ In: *Complex Algebraic Varieties*. Ed. by Klaus Hulek, Thomas Peternell, Michael Schneider, and Frank-Olaf Schreyer. Berlin: Springer, 1992, pp. 87–104. ISBN: 978-3-540-55235-2. DOI: [10.1007/BFb0094512](https://doi.org/10.1007/BFb0094512).
- [DGH98] Martin Dyer, Peter Gritzmann, and Alexander Hufnagel. „On The Complexity of Computing Mixed Volumes.“ In: *SIAM J. Comput.* 27.2 (1998), pp. 356–400. ISSN: 0097-5397. DOI: [10.1137/S0097539794278384](https://doi.org/10.1137/S0097539794278384).
- [Di +13] Sandra Di Rocco, Christian Haase, Benjamin Nill, and Andreas Paffenholz. „Polyhedral adjunction theory.“ In: *Algebr. Number Theory* 7.10 (2013), pp. 2417–2446. ISSN: 1937-0652. DOI: [10.2140/ant.2013.7.2417](https://doi.org/10.2140/ant.2013.7.2417).
- [Don02] Simon K. Donaldson. „Scalar Curvature and Stability of Toric Varieties.“ In: *J. Differential Geometry* 62.2 (2002), pp. 289–349. ISSN: 0022-040X. DOI: [10.4310/jdg/1090950195](https://doi.org/10.4310/jdg/1090950195).
- [DRo6] James H. Degnan and Noah A. Rosenberg. „Discordance of species trees with their most likely gene trees.“ In: *PLoS Genetics* 2.5 (2006), pp. 762–768. ISSN: 1553-7390. DOI: [10.1371/journal.pgen.0020068](https://doi.org/10.1371/journal.pgen.0020068).
- [DRo9] James H. Degnan and Noah A. Rosenberg. „Gene tree discordance, phylogenetic inference and the multispecies coalescent.“ In: *Trends Ecol. Evol.* 24.6 (2009), pp. 332–340. ISSN: 0169-5347. DOI: [10.1016/j.tree.2009.01.009](https://doi.org/10.1016/j.tree.2009.01.009).
- [DRS12a] James H. Degnan, Noah A. Rosenberg, and Tanja Stadler. „A Characterization of the Set of Species Trees that Produce Anomalous Ranked Gene Trees.“ In: *IEEE/ACM Trans. Comput. Biol. Bioinform.* 9.6 (2012), pp. 1558–1568. ISSN: 1545-5963. DOI: [10.1109/TCBB.2012.110](https://doi.org/10.1109/TCBB.2012.110).
- [DRS12b] James H. Degnan, Noah A. Rosenberg, and Tanja Stadler. „The probability distribution of ranked gene trees on a species tree.“ In: *Math. Biosci.* 235.1 (2012), pp. 45–55. ISSN: 0025-5564. DOI: [10.1016/j.mbs.2011.10.006](https://doi.org/10.1016/j.mbs.2011.10.006).
- [DS05] James H. Degnan and Laura A. Salter. „Gene tree distributions under the coalescent process.“ In: *Evolution* 59.1 (2005), pp. 24–37. ISSN: 0014-3820. DOI: [10.1111/j.0014-3820.2005.tb00891.x](https://doi.org/10.1111/j.0014-3820.2005.tb00891.x).
- [Dum+16a] Marcin Dumnicki, Alex Küronya, Catriona Maclean, and Tomasz Szemberg. „Rationality of Seshadri constants and the Segre-Harbourne-Gimigliano-Hirschowitz conjecture.“ In: *Adv. Math.* 303 (2016), pp. 1162–1170. ISSN: 0001-8708. DOI: [10.1016/j.aim.2016.05.025](https://doi.org/10.1016/j.aim.2016.05.025).

BIBLIOGRAPHY

- [Dum+16b] Marcin Dumnicki, Alex Küronya, Catriona Maclean, and Tomasz Szemberg. „Seshadri constants via functions on Newton-Okounkov bodies.“ In: *Math. Nachr.* 289.17-18 (2016), pp. 2173–2177. ISSN: 0025-584X. DOI: [10.1002/mana.201500280](https://doi.org/10.1002/mana.201500280).
- [Edm70] Jack Edmonds. „Submodular functions, matroids, and certain polyhedra.“ In: *Combinatorial Structures and their Applications (Proc. Calgary Internat. Conf., Calgary, Alta., 1969)*. Gordon and Breach, New York, 1970, pp. 69–87.
- [Edw70] Anthony W. F. Edwards. „Estimation of the Branch Points of a Branching Diffusion Process.“ In: *J. R. Stat. Soc., Ser. B, Methodol.* 32.2 (1970), pp. 155–164. ISSN: 1369-7412. DOI: [10.1111/j.2517-6161.1970.tb00828.x](https://doi.org/10.1111/j.2517-6161.1970.tb00828.x).
- [EH19] Laura Escobar and Megumi Harada. *Wall-crossing for Newton-Okounkov bodies and the tropical Grassmannian*. 2019. arXiv: [1912.04809](https://arxiv.org/abs/1912.04809).
- [Ein+06] Lawrence Ein, Robert K. Lazarsfeld, Mircea Mustață, Michael Nakamaye, and Mihnea Popa. „Asymptotic invariants of base loci.“ In: *Ann. inst. Fourier* 56.6 (2006), pp. 1701–1734. ISSN: 0373-0956. DOI: [10.5802/aif.2225](https://doi.org/10.5802/aif.2225).
- [FH13] Georges Francois and Simon Hampe. „Universal Families of Rational Tropical Curves.“ In: *Canad. J. Math.* 65.1 (2013), pp. 120–148. ISSN: 0008-414X. DOI: [10.4153/CJM-2011-097-0](https://doi.org/10.4153/CJM-2011-097-0).
- [Fin83] Jonathan Fine. „Resolution and completion of algebraic varieties.“ PhD thesis. University of Warwick, 1983. URL: <http://wrap.warwick.ac.uk/114676/> (visited on 11/24/2020).
- [Fis23] Ronald A. Fisher. „XXI.—On the Dominance Ratio.“ In: *Proc. R. Soc. Edinb.* 42 (1923), pp. 321–341. ISSN: 0370-1646. DOI: [10.1017/S0370164600023993](https://doi.org/10.1017/S0370164600023993).
- [Fuj16] Kento Fujita. „On K-stability and the volume functions of \mathbb{Q} -Fano varieties.“ In: *Proc. London Math. Soc.* 113.5 (2016), pp. 541–582. ISSN: 0024-6115. DOI: [10.1112/plms/pdw037](https://doi.org/10.1112/plms/pdw037).
- [Fuj79] Takao Fujita. „On Zariski problem.“ In: *Proc. Japan Acad., Ser. A* 55.3 (1979), pp. 106–110. ISSN: 0386-2194. DOI: [10.3792/pjaa.55.106](https://doi.org/10.3792/pjaa.55.106).
- [Ful71] Delbert R. Fulkerson. „Blocking and anti-blocking pairs of polyhedra.“ In: *Math. Program.* 1.1 (1971), pp. 168–194. ISSN: 0025-5610. DOI: [10.1007/BF01584085](https://doi.org/10.1007/BF01584085).
- [Ful72] Delbert R. Fulkerson. „Anti-blocking polyhedra.“ In: *J. Comb. Theory, Ser. B* 12.1 (1972), pp. 50–71. ISSN: 0095-8956. DOI: [10.1016/0095-8956\(72\)90032-9](https://doi.org/10.1016/0095-8956(72)90032-9).
- [Ful93] William Fulton. *Introduction to toric varieties*. Princeton, NJ: Princeton University Press, 1993. ISBN: 978-0-691-00049-7.

- [GK13] Concettina Galati and Andreas L. Knutsen. „Seshadri Constants of K_3 Surfaces of Degrees 6 and 8.“ In: *Int. Math. Res. Not.* 2013.17 (2013), pp. 4072–4084. ISSN: 1073-7928. DOI: [10.1093/imrn/rns174](https://doi.org/10.1093/imrn/rns174).
- [GM10] Angela Gibney and Diane Maclagan. „Equations for Chow and Hilbert quotients.“ In: *Algebr. Number Theory* 4.7 (2010), pp. 855–885. ISSN: 1937-0652. DOI: [10.2140/ant.2010.4.855](https://doi.org/10.2140/ant.2010.4.855).
- [Har77] Robin Hartshorne. *Algebraic Geometry*. New York, NY: Springer, 1977. ISBN: 978-1-4419-2807-8. DOI: [10.1007/978-1-4757-3849-0](https://doi.org/10.1007/978-1-4757-3849-0).
- [HHK16] Mark Hamilton, Megumi Harada, and Kiumars Kaveh. *Convergence of polarizations, toric degenerations, and Newton-Okounkov bodies*. 2016. arXiv: [1612.08981](https://arxiv.org/abs/1612.08981).
- [HK15] Megumi Harada and Kiumars Kaveh. „Integrable systems, toric degenerations and Okounkov bodies.“ In: *Inventiones Math.* 202.3 (2015), pp. 927–985. ISSN: 0020-9910. DOI: [10.1007/s00222-014-0574-4](https://doi.org/10.1007/s00222-014-0574-4).
- [HKW20] Christian Haase, Alex Küronya, and Lena Walter. *Toric Newton-Okounkov functions with an application to the rationality of certain Seshadri constants on surfaces*. 2020. arXiv: [2008.04018](https://arxiv.org/abs/2008.04018).
- [HNP12] Christian Haase, Benjamin Nill, and Andreas Paffenholz. *Lecture Notes on Lattice Polytopes: (preliminary version of December 7, 2012): Fall School on Polyhedral Combinatorics, TU Darmstadt*. 2012. URL: https://polymake.org/polytopes/paffenholz/data/preprints/ln_lattice_polytopes.pdf (visited on 11/24/2020).
- [HRS00] Birkett Huber, Jörg Rambau, and Francisco Santos. „The Cayley Trick, lifting subdivisions and the Bohne-Dress theorem on zonotopal tilings.“ In: *J. Eur. Math. Soc.* 2.2 (2000), pp. 179–198. ISSN: 1435-9855. DOI: [10.1007/s100970050003](https://doi.org/10.1007/s100970050003).
- [HS95] Birkett Huber and Bernd Sturmfels. „A polyhedral method for solving sparse polynomial systems.“ In: *Math. Comp.* 64.212 (1995), pp. 1541–1555. ISSN: 0025-5718. DOI: [10.2307/2153370](https://doi.org/10.2307/2153370).
- [Ito13] Atsushi Ito. „Okounkov bodies and Seshadri constants.“ In: *Adv. Math.* 241 (2013), pp. 246–262. ISSN: 0001-8708. DOI: [10.1016/j.aim.2013.04.005](https://doi.org/10.1016/j.aim.2013.04.005).
- [Ito14] Atsushi Ito. „Seshadri constants via toric degenerations.“ In: *J. Reine Angew. Math.* 695 (2014), pp. 151–174. ISSN: 0075-4102. DOI: [10.1515/crelle-2012-0116](https://doi.org/10.1515/crelle-2012-0116).
- [Jen16] Anders N. Jensen. *Tropical Homotopy Continuation*. 2016. arXiv: [1601.02818](https://arxiv.org/abs/1601.02818).

BIBLIOGRAPHY

- [Kin82a] John F. C. Kingman. „Exchangeability and the Evolution of Large Populations.“ In: *Exchangeability in Probability and Statistics*. Ed. by Giorgio Koch and Fabio Spizzichino. Amsterdam: North-Holland Elsevier, 1982, pp. 97–112. ISBN: 978-0-444-86403-1.
- [Kin82b] John F. C. Kingman. „On the genealogy of large populations.“ In: *J. Appl. Prob.* 19.A (1982), pp. 27–43. ISSN: 0021-9002. DOI: [10.2307/3213548](https://doi.org/10.2307/3213548).
- [Kin82c] John F. C. Kingman. „The coalescent.“ In: *Stoch. Proc. Appl.* 13.3 (1982), pp. 235–248. ISSN: 0304-4149. DOI: [10.1016/0304-4149\(82\)90011-4](https://doi.org/10.1016/0304-4149(82)90011-4).
- [KK12] Kiumars Kaveh and Askold G. Khovanskii. „Newton-Okounkov bodies, semigroups of integral points, graded algebras and intersection theory.“ In: *Ann. Math. (2)* 176.2 (2012), pp. 925–978. ISSN: 0003-486X. DOI: [10.4007/annals.2012.176.2.5](https://doi.org/10.4007/annals.2012.176.2.5).
- [KL17a] Alex Küronya and Victor Lozovanu. „Infinitesimal Newton–Okounkov bodies and jet separation.“ In: *Duke Math. J.* 166.7 (2017), pp. 1349–1376. ISSN: 0012-7094. DOI: [10.1215/00127094-0000002X](https://doi.org/10.1215/00127094-0000002X).
- [KL17b] Alex Küronya and Victor Lozovanu. „Positivity of Line Bundles and Newton-Okounkov Bodies.“ In: *Doc. Math.* 22 (2017), pp. 1285–1302. ISSN: 1431-0635. DOI: [10.25537/DM.2017V22.1285-1302](https://doi.org/10.25537/DM.2017V22.1285-1302).
- [KL18] Alex Küronya and Victor Lozovanu. „Geometric aspects of Newton–Okounkov bodies.“ In: *Banach Center Publ.* 116 (2018), pp. 137–212. ISSN: 0137-6934. DOI: [10.4064/bc116-7](https://doi.org/10.4064/bc116-7).
- [KLM12] Alex Küronya, Victor Lozovanu, and Catriona Maclean. „Convex bodies appearing as Okounkov bodies of divisors.“ In: *Adv. Math.* 229.5 (2012), pp. 2622–2639. ISSN: 0001-8708. DOI: [10.1016/j.aim.2012.01.013](https://doi.org/10.1016/j.aim.2012.01.013).
- [KM19] Kiumars Kaveh and Christopher Manon. „Khovanskii Bases, Higher Rank Valuations, and Tropical Geometry.“ In: *SIAM J. Appl. Algebra Geometry* 3.2 (2019), pp. 292–336. DOI: [10.1137/17M1160148](https://doi.org/10.1137/17M1160148).
- [KMM87] Yujiro Kawamata, Katsumi Matsuda, and Kenji Matsuki. „Introduction to the Minimal Model Problem.“ In: *Algebraic Geometry, Sendai, 1985*. Ed. by Tadao Oda. Advanced Studies in Pure Mathematics. Tokyo, Japan: Mathematical Society of Japan, 1987, pp. 283–360. DOI: [10.2969/aspm/01010283](https://doi.org/10.2969/aspm/01010283).
- [KMR19] Alex Küronya, Catriona Maclean, and Joaquim Roé. *Concave transforms of filtrations and rationality of Seshadri constants*. 2019. arXiv: [1901.00384](https://arxiv.org/abs/1901.00384).
- [KMS13] Alex Küronya, Catriona Maclean, and Tomasz Szemberg. *Functions on Okounkov bodies coming from geometric valuations (with an appendix by Sébastien Boucksom)*. 2013. arXiv: [1210.3523](https://arxiv.org/abs/1210.3523).

- [Knu08] Andreas L. Knutsen. „A Note on Seshadri constants on general K_3 surfaces.“ In: *C. R. Acad. Sci. Paris, Ser. 1* 346.19-20 (2008), pp. 1079–1081. ISSN: 1631-073X. DOI: [10.1016/j.crma.2008.09.008](https://doi.org/10.1016/j.crma.2008.09.008).
- [Lai17] Pierre Lairez. „A Deterministic Algorithm to Compute Approximate Roots of Polynomial Systems in Polynomial Average Time.“ In: *Found. Comput. Math.* 17.5 (2017), pp. 1265–1292. ISSN: 1615-3375. DOI: [10.1007/s10208-016-9319-7](https://doi.org/10.1007/s10208-016-9319-7).
- [Lazo4] Robert K. Lazarsfeld. *Positivity in Algebraic Geometry I: Classical Setting: Line Bundles and Linear Series*. Berlin: Springer, 2004. ISBN: 978-3-540-22533-1.
- [Lin+17] Bo Lin, Bernd Sturmfels, Xiaoxian Tang, and Ruriko Yoshida. „Convexity in tree spaces.“ In: *SIAM J. Discrete Math.* 31.3 (2017), pp. 2015–2038. ISSN: 0895-4801. DOI: [10.1137/16M1079841](https://doi.org/10.1137/16M1079841).
- [Liu+09] Liang Liu, Lili Yu, Laura Kubatko, Dennis K. Pearl, and Scott V. Edwards. „Coalescent methods for estimating phylogenetic trees.“ In: *Mol. Phylogenet. Evol.* 53.1 (2009), pp. 320–328. ISSN: 1055-7903. DOI: [10.1016/j.ympev.2009.05.033](https://doi.org/10.1016/j.ympev.2009.05.033).
- [LM09] Robert K. Lazarsfeld and Mircea Mustață. „Convex bodies associated to linear series.“ In: *Ann. Sci. Éc. Norm. Supér. (4)* 42.5 (2009), pp. 783–835. ISSN: 0012-9593. DOI: [10.24033/asens.2109](https://doi.org/10.24033/asens.2109).
- [LRS10] Jesús A. de Loera, Jörg Rambau, and Francisco Santos. *Triangulations: Structures for algorithms and applications*. Berlin: Springer, 2010. ISBN: 978-3-642-12970-4. DOI: [10.1007/978-3-642-12971-1](https://doi.org/10.1007/978-3-642-12971-1).
- [Lun20] Anders Lundman. „Computing Seshadri constants on smooth toric surfaces.“ In: *Interactions with Lattice Polytopes*. Ed. by Alexander M. Kasprzyk and Benjamin Nill. Springer, 2020 (in press).
- [Mad97] Wayne P. Maddison. „Gene Trees in Species Trees.“ In: *Syst. Biol.* 46.3 (1997), pp. 523–536. ISSN: 1063-5157. DOI: [10.1093/SYSBIO/46.3.523](https://doi.org/10.1093/SYSBIO/46.3.523).
- [Mal17] Gregorio Malajovich. „Computing Mixed Volume and All Mixed Cells in Quermassintegral Time.“ In: *Found. Comput. Math.* 17.5 (2017), pp. 1293–1334. ISSN: 1615-3375. DOI: [10.1007/s10208-016-9320-1](https://doi.org/10.1007/s10208-016-9320-1).
- [Mal19] Gregorio Malajovich. „Complexity of Sparse Polynomial Solving: Homotopy on Toric Varieties and the Condition Metric.“ In: *Found. Comput. Math.* 19.1 (2019), pp. 1–53. ISSN: 1615-3375. DOI: [10.1007/s10208-018-9375-2](https://doi.org/10.1007/s10208-018-9375-2).
- [Mal20] Gregorio Malajovich. *Complexity of Sparse Polynomial Solving 2: Renormalization*. 2020. arXiv: [2005.01223](https://arxiv.org/abs/2005.01223).

BIBLIOGRAPHY

- [MCoo] Tom Michiels and Ronald Cools. „Decomposing the Secondary Cayley Polytope.“ In: *Discrete Comput. Geom.* 23.3 (2000), pp. 367–380. ISSN: 0179-5376. DOI: [10.1007/PL00009506](https://doi.org/10.1007/PL00009506).
- [Mon+20] Anthea Monod, Bo Lin, Ruriko Yoshida, and Qiwen Kang. *Tropical Geometry of Phylogenetic Tree Space: A Statistical Perspective*. 2020. arXiv: [1805.12400](https://arxiv.org/abs/1805.12400).
- [MR15] David McKinnon and Mike Roth. „Seshadri constants, diophantine approximation, and Roth’s theorem for arbitrary varieties.“ In: *Inventiones Math.* 200.2 (2015), pp. 513–583. ISSN: 0020-9910. DOI: [10.1007/s00222-014-0540-1](https://doi.org/10.1007/s00222-014-0540-1).
- [MS01] Martin Möhle and Serik Sagitov. „A Classification of Coalescent Processes for Haploid Exchangeable Population Models.“ In: *Ann. Probab.* 29.4 (2001), pp. 1547–1562. ISSN: 0091-1798. DOI: [10.1214/aop/1015345761](https://doi.org/10.1214/aop/1015345761).
- [MS15] Diane Maclagan and Bernd Sturmfels. *Introduction to tropical geometry*. Providence, RI: American Mathematical Society, 2015. ISBN: 978-0-8218-5198-2.
- [Nei87] Masatoshi Nei. *Molecular evolutionary genetics*. New York, NY: Columbia University Press, 1987. ISBN: 978-0-231-06321-0.
- [Nye+17] Tom M. W. Nye, Xiaoxian Tang, Grady Weyenberg, and Ruriko Yoshida. „Principal component analysis and the locus of the Fréchet mean in the space of phylogenetic trees.“ In: *Biometrika* 104.4 (2017), pp. 901–922. ISSN: 0006-3444. DOI: [10.1093/biomet/asx047](https://doi.org/10.1093/biomet/asx047).
- [Ok096] Andrei Okounkov. „Brunn-Minkowski inequality for multiplicities.“ In: *Inventiones Math.* 125.3 (1996), pp. 405–411. ISSN: 0020-9910. DOI: [10.1007/s002220050081](https://doi.org/10.1007/s002220050081).
- [Oxl11] James G. Oxley. *Matroid theory*. 2nd ed. Oxford: Oxford University Press, 2011. ISBN: 978-0-19-960339-8. DOI: [10.1093/acprof:oso/9780198566946.001.0001](https://doi.org/10.1093/acprof:oso/9780198566946.001.0001).
- [PN88] Pekka Pamilo and Masatoshi Nei. „Relationships between Gene Trees and Species Trees.“ In: *Mol. Biol. Evol.* 5.5 (1988), pp. 568–583. ISSN: 0737-4038. DOI: [10.1093/oxfordjournals.molbev.a040517](https://doi.org/10.1093/oxfordjournals.molbev.a040517).
- [PS05] Lior Pachter and Bernd Sturmfels. „Biology.“ In: *Algebraic statistics for computational biology*. Ed. by Lior Pachter and Bernd Sturmfels. Cambridge: Cambridge University Press, 2005, pp. 125–160. ISBN: 9780511610684. DOI: [10.1017/CBO9780511610684.007](https://doi.org/10.1017/CBO9780511610684.007).
- [Roé16] Joaquim Roé. „Local positivity in terms of Newton-Okounkov bodies.“ In: *Adv. Math.* 301 (2016), pp. 486–498. ISSN: 0001-8708. DOI: [10.1016/j.aim.2016.05.028](https://doi.org/10.1016/j.aim.2016.05.028).

- [Ros02] Noah A. Rosenberg. „The Probability of Topological Concordance of Gene Trees and Species Trees.“ In: *Theor. Popul. Biol.* 61.2 (2002), pp. 225–247. ISSN: 0040-5809. DOI: [10.1006/tpbi.2001.1568](https://doi.org/10.1006/tpbi.2001.1568).
- [RY03] Bruce Rannala and Ziheng Yang. „Bayes estimation of species divergence times and ancestral population sizes using DNA sequences from multiple loci.“ In: *Genetics* 164.4 (2003), pp. 1645–1656. ISSN: 0016-6731.
- [San14] Taro Sano. „Seshadri constants on rational surfaces with anticanonical pencils.“ In: *J. Pure Appl. Algebra* 218.4 (2014), pp. 602–617. ISSN: 0022-4049. DOI: [10.1016/j.jpaa.2013.07.007](https://doi.org/10.1016/j.jpaa.2013.07.007).
- [Sma98] Steve Smale. „Mathematical problems for the next century.“ In: *Math. Intelligencer* 20.2 (1998), pp. 7–15. ISSN: 0343-6993. DOI: [10.1007/BF03025291](https://doi.org/10.1007/BF03025291).
- [Smi+04] Karen E. Smith, Lauri Kahanpää, Pekka Kekäläinen, and William Traves. *An Invitation to Algebraic Geometry*. New York, NY: Springer, 2004. ISBN: 978-1-4419-3195-5. DOI: [10.1007/978-1-4419-3195-5](https://doi.org/10.1007/978-1-4419-3195-5).
- [SS03] Charles Semple and Mike Steel. *Phylogenetics*. Oxford: Oxford University Press, 2003. ISBN: 978-0-19-850942-4.
- [SS04] David Speyer and Bernd Sturmfels. „The tropical Grassmannian.“ In: *Adv. Geom.* 4.3 (2004), pp. 389–411. ISSN: 1615-715X. DOI: [10.1515/advgeom.2004.023](https://doi.org/10.1515/advgeom.2004.023).
- [SS93] Michael Shub and Steve Smale. „Complexity of Bezout’s Theorem I: Geometric Aspects.“ In: *J. Amer. Math. Soc.* 6.2 (1993), pp. 459–501. ISSN: 0894-0347. DOI: [10.2307/2152805](https://doi.org/10.2307/2152805).
- [Sta86] Richard P. Stanley. „Two poset polytopes.“ In: *Discrete Comput. Geom.* 1.1 (1986), pp. 9–23. ISSN: 0179-5376. DOI: [10.1007/BF02187680](https://doi.org/10.1007/BF02187680).
- [Stu02] Bernd Sturmfels. *Solving Systems of Polynomial Equations*. Providence, RI: American Mathematical Society, 2002. ISBN: 978-0-8218-3251-6. DOI: [10.1090/cbms/097](https://doi.org/10.1090/cbms/097).
- [Sze01] Tomasz Szemberg. „On positivity of line bundles on Enriques surfaces.“ In: *Trans. Am. Math. Soc.* 353.12 (2001), pp. 4963–4972. ISSN: 0002-9947. DOI: [10.1090/S0002-9947-01-02788-X](https://doi.org/10.1090/S0002-9947-01-02788-X).
- [Sze12] Tomasz Szemberg. „Bounds on Seshadri Constants on Surfaces with Picard Number 1.“ In: *Commun. Algebra* 40.7 (2012), pp. 2477–2484. ISSN: 0092-7872. DOI: [10.1080/00927872.2011.579589](https://doi.org/10.1080/00927872.2011.579589).
- [Tak89] Naoyuki Takahata. „Gene genealogy in three related populations: consistency probability between gene and population trees.“ In: *Genetics* 122.4 (1989), pp. 957–966. ISSN: 0016-6731.

BIBLIOGRAPHY

- [Tav84] Simon Tavaré. „Line-of-Descent and Genealogical Processes, and Their Applications in Population Genetics Models.“ In: *Theor. Popul. Biol.* 26.2 (1984), pp. 119–164. ISSN: 0040-5809. DOI: [10.1016/0040-5809\(84\)90027-3](https://doi.org/10.1016/0040-5809(84)90027-3).
- [Tev07] Jenia Tevelev. „Compactifications of subvarieties of tori.“ In: *Amer. J. Math.* 129.4 (2007), pp. 1087–1104. ISSN: 0002-9327. DOI: [10.1353/ajm.2007.0029](https://doi.org/10.1353/ajm.2007.0029).
- [VVC94] Jan Verschelde, Pierre Verlinden, and Ronald Cools. „Homotopies Exploiting Newton Polytopes for Solving Sparse Polynomial Systems.“ In: *SIAM J. Numer. Anal.* 31.3 (1994), pp. 915–930. ISSN: 0036-1429. DOI: [10.1137/0731049](https://doi.org/10.1137/0731049).
- [Wak09] John Wakeley. *Coalescent Theory: An Introduction*. Greenwood Village, CO: Roberts & Company, 2009. ISBN: 978-0-9747077-5-4.
- [Wit12] David Witt Nyström. „Test configurations and Okounkov bodies.“ In: *Compos. Math.* 148.6 (2012), pp. 1736–1756. ISSN: 0010-437X. DOI: [10.1112/S0010437X12000358](https://doi.org/10.1112/S0010437X12000358).
- [Wit14] David Witt Nyström. „Transforming metrics on a line bundle to the Okounkov body.“ In: *Ann. Sci. Éc. Norm. Supér. (4)* 47.6 (2014), pp. 1111–1161. ISSN: 0012-9593. DOI: [10.24033/asens.2235](https://doi.org/10.24033/asens.2235).
- [Wri31] Sewall Wright. „Evolution in Mendelian Populations.“ In: *Genetics* 16.2 (1931), pp. 97–159. ISSN: 0016-6731.
- [Yan14] Ziheng Yang. *Molecular evolution: A statistical approach*. Oxford: Oxford University Press, 2014. ISBN: 978-0-19-960260-5.
- [Zar62] Oscar Zariski. „The Theorem of Riemann-Roch for High Multiples of an Effective Divisor on an Algebraic Surface.“ In: *Ann. Math. (2)* 76.3 (1962), pp. 560–615. ISSN: 0003-486X. DOI: [10.2307/1970376](https://doi.org/10.2307/1970376).
- [Zie95] Günter M. Ziegler. *Lectures on Polytopes*. New York, NY: Springer, 1995. ISBN: 978-0-387-94365-7. DOI: [10.1007/978-1-4613-8431-1](https://doi.org/10.1007/978-1-4613-8431-1).

LIST OF FIGURES

| | | |
|-------------|---|----|
| Figure 2.1 | The fan Σ of the first Hirzebruch surface $X_\Sigma = \mathcal{H}_1$ | 18 |
| Figure 2.2 | The polytope P_D with the monomials corresponding to its lattice points. | 19 |
| Figure 2.3 | The Newton–Okounkov body $\Delta_{Y_\bullet}(D)$ for the choice $Y_1 = \overline{\{xy^{-2} - 1 = 0\}}$ | 24 |
| Figure 2.4 | Adjacent rays $\rho_0, \dots, \rho_{k+1}$ of the prime divisors C_0, \dots, C_{k+1} | 30 |
| Figure 2.5 | Moving a copy of P_D in the direction of v to obtain $P_D \cap (P_D + tv) = P_{(D-tC)+}$ | 33 |
| Figure 2.6 | The mixed volume $MV(P_D \cap (P_D + t \cdot (0, -1)), \text{NP}(y^{-1} - 1))$ | 34 |
| Figure 2.7 | The Newton–Okounkov body $\Delta_{Y_\bullet}(D)$ | 34 |
| Figure 2.8 | Break points p_1, p_2 , and p_3 of shifting the sunny side sun(P_D, v) through P_D in the direction of v | 35 |
| Figure 2.9 | The chamber structure on P_D induced by the shifting process. | 35 |
| Figure 2.10 | Tilting the polytope P_D leftwards via the map Ψ_{left} | 36 |
| Figure 2.11 | Tilting the polytope $\Psi_{\text{left}}(P_D)$ downwards via the map Ψ_{down} | 37 |
| Figure 2.12 | The feasible region in P with respect to v and u , given $m \in P$ | 38 |
| Figure 2.13 | Star subdivision of the fan Σ relative to τ | 41 |
| Figure 2.14 | Values of the Newton–Okounkov function φ_Z associated to the distance to m_τ | 41 |
| Figure 2.15 | The fan Σ of the projective line $X = \mathbb{P}^1$ | 43 |
| Figure 2.16 | The fan $\Sigma \times D$ | 44 |
| Figure 2.17 | The fan $\hat{\Sigma}$ of $\mathbb{P}_{\mathbb{P}^1}(\mathcal{O}_{\mathbb{P}^1} \oplus \mathcal{O}_{\mathbb{P}^1}(1))$ | 45 |
| Figure 2.18 | The polytope $P_{\pi^*D+tX_\infty}$ for small t on the left and for $t = b$ on the right. | 48 |
| Figure 2.19 | Admissible region H^+ of rescaled exponent vectors associated to monomials of s inside the Newton–Okounkov body $\Delta_{Y_\bullet}(D)$ | 50 |
| Figure 2.20 | A non-empty region of points $(c, d) \in H^+$ that satisfy $c \geq a$ and $d \geq b$ forcing H to have positive slope. | 50 |
| Figure 2.21 | The scaled Newton polytope $\frac{1}{k} \text{NP}(s)$ of the section $s(x, y) = (x - 1)^{ka}(y - 1)^{kb}$ | 51 |
| Figure 2.22 | The coordinate system associated to the vertex p which lies at the opposite side of P_D with respect to the flag Y_\bullet | 52 |
| Figure 2.23 | Newton polytopes $\frac{1}{k} \text{NP}(s)$ of the respective sections s | 55 |
| Figure 2.24 | The values of the function φ on $\Delta_{Y_\bullet}(D)$ | 56 |
| Figure 2.25 | The values of the function φ' on $\Delta_{Y'_\bullet}(D)$ | 56 |

LIST OF FIGURES

| | | |
|-------------|---|----|
| Figure 2.26 | $SL_3(\mathbb{Q})$ -equidecomposable pieces of the Newton–Okounkov bodies $\Delta_{Y_\bullet}(D)$ on the left and $\Delta_{Y'_\bullet}(D)$ on the right. | 57 |
| Figure 2.27 | An instance of a centrally-symmetric polytope P that is not zonotopally well-covered. | 59 |
| Figure 2.28 | A polygon for which our approach does not work. | 60 |
| Figure 2.29 | The fan Σ with prime divisors E_1, \dots, E_{23} | 60 |
| Figure 2.30 | Local toric coordinates x, y for the Newton–Okounkov body $\Delta_{Y_\bullet}(D)$ | 60 |
| Figure 2.31 | Newton polytopes $\frac{1}{k} NP(s)$ of the respective sections s inside $\Delta_{Y_\bullet}(D)$ | 61 |
| Figure 2.32 | The values of the function φ on the Newton–Okounkov body $\Delta_{Y_\bullet}(D)$ | 62 |
| Figure 2.33 | The Newton–Okounkov body $\Delta_{Y'_\bullet}(D)$ | 64 |
| Figure 2.34 | The values of the function φ' on the Newton–Okounkov body $\Delta_{Y'_\bullet}(D)$ | 64 |
| Figure 2.35 | The fan Σ with associated torus-invariant prime divisors D_0, \dots, D_{15} | 69 |
| Figure 2.36 | The Newton–Okounkov body $\Delta_{Y_\bullet}(D) \cong P_D$ with $\text{core}(P_D)$ highlighted. | 70 |
| Figure 2.37 | The Newton–Okounkov body $\Delta_{Y'_\bullet}(D)$ with respective values of φ'_R | 70 |
| Figure 2.38 | Expected domains of linearity of the function φ_R on the Newton–Okounkov body $\Delta_{Y_\bullet}(D)$ | 71 |
| Figure 2.39 | The Newton polytope $NP(s)$ of the section $s(x, y) = x^3y^2 - 3xy + y + 1$ | 72 |
| Figure 2.40 | The values of φ on the Newton–Okounkov body $\Delta_{Y_\bullet}(D)$ | 72 |
| Figure 2.41 | The setup of the proof of Theorem 2.5.13 in the context of Example 2.5.10. | 74 |
| Figure 2.42 | Core versus Fine core. | 75 |
| Figure 2.43 | Examples of wide polygons $\Delta^{(d)}$ with small area for $d = 1, 2, 3$ | 76 |
| Figure 2.44 | Resolving $\Delta^{(1)}$, eliminating anti-canonical sections, and ensuring that the core is a point. | 76 |
| Figure 3.1 | Darwin’s tree of life. | 79 |
| Figure 3.2 | The Fisher–Wright model with $n = 4$ | 81 |
| Figure 3.3 | All 15 tree topologies of 4-trees. | 83 |
| Figure 3.4 | Two 4-trees T and T' of the same tree topology, but different ranked tree topology. | 84 |
| Figure 3.5 | The (ranked) tree topologies of 3-trees. | 90 |
| Figure 3.6 | Full- and lower-dimensional cones in the space MUM_3 | 90 |
| Figure 3.7 | The tree topology cone $\sigma_{((a,b),(c,d))}$ triangulated into two unimodular ranked tree topology cones $\sigma_{((a,b)_1,(c,d)_2)}$ (green) and $\sigma_{((a,b)_2,(c,d)_1)}$ (blue). | 94 |

| | | |
|-------------|---|-----|
| Figure 3.8 | The different ways to insert an n -th leaf to obtain a tree T in the preimage $\Phi_n^{-1}(\hat{T})$ | 99 |
| Figure 3.9 | Adding an n -th external branch within the k -th time interval. . | 100 |
| Figure 3.10 | The 4-tree \hat{T} and the resulting 5-tree T after attaching an additional external branch during the third time interval. | 101 |
| Figure 3.11 | A species tree T_S with specification times τ_S | 103 |
| Figure 3.12 | Non-matching species and gene tree topologies resulting from incomplete lineage sorting. | 104 |
| Figure 3.13 | Coalescent histories h_2 and h_3 | 108 |
| Figure 3.14 | Waiting times $t_j^{(S)}$ within the species $S \in \mathfrak{S}$ | 112 |
| Figure 4.1 | A regular subdivision of a line segment. | 118 |
| Figure 4.2 | The Minkowski sum of a square and a triangle. | 118 |
| Figure 4.3 | A regular mixed subdivision of the Minkowski sum of a square and a triangle. | 119 |
| Figure 4.4 | The Cayley embedding of a square and a triangle. | 120 |
| Figure 4.5 | The connection between the Cayley embedding and the Minkowski sum. | 121 |
| Figure 4.6 | The correspondence between Minkowski cells and Cayley cells. | 121 |
| Figure 4.7 | The combinatorics of the secondary polytope of five points on a line. | 123 |
| Figure 4.8 | Fine mixed subdivisions of the Minkowski sum of triangle and square. | 124 |
| Figure 4.9 | A signed circuit $c = (c_+, c_-)$ | 124 |
| Figure 4.10 | Some flips in the plane. | 125 |
| Figure 4.11 | Wall-crossing for a homotopy continuation in the secondary fan with start system $\bar{\omega}$ and target system ω | 127 |
| Figure 4.12 | Point configurations on the moment curve for $n = 4$ and $m = 4$. | 128 |

LIST OF TABLES

| | | |
|-----------|--|-----|
| Table 2.1 | Global sections of $\mathcal{O}_X(D)$ that realize lower bounds for the order of vanishing ord_R | 71 |
| Table A.1 | Sections s such that s^k are global sections of $H^0(X, \mathcal{O}_X(kD))$ that realize lower bounds for the order of vanishing ord_R for respective $k \in \mathbb{Z}_{\geq 1}$ | 135 |

ZUSAMMENFASSUNG

Die vorliegende Dissertation beschäftigt sich mit der Untersuchung von Problemstellungen aus der torischen und numerischen algebraischen Geometrie, sowie der mathematischen Populationsgenetik aus dem Blickwinkel der diskreten Geometrie.

Das einleitende Kapitel 1 enthält eine kurze Zusammenfassung der Ergebnisse. Des Weiteren führen wir die Objekte aus der diskreten Geometrie ein, die im Folgenden eine zentrale Rolle spielen und fixieren die entsprechende Notation.

Kapitel 2 widmet sich der Untersuchung von Newton–Okounkov–Körpern und Newton–Okounkov–Funktionen. Wir betrachten den Fall torischer Varietäten. Zunächst geben wir einen kombinatorischen Beweis für die Existenz und Eindeutigkeit der Zariski–Zerlegung auf torischen Flächen. Darauf aufbauend konstruieren wir einen Isomorphismus zwischen dem zu einem torusinvarianten Divisor gehörigen Polytop und dem Newton–Okounkov–Körper einer nichttorischen Fahne. Anschließend geben wir eine explizite Beschreibung von Newton–Okounkov–Funktionen im vollständig torischen Fall und einen Ansatz für die Bestimmung von Funktionen, die von Bewertungen im allgemeinen Punkt kommen. Wir formulieren kombinatorische Kriterien an die involvierten Polytope und beweisen, dass sich in diesen Fällen die Funktion mithilfe unseres Ansatzes vollständig beschreiben lässt. Die entwickelten Techniken lassen sich anwenden, um die Rationalität gewisser Seshadri–Konstanten zu beweisen. Wir erläutern den Zusammenhang und zeigen Rationalität in Abhängigkeit von einer kombinatorischen Bedingung. Darüber hinaus konstruieren wir eine Klasse von Beispielen, für die bisherige Kriterien nicht greifen und zeigen Rationalität in diesen Fällen.

Im Rahmen von Kapitel 3 beschäftigen wir uns mit Modellen aus der mathematischen Populationsgenetik und ihrer Beschreibung in polyedrischer Sprache. Zunächst definieren wir verschiedene Räume von phylogenetischen Bäumen und definieren darauf den Kingman– n –Koaleszent–Prozess in Form einer entsprechenden Dichte. Darauf aufbauend definieren wir eine Vergissabbildung für variierende Stichprobengröße und zeigen, wie sich die entsprechende Dichte davon ableiten lässt. Wir betrachten schließlich den Multispezies–Koaleszent–Prozess und beschreiben auch diesen in polyedrischer Sprache. Insbesondere beweisen wir, wie sich die bedingte Wahrscheinlichkeit des Auftretens eines bestimmten Genbaumes, gegeben ein Speziesbaum, in Form einer Dichte auf unserem Raum von phylogenetischen Bäumen beschreiben lässt.

Im Fokus von Kapitel 4 steht die Untersuchung der tropischen Version von Smales berühmtem 17. Problem. Die ursprüngliche Fragestellung, ob es möglich ist, zu n gegebenen Polynomen in n Unbekannten in erwarteter polynomieller Zeit eine gemeinsame Lösung zu finden, übersetzt sich in ein Problem aus der diskreten Geometrie: das Finden einer vollständig gemischten Zelle in einer, von den randomisierten Inputdaten induzierten, Triangulierung eines Cayleypolytops. Wir erläutern diese Variante der Fragestellung und untersuchen darauf aufbauend einen Ansatz zur Lösung mittels eines Homotopieverfahrens. Insbesondere geben wir ein Beispiel, das zu einer unteren Schranke führen kann, die exponentiell in den Eingabedaten ist.

ABSTRACT

The present dissertation is concerned with the study of problems from toric and numerical algebraic geometry, as well as mathematical population genetics from the perspective of discrete geometry. The introductory Chapter 1 contains a short summary of the results. Furthermore, we introduce the objects stemming from discrete geometry which play a central role in the following, and fix the corresponding notation.

Chapter 2 is devoted to the examination of Newton–Okounkov bodies and Newton–Okounkov functions. We consider the case of toric varieties. First, we give a combinatorial proof for the existence and uniqueness of Zariski decomposition on toric surfaces. Based on this, we construct an isomorphism between the polytope associated to a torus-invariant divisor and the Newton–Okounkov body of a non-toric flag. Subsequently, we give an explicit description of Newton–Okounkov functions in the completely toric case and an approach to determining functions coming from valuations in a general point. We formulate combinatorial criteria on the polytopes involved and prove that in these cases the function can be fully described using our approach. The developed techniques can be applied to prove the rationality of certain Seshadri constants. We explain the connection and show rationality as a dependency of a combinatorial condition. Furthermore, we construct a class of examples to which existing criteria do not apply, and show rationality in these cases.

In Chapter 3, we deal with models from mathematical population genetics and their description in polyhedral language. First, we define different spaces of phylogenetic trees and then define the Kingman n -coalescent process in terms of a suitable density. Based on this, we define a forgetful map for varying sample sizes and show how the corresponding density can be derived from it. Finally, we consider the multispecies coalescent process and describe it in polyhedral language. In particular, we show how the conditional probability of the occurrence of a certain gene tree, given a species tree, can be described in terms of a density on our space of phylogenetic trees.

The focus of Chapter 4 is the investigation of the tropical version of Smale’s famous 17th problem. The original question, whether it is possible to find a common solution of n given polynomials in n unknowns in expected polynomial time, translates into a problem from discrete geometry: finding a fully mixed cell in a triangulation of a Cayley polytope induced by the randomized input data. We explain this version of the problem and, based on it, analyze an approach to solving it by means of a homotopy continuation. In particular, we give an example that could lead to a lower bound in the input data that is exponential.

SELBSTSTÄNDIGKEITSERKLÄRUNG

Ich erkläre gegenüber der Freien Universität Berlin, dass ich die vorliegende Dissertation selbstständig und ohne Benutzung anderer als der angegebenen Quellen und Hilfsmittel angefertigt habe. Die vorliegende Arbeit ist frei von Plagiaten. Alle Ausführungen, die wörtlich oder inhaltlich aus anderen Schriften entnommen sind, habe ich als solche kenntlich gemacht. Diese Dissertation wurde in gleicher oder ähnlicher Form noch in keinem früheren Promotionsverfahren eingereicht.

Mit einer Prüfung meiner Arbeit durch ein Plagiatsprüfungsprogramm erkläre ich mich einverstanden.

Berlin, November 24, 2020

Lena Walter